

Commissariat à l'énergie atomique

e-den

A Nuclear Energy Division  
Monograph

# Nuclear Waste Conditioning



EDITIONS  
**LE MONITEUR**



---

## DEN Monographs

A Nuclear Energy Division Monograph  
Commissariat à l'énergie atomique,  
91191 Gif-sur-Yvette Cedex (France)  
Tel: +33 (0)1 64 50 10 00

### Scientific Committee

Michel Beauvy, Georges Berthoud, Mireille Defranceschi, Cheikh Diop, Gérard Ducros, Damien Féron, Yannick Guérin, Christian Latgé, Hervé Lemonnier, Yves Limoge, Charles Madic †, Philippe Moisy, Gérard Santarini, Jean-Marie Seiler, Pierre Sollogoub, Étienne Vernaz, François Willaime, Directeurs de Recherche.

**Topic Editor:** Etienne Vernaz.

### Contributors to this Monograph:

Thierry Advocat, Catherine Andrieux, Isabelle Bardez, Florence Bart, Roger Boën, Pascal Bouniol, Guy Brunel, David Chartier, Céline Cau dit Coumes, Jean-Marc Delaye, Xavier Deschanel, Sylvain Faure, Cécile Ferry, Catherine Fillet, Bruno Fournel, Fabien Frizon, Christophe Gallé, Stéphane Gin, Christophe Girold, Agnès Grandjean, Damien Hudry, Christophe Jousot-Dubien, David Lambertin, Aurélien Ledieu, Florent Lemont, Nicolas Moulin, Sylvain Peugeot, Olivier Pinet, Jean-Paul Piron, Guillaume Ranc, Isabelle Ribet, Stéphane Sarrade, Magaly Tribet, Étienne Vernaz (Topic Editor).

**Editorial Director:** Philippe Pradel.

**Editorial Board:** Bernard Bonin (Editor in chief),  
Bernard Bouquin, Martine Dozol, Michaël Lecomte, Alain Forestier.

**Administrator:** Fanny Bazile.

**Editor:** Jean-François Parisot.

**Graphic concept:** Pierre Finot.

**Correspondence:** all correspondence should be addressed to the Editor or to CEA/DEN Direction scientifique, CEA Saclay 91191 Gif-sur-Yvette Cedex (France)  
Tel: +33 (0)1 69 08 16 75

© CEA Saclay and Groupe Moniteur (Éditions du Moniteur), Paris, 2009

ISBN 978-2-281-11380-8  
ISSN pending

The information contained in this document may be freely reproduced, subject to agreement by the Editorial Board and due acknowledgement of the source.

Commissariat à l'énergie atomique

e-den

A Nuclear Energy Division  
Monograph

# Nuclear Waste Conditioning



## Foreword

**A**fter a dazzling start in the 1950's as a promising, inexhaustible, cost-effective energy source, nuclear energy was rejected by majority opinion in several Western countries three to four decades later, which suddenly brought its development to a halt.

Although the 1973 and 1979 oil crises marked the beginning of massive construction programs in some countries most heavily penalized by oil imports, France and Japan in particular, they were paradoxically followed by a gap in nuclear spending, first in the United States and then in Western Europe. However, repeated oil market tensions and emerging concerns over non-renewable natural resources should have increased such spending.

There are surely many reasons for this pause, which can in part be explained by the accidents in Three Mile Island in 1979 and Chernobyl in 1986, which deeply impacted public opinion. On top of this, ecological movements and Green parties made their (highly publicized) fight against nuclear energy a key part of their platform.

In France, whose population, with the exception of one case, had never disputed nuclear plant construction, negative attitudes began to surface in the late 1980's concerning the nuclear waste issue. Given Andra's growing difficulties in finding an underground laboratory site, the Government decided to suspend work in favor of a one-year moratorium and submitted the issue to the OPECST (French parliamentary evaluation office for scientific and technological choices).

The French Act of 30 December 1991 on nuclear waste management implemented the essence of the OPECST's recommendations, in particular its definition of a diversified research program and the basis for democratic discussion, thus helping calm the debate. It paved the way for a fifteen-year research period in which various options for long-term radioactive waste management were investigated. This led to the Act of 28 June 2006, which set out the basic framework for this management, to be recognized as a necessity from now on.

In addition, the starting century is marked by renewed collective awareness that our generation's energy needs cannot be met without concern for the environment and without preserving future generations' rights to satisfy these same needs. This concept of sustainable development is an inevitable challenge to our society.

Today, it goes unquestioned that global warming due to increasing greenhouse gas emissions is a human-caused problem. The only remaining debate concerns the extent and consequences of this climate change. Industrialized countries, which are for the most part responsible for the current situation, should feel particularly obliged to voluntarily take steps towards reducing emissions of these gases. Nuclear energy can but gain considerable ground since, by nature, it does not produce this type of emissions and yet is a relatively abundant, reliable and cost-effective energy source.

*Even if the situation still varies from country to country, more especially in Europe, several countries (China, South Korea, Finland, India, South Africa...) have already decided to make huge investments in developing nuclear energy. Others are very close to taking this step, in particular Great Britain and the United States who seem to be determined to launch programs for the construction of new nuclear power plants by the end of the decade, picking up a process that had been on hold for over a quarter-century.*

*Following France's national energy debate that took place in the first half of 2003, the Energy Act on energy passed in June 2005 established the decision to build an EPR demonstrator in preparation for the replacement of currently operating power plants.*

*A number of signs lead us to believe that a worldwide boost of nuclear energy is taking place. Nevertheless, the future of nuclear energy in our country, as in many others, will depend largely on its capacity to properly address the following two concerns:*

*- First, its social acceptability: nuclear energy must be deployed under stringent safety and security conditions, generating as little ultimate waste as possible, with perfect control of the waste that is produced in terms of its possible impact on human health and the environment.*

*- Secondly, the availability of nuclear resources: it is important to guarantee a long-term supply of fuel, by preparing to resort to systems which are more economical in terms of natural fissile materials and, above all, less dependent on market fluctuations.*

*These topics are a key part of the CEA Nuclear Energy Division's work. Indeed, this Division is a major player in the research aimed at supporting the nuclear industry's efforts to improve reactor safety and competitiveness, providing the Public Authorities with the elements necessary for making decisions on long-term nuclear waste management, and, finally, developing the nuclear systems of the future. These systems, essentially fast neutron reactors, afford highly promising innovations in waste management and raw material use.*

*As a fervent partisan of the broadest possible dissemination of scientific and technical knowledge, I believe that this research work, which calls upon a wide range of scientific disciplines often at top worldwide level, should be presented and explained in priority to all those who would like to form their own opinion on nuclear energy. This is the reason why I welcome the publication of these DEN monographs with deep satisfaction, indeed. No doubt that close reading of these works will afford an invaluable source of information to the, I hope, many readers.*

*I would like to thank all the researchers and engineers who, by contributing to this project, willingly shared their experience and knowledge.*

*Bernard BIGOT,  
High Commissioner for Atomic Energy*

# Introduction

**W**aste\* arising from nuclear power is produced in very small amounts, compared with that resulting from other energy sources. Indeed, for an equal amount of power produced, the amounts of materials converted through nuclear reactions are very small, contrasted with those produced by chemical reactions in coal or oil combustion, i.e., one million times smaller !

However, their potential toxicity makes it necessary to protect man and the environment from the related risk. Managing this **radioactive\*** waste therefore requires specific methods.

## Waste volumes and streams

The major part of nuclear-derived waste directly results from electricity generation in reactors and from **fuel cycle\***, which it is part of. The so-called “closed cycle” consists in treating **spent fuels\*** in order to separate still valuable materials and ultimate waste. It currently allows energy materials (uranium and plutonium) to be recovered so that high-level waste (**fission products\*** and **minor actinides\***), i.e., a very small part of the total radioactive waste volume (Table 1), may be recycled and conditioned in a safe and durable way.

France has got involved in the first step of the closed cycle, which means treating spent fuels arising from nuclear power plants and recycling recovered plutonium as **MOX\*** fuel in **PWR\*** reactors. This option is at the core of the French strategy oriented to ultimate waste minimization, with a twofold benefit: consuming a portion of the plutonium initially produced for power generation, and concentrating the remaining portion in spent MOX fuel pending further use.

Operating nuclear reactors as well as fuel manufacturing and processing plants also causes **effluents\*** and waste to be generated. So is it of filters which prevent radioactive gas discharges to the atmosphere, of pumps replaced, or of liquids resulting from facility washing.

This is operational waste, far less radioactive, but of much higher volume than the waste separated from fuel.

Another type of waste results from the cleanup and dismantling of former facilities. It is conditioned and sent to existing waste disposal streams.

Last but not least, research centers and hospitals generate a small amount of radioactive waste.

Table 1.

Volume of radioactive waste in France in late 2002 (excluding very low-level waste)	
High-Level Waste (HLW)	1,639 m <sup>3</sup>
Intermediate-Level, Long-Lived (IL-LL) waste	43,359 m <sup>3</sup>
Low-Level, Long-Lived (LL-LL) waste	44,559 m <sup>3</sup>
Low- or Intermediate-Level, Short-Lived (LL- or IL-SL) waste	778,322* m <sup>3</sup>

\* Including 663,562 m<sup>3</sup> disposed of at two centers, Centre de l'Aube and Centre de la Manche.

All radioactive waste occurring on the French territory is localized and quantified in a national inventory built up by the **ANDRA\*** which is updated every year. The first edition of this document was issued in November 2004.

## Waste management in terms of strategy and steps

Radioactive elements contained in radioactive waste emit various types of **radiation\*** (*alpha, beta, gamma*), which can have harmful biological effects on living systems. It is therefore necessary to protect man and his environment from these radiations by isolating radioactive waste. This means implementing several protection **barriers\*** which confine waste in juxtaposed envelopes. The first of these barriers is the confining matrix.

Two major steps can be differentiated in waste management:

- **storage\*** (temporary, by definition), which consists in orderly placing waste or spent fuel in a safe place with the intent to retrieve it at a later date to provide it a more permanent future. Following this step, part of the occurring radionuclides may be transmuted to reduce **potential radiotoxicity\*** in ultimate waste.
- **disposal\*** (final, although possibly reversible during a given period of time), which consists in placing ultimate waste in a deep geological formation so as to protect it from the natural environment's and man's aggressions till the end of radioactive decay.

Waste conditioning has to be compatible with these two complementary, non-exclusive major steps, which will take place in succession. Consistently, easy handling of conditioned

waste packages is required, in compliance with safety and radiation protection rules. This involves the possibility of retrieving these packages under constantly safe conditions at the end of the storage period. Besides, the conditioning material selected must show a suitable behavior in the very long term, in accordance with the future disposal step. In this very context, the aggressive component is underground water, which will inevitably come into contact with the material in the geological environment after a period of variable duration.

Referring to this context, the French Act of 30 December 1991, which postponed to 15 years later any industrial decision concerning the long-lived waste future, defined three research axes (Fig. 1): partitioning-**transmutation\***, geological disposal, waste conditioning and long-term storage. For the CEA, that meant mobilizing more than 300 research workers, and a budget of 1.5 billion euros over a 15-year period.

Those studies, carried out quite actively since 1992, benefited from significant international and national collaborations (EDF, AREVA, ANDRA, CNRS, and universities).

## Waste conditioning in steady progress

As any other waste, radioactive waste is generated in solid or liquid form: this is raw waste. It is turned into waste **packages\*** so that it may be handled easily and safely. The package guarantees that radioactive elements will not be disseminated. It constitutes a barrier between radioactive elements and the environment. It also complies with standards for transportation, storage, or disposal.

**Conditioning\*** thus includes all the successive operations required for manufacturing this package.

As early as the 1990's, when La Hague spent fuel **treatment\*** plants currently in operation were commissioned, AREVA tried to decrease the volume and activity level of the waste generated at these plants. This resulted in PURETEX, a large-scale research program jointly managed by AREVA and the CEA. Various routes were explored as part of this program, such as modifying currently applied chemical treatments, and using new conditioning modes. Plant operation was also optimized

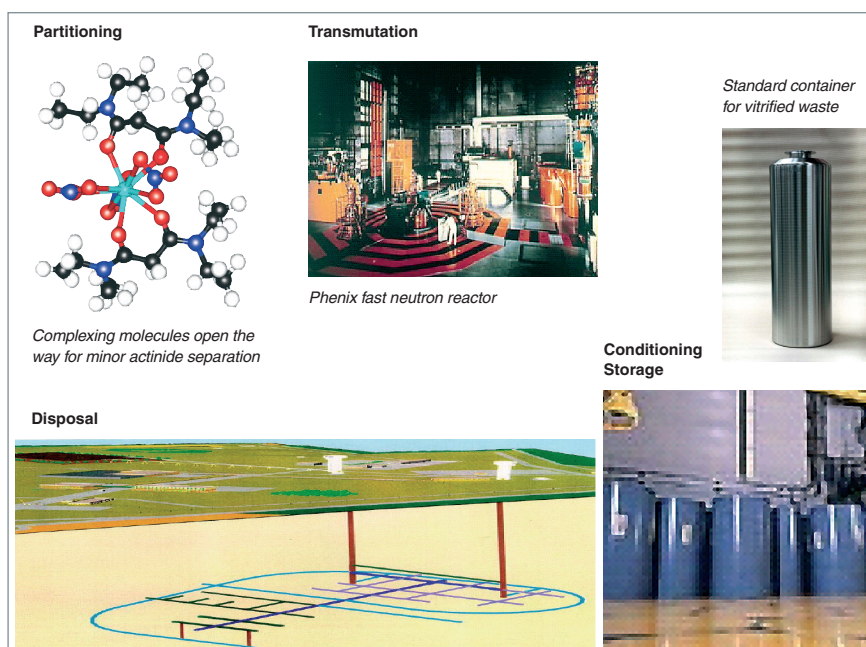


Fig. 1. Current research axes for managing waste, especially long-lived high-level waste: partitioning, intended to keep as waste only materials intended to keep as waste only materials which are actually non-valuable and lead this extracted fraction to a suitable and optimal end (transmutation); transmutation, which seems to be applicable to actinides in fast neutron reactors so as to reduce waste potential radiotoxicity; conditioning, designed to give waste a stable and reliable form; storage, intended to allow conditioned waste to cool ... and human beings to think; and deep geological disposal, designed for durably isolating ultimate waste.

with a view to reducing the amounts of products used (potential radioactive waste) in the various spent-fuel treatment operations.

Combining all these improvements led to very significant results (Fig. 2). Radioactivity released to the sea could be divided by ten owing to changes in liquid waste chemical treatment. The volume of long-lived solid waste was divided by six, especially owing to compaction which is a new conditioning mode for spent-fuel structural waste (hulls and nozzles,...). This compacted waste is introduced into a container of the same type as that used for vitrified waste, which ensures standardized conditioning for the ultimate waste generated at La Hague plants.

## Waste and effluents

Not only solid waste, but also liquid or gaseous waste arise from chemical treatment operations in the fuel cycle, as well as from power-generating or nuclear research centers. In some cases this waste is directly released to the environment. In most cases, however, its activity is too much high to do so.



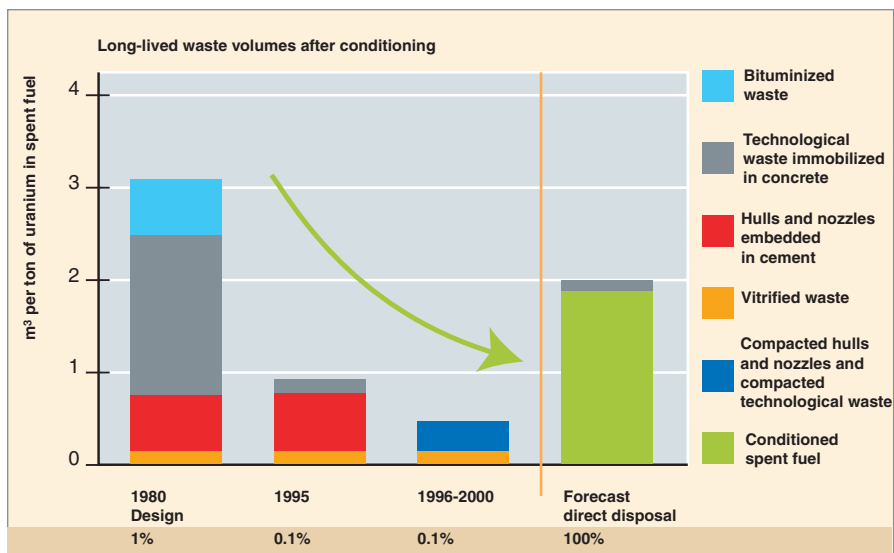


Fig. 2. Production record of waste volumes generated at La Hague UP3 facility, the capacity of which is 800 tons of spent fuel per year. The percentage mentioned at the bottom of the figure is the plutonium fraction left in waste.

It is then necessary to extract the waste toxic fraction, and condition it in a suitable matrix prior to releasing the harmless fraction to the environment. (See “Organic waste treatment”, pp. 19-26).

## Conditioning processes

High-level waste separated from spent fuel is conditioned in a glassy matrix, i.e., it is mixed with melting glass at very high temperatures (1,150 °C).

This mixture is then poured into a 200-liter stainless steel container. The resulting vitrified waste package thus consists of a homogeneous glass block containing radioactive elements in its intimate structure, surrounded by a stainless steel sealed envelope.

Nowadays **vitrification\*** is the industrial process in France for conditioning fission products solutions generated in spent fuel treatment.

The main improvements achieved in the last ten years are the following:

- a volume reduction by a factor 2 to 3 for operational waste arising from the vitrification process,
- an approximate 25% gain over the vitrified waste volume, by increasing the proportion of the radioactive elements contained in the vitrified waste package.

The ultimate waste volume will be further reduced with the cold crucible vitrification process, the implementation of which is under way at La Hague Areva NC plant (see “Cold crucible vitrification”, pp. 67-70).

Operational waste is most often cemented. In the case of solid waste, it is placed in a metal or concrete container into which cement is poured: this is the so-called “cement-immobilized waste”. As regards liquid waste, it is used in cement manufacturing as a mixing liquid prior to cement pouring into a metal or concrete container. Several container models are available, adapted to the form and size of the waste to be conditioned (see “Cements as confining materials”, pp. 71-89).

Some operational waste in liquid form may be bituminized rather than cemented.

It is presumable that the bituminization process will be decreasingly used, for today’s trend is minimizing the amount of combustible organic matter introduced into disposal facilities, and favoring inorganic matrices such as glass and concrete. Yet a few studies are still being carried out to adapt this process to the conditioning of legacy sludges stored in some silos, as their chemical characteristics could make it difficult to use vitrification or cementation. The aim is to minimize the number of packages to be produced, which implies maximizing the radioactive content acceptable for each package. In addition, given the high number of existing packages, other studies are under way to predict the long-term behavior of these packages at storage and disposal sites (see “Bitumens”, pp. 91-97).

Some solid waste may be simply compacted by press crushing, then put into a container without being immobilized (see “Metallic structure waste conditioning”, pp. 99-103).

Even if glasses, cements, bitumens, or compacted clads are proven matrices, indeed (Fig. 3), it is worthwhile carrying out prospective research on new conditioning modes in order to propose new options for some specific (organic, mixed...) waste classes. This will also pave the way for taking up future challenges in relation to new-generation reactors, whilst preserving a dynamic approach oriented to continuous improvement (see “Plasma benefits for incineration vitrification waste treatment. The Shiva process”, pp.105-110).

Generally, radioactive waste is conditioned at the site where it has been generated. Nuclear power plants as well as research centers are endowed with cementation and, possibly,

bituminization facilities. Vitrification facilities are also available in spent fuel treatment plants. In France, about 3,000 vitrified waste packages could thus be produced at Marcoule research center, where the first French spent fuel treatment plant (UP1) was in operation from 1958 to 1997.

Since 1990 vitrified waste packages have been produced at La Hague spent fuel treatment plant. About 13,000 packages have already been made, and the current manufacturing volume is approximately 600 packages per year.

Short-lived low- or intermediate-level waste is transferred to Soulaines disposal center in Aube, which is managed by ANDRA.

Long-lived waste is kept at its production site in specific storage facilities adapted to the package type. For instance, packages of waste vitrified at La Hague are also stored there.

## Conditioning systems designed for durability

The package is the first of the successive barriers separating radioactive elements from the environment. Consequently, a long-term management of packages implies evaluating the quality of this barrier as time elapses.

Now, given the long periods of time to be considered, especially for geological disposal, it is not sufficient to simply perform time extrapolation of laboratory-scale results obtained over only a few years.

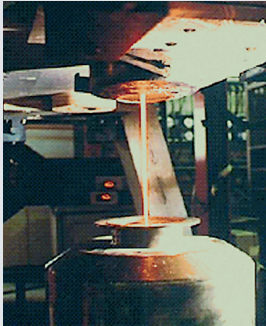
As a first step, it is necessary to understand and hierarchize the phenomena occurring in package lifetime under storage or geological disposal conditions. This can be done, in particular, performing laboratory experiments, and observing natural or archeological analogues. Basing upon the data collected, the package evolution can be mathematically described with models which simulate the intervening phenomena, ranging from matrix deterioration (atomic-, meso-, and macroscopic scale modelling) to near-field radionuclide migration (chemistry-transport modelling). This first step aims at getting the assurance, through a wide range of concording data, that matrix alteration mechanisms are well understood and thoroughly reproduced by modelling.

Such studies of waste package and confining matrix long-term behavior stand as the first step in the safety assessment related to a disposal facility.


Owing to the works carried out in the past few years, evolution models could be established for any type of package.

- Glass was selected for confining long-lived high-level waste due to its flexible use and durability. However, the very long periods of confinement required for long-lived waste disposal made it necessary to closely investigate long-term glass behavior under disposal conditions. Such studies confirmed that glass showed good behavior. First, although glass is normally metastable, and, thus, likely to recrystallize into a form thermodynamically more stable than the initial amorphous form, this process is outstandingly slow if glass composition is well chosen. Besides, this already **amorphous\*** material undergoes few structural changes under self-irradiation. Last but not least, glass exhibits

- The fission products solution, which also contains minor actinides and about 0.1% of uranium (U), is vitrified.



- Hulls and nozzles are flushed out and then compacted.



**The annual waste volume produced by treating fuel from a 1-GWe reactor is as follows:**

- 2.5 m<sup>3</sup> of high-level waste (glass)
- 5 m<sup>3</sup> of intermediate-level waste (compacted metallic clads)
- 12 m<sup>3</sup> of low-level waste (cemented waste)

- Technological waste is cemented.




Fig. 3. Ultimate waste arising from spent fuel treatment.

good resistance to water: it is true that glass oxides are slowly turned into hydroxides, but this transformation is very slow. The phenomena involved, such as interdiffusion and hydrolysis, are now well understood. Yet, glass alteration in the very long term is still thoroughly investigated, since it is much dependent on its environment.

- Concerning cemented waste packages, the main risk to be considered in relation with storage is concrete cracking due to its physico-chemical evolution, as well as some waste/cement interactions, and reinforcement corrosion. Such risk can be reduced using tailored concrete formulations and reinforcing materials (fibers or reinforcement).

As part of an exploring approach, other studies have been carried out to optimize cementation in two ways: performing waste pretreatment, and improving cement formulation for better compatibility with the waste to be conditioned.

In the case of a geological disposal site, the major phenomenon affecting cementitious material behavior is chemical degradation, which strongly depends upon the sulfate and carbonate ion content in the site water. Various models have been developed, especially to predict the evolution of radioactive element confinement in cases when a concrete container is externally degraded by water.

- Two main phenomena may significantly affect the long- and medium-term behavior of bituminized sludge packages:
  - Bitumen swells under the effect of **radiolysis**\* gases generated by radioactivity in the package, in the case of high radioactivity. Such gas release decreases with time. This swelling may affect the package behavior under storage conditions;
  - Bitumen releases the radioactive elements contained as a result of slow water inflow to the package under disposal conditions.

The first estimates of bituminized sludge package performances were based upon the models developed. For example, it can be predicted that package degradation under geological disposal conditions will last a few dozen thousand years following water inflow.

- Concerning the compacted waste package which contains metallic pieces, the proposed model is based upon the localization of radioactive elements in the package. Radioactive elements located at the surface of metallic pieces are directly driven away by water, whereas those included within metallic pieces are released progressively as metal corrodes. For example, according to laboratory-scale corrosion experiments, radioactive elements included in stainless steel pieces are released within a hundred thousand years.

- Spent fuel **direct disposal**\* has also been studied at the CEA though it is not part of the French strategy for the back-end of the fuel cycle. Studies carried out on the physico-chemical state of out-of-pile spent fuel have demonstrated that, indeed, fuel rod clads can still confine radionuclides over a period of time compatible with a dry or pool storage of about one hundred years. Yet, it was also evidenced that fuel rod clads cannot ensure conditioning with suitable confinement over longer periods of time, which implies the use of other engineered barriers (see “Spent fuel: a possible confining matrix ?”, p. 123).

**Étienne VERNAZ,**

*Research Department of Waste Treatment and Conditioning*

**Bernard BONIN,**

*Scientific Division*



## Aiming at “cleaner” waste and effluents

As any industrial activity, nuclear industry generates waste. The main nuclear waste arising from the nuclear power industry is the so-called “process waste” which directly results from spent fuel treatment. It consists of fission products and minor actinide solutions to be vitrified, or fuel assembly structural waste to be compacted. The conditioning of this waste will be dealt with in the following pages of the monograph. Another type of waste, the so-called “technological waste”, results from plant and laboratory operation. Some waste is solid such as, e.g., gloves, ion-exchange resins, small pieces of equipment, or dismantling waste; others are liquid such as, e.g., decontaminating effluents, spent solvents, or scintillating liquids used for analytical purposes. Although activity levels involved are much lower than in process waste, the volumes of technological waste may be relatively significant. Given the radioactive materials involved, treating this waste requires a specific, adapted methodology.

The strategy adopted in most applications is decontaminating waste prior to considering its future. The decontamination operation is a preliminary step which consists in removing as much radioactivity as possible from the technological waste considered, thereby making the waste “cleaner”, and allowing its easier management. In most cases radioactive contamination is located at the surface of solid waste, making it possible to collect it by various “washing” operations.

The main challenge of radioactive decontamination is to perform such an operation generating but a minimal quantity of secondary waste or effluents. Now, for every process, minimizing the quantity of waste generated requires taking into account a number of parameters in the process development: the nature of contamination, accessibility conditions, temperature, moistness, the nature of the material to be processed... For all these reasons, it is difficult to use a universal process. For each decontamination operation, it is necessary to think out a process adapted to it.

Practically the decontamination of solid pieces of equipment can be achieved with imbibed pads or lyes. Such rustical processes, however, mean producing significant volumes of waste, and it may be interesting to consider more recent processes. For example, decontaminating solids with foams allows the amount of secondary effluents to be divided by a factor 10. Surface decontamination with gels, when feasible, makes it possible to consider dry treatment which results in solid by-products, easy to be conditioned. In fine, the decon-

taminated solid will show low residual contamination, and, from the technico-economic viewpoint, it will be easier to immobilize it.

Concerning contaminated aqueous effluents, especially those resulting from the effluent treatment stations (**STEL\***, for *Stations de Traitement d'Effluents Liquides*), the technical challenge of decontamination is optimizing radionuclide precipitation using the most selective reagents with the lowest concentrations as possible. As a consequence, the amount of resulting sludges is minimized, which optimizes the final volume to be immobilized.

Concerning organic waste treatment, the challenge is quite different.

One possible process, particularly well adapted to organic effluents and waste, lies in drastically reducing their volume by incineration, which concentrates the contamination within a mineral ash easy to condition.

Another option, well adapted to small volumes of organic liquids, is supercritical water oxidation, which also destroys the organic effluent, and concentrates contamination within a small volume of aqueous effluent that may be sent to effluent treatment stations.

All those processes are described in the following chapter which gives an overview on the CEA's technological breakthroughs in this subject field.

**Stéphane SARRADE,**  
Research Department of Waste Treatment  
and Conditioning



## Decontamination processes

**D**econtamination operations in the nuclear industry are carried out simultaneously on solids, liquids and gases every day. The laboratory for decontamination advanced processes at the CEA-Marcoule improves existing processes for liquid and solid decontamination, and also develops new processes.

Decontaminated liquids have to be either recycled or released through a conventional processing stream (evaporation or dilution and, then, release into the sea). The difficulty when decontaminating an aqueous or organic liquid lies in occurring radioactive ions solubilized in the solvent, or traces of ions sorbed onto solid submicronic or colloidal particles (10 to 1,000 nm). The CEA currently investigates a coprecipitation process coupled to solid particle sedimentation.

As regards solids, the challenge is the same: decontaminating a small-sized piece of equipment (pump, valve, package) makes it possible to use it again. When dealing with a bigger facility (hot cell, fission products tank, piping, steam generator...), decontamination allows the facility to be maintained or dismantled. The difficulty to be faced in decontaminating a solid often originates in the following conditions:

- an oxide layer where radionuclides are trapped, a case often observed in metals,
- radionuclides which have migrated or diffused deeply inside the solid (such as tritium in metals, or caesium in porous concretes).

### Liquid waste decontamination

#### Coprecipitation-settling process

The coprecipitation-settling process for liquid waste treatment in the nuclear industry has been adopted in most effluent treatment stations (STEL, for *Stations de Traitement d'Effluents Liquides*) for a number of years. That process is simple and robust. It is still the basic one for effluents of complex composition [1]. For example, barium sulfate is used to make strontium insoluble or sorb it. Iron and copper hydroxides are used to trap *alpha* emitters and ruthenium. Solid particles are then separated by settling, and the resulting radioactive slurries are embedded in bitumen or in a cementitious matrix. A major challenge is optimizing reagent choices and quantities in relation to waste characteristics so as to reach the highest decontamination with the lowest waste production.

Coprecipitation consists in precipitating an adsorbent in the effluent to be decontaminated in the presence of the radionuclide to be trapped on the solid. The model most investigated at the CEA is the decontamination of effluents in strontium by barium sulfate. For this adsorbent used in most effluent treatment stations also displays the advantage of being a reference precipitate for precipitation studies. The experiment approach aims at observing the impact of the process variables (reagent inflow mode and rate, mixture...) on the size of adsorbing particles and *in fine* on their capacity to make radionuclides insoluble. As a first step, conventional implementation procedures are tested, such as processing in online operating continuous-feed reactors, as in La Hague plant, or semi-continuous reactor processing, as in the effluent treatment station at Marcoule. From the chemical process engineering viewpoint, the reactor mode of operation is generally chosen as a function of the waste volume to be processed. If the volume is high, treatment is performed in online operating reactors continuously fed with liquid waste and reagents (such as the STE3 line at La Hague). If the volume is lower, the process used is semi-continuous, i.e., reagents alone are introduced into a given waste volume.

The impact of both processes was determined in a laboratory pilot unit designed for this purpose, representative of an industrial-scale reactor by its hydrodynamic features. It was thus possible to demonstrate how decontamination may be affected by chemical process engineering parameters such as power dissipation through stirring, transit time (for a continuous-feed reactor, the ratio of the reactor volume and the total fluid flow rate passing through it), or reagent feed time (for a semi-continuous reactor). Figure 4 illustrates this research work showing two noteworthy results in continuous-feed reactors: the increase by a factor 2.5 in the decontamination factor (defined as the ratio of incoming or initial radionuclide concentration [depending upon the reactor type] to concentration in the reactor) when the transit time rises from 5 to 20 min, and the increase in the same factor when the dissipated power is increased from 0.04 to 0.4 W/kg.

Another outstanding result is the decontamination factor obtained with a semi-batch processing, which is 10 times higher than with a continuous-feed processing for the same concentration in BaSO<sub>4</sub>.

Coprecipitation results from the coupling of two phenomena: adsorptive particle formation by precipitation and radionuclide

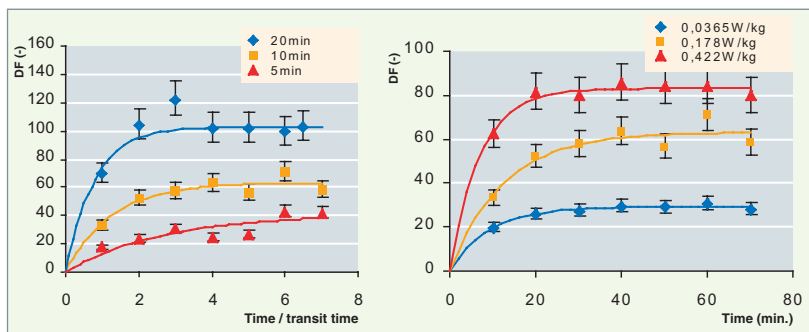


Fig. 4.- Evolution of the strontium decontamination factor (DF) as a function of a non-dimensional time for three transit times 5, 10, and 20 minutes (left), and for three powers dissipated by stirring 0.04, 0.2, and 0.4 W/kg with a 10-minute transit time (right).

capture. As the modelling of precipitation with  $\text{BaSO}_4$  has already been well established, the CEA has focused on modelling the radionuclide capture on the precipitate under formation in both types of reactors [2].

Optimizing the process means controlling particle formation. For process efficiency is governed by the characteristics and formation kinetics of the particle population. It was proved that operating conditions had a direct effect upon crystals granulometry and, so, their decontamination potential. Such an observation induces to contemplate new processes likely to favorably affect the size distribution of crystals.

## Solid waste decontamination

The CEA is developing new processes which reduce the volume of the secondary waste generated, thereby affording an alternative to conventional acid-base flushes, that generate significant quantities of liquid waste.

### *Decontamination by self-drying gels, the so-called “vacuumable gels”*

The benefits of such a treatment are numerous when comparing it with other existing processes [3]. First, in the case of onsite decontamination of radioactive facilities, gel treatment makes it possible to avoid aqueous solution projections which produce high quantities of radioactive effluents while showing limited efficiency, owing to the short time of contact with the equipment parts. Second, this approach allows the conventional operation of gel flushing by water to be given up, so that it does not generate any liquid waste requiring further treatment. As a consequence, the whole contamination treatment stream is simplified (250 g/m<sup>2</sup> of solid waste). Last but not least, these new gels can easily be used on the surface to be decontaminated as a film deposited on the surface by sputtering or brushing. After full drying in a few hours, gels result in solid flakes that can be removed by brushing or vacuum cleaning (suction), still bearing radioactivity fixed on them (Fig. 5 and 6).

Gels already developed can be described as concentrated colloidal solutions which include one or more viscosity-increasing, generally mineral, agents, such as alumina or silica, and an active decontaminating agent, e.g., an acid, a base, an oxidizing agent, a reducing agent or a mixture of these agents, especially selected taking account of the contamination and surface nature. For instance, in order to decontaminate stainless steel in a

small decontamination cell at Marcoule, the CEA has developed the first formulations of vacuumable cerium-IV-based



Fig. 5. Freshly prepared vacuumable gel.

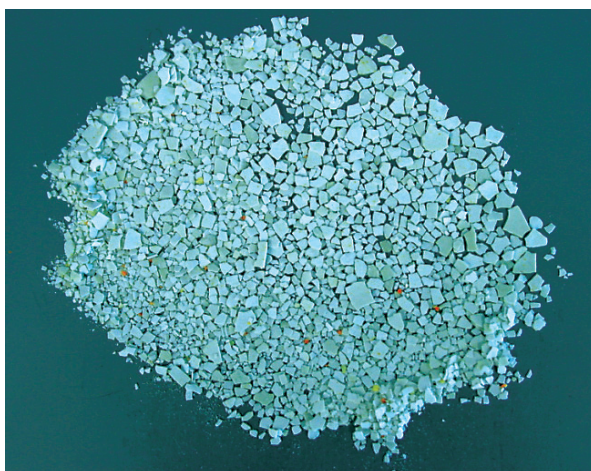


Fig. 6. Millimetric flakes as obtained after drying a gel film.

oxidizing gels. For the first time, concentrations up to 0.3-1 mol/L of cerium as nitrate salts could be reached through formulations allowing the gel to be fast dried in a few hours. This formulation uses an original mixture of silicas as a viscosity-increasing mineral base. A thin film of uniform gel



approximately 500  $\mu\text{m}$  thick can be deposited, similar to that obtained through paint sputtering. The quantity of deposited gel is lower than 700  $\text{g}/\text{m}^2$ . The gel developed for this operation is now marketed by the FEVDI company and is known as ASPIGEL 100. It dries naturally in less than eight hours at 22  $^{\circ}\text{C}$ , the usual temperature condition, and a relative moistness of 40%. It induces a homogeneous corrosion of the surface 1  $\mu\text{m}$  deep, and results in dry residues easily detached by brushing from the treated surface. It has recently been used by the STMI Company to decontaminate the cells “Candide” and “Guyenne” at the CEA Center of Fontenay-aux-Roses.

In addition, new gels are under development and are the subject of theses. For example, adding surfactants makes it possible to alter the visco-elastic properties of a gel as well as the size of the flakes obtained, while controlling the drying time.

### Decontamination by aqueous foams

Decontaminating aqueous foams are complex two-phase fluids which contain about 90% air. Foam decontamination allows to reduce the quantity of reagents used and the waste volume produced. In addition, foam filling allows facilities with complex shapes to be decontaminated (Fig.7). A decontaminating foam contains at least one foaming surfactant likely to produce foam, and one or several chemical reagents likely to dissolve the contaminating deposit adhering to the wall.

#### Foams stabilized by viscosity-increasing agents or cosurfactants

A new decontamination process known as “Procédé Mousse Statique” (Static Foam Process) has recently been patented by the CEA. It merely consists in filling the facility to be decontaminated (steam generator, tank, cell...) with a foam containing biodegradable anionic surfactants and low quantities of viscosity-increasing organic agents (1 to 3  $\text{g}/\text{L}$ ) [4]. This makes it possible to increase foam lifetime as well as the chemical reagent contact time with the wall to be decontaminated. This process is to be tested on the fission products tank at La Hague in 2009.

Besides, more fundamentally, the CEA has demonstrated that adding low quantities of cosurfactant (100 to 150  $\text{mg}/\text{L}$ ) to the foaming formulation stabilizes not only the foam, due to the interface rigidification effect, but also the liquid film thickness at the foam/wall interface. [5]

That demonstration was performed on a model system with an anionic surfactant, SDS (Sodium Dodecyl Sulfate), of concentration 3  $\text{g}/\text{L}$ , and dodecanol (DOH) as a cosurfactant (150  $\text{mg}/\text{L}$ ).

Such results can be exploited in a decontamination operation to increase mass transfer in the wall film and so the process



Fig. 7. Decontaminating foam in a tank contaminated by adhering deposits.

efficiency. This foam stabilization route, which increases interface rigidity, and slows down drainage, is an interesting alternative to that based on adding high quantities of viscosity-increasing agents (2 to 3  $\text{g}/\text{L}$ ). For that means an economy of organic matter, and allows for easier treatment of the effluent generated prior to conditioning.

As a result, research work on formulation is now focused on finding a cosurfactant for anionic foaming surfactants.

#### Foams stabilized by particles

The possibility to stabilize decontaminating foams with additional mineral nanoparticles is under study at the CEA, in order to decrease the quantity of surfactants used. Practically, adding thin particles of solids during a decontamination process may also bring another benefit if radioactivity is adsorbed onto the particle. For an increase in the decontaminating foam efficiency may be expected then, and solid particles may be separated by filtration after foam drainage, which results in easier management of the liquid waste generated.

Two main types of particles likely to stabilize aqueous foams have been identified at the CEA: hydrophilic nanoparticles, on the one hand, and more hydrophobic particles located at the air-liquid interface, on the other hand. The first type of particle stands for the naked and hydrophilic particles: it is chiefly located in inter-bubble liquid films. The effect of adding to formulations (7 nm diam.) pyrogenated silica particles of known gellification properties is currently being investigated [3]. As shown by the first results, for a concentration of 20  $\text{g}/\text{L}$  the liquid retention time within the foam may reach 30 minutes [8]. Two stabilization mechanisms have been proposed to explain such a stability: the plugging of the drains, and the solution gellification by particles.

Other investigations are being carried out in relation to hydrophobic particles which stabilize the foam locating at the air-liquid interfaces. The aim is to develop particles endowed with both a hydrophilic and a hydrophobic part, as in a conventional organic surfactant.

### **Decontamination by degreasing using acid surfactant solutions**

Soda is currently used for degreasing tri-n-butyl phosphate (TBP) used in spent fuel treatment. Yet, the drawback of this method is that waste is contaminated by a small quantity of sodium, an undesirable element in glasses used for conditioning. An interesting alternative would be to replace soda with a new degreasing, non-foaming liquid reagent. In 2007 the CEA developed a new acid solution, the surface-active formulation of which makes it possible to extract removable organic contamination shown at the surface of spent fuel treatment equipment. In most cases surfaces have been in contact with a fat organic phase containing TBP and its degradation products (HDBP and H2MBP). The newly developed surface-active solution detaches fat deposits adhering to the surface, and makes them soluble in **micelles\*** or micro-emulsions, in coherence with the general principles of detergency. During the experiments, contact angle and interfacial tension measurements were performed in order to study the capacity of various solutions to detach tri-n-butyl phosphate (TBP) deposited on a stainless steel surface. Two mechanisms of TBP detachment could thus be pinpointed: emulsification mechanism, and roll-up mechanism in which the contact angle of the droplet increases up to detachment (Fig. 8). The formulation proposed by the CEA combines two surfactants in low quantities (>10 g/L) so as to reach synergy: one wetting, and the other emulsifying for TBP. The selection of the latter, in particular, required a number of experiments, which finally highlighted the family of Pluronics (amphiphilic triblock copolymers  $EO_n-PO_m-EO_n$ ) as the more relevant [6,7]. Among the compounds tested, Pluronic P123 shows the highest emulsifying power for TBP. As for the micelles containing TBP, they were characterized using small-angle neutron scattering at the Léon-Brillouin Laboratory of Saclay: it was demonstrated that, in the case of TBP excess, the resulting emulsions remain stable for several weeks, and avoid any risk of criticality related to a possible reconcentration of plutonium.



Fig. 8. A TBP drop as it is being detached from the film: by emulsification (left), and by roll-up (right).

### ► References

- [1] IAEA Technical Report No. 337, 1992, 1-24.
- [2] V. PACARY, Y. BARRE, E. PLASARI, "Modelling and comparison of continuous and semi-continuous processes for the decontamination of liquid nuclear wastes by the coprecipitation of radioactive Sr<sup>2+</sup> with barium sulphate", an article submitted to *International Journal of Chemical Engineering Reactor*, 2007.
- [3] S. FAURE, B. FOURNEL, P. FUENTES, Y. LALLOT, French Patent FR 2 827, 530, 2001.
- [4] S. FAURE et al., International Patent No. 0208537, 2002.
- [5] C. DAME, C. FRITZ, O. PITOIS, S. FAURE, "Relations between physico-chemical properties and instability of decontamination foams", *Colloids and Surfaces A: Physicochem. Eng. Aspects*, **282**, 2005, pp. 65-74.
- [6] J. CAUSSE, S. LAGERGE, L.-C. DE MÉNORVAL, S. FAURE, B. FOURNEL, "Turbidity and proton NMR analysis of the solubilization of tributylphosphate in aqueous solutions of an amphiphilic triblock copolymer", *Colloids and Surfaces A: Physicochem. Eng. Aspects*, **252** (1), 2005, pp. 51-59.
- [7] J. CAUSSE, S. LAGERGE, S. FAURE, "Micellar solubilization of TBP in aqueous solutions of Pluronic block copolymers. Part I: Effect of the copolymer structure and temperature on the phase behaviour", *Journal of Colloid and Interface Science*, **300**, 2006, pp. 713-723.

**Sylvain FAURE,**

*Research Department of Waste Treatment and Conditioning*

## Organic waste treatment

### Incineration processes for organic technological waste

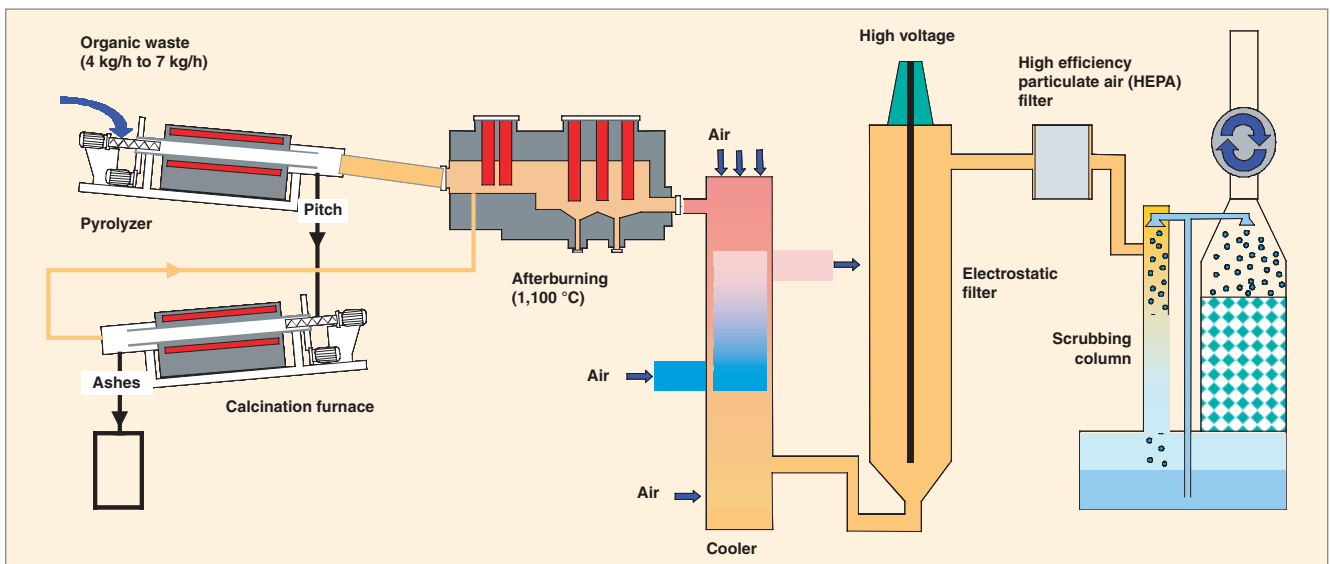
Several sectors of the nuclear industry generate various types of organic waste. For example, facility or equipment maintenance generates the chiefly solid, so-called “technological waste”, such as papers, plastics, or ion-exchange resins. On the other hand, some basic research activities can produce liquid waste such as scintillating liquids (used for measuring tritiated compound radioactivity). Whatever their origin may be, the organic nature of these various wastes makes incineration processes very attractive, for they afford the benefit of converting waste fuel load into inert gases, and reducing their weight and volume strictly to their mineral load.

For several years the CEA has been developing this type of processes in order to find an optimal solution for organic waste management. Some of them, such as the IRIS process devoted to the treatment of contaminated solid *alpha*-bearing waste, have an industrial application. Others are still under development, e.g., the IDOHL process devoted to the treatment of carbon-14 loaded or tritiated liquids.

### The IRIS process - Treating a wide range of organic waste

The CEA has to process organic waste arising from the nuclear industry glove boxes, contaminated with *alpha*-emitting actinides and highly chlorinated. For this purpose, the CEA has developed an incineration process bearing the name of its pilot facility: IRIS (pilot solid incineration unit). This type of process draws its robustness and efficiency from its breaking down into two processing steps, i.e., on the one hand, the removal of corrosive materials such as chlorine and, on the other hand, organic load combustion. This is obvious in the diagram below: the organic waste is first sent to a medium-temperature pyrolyzer system (500 °C) in order to remove the most corrosive gaseous compounds, and then to an oxygen-fed calcination system (900 °C) which completes combustion, while concentrating contamination into mineral ashes.

The resulting ashes contain no carbon and concentrate nearly all the initial activity (~ 99%) due to the relatively long residence times in the solid processing furnaces combined with low gas flow rates. The off-gas treatment system consists of an afterburning chamber followed by an electrostatic filtration system, and ensures high-performance scrubbing: after treatment, the activity level of gaseous waste is lower than detection thresholds.



General overview of the IRIS process for organic waste treatment.

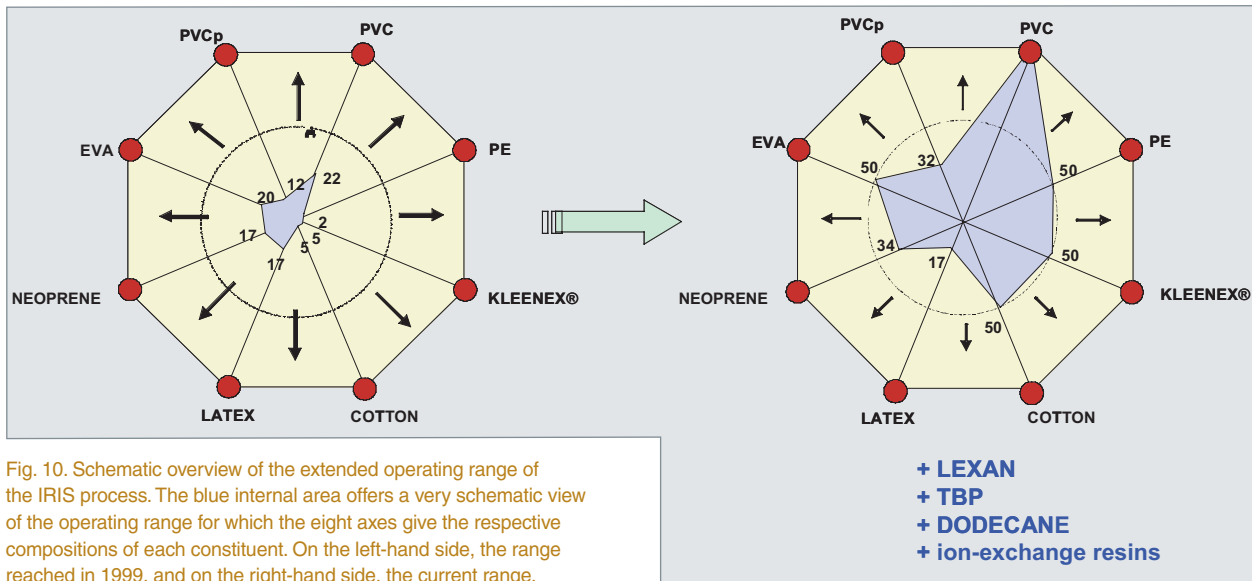


Fig. 10. Schematic overview of the extended operating range of the IRIS process. The blue internal area offers a very schematic view of the operating range for which the eight axes give the respective compositions of each constituent. On the left-hand side, the range reached in 1999, and on the right-hand side, the current range.

The significant volume of research work carried out in this area paved the way for the building at the Valduc Center of a facility designed to process waste from glove boxes. The incinerator started to operate as an active facility on 10 March 1999. It made it possible to treat several tons of waste, the average composition of which included 50 weight % PVC among other materials. Since that industrial achievement the technology and parameterization of the process have still been evolving to a higher level of performance, flexibility, and safety. For instance, better understanding of materials flow in the incinerator helped propose a fairly efficient method to prevent the formation of volatile chlorides, which induce generalized corrosion phenomena. This method is based on adding phosphorus

to the system, so as to turn chlorides into phosphates in the afterburning chamber.

Similarly, new modes of operation have emerged as a result of other advances in research, such as analyzing the processes of waste conversion into carbonated residues and, then, into ashes [1], the study of coupled kinetics, or the understanding of solid flow phenomena [2]. As a result, this has extended quite significantly the operation range of the incinerator, which can now process mixtures containing liquids such as TBP-Dodecane extractants, as well as ion-exchange resins, as shown on Figure 10.

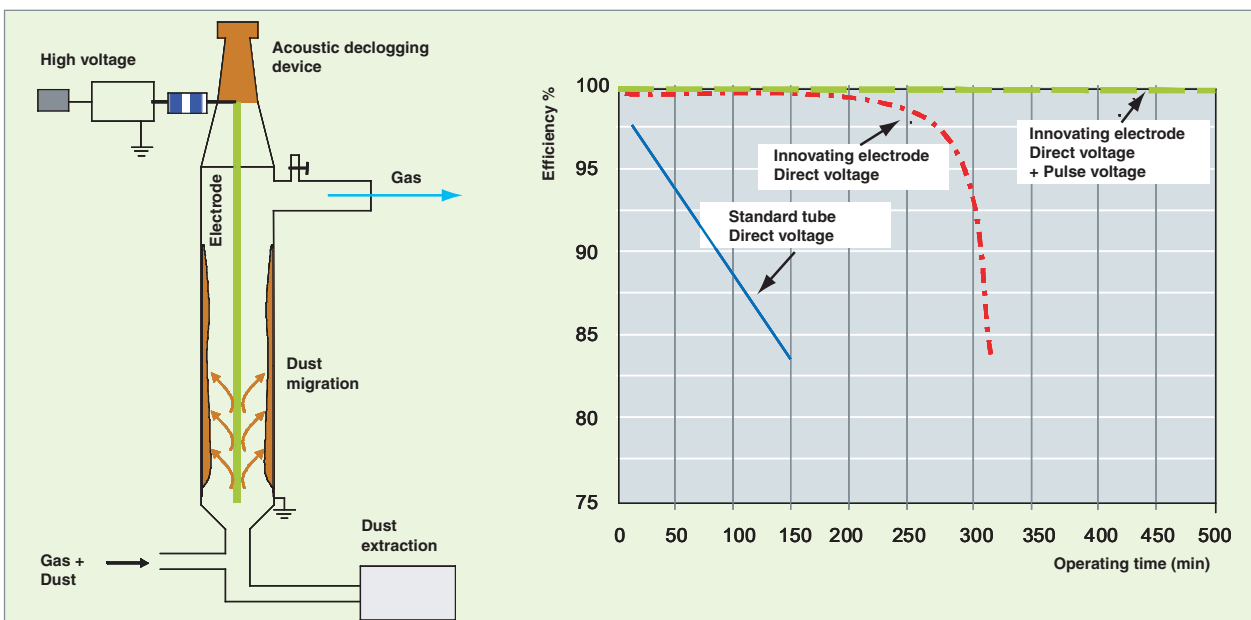


Fig. 11. Schematic overview of an electrofilter and view of the filtration endurance evolution according to the various techniques applied.

The various industrial demands have also induced an outstanding development of the gas processing system. For instance, a new concept of afterburning chamber was developed to ensure very fast thermal cycling. Moreover, the electrostatic filtration device, a very attractive one generating no head loss or secondary waste, was significantly improved as developing new electrodes coupled with high pulse voltages made it possible to get filtration endurance with the highest efficiency over very long periods of time (Fig. 11). Obviously, it is impossible to durably sustain a maximum efficiency when using a reference electrode to which a direct voltage is applied. Reversely, a maximum efficiency can be maintained for several hours using new optimized electrodes activated by electrical pulses superimposed on a direct voltage.

As this research work has been brought to completion, the CEA is endowed with a highly performing, very flexible, and safe use tool which can turn a high portion of solid or liquid organic waste into ashes, a stable ultimate waste likely to be compacted, vitrified, left untreated, or possibly treated to extract some valuable materials. Mass reduction factors recorded vary from 20 to 80 according to the mineral load of the waste to be treated. It is worth noting that developments performed for the various incinerator components may contribute to the optimization of other processes. For example, electrostatic filtration, a highly performing and enduring technique, is likely to be of interest for any other heat treatment.

### IDOHL process - Organic halogen liquid treatment

Industrial or research activities generate solid waste with variable activity level. They also generate liquid waste, the activity levels of which are too low to allow for its cost-effective treatment using conventional equipment, while being too high to allow for its treatment with Very Low-Level (VLL) Waste-dedicated equipment. Such is the case of effluents with no stream, e.g., carbon-14 or tritiated scintillation solutions used in various laboratories of research centers such as those of CEA's Life Sciences Division.

In order to find an outlet for that type of waste, the CEA is developing an innovating process based on the use of inductive plasmas similar to those used in ICP-type analytical systems. In this process the effluents to be treated substitute for the solutions to be analyzed at the center of the inductive plasma torch coil (see Fig. 12).

Using halogens in the solutions to be processed makes the whole process more complex as these products are corrosive. Another problem to cope with is avoiding the formation of harmful species such as phosgens. These constraints have been taken into account in the reactor design, since it combines a technology allowing an optimal destruction of initial compounds, and a high-temperature chemistry that ensures recombination of dissociated species into neutral compounds acceptable for release into the atmosphere, excluding halogens. Figure 13 gives a schematic overview of the technology under development in which the inductive torch can be seen at the top of the reactor. Compound degradation and recom-

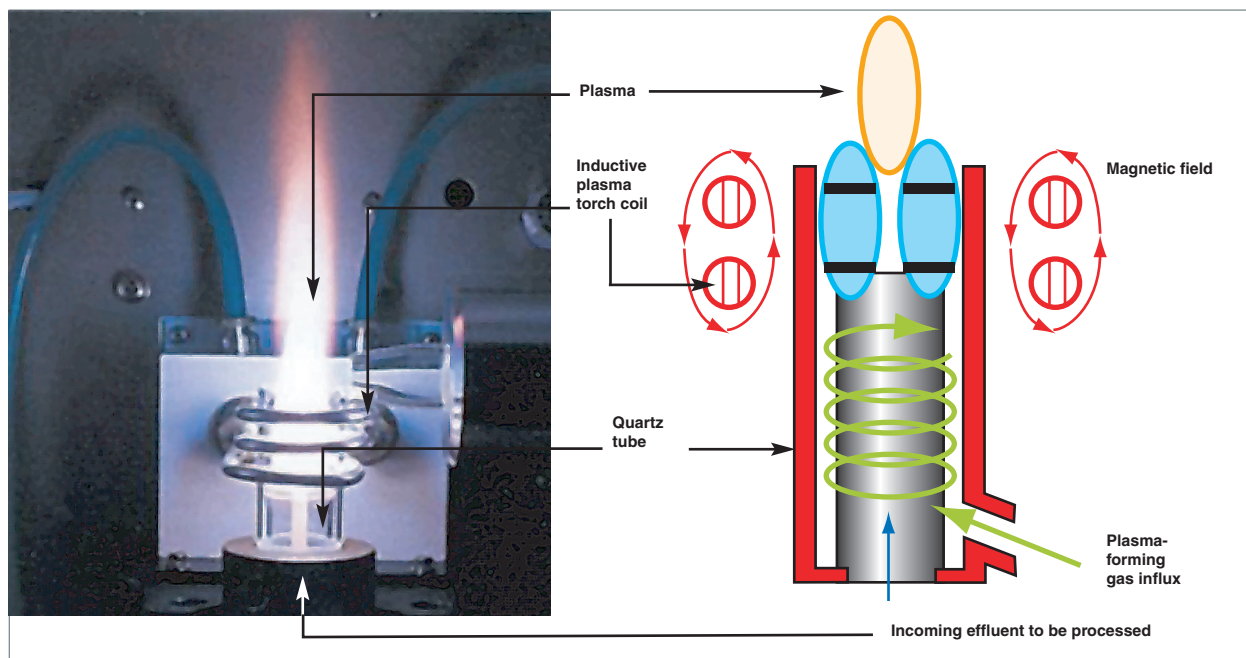


Fig. 12. Inductive plasma torch used for liquid waste treatment.

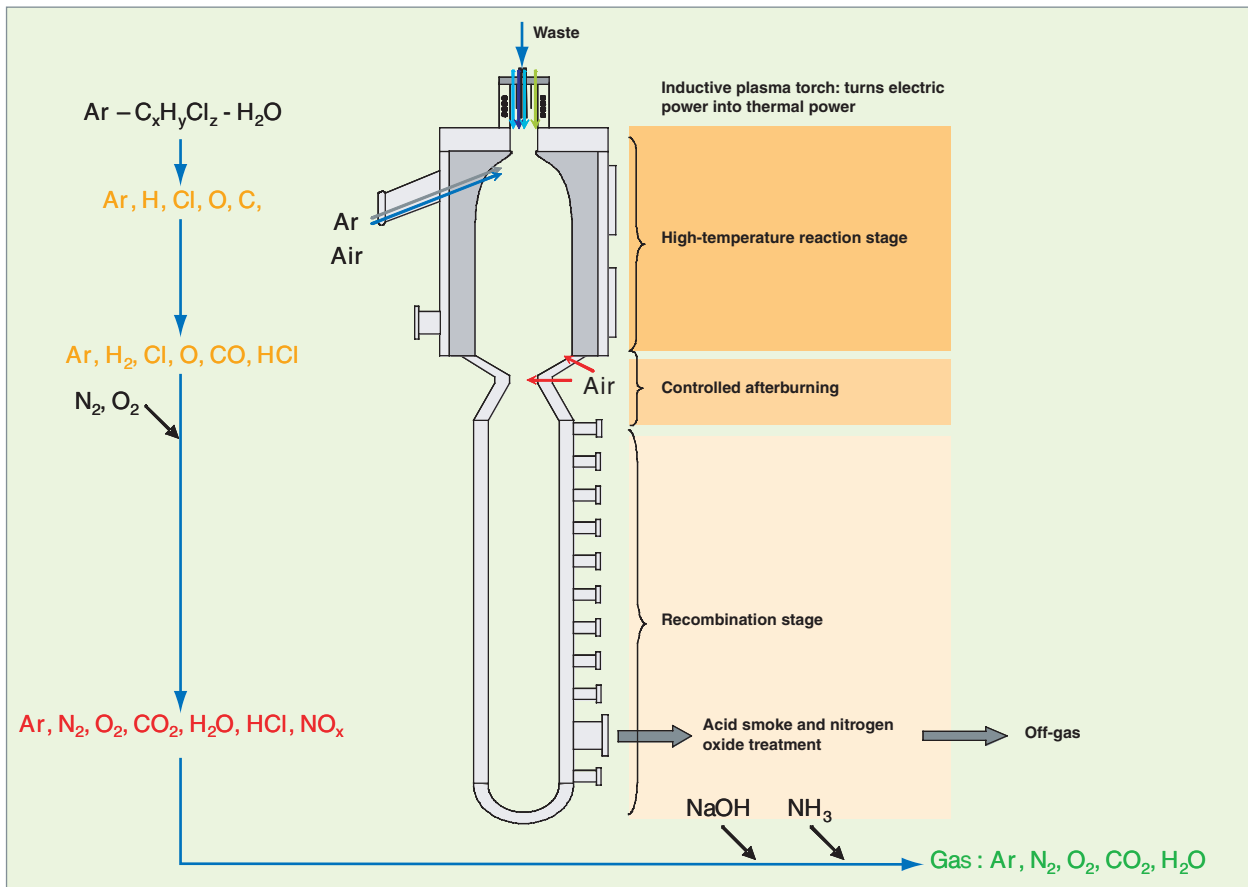


Fig. 13. Schematic overview of the IDOHL process reactor. Organic halogen compounds are continuously transformed as the gases flow through the reactor.

Recombination are carried out continuously in an up-down process, resulting in the generation of neutral gases such as  $\text{CO}_2$  or  $\text{H}_2\text{O}$ .

No substance likely to be harmful to the environment shall be released by the IDOHL process. For this reason a gas processing system has to be set up immediately after the reactor final part. This system ensures gas cooling, halogen neutralization, e.g., in a basic solution, and final filtration.

To sum up it all, the reactor as the main technological unit is integrated into a process unit as seen on Fig. 14, which includes all tools required for optimal effluent conversion.

Although this process is not yet used in active conditions, its qualification allowed a number of destruction tests to be performed for a wide range of

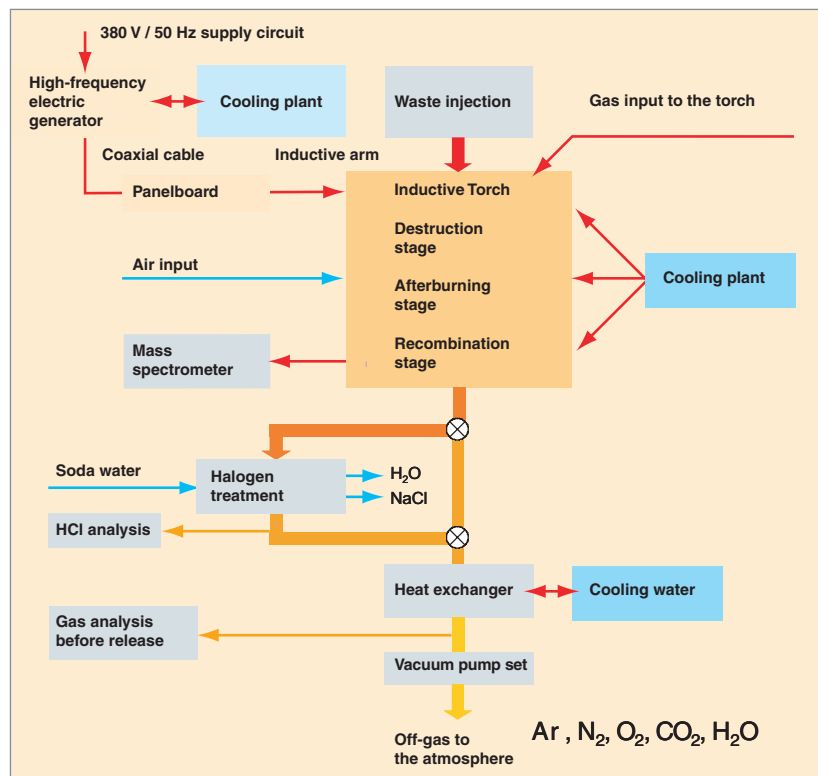


Fig. 14. Block diagram of an IDOHL-type process.

compounds including chloroform, dichloromethane, or dioxane. The tests showed highly efficient destruction of compounds as well as with high halogen capture.

As a general rule, if efficient decomposition of waste organic loads can be achieved using thermal energy, the plasma torch brings out an additional benefit: its high temperatures make it possible to reach fairly high kinetics in compound degradation, which allows for relatively compact processes. Figure 15 shows a 3-D representation of the IDOHL process. The first small-scale pilot unit for this process is under construction at the Marcoule site. It is worth noting that the compactness of the whole process could pave the way to mobile on-board systems likely to process some effluents quite near their production site. Far from being reserved to tritiated low-level effluents, such an alternative could also be of interest in other applications to treat the broad range of organic halogen compounds present in civil- or military-dedicated industrial processes.

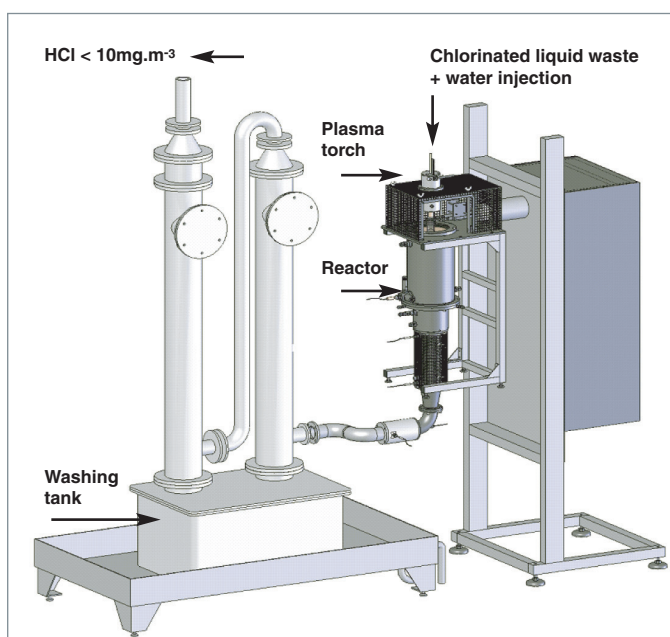


Fig.15. 3-D view of the IDOHL process.

## Chemical and thermal oxidation of organic waste in supercritical water phase (SCWO)

Since 1994 the Laboratory of Supercritical Fluids and Membranes (LFSM) has developed a supercritical water oxidation in order to destroy radioactive organic waste [3]. The process lies in the use of water properties in the supercritical phase ( $T > 374\text{ }^{\circ}\text{C}$  and  $P > 22.1\text{ MPa}$ ). In this region of the phase diagram, the value of the water dielectric constant is low, close to that of an organic liquid. The destruction reaction of organic molecules thus takes place in a homogeneous phase, in the presence of an oxidizing agent, generally air. This ensures high destruction kinetics (a few seconds) due to the increasing mass transfer and the increasing diffusivity value of species in the supercritical medium, close to that of gases. By comparison with conventional incineration, temperatures are moderate, so that no toxic gas ( $\text{NO}_x$ ,  $\text{SO}_x$ ) is released. In addition, the system temperature can be maintained due to the heat of the oxidation reaction. Last but not least, the process allows for continuous operation, which can be a benefit for its nuclearization (compactness, easy implementation) [4].

The supercritical water oxidation (SCWO) was preferred to other competing processes for organic molecule destruction such as UV treatment, ozonation, or silver-II electrochemical treatment, at least for three reasons:

- the ability to reach very high destruction rates, whatever the chemical nature of organic molecules may be,
- high treatment capacity,
- the generation, downstream the SCWO treatment, of a radioactive aqueous waste which is fully consistent with input specifications of effluent treatment stations.

### Developing an innovating reactor concept

The first reactor built was a continuous-mode tubular reactor (5 m long), made of nickel-based Inconel-718 alloy, with an operating range of 400 to 600  $^{\circ}\text{C}$  and 20 to 60 MPa. The water flow rate ranged from 1 to 4 kg/h, which made it possible to process 50 to 400 g/h of organic solvent. This reactor helped demonstrate that destroying organic compounds with supercritical water oxidation was achievable with yields higher than 99%.

The advantage of the continuous-mode tubular reactor technology lies in its easy implementation together with low investment costs. Besides, that is the only technology developed on the industrial scale. Yet, as far as nuclear applications are concerned, it displays two major drawbacks.

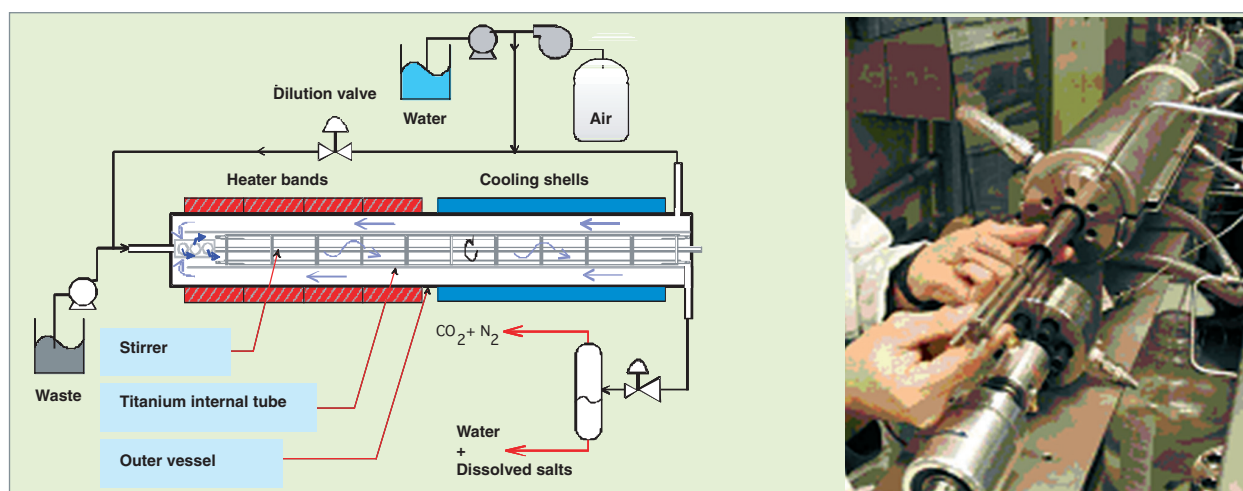


Fig. 16. Schematic view of the double-shell reactor POSCEA 2 and view of the reactor internals.

The composition of the waste likely to be destroyed with this technology is limited to C, H, O, and N type species. The occurrence of mineral salts for concentrations as low as 0.1 wt% can indeed result in mineral precipitates that are insoluble in supercritical phase, and may induce a reactor blockage.

Another limitation is the occurrence of a few milligrams of chloride (or any other halogenated compound) which results in significant corrosion in stainless steels or nickel-based materials.

Consistently, the research strategy adopted was focused on a reactor concept likely to solve both problems at one and the same time. In 2000 a patent was issued for the double-shell stirred reactor, a fairly original concept (see Fig. 16) [6]. This new reactor ensures that mineral precipitates are kept as a suspension up to their solubilization in the colder zone of the reactor. In addition, the internal reactional tube, which withstands corrosion, and operates with equal pressure between the outflowing fluid (water preheating) and the internal reactional medium, becomes an easily interchangeable component, with no limitation on the nature of the materials to be used as a function of their corrosion resistance. As for the stainless steel outer vessel, it is subject to the mechanical effects of pressure, but not to the corrosive products released by the waste [7].

A first inactive reactor named POSCEA 2 was designed, featuring a 600-ml volume, a 200-g/h capacity for organic liquid treatment, and an internal tube in titanium. The tests performed made it possible to validate the reactor resistance to chloride concentrations higher than 100 g/l as well as its operation with high salt concentration (40 wt%  $\text{Na}_2\text{SO}_4$  in the waste stream). This system also allows temperature control both inside the reactor and in the output effluent through a longitudinal temperature regulator.

### Developing a treatment tool for CEA's radioactive organic effluents

Jumping from the inactive laboratory scale to an active tool of suitable capacity made it necessary to cope with two difficulties:

- nuclearizing the process, while preserving the principle of dynamic contamination confinement,
- extrapolating the reactor POSCEA 2 by a factor 5, so as to reach a treatment capacity likely to take into account the whole inventory of the so-called “without stream” organic waste already existing, as well as the future waste to be generated.

The first point led to the development of the mini-reactor DELOS, of a 100 ml volume, put in a **glove box\*** and operating as an active facility. The dynamic confinement is achieved inserting the reactor into a shielded enclosure, designed for absorbing sudden pressure increases due, e.g., to reactor rupture. This enclosure, put in a glove box, maintains a negative pressure and, thereby, process confinement. This first reactor served as a reference for the concept validation by the safety authorities.

Concerning the second point, a three-step approach was adopted as follows:

- setting up an active DELOS reactor designed for the treatment of all radioactive organic liquids in ATALANTE, with an initial capacity equivalent to that of the reactor POSCEA2,
- setting up an inactive DELIS reactor endowed with all the DELOS functions related to nuclearization (see Fig. 17),
- setting up a numerical simulation approach oriented to fine



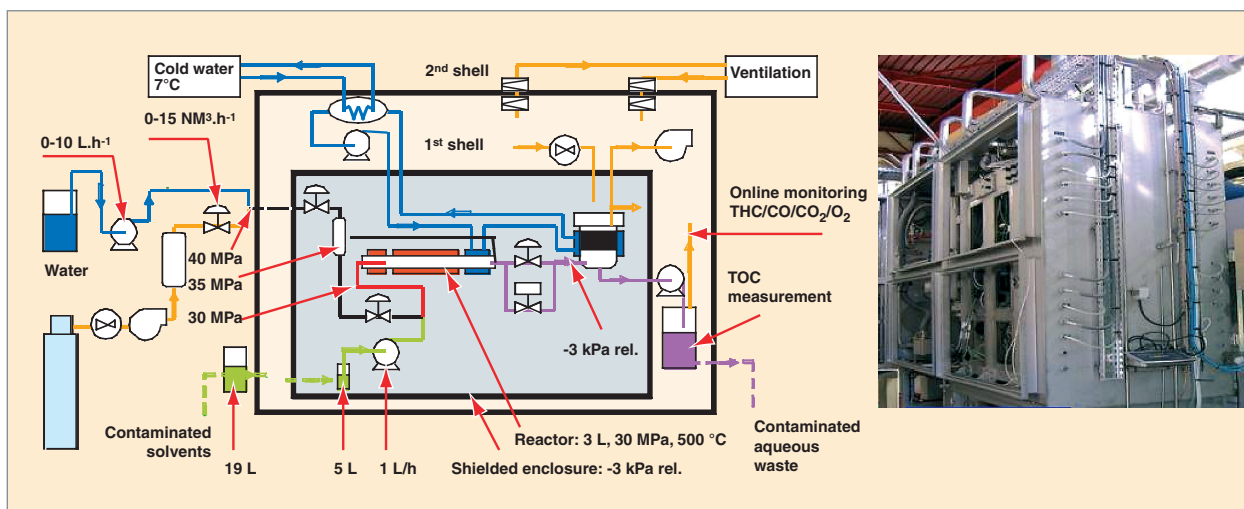


Fig. 17. Basic diagram of the nuclearized process and view of the DELIS pilot designed for radioactive organic effluent treatment.

modelling of the velocity field, coupling with the oxidation reaction, and simulation of heat transfers, so as to carry out the predictive studies required for the extrapolation.

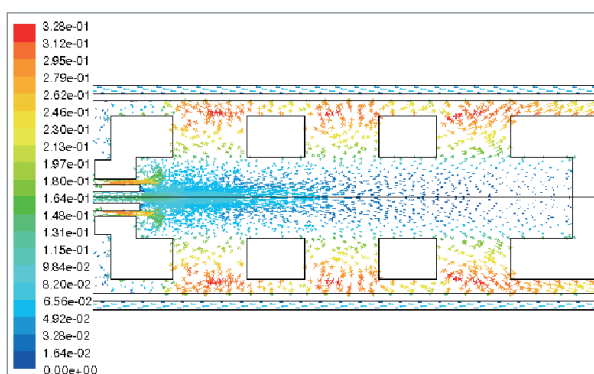


Fig. 18 a. Velocity field in m/s at the top of the stirrer.

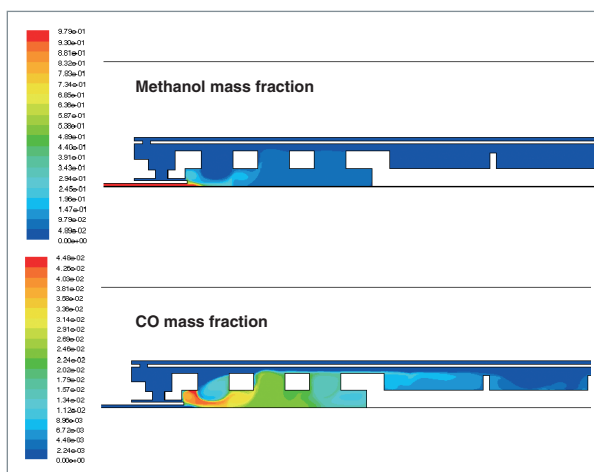


Fig. 18 b. Local concentrations of methanol (waste selected as a model) and CO, an intermediate species formed during the oxidation reaction.

The DELOS process in its current configuration is scheduled to start in 2009, prior to a scale increase expected around 2010-2011.

The process DELIS was qualified in 2007. Its operation as an experimental basis will help improve the numerical simulation models, until the DELOS start-up in its final version, i.e., a capacity equivalent to the pilot DELIS.

The supercritical oxidation process in the double-shell reactor was reproduced by fluid-dynamics numerical simulations using the code Fluent®, including reactivity through a combustion model [8, 9]. The aim is to generalize this approach, which affords the advantage of coupling the effects of chemical kinetics with the effects of hydrodynamics. Fig. 18 puts forth the results of the hydrodynamical simulation alone (a), and the results obtained by coupling with the combustion model (b).

### Other applications of supercritical water under study

Considering the supercritical water applications of interest, the laboratory currently focuses on two development axes which directly or indirectly address waste or energy problems:

- hydrogen production from waste rich in organic matter (whether or not biomasses). This purpose calls for a hydrolysis-type reaction. The oxidant is added substoichiometrically in order to achieve partial oxidation. Gases enriched in hydrogen (about 30% of the total composition) and CO can be generated. The interest of this technique lies in its twofold benefit, as the waste (distillation effluents, paper industry waste) can be both processed and recycled for energy purposes;

- organic solid treatment. There is a strong demand for treating this type of product, such as, e.g., ion-exchange resins used in nuclear power stations. So the aim is to achieve a polyphasic oxidation reaction in a supercritical water medium, while maintaining the continuous mode of the reactor.

## Overview and Outlooks

All things considered, alternatives available for the treatment of industrial organic effluents are relatively few. In the case of low concentrations of organic matter in water (generally <1%), it is possible to turn to biological, efficient, and low-cost processes. Incineration is a conventional technology of interest, especially for effluents with organic matter concentrations higher than 25%. Yet, it requires to manage the combustion gas release to the atmosphere. As for supercritical water oxidation processes, their field of application includes effluents of intermediate concentration (5-20%) or toxic, dangerous organic waste.

Research work related to supercritical water oxidation has paved the way for the development of a nuclearized tool able to process all contaminated organic liquids handled at the CEA as well as those to be generated in the future. The bottom effluent is an aqueous medium compatible with the specifications of effluent treatment stations. Complementary routes are also being investigated so as to make this process exploitable. As regards modelling, emphasis is given to the coupling of hydrodynamics with a combustion-type approach.

Optimization of the current process will break into the following steps:

- managing solids in a continuous-mode reactor (patented process) [10];
- fully exploiting the concept of interchangeable reactional tube by scheduling operation cycles, and by preparing to adapt at any time, if need be, the nature of the reactor constituent material to the effluent being processed, in order to extend the material lifetime as much as possible;
- achieving the separation of mineral solids in the supercritical phase when they are precipitated, in order to remove the salt load from the effluent as a pre-treatment step.

Beyond the investigations still under way, other outlooks seem to be of interest in relation with the supercritical water oxidation process:

- supercritical water synthesis of solids for a wide range of applications: fuel manufacturing, catalyzers, membranes, pharmaceutical or cosmetic products... In this case, the technological challenge to be taken up is related to the reaction process control and reproductibility due to fast kinetics;

- using supercritical water for decontamination effluents treatment during cleanup operations. The challenge is then to develop a nuclearized mobile unit.

## References

- [1]. F. LEMORT, J.-P. CHARVILLAT, "Incineration of chlorinated organic nuclear waste: In situ substitution of phosphates for chlorides", *ICEM'99 Conference*, September 26-30, 1999, Nagoya – Japan.
- [2]. Y. SOUDAIS, I. MOGA, J. BLAZEK, "Comparative Study of Pyrolytic Decomposition of Polymers Alone or in EVA/PS, EVA/PVC and EVA/Cellulose Mixtures", *Journal of Analytical and Applied Pyrolysis*, **80** (1), August 2007, pp. 36-52.
- [3]. C. JOUSSOT-DUBIEN, "Étude de l'oxydation hydrothermale de déchets organiques. Cas de deux molécules modèles: le dodécane et le méthanol", Thesis, Bordeaux I University, 1996.
- [4]. G. LIMOUSIN, "Oxydation hydrothermale de déchets organiques contaminés", Thesis, Bordeaux I University, 2003.
- [5]. E. FAUVEL, C. JOUSSOT-DUBIEN, *et al.*, "A Porous Reactor for Supercritical Water Oxidation: Experimental Results on Salty Compounds and Corrosive Solvents Oxidation", *Industrial & Engineering Chemistry Research*, **44** (24), pp. 8968-8971, 2005.
- [6]. C. JOUSSOT-DUBIEN, H.-A. TURC, G. DIDIER, "Procédé et dispositif pour l'oxydation en eau supercritique de matières", Patent No 00/12929.
- [7]. Y. CALZAVARA, C. JOUSSOT-DUBIEN, H.-A. TURC, E. FAUVEL, J. S. SARRADE, "A new reactor concept for hydrothermal oxidation", *Journal of Supercritical Fluids*, **31**, pp. 195-206, 2004.
- [8]. S. MOUSSIÈRE, "Étude par simulation numérique des écoulements turbulents réactifs dans les réacteurs d'oxydation hydrothermale: Application à un réacteur agité double-enveloppe", Thesis, Paul-Cézanne Aix-Marseille III University, 2006.
- [9]. S. MOUSSIÈRE, C. JOUSSOT-DUBIEN, P. GUICHARDON, O. BOUTIN, H.-A. TURC, A. ROUBAUD, B. FOURNEL, "Modelling of heat transfer and hydrodynamic during supercritical water oxidation process", accepted to *J. of Supercritical Fluids*, 20-06-2007.
- [10]. C. JOUSSOT-DUBIEN, H.-A. TURC, "Dispositif d'injection de particules dans un procédé d'oxydation hydrothermale", Patent E.N. 04/51902.

**Bruno FOURNEL and Florent LEMONT,**  
*Research Department of Waste Treatment  
 and Conditioning*

## Glass packages and manufacturing processes

As early as the late fifties, the CEA's Directorate became aware of the management problem related to fission products solutions, and started research programs in order to solve it.

After being preconcentrated so as to reduce their volume, fission products solutions are stored in stainless steel tanks which are constantly stirred and cooled. Their activity, related to spent fuel burnup, may reach  $3.75 \cdot 10^{13}$  Bq/L and the power released is significant (up to 7 W/L). These nitric solutions (1 to 2 N) feature high physico-chemical complexity. Their chemical composition generally includes inactive elements such as:

- corrosive products (iron, nickel, chromium),
- additive products (aluminium, sodium...),
- solvent degradation products (phosphorus),
- elements issued from clad materials (aluminium, magnesium, zirconium...).

There is a broad range of radioactive elements, fission products and actinides concerned, since more than 40 different elements can be numbered ranging from germanium ( $Z=32$ ) to californium ( $Z=96$ ).

Contrary to what is suggested by the word "solution", usually reserved for homogeneous liquids, "fission products solutions" also prove physically complex: for they contain flocculates and precipitates (zirconium phosphates and molybdates...) as well as fine metallic particles (undissolved platinoids such as ruthenium, palladium, rhodium, or intermetallics, e.g., with molybdenum), and fines resulting from fuel clad shearing (zirconium, for PWR fuels).

### Glass as a confining material

The conditioning of fission products solutions is aimed at:

- turning waste from the liquid to the solid state,
- reducing the volume to be stored and, then, disposed of,
- getting a material which complies with the safety requirements peculiar to storage and disposal.

The material selected for conditioning these solutions must display very specific properties due to the complexity of the problem. Early research routes were first focused on mica- or feldspath-type crystalline materials prior to being re-oriented to

amorphous materials making in the late fifties. During the sixties, glass was selected by France and the world's community as the confinement material for fission products solutions, due to the flexibility of its disordered structure that enables glass to confine many chemical elements. It must be emphasized that the aim is not a mere embedding, but an atomic-scale confinement (Fig. 19), since radionuclides are intimately incorporated in glass structure.



Fig. 19 a. Confinement glass block.

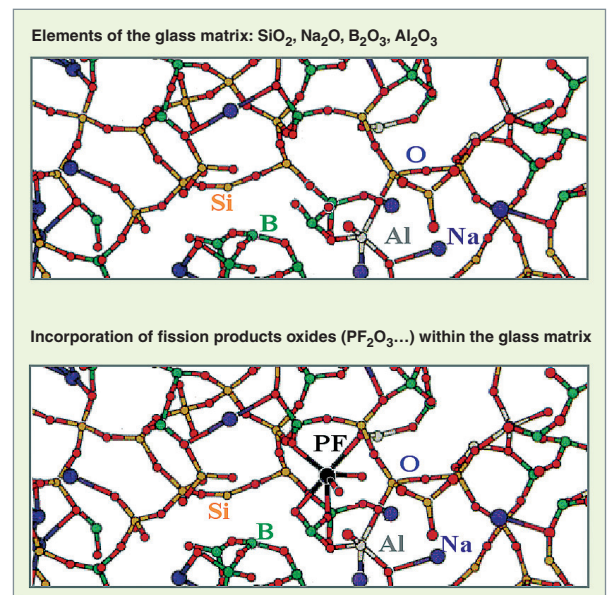


Fig. 19 b. Principle of element confinement within a vitreous structure.

In addition, as will be shown hereafter, glass is endowed with satisfactory properties of:

- thermal stability,
- chemical durability,
- resistance to self-irradiation.

Determining a glass composition means making a compromise between the material properties and the technological feasibility of its industrial-scale fabrication. France has thus selected alumino-borosilicate glasses as confining materials for fission products solutions resulting from the treatment of “graphite-gas” and “light-water” reactor fuels.

Regarding “light-water” solutions, the glass fabricated at La Hague is referenced “R7T7” after the name of the AREVA plant workshops in which it is manufactured. It consists of SiO<sub>2</sub>, B<sub>2</sub>O<sub>3</sub>, AlO<sub>3</sub>, and Na<sub>2</sub>O in the major proportion (80%). Silicon, aluminium, and boron act as forming elements, i.e., they polymerize the vitreous network with their strong bindings, whereas alkaline elements are modifying elements which generally depolymerize the network: they make it possible to reduce the melting point and viscosity, and increase molten glass reactivity, which makes its fabrication easier. The incorporation rate for fission product oxides is currently limited to 18.5% (see Table 2).

Table 2.

Chemical composition range of R7T7 glasses produced in the AREVA - La Hague plant workshops			
Oxides	Specified interval for the industry (wt%)		Average composition of industrial glasses (wt%)
	min	max	
SiO <sub>2</sub>	42.4	51.7	45.6
B <sub>2</sub> O <sub>3</sub>	12.4	16.5	14.1
Al <sub>2</sub> O <sub>3</sub>	3.6	6.6	4.7
Na <sub>2</sub> O	8.1	11.0	9.9
CaO	3.5	4.8	4.0
Fe <sub>2</sub> O <sub>3</sub>	< 4.5		1.1
NiO	< 0.5		0.1
Cr <sub>2</sub> O <sub>3</sub>	< 0.6		0.1
P <sub>2</sub> O <sub>5</sub>	< 1.0		0.2
Li <sub>2</sub> O	1.6	2.4	2.0
ZnO	2.2	2.8	2.5
Oxides (PF + Zr + actinides) + Fines suspension	7.5	18.5	17.0
Actinide oxides			0.6
SiO <sub>2</sub> +B <sub>2</sub> O <sub>3</sub> +Al <sub>2</sub> O <sub>3</sub>	> 60		64.4

Excepting the platinoids occurring in glass as RuO<sub>2</sub> crystals and metallic phases (Pd, Rh, Te), glass R7T7 is homogeneous on the microscopic scale after fabrication and natural cooling.

The physico-chemical properties of nuclear glasses R7T7 were determined for compositions of inactive glass **simulants**<sup>\*</sup>, and then validated on radioactive glass samples made on the laboratory scale or collected in La Hague plant industrial workshops.

## The confinement process

The main operations allowing solution-to-glass conversion are as follows:

- water evaporation;
- calcination - in a temperature range of 100-400 °C - which turns most elements into oxides by decomposition of nitrates excluding alkalines and a portion of alkaline earths;
- vitrification, through a reaction between the calcinate resulting from the previous operation and raw materials, which mainly bring vitreous-network forming elements such as silica (these raw materials generally are a preformed glass called glass frit). These reactions require temperatures in a range of 1,050-1,300 °C according to the composition of the glass under fabrication.

Implementing these operations means coupling the process with a sufficiently basic technology likely to be compatible with operation in highly active conditions.

In the sixties, the CEA started developing batch processes in which online operations similar to those described above were performed sequentially in the same system. These processes finally led to the building and operation of two active facilities at the Marcoule pilot workshop:

- GULLIVER, which was in operation from 1964 to 1967.

Evaporation, calcination, and vitrification were performed in a graphite crucible heated by a resistance furnace. After controlled cooling, a 4-kg glass “pancake” was retrieved using a suction cup handling device (Fig. 20). 50 pancakes could be made in this way, which represents the treatment of 250 liters of fission-products solution.

- PIVER, in operation from 1968 to 1980, in which 25 m<sup>3</sup> of solution were processed.

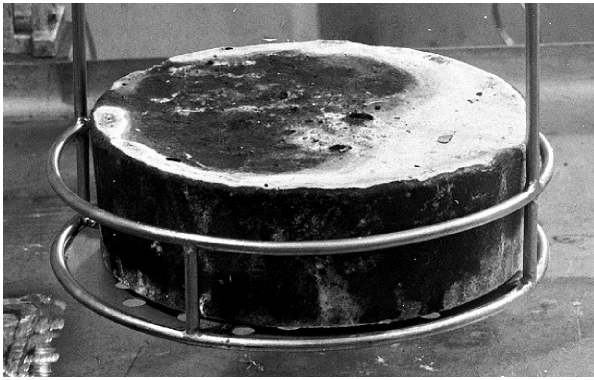


Fig. 20. . Glass “pancake” manufactured in the GULLIVER facility at the CEA Center of Marcoule.

The evaporation, calcination, and vitrification operations were performed in an inductively-heated metal pot (made of Inconel so as to withstand molten glass corrosive action). The resulting liquid glass was then poured into a container. 176 containers, of about 70 kg glass per container, were produced (the total activity of which was equal to 52 *beta gamma* PBq and 56 *alpha* TBq in 2002). This production divided into two successive steps: 164 containers of fission products confinement glass resulting from the treatment of SICRAL “graphite-gas” fuels, and 10 containers of fission products confinement glass resulting from the treatment of PHENIX “fast neutron reactor” fuels.

This PIVER facility (Fig. 21) allowed FPs-solution vitrification on the industrial scale, especially the inductively-heated metal pot technology with its pouring system, to be qualified in highly active conditions. This process, however, could not have industrial-scale outlets in France due to the batch mode and the too low resulting productivity (about 5 kg/h of glass). A version very close to the PIVER process is currently used in India.

In the 70's, in order to reach a productivity compatible with the demand of spent fuel treatment plants, the CEA has refocused R&D work on the development of a continuous process with the related technology. This process consists of two steps of operations, online performed in two separate devices (Fig. 22): evaporation-calcination of fission-products solutions, and vitrification of the calcinate previously produced:

- the calcination unit, consisting of a rotative tube heated by a resistance furnace, also receives reagents and a recycled solution arising from gas treatment. It especially allows the partial nitrates occurring in solutions to be evaporated and turned into oxides, among other operations. Adding a calcination organic adjuvant, which decomposes under the effect of temperature, makes the calcinate fragmentation easier, while reducing the volatility of some elements (e.g., ruthenium).

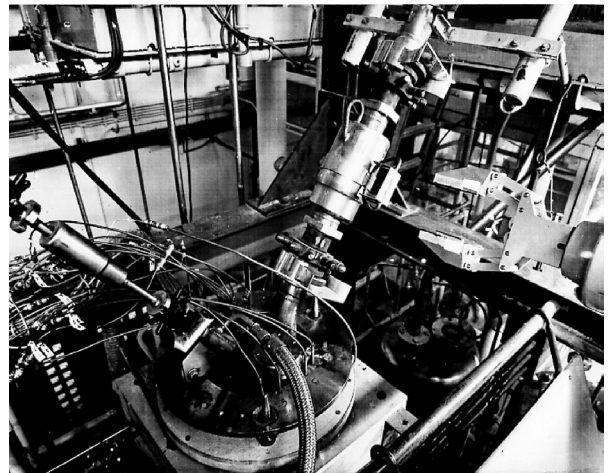
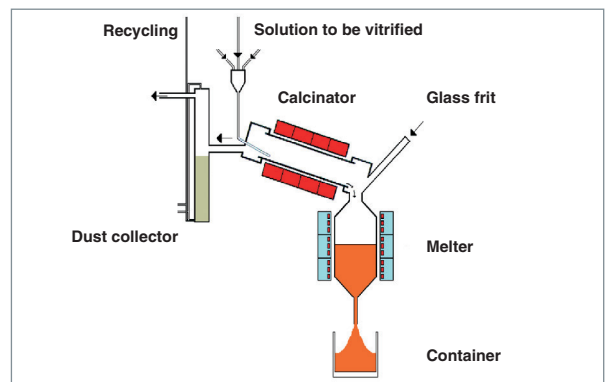


Fig. 21. The melter top in the vitrification facility PIVER at the CEA Center of Marcoule.

- the vitrification melter, which receives the calcinate coming from the rotative tube, as well as the glass frit required for confinement glass formation. This glass is made in an inductively-heated metal pot at a temperature of about 1,100 °C. It is then poured as 200-kg batches into refractory stainless steel containers (2 batches per container in La Hague vitrification workshops). After lid welding and external decontamination these containers can finally be transferred to a storage site.

The off-gas from the calcinator is processed in several pieces of equipment designed to stop dust – to be recycled –, condense water vapor, and recombine nitrous vapors. One of the basic functions of off-gas treatment is the recovery of fission products carried over by volatility, mainly Ru, Cs, Te, and Se.

As a conclusion, the whole series of operations results in decontamination factors allowing for off-gas release to the atmosphere in compliance with chemical and radioactive release standards.



The two-step continuous vitrification process.

Small size is a feature common to all the devices used in this process, especially the metallic melting pot, which has the shortest lifetime (about 5,000 hours), and their design allows for easy replacement in a shielded cell. This results in relatively low values for the total fission products content of the vitrification facility, and for the technological waste amount resulting from the process implementation. In addition, another benefit of this design is its high flexibility in operation, allowing for use in small-sized shielded hot cells tailored to remote-handling conditions. Conversely, the capacity is limited, so that several vitrification lines have to be in operation in parallel.

After scale-1 validation with inactive simulated waste, this two-step continuous vitrification process was commissioned:

- in 1978 at the CEA Center of Marcoule, in the Marcoule Vitrification Workshop (AVM, for *Atelier de Vitrification de Marcoule*) coupled with the UP1 treatment plant.

Featuring a solution treatment capacity of 40 L/h and a glass-making capacity of 15 kg/h, the AVM could vitrify all the fission products resulting from the UP1 plant operation. Being now close to the end of its lifetime, it currently vitrifies effluents arising from the plant decontamination. The containers produced by the AVM hold 360 kg glass resulting from three successive 120-kg pouring steps.

- in 1989 and 1992 at La Hague, in the R7 and T7 workshops coupled with the UP3 and UP 2 800 plants.

Each of these workshops is endowed with three vitrification lines with an initial solution treatment capacity of 60 L/h and a glass-fabrication capacity of 25 kg/h. The containers resulting from the workshops R7 and T7 contain 400 kg glass coming from two successive pouring steps of 200 kg each. The maximum capacity of these workshops is of about 950 **CSDV\*** a year (CSDV: *Conteneur ou Colis Standard de Déchets Vitrifiés*: standard container for vitrified waste).

- in 1990 at Sellafield in Great Britain, in the WVP (Windscale Vitrification Plant) workshop.

In parallel to the operation of these workshops R&D was carried out with the following results:

- the glass volume was reduced by an approximate 25% by increasing the fission products feed rate;
- the technological waste amount was decreased by extending the lifetime of the metal melting pot to near 5,000 hours;
- the process and technology were tailored to the higher burn-up rates of the fuels processed and the higher glass incorporation rates of metal particles (platinoids), up to 3 wt% (e.g., by implementing highly-performing stirring systems);

- the treatment capacity was increased (about 90 L/h for each calcinator).

## How to manage glass packages

The Marcoule vitrification workshop (AVM\*, for *Atelier de Vitrification de Marcoule*) has produced more than 3,000 containers since it was commissioned.

The glass produced by the two vitrification workshops at La Hague is poured into standard containers for vitrified waste (CSDV) made of refractory stainless steel, the dimensions of which are given in Figure 23.

From the date of their commissioning to September 2007 the two workshops R7 and T7 have produced more than 13,000 CSDV confining a total initial radioactivity of  $2.10^8$  TBq *beta gamma*. These containers are either stored at La Hague site, in the case of waste arising from French spent fuels, or sent to foreign customers.

Glass containers are stored in ventilated vaults. This first step in package management is meant to allow waste to cool.

Indeed, cooling is a crucial issue in glass storage. For glass packages are subject to heating problems due to the radioactive decay of confined radioelements.

This decay heat generation makes necessary a cooling step so as not to go beyond the maximum allowable temperatures for glass and its environment. The specific powers of R7T7-type glasses arising from PWR fuels are approximately 2.5 kW per package at the conditioning step, 1 kW after 10 years, and 0.4 kW after 50 years.

The maximum allowable temperature for the material is defined taking into account glass crystallization characteristics, which vary according to its composition. As regards R7T7

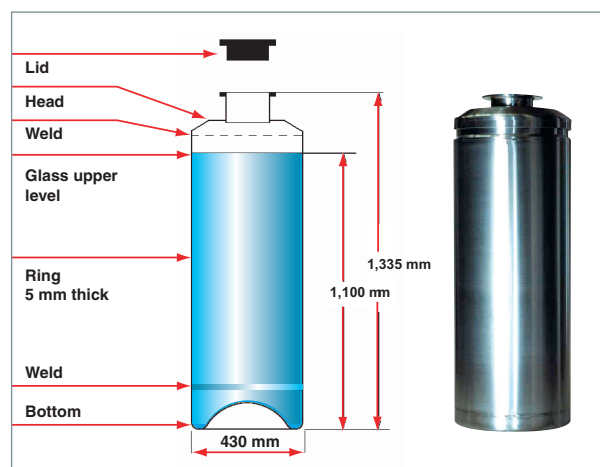


Fig. 23. The standard container for vitrified waste (CSDV).



Fig. 24. Storage facilities at the CEA Marcoule Center (for claddings) and La Hague plant (for vitrified waste).

glass, the minimum crystallization temperature is about 610 °C. That means that stored glass in the equilibrium state has to be kept at a maximum temperature of 510 °C.

Glass package storage has been recognized a proven industrial alternative for decades (Fig. 24).

At the CEA Marcoule, the first glass packages made in the PIVER facility in the seventies have been stored there since that time. As for the 3,146 glass packages produced by the AVM since its commissioning in 1978, they are stored in the workshop storage vaults.

At La Hague, each vitrification workshop has its own storage capacities, not to mention a complementary glass package storage facility available at the site.

## Waste vitrification in other countries

The two industrial techniques for vitrification are the following:

- the continuous vitrification process using a metallic pot melter, hereabove described, which has been implemented in France and the United Kingdom, as well as in India in its batch version;
- the ceramic-lined melter process in which glass is heated by an electric current flowing between electrodes, known as “LFCM” (*Liquid Fed Ceramic Melter*). This process is characterized by the use of a very big-sized ceramic furnace: it shows extended lifetime compared with metallic pots (up to six years); yet, it is hard to replace at the end of lifetime, and gives rise to a huge quantity of waste. The furnace is directly fed with the solution to be processed, so that the water evaporation and calcination steps take place on the molten glass surface. This process has already been implemented in former facilities in Belgium (Pamela) and the United States (West Valley). It is now in operation in the United States

(Savannah), Japan (Tokai Mura), and Russia (Mayak), and will be implemented in Germany (Karlsruhe) or Japan (Rokkashomura) in the future.

## Prospects for vitrification

The vitrification processes currently in industrial operation in the world (ceramic furnace or metallic pot) display limitations as regards the following features:

- the lifetime (about 5,000 hours) of metallic pots, which stand as a source of secondary waste;
- the capacity of metallic pots (about 25 kg/h in the case of R7T7 glass), which requires several parallel treatment lines;
- dismantling difficulties for end-of-life metallic furnaces, as they account for a big volume of technological waste;
- a composition range limited to glasses with a glassmaking temperature of 1,150 °C both in metallic pots and the LFCM.

A new melting technology has been developed in order to cope with all these limitations. It is based upon the use of a cooled metallic crucible coupled with direct induction heating in glass (see “Cold crucible vitrification”, p. 67).

This technology makes it possible to reach higher melting temperatures (1,200-1,400 °C), thereby paving the way to the fabrication of new confining matrices. It is worthwhile to mention, for instance, the following matrices:

- a vitrocristalline matrix with 13 wt% molybdenum oxide, which was developed to confine solutions formerly used for UMo fuel treatment;
- new rare-earth-oxide-based glasses likely to allow for fission products incorporation rates up to 25 wt%, i.e., an almost 40% gain compared with current glasses.

The cold crucible technology also makes it possible to anticipate future evolutions of spent fuel treatment plants, and reach such goals as process simplification, operating cost reduction, and treatment of a wider range of waste, for example:

- sodic solutions of the LILW type, which can be processed with increased capacity using a simplified process based upon direct feeding of the solutions to the molten glass bath surface;
- chlorinated combustible organic waste which can undergo oxygen incineration together with ash vitrification. The process feasibility was demonstrated for combustible technological waste mixed with ion-exchange resins, resulting in the generation of reduced glass volume. A reactor waste treatment facility is under construction in Korea;
- combustible organic waste difficult to oxidize (e.g., highly loaded with ion-exchange resins), for which a compact process coupling a cold crucible and oxygen plasma torches was developed and tested on the SHIVA pilot facility (see “Plasma benefits for incineration/vitrification waste treatment. The Shiva process”, pp. 105-110).

**Roger Boën,**

*Research Department of Waste Treatment  
and Conditioning*



# Nuclear glass formulation, structure and properties

## Tailored glasses for various types of waste

Confining glasses are “tailored” materials, the chemical composition of which is adapted to ensure both their compatibility with the waste to be vitrified, and the optimization of their physico-chemical properties. These properties must be satisfactory, whether considering the molten state or the solid state. In the eighties a large-scale research program was carried out to characterize glasses for confining fission products arising from **UOX\*** fuel treatment. These so-called “R7T7” glasses have been produced at an industrial scale at the La Hague R7 and T7 workshops since 1989.

However, nuclear fuels are still evolving, with a general trend to extended in-pile residence time and burnup. Consequently, the solutions to be vitrified contain more **fission products** (FPs) and **minor actinides** (MA).

For instance, new-generation glasses are under development in order to confine FPs resulting from the treatment of high-burnup (45 GWe.d/t - 60 GWe.d/t) **UOX\*** spent fuels (Fig. 25).

Other developments aim at tailoring glass formulation to the new “cold crucible” vitrification process (see “Cold crucible vitrification”, pp. 67-70), so as to make it possible to confine high-level effluents from high-burnup fuel treatment as well as metallic (i.e., UMo) fuel treatment, or decontamination effluents from end-of-life plants.

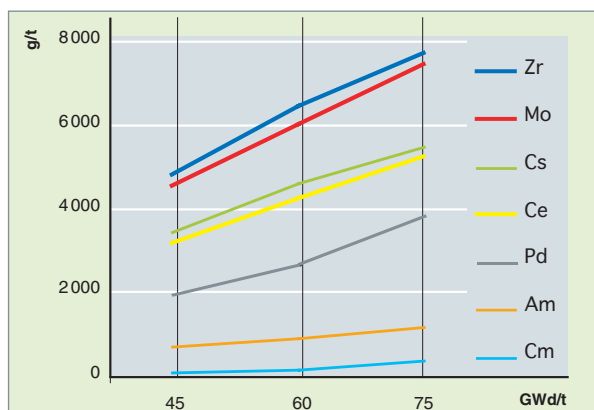


Fig. 25. Quantities of FPs and MAs (in gram) generated per tonne of initial uranium in UOX type fuels with an initial enrichment of 4.9 % <sup>235</sup>U, versus the burnup rate.

Determining the compositions of confining glasses always depends upon a compromise between three goals, i.e., the chemical flexibility of the glass, which must be able to contain about thirty chemical elements at least in its atomic-scale structure, the technological feasibility of vitrification, and the long-term behavior of the glass package, which must ensure radionuclide confinement.

Useful guidelines for glass formulation may be derived from the physico-chemical properties of the radwaste mixtures to be vitrified. The most important topics are the following:

- the solubility of the waste element oxides (Mo, Pu, Am, Np, rare earths, platinoids, etc.) in glass;
- the structure of fission products glasses;
- the **rheology\*** of glass melts;
- the chemical durability of glasses and their thermal stability (ability to withstand devitrification);
- electrical and thermal transport properties of these glass melts.

## Determining glass composition

After calcination FPs solutions are complex mixtures of oxides and nitrates. They do not contain any significant amount of glass-forming element oxide. Now, introducing FPs in an oxide glass can only be achieved through adding of at least two types of oxides:

- one aims at forming the glass network. The glass network former most often used is SiO<sub>2</sub>, or P<sub>2</sub>O<sub>5</sub> to a lesser extent. A second glass former such as B<sub>2</sub>O<sub>3</sub> is systematically added, for it can significantly increase the solubility of the waste element oxides such as molybdenum and rare earths.
- the other aims at modifying the glass network in order to increase its chemical flexibility to the various groups of chemical elements which characterize the FPs. The glass network modifier is an ionic oxide such as Na<sub>2</sub>O. The latter choice is often imposed by the very composition of the FPs solution, as the sodic solutions used for solvent cleaning or facility decontamination are mixed with FPs solutions.

A high-level nuclear glass thus consists of about 70-80 wt% inactive element oxides, the so-called “vitrification adjvants” (mostly  $\text{SiO}_2 + \text{B}_2\text{O}_3 + \text{Na}_2\text{O} + \text{Al}_2\text{O}_3$ , in the case of borosilicate glasses). This vitrification adjvant is introduced in the form of glass frit flakes.

Typically, high-level nuclear glasses manufactured at the R7 and T7 workshops confine FPs oxides up to 18.5 wt%.

The second part of the research program includes the addition of oxides with special characteristics to optimize glass formulation. Typically,  $\text{Li}_2\text{O}$  is added to increase the glass melt fluidity. Cobalt and nickel oxides can also be added to “blacken” the glass melt, in order to control the overall thermal conductivity<sup>1</sup> of the molten bath at the vitrification-process scale. This is of prime interest, indeed, for the technology of the cold-crucible fusion, which requires a bath thermal conductivity of 1-10  $\text{W.K}^{-1}.\text{m}^{-1}$ . At this step a so-called “reference” glass composition is selected.

As part of a parallel process, technological-scale vitrification tests are performed on an inactive industrial pilot unit with a view to determining the characteristics of the process. This involves characterizing the glasses made on this scale so as to validate the properties previously determined on the laboratory scale (i.e., on a few dozen or hundred grams of material).

Consistently the chemical and radiochemical nature of the waste to be conditioned stringently determines the incorporation rate in the glass matrix. For the atomic-scale insertion of the radioactive waste elements in the glass network is based upon the use of iono-covalent chemical bonds. High-temperature fabrication aims at getting a homogeneous liquid through chemical reactivity between the waste and the vitrification adjvants. Glass is finally produced through the molten bath quench, which involves the dissolution of the waste element oxides at high temperature in a silicate glass bath. The step of chemical reactivity between the constituents is of prime concern, indeed.

## Chemical reactivity during glass making

The melting process is a complex succession of chemical reactions, often in a thermodynamic non-equilibrium state, between the initial products. Several steps succeed, such as heating, primary melting, degassing, refining, and homogenization prior to melting into the final canister.

1. Too low a thermal conductivity means poor homogeneity in the molten bath temperature while too high a conductivity leads to too much significant thermal losses in the cold crucible.

In the special case of high-level borosilicate nuclear glasses, made through a reaction between a FPs calcinate and glass frit, the series of steps is the following (Fig. 26):

- the glass frit centimetric plates (a few millimeters thick) are turned discontinuously from the elastic solid state to the viscous liquid state, beyond the glass transition region around 510°C;
- the viscous frit impregnates the calcinate fragments, which consist of FPs nitrate- and oxide-type complex compounds. The calcinate is a highly refractory product, as it is rich in rare-earth oxides, zirconium, and aluminium. Crystals such as rare-earth silicates and cerium oxides, as well as chromites (mixed oxides of iron, zinc, and chromium) are formed as a result of localized oversaturations. This results in the formation of a heterogeneous product;
- the following step - the stirring of the mixture - dilutes the crystallized aggregates, which are then dissolved. The final glass becomes homogeneous in chemical composition. In this final step, only insoluble particles of noble metals remain, the size of which is about 10-100 micrometers.

As far as chemical reactivity are concerned, investigations are under way to evaluate the benefits of adding vitrification adjvants such as silica sand, sodium and calcium carbonates, and alumina. This vitrification technique has already been implemented abroad (USA, Japan, China, Russia) in the nuclear industry using high-capacity ceramic melters directly fed with liquid-phase waste. This method is based upon batch operation, which makes it possible to tailor the target final composition of glass. It proves to be especially adapted to the treatment of radioactive effluents showing high chemical variability, such as decontamination effluents from plants generally endowed with very rich sodium stores. This method is also highly flexible, and makes it possible to reach optimum waste loading rates in glass. It is noteworthy that glass frit has to be made through melting at temperatures lower than 1450 °C in order to limit volatilizations. For this reason it must contain alkaline oxides likely to decrease the melting temperature of glass forming oxides such as silica.

Investigations have been performed on the vitrification of the sodium-rich waste resulting from La Hague UP2-400 plant final shutdown (“MAD” in French, for *Mise à l'Arrêt Définitif*). The results show that the  $\text{Na}_2\text{O}$  content in glasses should not exceed about 20 wt%. For most glasses beyond this content display degraded properties in long-term chemical durability. In addition, a high  $\text{Na}_2\text{O}$  content of the effluent makes it difficult to calcine it due to the forming of phases with high adherence to the walls. Indeed, calcination can be controlled from the technological viewpoint using ( $\text{Al}_2\text{O}_3$ - and rare-earth oxide-based) clogging inhibitors. But the resulting drawback is a reduction in the waste loading rates in glass. As regards vitrification processes based upon direct liquid feed, adding vitri-

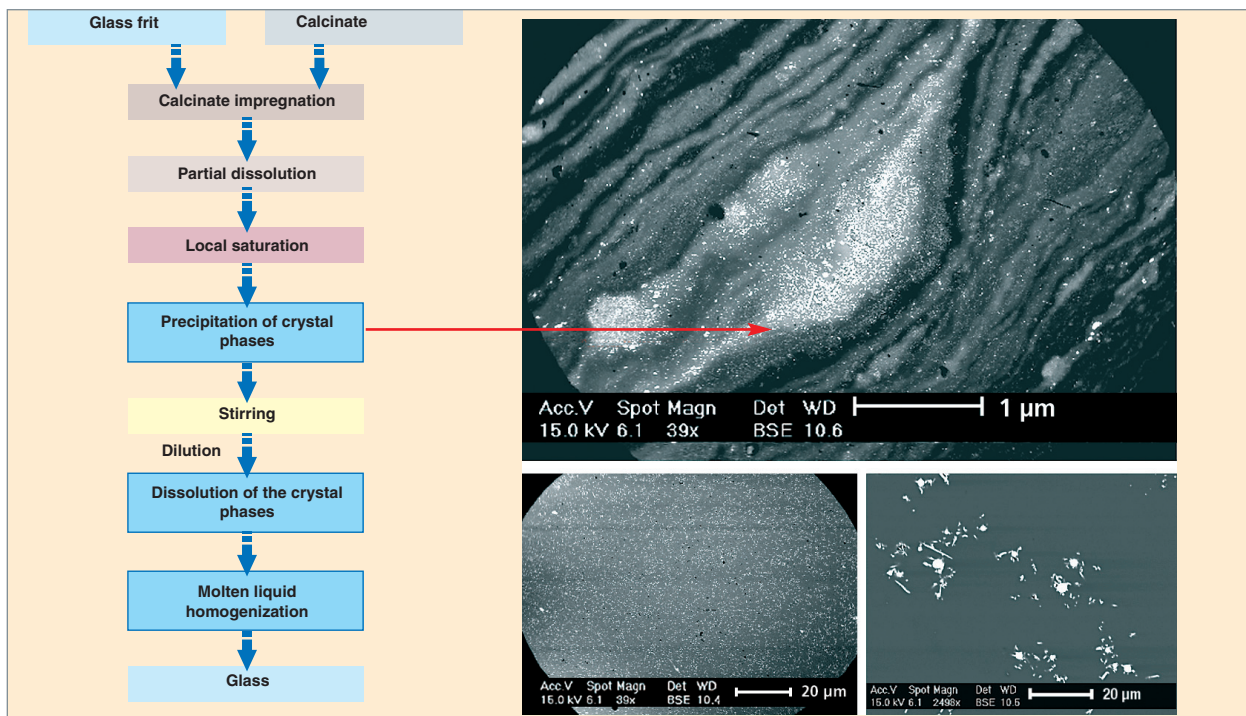


Fig. 26. Reaction steps as the fission products calcinate and glass frit come into contact at 1,100 °C. Glass photographs have been taken using a scanning electron microscope (the backscattered electrons highlight the contrasts in chemical composition).

ification adjuvants such as silica and sodium carbonates would significantly increase waste loading in glass (about 50%).

## Glass structure

Glass melt and glass properties depend upon the atomic ordering of the elements. The setting up of this structure is governed by local rules and medium-range constraints (radius, electric charge, negative electric charge property, field force...).

The cohesion of the oxide glass skeleton is ensured by the ionic-covalent chemical bonds which are formed by the glass network formers (Si, B, Al) in combination with oxygen atoms. One oxygen atom bound with two network formers is said to be “bridging”, whereas one oxygen atom bound with a single network former is said to be “non-bridging” (in French, ONP, for *Oxygène Non Pontant*: NBO, non-bridging oxygen). These bonds are oriented and take part in the formation of the tetrahedrons  $\text{SiO}_4$ ,  $\text{BO}_4$ ,  $\text{AlO}_4$ , and of the triangles  $\text{BO}_3$ . They coexist with the more strongly ionic bonds formed between the alkaline or alkaline-earth metals (Na, Ca), and the oxygen atoms.

The Na and Ca elements may play two distinctive roles within the glass network. They may either behave as charge-com-

pensators near a locally negative-charged  $\text{BO}_4$  or  $\text{AlO}_4$  type group, or they may behave as modifying elements, forming a  $\text{F—O—Na}$  or  $\text{F—O—Ca}$  bond (with F being a network former).

The atomic structure can be identified through various structural investigations of glass samples using such spectroscopic techniques as NMR, EXAFS, EPR, and optical spectroscopy. These studies demonstrate the high degree of polymerization displayed by FP confinement glasses. Indeed, all the glass network intermediate cations “M” (M = metallic cations of the Fe-, Al-, Zr-, U-, Nd-... type) occurring in the FPs behave as glass network “formers”: their substitution to  $\text{Si}^{4+}$ , the main glass network former, causes a charge loss which is compensated by a glass network modifying cation such as  $\text{Na}^+$ . That ensures the electroneutrality of the material. The numerous mixed  $\text{Si—O—M}$  bonds are formed during the step of high-temperature glass making. For instance, regarding R7T7-type glass, the balance of the negative charges produced by groups ( $\text{AlO}_4^-$ ), ( $\text{ZrO}_6^{2-}$ ), ( $\text{FeO}_4^-$ ), and ( $\text{BO}_4^-$ ) within the network was calculated to be 5.2 moles for 100 moles of elements (this calculation being based upon molar percentages of elements). As a counterpart, the balance of alkaline and alkaline-earth metals is 9.4 moles. This very difference accounts for all M-type intermediate cations being incorporated into the glass network as elements behaving like “network formers”.

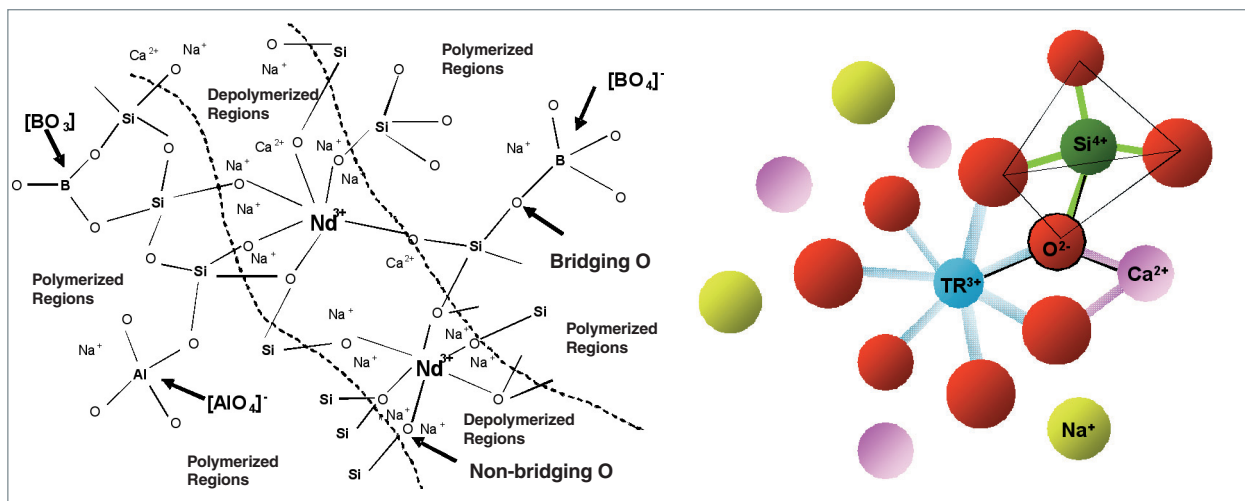


Fig. 27. Plane schematic view of the simplified glass network of rare-earth-oxide-rich glasses (from [1] and [2]). Detailed view of the arrangement of oxygen polyhedrons around the rare-earth and silicon ions. It is worthwhile noting the role of charge compensator played by the  $\text{Na}^+$  ions.

The incorporation of rare earth ions, high field force elements, within a borosilicate vitreous network, is boosted by the addition of  $\text{Al}_2\text{O}_3$ , alkaline oxides ( $\text{Na}_2\text{O}$ ), and alkaline earth metals ( $\text{CaO}$ ). The spectroscopic investigations (performed in collaboration with the ENSCP) have shown that rare earths prove to be cations endowed with an intermediate behavior between glass network formers and modifiers (see “Actinide solubility in glass”, pp. 45-47). They bind to non-bridging oxygen atoms (NBO), but remain localized in a neighbouring environment such as, typically bridging-oxygen- rich silicate.

To sum up it all, alkaline and alkaline earth cations play several roles within the vitreous network. First, they allow lanthanide ions to be incorporated in the neighborhood of Non Bridging Oxygens, which the partly help form, and they comensate for the local negative charge excess at the  $\text{Nd}^{3+}$ -ONP bonds in the depolymerized regions (RD, on Fig. 27). Secondly, in polymerized regions (RP on Fig. 27), alkaline cations preferentially compensate for the negative charge of units  $\text{BO}_4^-$  and  $\text{AlO}_4^-$ .

## Atomistic modelling of glasses: structure, physical properties, and quench effects

As previously seen, nuclear glasses mainly are silicate glasses which both contain alkaline or alkaline-earth-type network formers and modifiers. The too high complexity of a real nuclear glass (i.e., more than thirty constituents or so) makes it impossible to model it. Yet, atomistic simulation, and more especially classical molecular dynamics, have been used to reproduce nuclear glasses representative of actual glass.

Classical molecular dynamics method focuses on empirically reproducing the bonds between ions, with a view to simulating a glass structure representative of real structures. The basic principle of molecular dynamics is, first, to define interaction potentials which characterize force fields between ions. Molecular dynamics calculations are performed on several thousands, or even millions, of time steps for a given set of atoms. At each step, the forces applied to each atom are calculated and atoms are displaced accordingly. The dynamics of all the atoms can thus be reproduced step by step. The value of one time step is of the order of the femtosecond (10-15s), which ensures good accuracy in atomic path calculations. The algorithm used enables the whole of the structure to tend to a minimum potential energy, thus making it possible to make stable, crystalline, or **amorph**\* structures from an initial random configuration.

Iono-covalent and ionic interactions between the ions of an oxide glass are simulated by pair potentials, corrected with three-body angular potentials so as to incorporate the directionality of network former-oxygen iono-covalent bonds.

Pair potentials are of Buckingham type [3]:

$$\phi(r_{ij}) = A \exp\left(-\frac{r_{ij}}{\rho}\right) + \frac{q_i q_j}{r_{ij}} \operatorname{erfc}(\alpha r_{ij}) - \frac{C}{r_{ij}^6}$$

to be possibly completed with a  $1/r^3$  term. In other terms, the interaction energy between a pair of atoms i-j depends upon the distance  $r_{ij}$  between the atoms i and j, the charges  $Q_i$  and  $Q_j$  borne by these atoms, and adjustable parameters A,  $\rho$ ,  $\alpha$  and C. Figure 28 shows the example of Si-O pair interaction potential.

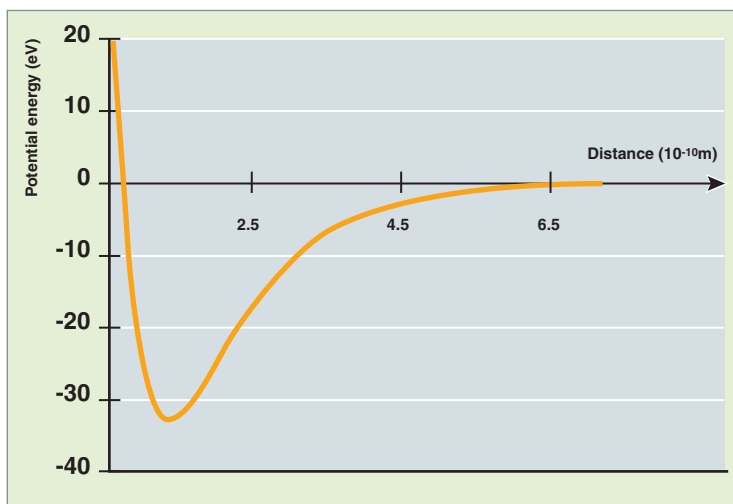


Fig. 28. Interaction potential of Si-O pairs as a function of the ion separation distance.

Three-body angular potentials take the following form (initially put forth by F.H. Stillinger and T.A. Weber [4]):

$$\phi(r_{ij}, r_{ik}, \theta_{jik}) = \lambda \exp\left(\frac{\gamma}{r_{ij} - r_c} + \frac{\gamma}{r_{ik} - r_c}\right) (\cos\theta_{jik} - \cos\theta_0)^2$$

A potential energy  $\phi(r_{ij}, r_{ik}, \theta_{jik})$  is coupled to an atom triplet j-i-k characterized by the two interatomic distances  $r_{ij}$  and  $r_{ik}$  and the angle  $\theta_{jik}$ .  $\lambda$ ,  $\gamma$ ,  $r_c$ , and  $\theta_0$  are adjustable parameters. These three-body potentials are applied to the triplets O-Si-O, Si-O-Si, O-Al-O, and O-B-O. The forces are the opposite of the interaction potential gradient with respect to atomic coordinates.

Once the interaction potentials have been defined, it is possible to make vitreous networks referring to a scheme which, though close to experimental methods, includes much higher quenching rates owing to computational times. For instance, we have investigated 4-, 5-, and 6-oxide glasses, the size and

Table 3.

Composition of simulated glasses in molar %						
	SiO <sub>2</sub>	B <sub>2</sub> O <sub>3</sub>	Na <sub>2</sub> O	ZrO <sub>2</sub>	Al <sub>2</sub> O <sub>3</sub>	CaO
4 oxides	67.3	17.7	13.2	1.7	-	-
5 oxides	64.1	16.8	13.3	1.8	4.0	-
6 oxides	60.1	16.0	12.6	1.7	3.8	5.7

compositions of which are given in Table 3. These simplified glasses include the molar ratios of R7T7 nuclear glass, and the more complex of them contains 65% of the R7T7 glass elements. [5]

The whole set of atoms is contained in a cubic simulation box containing 5,184 atoms, and subject to periodic conditions. This means that whenever an atom goes out of the simulation box, it is automatically re-injected by the opposite side. This method makes it possible to simulate pseudo-infinite systems with only a few thousand atoms.

Initially, the whole of the atoms is randomly positioned in the simulation cell. Then, a liquid is stabilized at high temperature in a 4,000-6,000 K range over about 20,000 time steps, each time step being equal to  $10^{-15}$ s. This liquid is then quenched to room temperature by steadily decreasing atomic velocities. As a final step, glass is stress-relieved so as to stabilize the vitreous structure at room temperature. Quench temperatures remain very high - around  $10^{14}$ K/s - contrasted with experimental velocities, owing to calculation times. Even with the most powerful computers, it is currently impossible to simulate "experimental" quenching rates.

As part of the quenching phase, the system progressively moves to a metastable state equivalent to a minimum value of the potential energy. This metastable state stands for a glass structure, i.e., a liquid structure progressively frozen following temperature decrease. Figure 29 shows a slice of such a structure. It is easy to pinpoint the various local entities surrounding the network formers, as well as their chains which constitute glass skeleton (see the tetrahedra SiO<sub>4</sub>, tetrahedra and triangles BO<sub>4</sub> and BO<sub>3</sub>...). Alkalis depolymerize the structure as they insert themselves into the vitreous network skeleton to open chemical bonds.

To put it in a nutshell, classical molecular dynamics method thus enables us to make glass structures the atomic positions of which are all known. However, this numerical model still has to be validated by proving its consistency with experimental data. The numerical structure can be characterized both statically, basing upon atomic positions, and dynamically, refer-

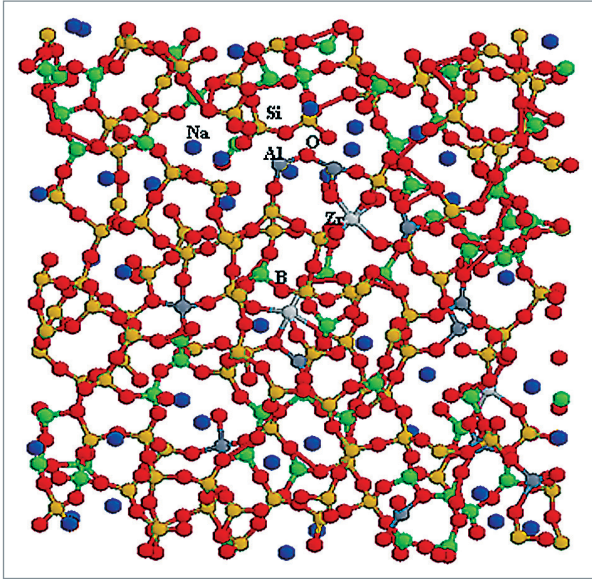


Fig. 29. A slice of a glass 5Å thick containing 5 simulated oxides. Si: gold, O: red, B: green, Na: blue, Zr: light grey, Al: dark grey.

ring to atomic motions. For the whole atomic dynamics is known for 10-100 picosecond intervals, through the successive positions at each time step.

It is difficult to characterize a glass at the experimental level owing to the lack of long-range order. Yet, short-range orders are accessible through such techniques as Nuclear Magnetic Resonance (NMR\*) or X-ray absorption spectroscopies (EXAFS\* or XANES\*). These techniques make it possible to determine first-neighbor distances and coordination numbers around elements.

It is also worthwhile to mention X-ray or neutron diffraction spectroscopies which provide data on intermediate-range order through structure factors.

As all the atomic positions in modelled glass are known, it is possible to calculate local coordination numbers and first-neighbour distances, as well structure factors.

A structure factor can be expressed as follows [6]:

$$S(Q) = \sum_{\alpha, \beta} W_{\alpha\beta}(Q) S_{\alpha\beta}(Q)$$

where  $S_{\alpha\beta}(Q)$  is the partial structure factor for element pairs

and

$$W_{\alpha\beta}(Q) = \frac{c_{\alpha} c_{\beta} \Re(f_{\alpha}(Q, E) f_{\beta}^{*}(Q, E))}{\left| \sum_{\alpha} c_{\alpha} f_{\alpha}(Q, E) \right|^2} (2 - \delta_{\alpha\beta}),$$

where  $c_{\alpha}$  and  $c_{\beta}$  are the atomic fractions of species  $\alpha - \beta$   $f_{\alpha}$  and  $f_{\beta}$  are the atomic diffusion factors for species  $\alpha - \beta$ ,  $Q$  is the diffusion vector, and  $E$  is the X-ray energy.

Each partial structure factor is weighed in the total structure factor by the atomic diffusion factors and the atomic fractions of each species.

Figure 30 shows the comparison between the simulated structure factors and the experimental structure factors for the 4-, 5-, and 6-oxide glasses. A few discrepancies can be pinpointed, especially in the shape of the first peak: a double peak emerges in the simulated structures whereas the experimental data display a single peak. Such discrepancies can be suppressed through finer structures using the so-called “reverse Monte-Carlo” method.

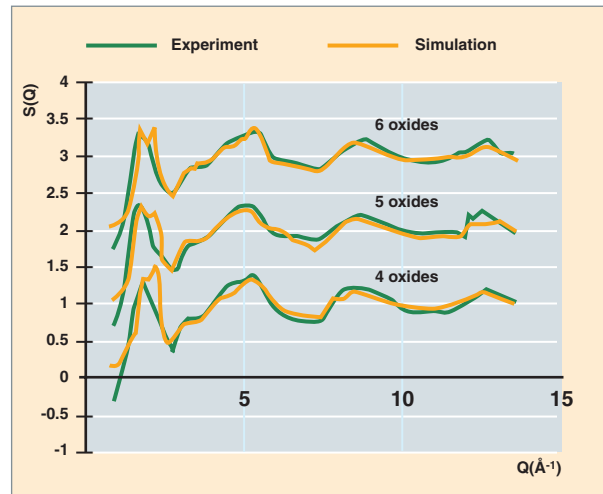


Fig. 30. Comparison between the measured (green) and simulated (orange) structure factors for 4-, 5- and 6-oxide glasses.

The “reverse Monte-Carlo” method [7] allows the simulated structure to be corrected through a series of atomic displacements so as to be fit to a set of experimental data. One atom is randomly selected and is moved in a similar random way over a distance of a few angström fractions. The structure factor is then recalculated. If the structure factor is improved comparing with the experimental reference, the atomic displacement is then maintained. In the opposite case, the atomic displacement is maintained, but the higher is the discrepancy between the simulated and experimental structure factors, the

lower is the probability of the atomic displacement. Consequently, the simulated structure can be corrected through a series of atomic displacements.

As regards 4-, 5-, and 6-oxide glasses, about 20,000 atomic displacements have been necessary to correct structure factors. Figure 31 shows the comparison between the structure factor obtained for the corrected atomic structure and the experimental structure factor for the 6-oxide glass. The resulting correspondence is now perfect. Similar results have been reached for 4- and 5-oxide glasses.

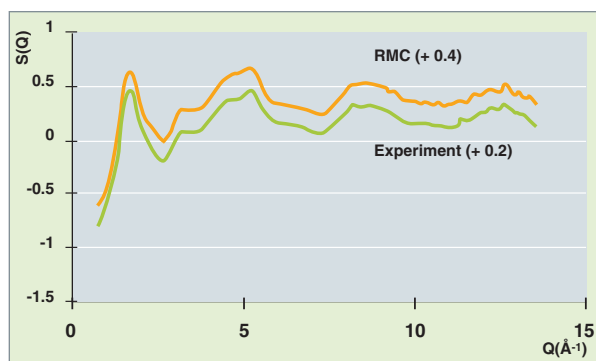


Fig. 31. Comparison between the real structure factor (green) and the structure factor simulated and corrected by the “reverse Monte Carlo” method (orange) for the 6-oxide glass. Actually the two curves are nearly superimposed. The above figure shows a slight distance between the curves for the mere purpose of differentiating them.

When focusing on the nature of the atomic displacements that proved necessary, it becomes obvious that the corrected environments chiefly are those of Na and A. Initially Na and Ca environments were not sufficiently ordered, i.e., they featured too high a dispersion in first-neighbor and coordination distances.

As a result, the benefit of the “reverse Monte-Carlo” calculation step proves to be twofold: on the one hand, the atomic structure was corrected in order to best reproduce the experimental structure factors, and, on the other hand, the interaction potentials Na-O and Ca-O were improved on account of the new atomic displacements required.

Local orders were analyzed on 4-, 5-, and 6-oxide glasses corrected by the reverse Monte-Carlo method. Tables 4 and 5 provide a comparison of first-neighbor distances and 4-coordinated boron atom percentages with data acquired by Nuclear magnetic Resonance. As can be seen, this resulted in a good correlation for first-neighbor distances and coordination numbers but for the 5-oxide glass: in the latter, the 4-coordinated boron percentage shown is too much high, contrasted with the experimental data. Yet, new measurements have been recently performed by Nuclear Magnetic Resonance and EXAFS

spectroscopy on a glass nearly identical to the 5-oxide glass: they exhibit 4-coordinated boron percentages respectively equal to 50% and 56%, i.e., closer to the simulated value. As a conclusion, there may have been a strong uncertainty in the first nuclear magnetic resonance spectrum relating to the 5-oxide glass.

Table 4.

Comparison of the first-neighbor distances in experiment and simulation.				
	Si-O	B-O	Na-O	Zr-O
Experiment	1.61Å	1.41Å	Between 2.29Å and 2.60Å	2.08Å
Simulation (5-oxide glass)	1.60Å	1.39Å	Between 2.20Å and 2.55Å	2.10Å

Table 5.

Comparison of the percentages of 4-coordinated boron atoms in experiment and simulation (after correction by the reverse Monte-Carlo method).		
	Simulation (reverse Monte-Carlo)	Experiment (NMR)
4-oxide glass	57.8	60.8
5-oxide glass	58.7	37.6
6-oxide glass	46.3	46.0

### Effects of quenching rates

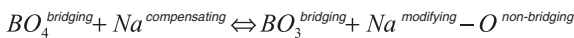
It is well known that the structure and properties of a glass depend upon its thermal history and, particularly, upon its quenching rate. This phenomenon can be quantified basing upon the concept of fictive temperature. This point is important for understanding the nuclear glass behavior under disposal or storage conditions, for the irradiation effect – especially that of  $\alpha$  disintegrations – could be much alike a quench effect. In this phenomenon, the core of each trace of recoil nuclei is locally melt – it must be stressed here that this melting is forced by the surrounding environment and that the liquid state formed probably does not have sufficient time to reach equilibrium –. Then, it is quenched again with a cooling velocity far higher than in the initial cooling used for glass making, owing to the very small size of the molten zone. Consequently, the initial structure prepared by quenching is progressively replaced by a structure which, area by area, will be quenched again far more rapidly.

Now, classical molecular dynamics can be used for investigating how a structure evolves as a function of its thermal history, confronting different quenching rates. Consistently, in parallel with the simulation of ballistic effects, a topic dealt with in the following pages (see “Long-term behavior of glasses”, pp. 51-65), several separate calculations have been performed on a

glass of composition 67.7% SiO<sub>2</sub> - 18.0% B<sub>2</sub>O<sub>3</sub> - 14.2% Na<sub>2</sub>O (molar percentages), focusing on quenching rates ranging from 2.10<sup>12</sup> K/s and 10<sup>15</sup> K/s. This series has been completed with a last structure, which corresponds to a liquid instantaneously frozen.

It is worthwhile to highlight that the quenching rate effect reproduces that of ballistic shocks: in the fastest quenching processes, the glass is slightly less polymerized (i.e., the number of non-bridging oxygen atoms increases) and the density is lower. Structural relaxations are limited with increasingly faster quenching, that contributes to keep glass in a slightly more disordered state.

As shown in Figure 32, the percentage of 3-coordinated boron atoms also evolves with the quenching rate. As the glass quenching rate increases, so does obviously the concentration in 3-coordinated boron atoms detrimentally to 4-coordinated boron atoms. In parallel, there is an obvious increase in the number of non bridging oxygen atoms and sodium atoms behaving as network modifiers. In the equilibrium expressed hereunder, the direct reaction is enhanced when the quenching rate increases:



Glass disordering process under the effect of an increasing quenching rate is a global effect which takes the form of a systematic broadening of distributions: angular distribution, ring size distribution, broadness of radial distribution function first peaks. Besides, an increase in the species mixing can be observed, and the concentrations of the various triplets of type F1-O-F2 (F1 and F2 being two network formers) come close to those of a homogeneous mixture.

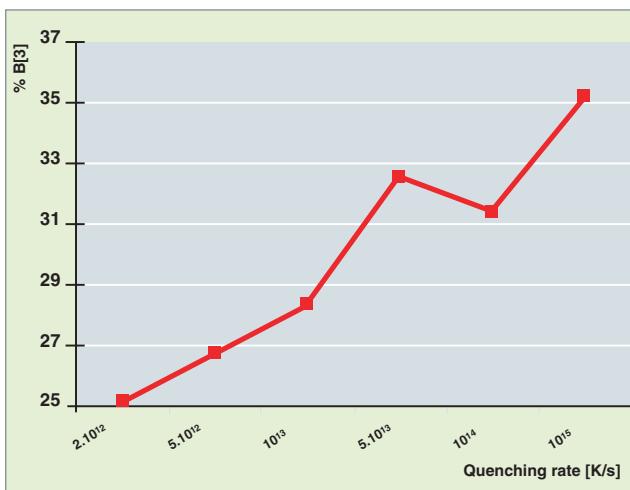


Fig. 32. Evolution of the average coordination number of boron atoms versus quenching rate.

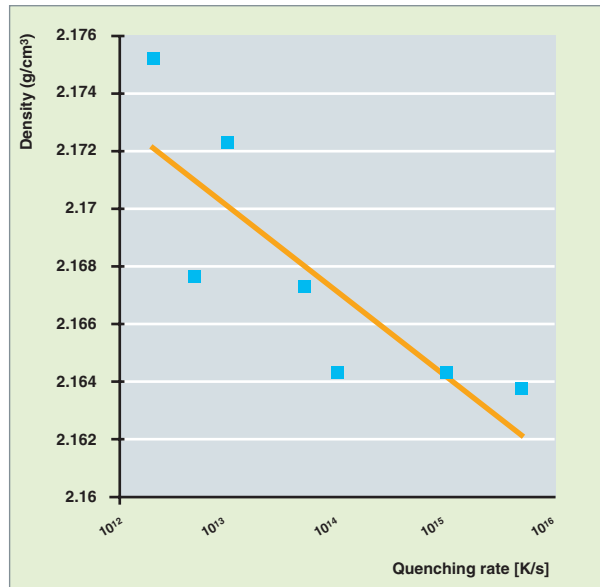


Fig. 33. The density of the glass of formulation 67.7% SiO<sub>2</sub> - 18.0% B<sub>2</sub>O<sub>3</sub> - 14.2% Na<sub>2</sub>O versus the quenching rate. By convention, the instantaneous quenching rate is 5 10<sup>15</sup> K/s.

Figure 33 shows how density evolves versus quenching rate. The structure depolymerization is coupled with a decrease in glass density. A similar phenomenon of coupled glass depolymerization/swelling was evidenced in the simulation of ballistic effects in glass structures (see “Long-term behavior of glasses”, pp. 51-65).

It may be hard to establish a direct relationship between experiment and simulation, because experimental quenching rates are far lower than simulated quenching rates. However, swelling phenomena observed under simulation conditions between slow and rapid quenching bear close resemblance to experimental swelling phenomena observed in ternary glass (67.7%, SiO<sub>2</sub> - 18.0% B<sub>2</sub>O<sub>3</sub> - 14.2% Na<sub>2</sub>O) following heavy-ion irradiation. Consequently, experimental swelling under irradiation could possibly be interpreted as a quenching rate effect. An additional factor in favor of this interpretation lies in the local quenching rates are around 10<sup>15</sup> K/s - 10<sup>16</sup> K/s, as shown through the analysis of atomic agitation within displacement cascades.

## How to optimize physico-chemical properties in nuclear glasses

The glass melt viscosity is a major parameter, since it has a deep impact on the feasibility of glass making in a melter. Too low a viscosity generally increases the corrosion rate of the furnace wall constitutive materials. It also enhances element volatility, as well as the sedimentation of little-solubility or refractory species at the bottom of the fusion pot. It may increase pouring times and affect the container filling rate.



As a general rule, the viscosity aimed for nuclear glasses ranges between 2 and 15 Pa.s at the glass-making temperature<sup>2</sup>.

Glass melt electrical conductivity is another major parameter, to be considered strictly in the case of electrode-heated ceramic furnaces and cold crucible melters heated by direct electromagnetic induction in the molten glass bath (see “Cold crucible: a promising technology”, pp. 67-70). For in these furnaces the melting energy is supplied by Joule effect, as electric current flows through the glass melt mass. Typically, glass electrical conductivity must range between 0.1 and 1 S/cm at the glass-making temperature. The electrical conductivity of an oxide glass melt significantly increases (see Table 6) when adding a small volume of insoluble RuO<sub>2</sub> particles [8]. Such an increase in electrical conductivity has a strong impact on the operation of Joule-heated melters. In a matrix of type SiO<sub>2</sub>-B<sub>2</sub>O<sub>3</sub>-Na<sub>2</sub>O with no RuO<sub>2</sub>, the alkaline transport is mainly responsible for ionic conductivity. Temperature dependence of conductivity can be thus formulated as a unique equation on the temperature range under consideration (from T<sub>g</sub> to the glass-making temperature). This equation stands for a microscopic model which describes sodium diffusion above and under the glass transition temperature T<sub>g</sub>.

In a glass-RuO<sub>2</sub> microcrystals composite, the ionic conductivity supplied by the matrix is completed with an electronic conductivity contribution for a RuO<sub>2</sub> critical volume percentage of about 1% in the case of spherical particles, or about 0.4% if RuO<sub>2</sub> is available as pins. The occurrence of dissolved Ru in the glass network, not exceeding a few dozen ppm, is a key factor of electronic conductivity.

Last but not least, the glass melt thermal properties (specific heat, thermal conductivity) are parameters to be monitored and optimized, through chemical composition, to ensure melter operation and optimum heat dissipation. At high melting temperatures heat is mainly transferred by radiation. The absorption properties of silicate molten glass lie in the wavelength range of 0.5-4 μm. Consistently, adjusting the thermal conductivity of a molten glass depends upon the nature and quantity of absorbing elements in this very range. Typically,

Table 6.

Values for the electrical conductivity of an UOx1-type borosilicate glass as a function of the RuO <sub>2</sub> ' volume fraction		
	σ(S/cm)	
	800 °C	1,100 °C
with RuO <sub>2</sub> as pins (1.3 vol.%)	5.6.10 <sup>-2</sup>	4.5.10 <sup>-1</sup>
without RuO <sub>2</sub>	1.0.10 <sup>-2</sup>	3.0.10 <sup>-2</sup>

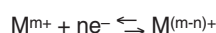
2. In the international system, the viscosity unit is the pascal second (Pa.s). One Pa.s = 10 dPa.s = 10 poises (CSG system unit).

adding Ni and Co oxides makes it possible to reach a molten glass thermal conductivity adjusted around 5 W.K<sup>-1</sup>.m<sup>-1</sup>, within the range of interest for the cold crucible melting technology. Now, the addition of platinoids proves to have a positive effect with respect to this property: at 1,200 °C, the conductivity of a glass with no platinoid equals 7 W.K<sup>-1</sup>.m<sup>-1</sup>, whereas it decreases to 4 with 2 wt% platinoids.

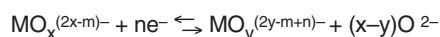
## Redox phenomena in glasses

Several chemical elements occurring in FP solutions can be stabilized in glass matrices under various oxidation states (Ce, Fe, Cr, Ni, Mn, S, Mo, Ru, actinides...). Taking into account element oxidation states aims at increasing the waste loading rate or improve the fabrication conditions.

In an oxide glass melt the solvent consists of oxygen ions. So the ratio of the reduced species to the oxidized species of multivalent metallic cation M<sup>m+</sup>/M<sup>(m-n)+</sup> is determined in relation with the couple O<sub>2</sub>/O<sup>2-</sup>. The redox half-equation of the couple M<sup>m+</sup>/M<sup>(m-n)+</sup> can be written as follows:



In order to take account of the oxygen environments of the oxidized and reduced forms of the couple, the system can also be written as follows, with a reference potential redox E<sub>OM</sub>:

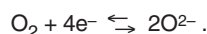


The redox potential is given by the Nernst formula:

$$(1) \quad E = E_{OM} + \frac{RT}{nF} \ln \frac{[MO_x^{(2x-m)-}]}{[MO_y^{(2y-m+n)-}]} + \frac{RT}{nF} \ln \frac{\gamma_{MO_x^{(2x-m)-}}}{\gamma_{MO_y^{(2y-m+n)-}}} - \frac{RT}{nF} \ln a(O^{2-})^{(x-y)}$$

where:

$\gamma_{MO_x^{(2x-m)-}}$  is the activity coefficient of the ion MO<sub>x</sub><sup>(2x-m)-</sup> in the glass melt, and  $\gamma_{MO_y^{(2y-m+n)-}}$  is the coefficient of the ion MO<sub>y</sub><sup>(2y-m+n)-</sup>. In equilibrium in the glass melt, the potential equals that of the couple O<sub>2</sub>/O<sup>2-</sup>, described by the following equation:



The couple O<sub>2</sub>/O<sup>2-</sup> is chosen as the reference for the redox scale of the glass melt:

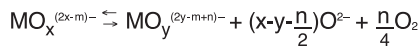
(2)

$$E = \frac{RT}{nF} \ln \frac{f_{O_2}}{a(O^{2-})^2}$$

where:

f<sub>O<sub>2</sub></sub> is the oxygen fugacity\* in the glass melt, and a(O<sup>2-</sup>) is the O<sup>2-</sup> ion reactivity\*.

The overall balance equation is then as follows:



The redox rapport  $\frac{Red}{Ox} = \frac{[\text{MO}_y^{(2y-m+n)-}]}{[\text{MO}_x^{(2x-m)-}]}$

is consistent with the following relation:  
(3)

$$\log \frac{Red}{Ox} = \frac{nF}{2.3 \cdot RT} E_{0M} - \log a + \left( y - x + \frac{n}{2} \right) \log a(\text{O}^{2-}) - \frac{n}{4} \log f_{\text{O}_2}$$

where  $\frac{\gamma_{\text{MO}_y^{(2y-m+n)-}}}{\gamma_{\text{MO}_x^{(2x-m)-}}}$  and  $E_{0M} = -\frac{\Delta G^0}{nF} = -\frac{\Delta H^0}{nF} + T \frac{\Delta S^0}{nF}$

Equation (3) highlights the major parameters which affect the redox state of glass melt:

- the glass melt basicity, or O<sup>2-</sup> ion activity;
- the oxygen fugacity in the glass melt, equivalent to the glass oxygen pressure, PO<sub>2</sub> (the glass melt being all the more oxidizing as fugacity increases);
- the temperature T (the redox equilibrium being shifted to reduced species as T increases).

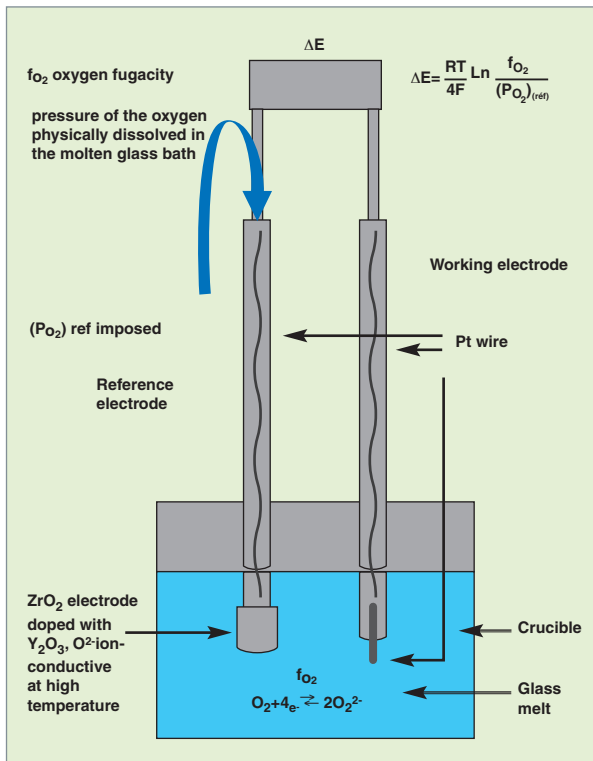


Fig. 34. Device for measuring the oxygen fugacity of glass melts.

Redox reaction mechanisms [9] could be identified through implementing specific electrochemical techniques to measure the redox state of glass melts (Fig. 34).

For instance, measuring the oxygen fugacity, f<sub>O<sub>2</sub></sub>, in glass melts, led to determining the characteristic potentials of the redox species couples as a function of temperature. Various redox couples were classified for borosilicate glass melts, defining a specific oxygen fugacity for each couple under consideration with respect to the oxygen fugacity of the glass melt:

$$\log \frac{Red}{Ox} = \frac{n}{4} (\log f_{carO_2} - \log f_{O_2})$$

After integration into equation (3), this results in the following equation:

$$\log f_{carO_2} = \frac{4F}{2,3 \cdot RT} E_{0M} - \frac{4}{n} \log \beta_M + \left( 4 \left( \frac{y-x}{n} \right) + 2 \right) \log a(\text{O}^{2-})$$

The physical meaning of this quantity is the following: it gives the value beyond which the oxidized form of a couple prevails in the glass melt:

- If log f<sub>O<sub>2</sub></sub> > log f<sub>car O<sub>2</sub></sub> then Red/O<sub>X</sub> < 1
- If log f<sub>O<sub>2</sub></sub> < log f<sub>car O<sub>2</sub></sub> then Red/O<sub>X</sub> > 1

Thermodynamical models coupling the redox ratios of glass multivalent species could thus be developed for the main multivalent species included in the confinement glass composition (Ce, Fe, Cr, Mn, S). Comprehensive models were also established for specific redox couples (Ce<sup>4+</sup>/Ce<sup>3+</sup>, Fe<sup>3+</sup>/Fe<sup>2+</sup>) basing upon electrochemical measurements [10]. Chemical compositions of glass melts can thus be improved basing upon these models.

For instance, it was demonstrated that cerium-rich waste incorporation rate increases with the reducing feature of glass melt. Moreover, some redox phenomena are intrinsically likely to generate foaming phenomena which are detrimental to the control of vitrification processes and glass final quality. For instance, glass melt foaming results from oxygen off-gassing, which takes place when cerium oxide Ce<sup>4+</sup> is reduced to cerium oxide Ce<sup>3+</sup> at high temperatures.



Understanding elementary processes made it possible to test several methods for redox ratio control in glass melts: adding oxidizing or reducing material, controlling the gases above the molten glass bath, modifying the temperature, and altering glass basicity. As shown in these investigations, adding oxidizing and reducing species proves to be the most suitable method for controlling redox conditions in glass melts on the radwaste vitrification process scale. A controlled redox glass frit was designed and successfully tested on the technologi-

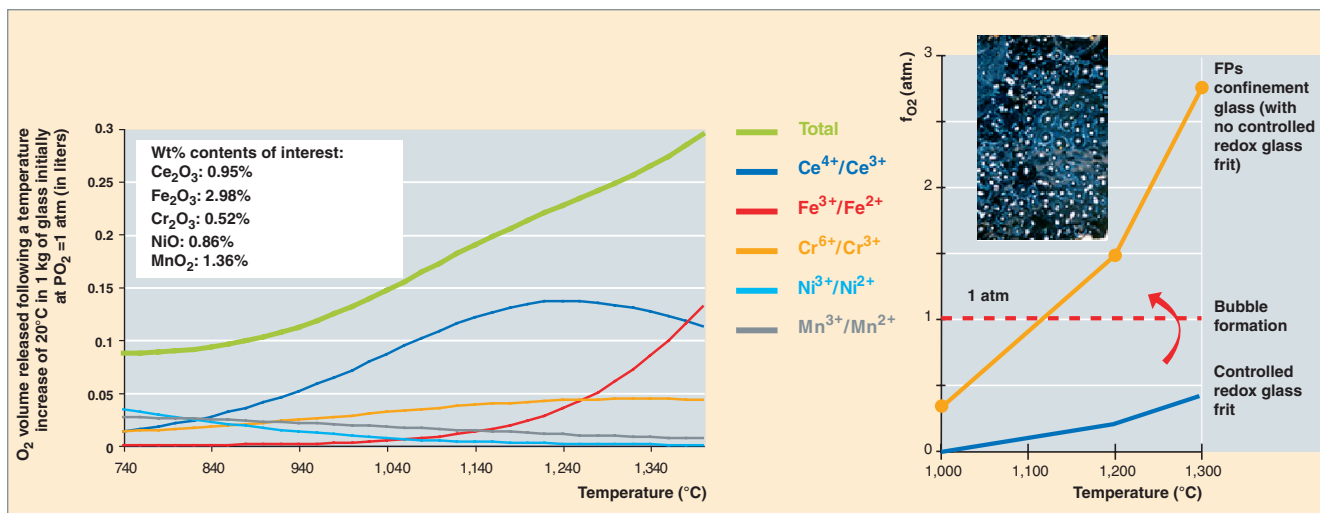


Fig. 35. Curves showing the gaseous oxygen release from a molten glass, in relation to the various redox couples present in a FPs glass (left). Evolution of the oxygen fugacity of the molten glass versus temperature (right).

cal scale in order to prevent glass swelling phenomena. In addition to providing glass-forming chemical elements, the controlled redox glass frit provides iron atoms under the reduced form Fe<sup>2+</sup> which turn into Fe<sup>3+</sup> by consuming the oxygen released through Ce<sup>4+</sup> reduction. This results in the suitable adjustment of the glass melt oxidation state to the desired values, thereby avoiding any foaming (see Fig. 35, left side).

Redox kinetics of multivalent species in glass melts is also investigated. For glass-making duration on the process scale may extend over several hours, thereby delaying equilibrium establishing. Evolution in time of glass sample redox at high temperature can be quantified through spectroscopic (XANES or RAMAN) analyses of the ratio of tracer elements such as Fe<sup>2+</sup> and Fe<sup>3+</sup> (collaboration with the IPGP). The prevailing mechanism was identified through comparing the diffusion coefficients specific of redox equilibrium establishment with those of the chemical species involved [11]. It is thus demonstrated that, at temperatures close to the glass transition temperature T<sub>g</sub>, redox kinetics is limited by the diffusive transport of divalent cations (e.g., Ca<sup>2+</sup>), whereas at higher temperatures the reaction kinetics is limited by the diffusive transport of ionic or molecular oxygen [12].

To sum up it all, for each glass composition range it can be found a redox couple suitable for oxygen pressure control in glass melt. A clever procedure may be incorporating it as additives (glass frit) into the mixture to be vitrified.

## Specific oxide solubility

Some elements in waste solutions to be vitrified make it difficult to obtain homogeneous glasses. Indeed, the glassmaking temperature plays a key role here. In most vitrification processes which have been implemented, the melting temperature is limited to 1,150 °C. Consequently, only combining with specific oxides can increase the incorporation limit into the glass network for some limited-solubility elements.

Glass melt homogenization is delayed by aluminium and cerium, available in high amounts (respectively more than 10 wt% and 1 wt% oxides). Oxide contents are generally limited as the glass frit/calciate contact time strictly depends upon the process. However, for vitrification processes at higher temperatures (1,200-1,300 °C), these solubility limits are increased.

Chromium tends to form nickel-, iron-, and zinc-based chromites (spinel) beyond an approximate 1 wt% oxide. It is not rare to find some again in the final glass, for only a temperature generally higher than 1,100 °C allows for these compounds to be dissolved in a glass melt. Consequently, increased solubilization of this element in a glass can be considered under the condition that the melting temperature of the mixture is higher than 1,200 °C.

Whatever the form of platinumoids when they are introduced into glass, they are finally dispersed as RuO<sub>2-x</sub> precipitates, and Rh and Pd-Te metal particles. The latter can be found as metal alloys with relatively low melting points (typically around 700 °C).

MoO<sub>3</sub> and P<sub>2</sub>O<sub>5</sub> oxides result in phase separations with contents higher than 2-3 wt%. The phenomenon of separation into two phases, one silicate-based and the other molybdenic or phosphatic, is triggered when the glass-making temperature drops to under a specified value. It is worthwhile to mention that the homogeneous distribution of a secondary vitreous or, possibly, microcrystalline phase may be tolerated provided that it does not entail deterioration of the confining matrix chemical stability, or its physical properties (resistance to irradiation). Such is the case of the “SPNM”-type glass which was developed to confine FP solutions highly rich in Mo and P. These FP solutions arise from the treatment of metal fuels consisting of uranium and molybdenum. As part of experimental work on a tailored glass matrix, three outstanding areas could be identified in a broad range of borosilicate-based composition (see Fig. 36). One of them results in a stratified material (Area 1), the other in a homogeneous glass (Area 2), and the third area in an opaque glass material consisting of separate microbeads uniformly distributed within an encapsulating borosilicate glass (Area 3). These microbeads are partially crystallized. They are formed during the cooling of the glass melt, which is homogeneous at high temperature. This composition area has been selected owing to its broadness, which allows composition changes even higher than in Area 2. In addition, Area-3 compositions feature high silica contents suitable for chemical durability.

In the glass matrix under investigation, the MoO<sub>3</sub> contents may go beyond 10 wt%. An example of glass composition determined in this research is given in Table 7.

This matrix is made by melting at 1,250 °C. Following the cooling step, it is characterized by a major vitreous phase encap-

Table 7.

Typical composition of a UMo glass (wt% oxides)	
	<b>SUMo 2-12-c</b>
SiO <sub>2</sub>	35.99
Na <sub>2</sub> O	8.79
B <sub>2</sub> O <sub>3</sub>	12.96
Al <sub>2</sub> O <sub>3</sub>	6.18
P <sub>2</sub> O <sub>5</sub>	3.69
MoO <sub>3</sub>	12.00
ZnO	5.62
ZrO <sub>2</sub>	7.14
CaO	5.67
Remainder	1.97

ulating secondary phases (the so-called “major encapsulating vitreous phase”) (Fig. 37). Its resistance to water corrosion is predominantly governed by the durability of this vitreous phase, which, all things considered, makes it very close to that of a homogeneous borosilicate glass.

Last but not least, the actinide solubilization in the borosilicate glass network plays a key role with respect to *alpha* decay processes. Understanding the rules which govern their dissolution within the glass network, can also help reach an industrial goal, in relation with higher-burnup spent fuel treatment.

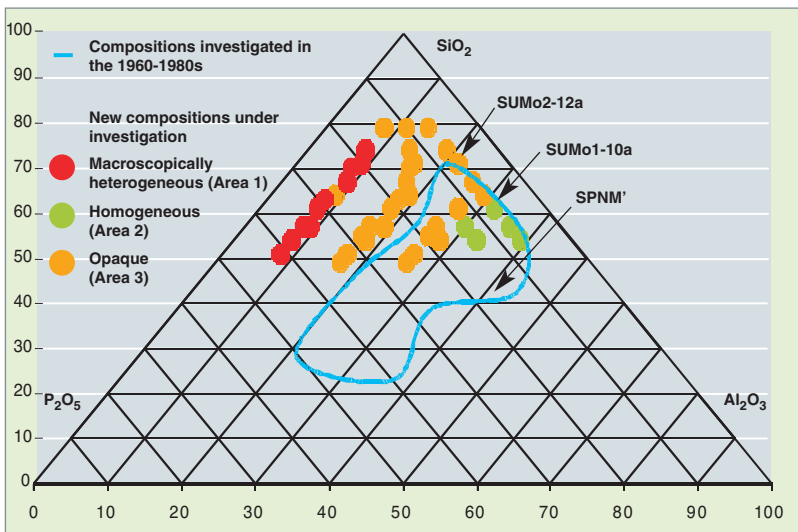


Fig. 36. Projection of the MoO<sub>3</sub>-rich glass compositions on the diagram SiO<sub>2</sub>-P<sub>2</sub>O<sub>5</sub>-Al<sub>2</sub>O<sub>3</sub> (wt%).

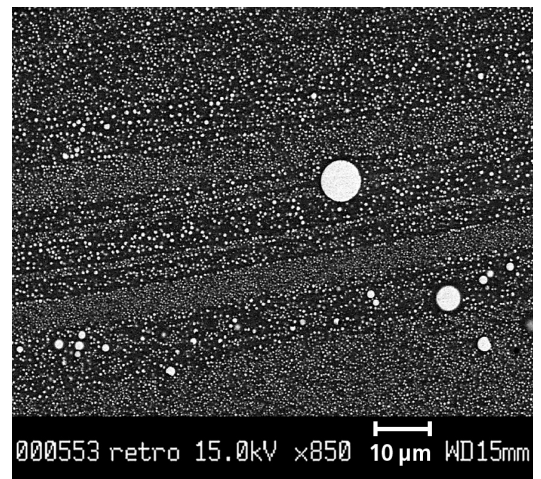


Fig. 37. Microstructure of the vitrocrySTALLINE UMo showing the dispersion of separate phases as MoO<sub>3</sub>-rich droplets in a glass including secondary phases (SEM picture of backscattered electrons).

## Actinide solubility in glass

Nuclear fuel burnup steadily increases, along with the actinide content in fission products solutions to be vitrified. This evolution raises new concerns over actinide solubility in glasses. Today, in contrast, the industrial borosilicate glass (R7T7) contains but very few actinide oxides (0.4 wt%) and these low contents result in a complete dissolution within the vitreous network, as was evidenced in the eighties in the fabrication of glass specimens doped with PuP<sub>2</sub>, AmO<sub>2</sub>, and NpO<sub>2</sub>.

An example of the results obtained regarding actinides is detailed in Table 8. The actinide incorporation limit varies depending on the glass composition and fabrication parameters (temperature, redox state). As regards multivalents (U, Pu, Np), modifying the redox conditions entails a change in the oxidation degree of the element of interest. The influence of this parameter is particularly drastic in the case of uranium, the incorporation limit of which is either 9 or 40 wt%, depending upon whether this element has an oxidation degree of (IV) or (VI). This singularity can be explained by the fact that the uranyl configuration (UO<sub>2</sub><sup>2+</sup>) allows uranium to form polymerized

chains within the vitreous network. A similar effect could be observed for neptunium in sodium silicate glasses. This element similarly develops an actinyl configuration, which causes its incorporation limit to increase from 19 to 33 wt% at 1,250 °C.

These fragmentary results have recently induced the CEA to undertake work in order to assess the true impact of fabrication parameters (redox conditions and temperature) on the incorporation limit of actinides and their simulants (hafnium and lanthanides) in borosilicate glasses. The local environment around the actinide or simulants has been investigated through various spectroscopies XAS\* and NMR\*.

### Apparent solubility: defining and measuring this quantity

The solubility limit of an element in a glass stands for the maximum concentration of this element that can be dissolved at a given temperature, as is the case in a liquid or a solid. Strictly speaking, this solubility should be measured at the glass melt making temperature. However, such measurement is not easy to achieve in these conditions owing to technical reasons relating to melting glass aggressiveness. Therefore, two methods are currently used to measure this quantity in the cooled glass at room temperature. The first one consists in measuring the concentration of the element under consideration by X micro-analysis in glasses which contain an excess amount of this element, i.e., displaying structural heterogeneities. The second method consists in determining emerging heterogeneous phases (crystallization or demixtion) through optical and electronic microscopy, gradually increasing the concentration of the element of interest. Solubility is then defined as the maximum concentration of the element of interest which can be incorporated in the the glass while preserving its homogeneous feature on the micrometer scale. It is this second method which has been used, because it is the most relevant in the context of confining matrices.

Whatever the method selected for measuring solubility, a challenge to be faced is reaching the dissolution thermodynamical equilibrium between molten glass and the compound to be dissolved. The difficulty to reach the equilibrium state originates in the high viscosity of the environment: about 8 Pa.s at 1,000 °C versus 10<sup>-3</sup> Pa.s for water at 20 °C. As shown by the results set forth in reference [6], which have been confirmed by the CEA's investigations, reaching the equilibrium between the species Ce(III) and Ce(IV) at 1,400 °C in a borosilicate glass takes about 60 hours. This relatively long duration is not compatible with such systematic laboratory experiments as those already performed. Besides, it does not account for the duration of industrial-scale vitrification, which is far shorter (about ten hours). This is the reason why a 3-hour duration was finally retained for the period of time when glass is maintained at the melting temperature. In addition, the concept of apparent solubility has been introduced, in contrast with thermodynamic

Table 8.  
Bibliographical data relating to the immobilization limit for U, Pu, Am, Cm, and Np in various glass compositions from References [13-14-15].

Incorporation limit of U, Pu, Am, Cm, and Np in various glass compositions.			
Glass type	Fabrication parameters	Actinide of interest (An)	Solubilité AnO <sub>2</sub> (% mass)
Borosilicate	1,150 °C	U(IV)	9
	1,150 °C	U(VI)	40
	1,200-1,300 °C	U	25-28
	1,100 °C air	Pu(IV)	0.55
	1,200 °C, air	Pu(IV)	<2
	1,500 °C, air	Pu(IV)	<10
	1,400 °C + graphite	Pu(III)	13<S<25
	1,000 °C	Am	2
	1,175 °C	Am	5
	1,000 °C, air	Np(IV)	2
	1,250 °C, air	Np(IV)	3
	1,350 °C	Np(III)/Np(IV)	>5
ATS (Alkali-Tin-Silicate)	1,150 °C	Pu	>5
LaBS	1,450 °C air	Pu	7<S<10
	1,500 °C	Pu	>11.4
	1,450 °C air	Am	0.1
Sodium silicate	1,250 °C, CO/CO <sub>2</sub>	U(VI)	19
	1,250 °C under air	U(VI)	52.7
	1,250 °C under reducing conditions	Np(IV)	19
	1,250 °C under oxygen	Np(V)	33
Phosphate glasses	1,100 °C	Pu(III)	2<S<10

solubility. This quantity allows for intercomparisons of the experiment results as regards the incorporation limit of the various elements investigated.

### Solubility of actinides and related simulants in borosilicate glasses

Glass composition is presented in Table 9. A simplified composition was used for the glasses made under reducing conditions, so as to avoid possible interactions between the multivalent elements (Cr, Fe...) occurring in glass with the multivalent couples investigated: Pu(III)/Pu(IV) or Ce(III)/Ce(IV). This composition contains the main elements of the complex glass and presents structural similarities with the latter as was shown through molecular dynamics. Each specimen, consisting of a few grams of glass, was manufactured through melting of oxide, nitrate, or carbonate precursors in platinum or zirconia crucibles. The actinides were added under the form of a nitric solution. The resulting slurry was heated and kept at the glass-making temperature during three hours. Then the glass underwent fast cooling in the melter in order to prevent any crystallization. Reducing conditions were obtained by adding to the blend to be vitrified a reducing compound, e.g., silicon nitride, as the melting was performed under argon atmosphere. Reversely, so-called "standard" conditions refer to glasses manufactured without any addition of reducing compound in air or under neutral atmosphere (Ar).

It is worthwhile to mention that Table 10 indicates the oxidation degrees known to exist in the glass elements investigated. As a general rule, apparent solubility increases with the glass-making temperature (Fig. 38). In addition, the trivalent elements (Gd, La, Nd) are endowed with an apparent solubility

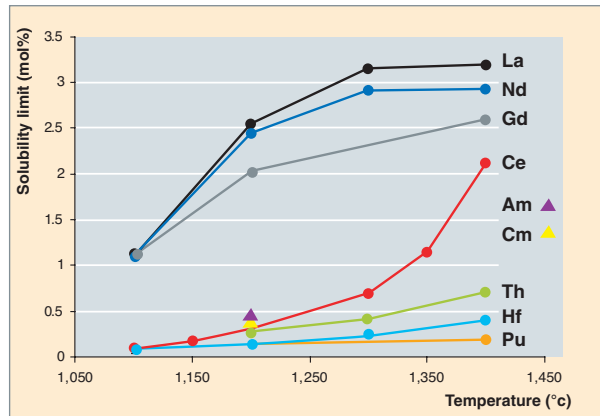


Fig. 38. Solubility limit of various elements versus temperature in borosilicate glasses manufactured under standardized conditions. The results reported for americium and curium stand for the highest content incorporated without reaching their limit of solubility.

much higher than their tetravalent counterparts (Hf, Pu, Th). The most significant increase in apparent solubility was observed in the case of cerium. This result accounts for the fact that this element is reduced to a trivalent state with the increase of the glass-making temperature. The apparent solubility of the multivalent elements increases with the varying redox potential of the environment.

In order to verify this postulate, glasses containing multivalent elements (Pu, Ce) were fabricated under reducing conditions, with addition of a reducing compound. Silicon nitride Si<sub>3</sub>N<sub>4</sub> was selected for this purpose among several families of reducing compounds (hydride, carbide, nitride), for its chemical and physical characteristics (melting temperature, density, chemical composition) are compatible with those of a borosilicate glass melt. The apparent solubility of cerium and plutonium proved to increase significantly when glasses were made under reducing conditions (Fig. 39). At 1,100 °C the apparent

solubility of cerium is multiplied by twenty; at 1,400 °C, that of plutonium is multiplied by 1.5 without reaching its limit of solubility. Experiment work with higher plutonium contents is under way to determine this limit. Plutonium and cerium reduction to the trivalent state was respectively evidenced by XANES\* spectroscopy and chemical analysis.

Table 9.

Nominal chemical composition of the borosilicate glasses under study									
(a) Complex composition (wt%)									
SiO <sub>2</sub>	45-46	Al <sub>2</sub> O <sub>3</sub>	5	Fe <sub>2</sub> O <sub>3</sub>	3	ZnO	2-3	SrO	0.3-0.4
B <sub>2</sub> O <sub>3</sub>	14-15	CaO	4	MoO <sub>3</sub>	2-3	CsO <sub>2</sub>	1	Rare-earth oxides	3-4
Na <sub>2</sub> O	10-11	Li <sub>2</sub> O	2	ZrO <sub>2</sub>	2-3	BaO	0.5-0.6	Other oxides	2-3
(b) Simplified composition (wt%)									
SiO <sub>2</sub>	59	Na <sub>2</sub> O	7	CaO	5.2	ZnO	3.2		
B <sub>2</sub> O <sub>3</sub>	18	Al <sub>2</sub> O <sub>3</sub>	4.3	Li <sub>2</sub> O	2.6	ZrO <sub>2</sub>	0.7		

Table 10.

In-glass oxidation degree of the actinides and simulants investigated in this research work										
U	Pu	Np	Am	Cm	Th	Ce	Nd	Gd	La	Hf
(III)	(III)	(III)	(III)	(III)	(IV)	(III)	(III)	(III)	(III)	(IV)
(IV)	(IV)	(IV)				(IV)				
(V)		(V)								
(VI)										

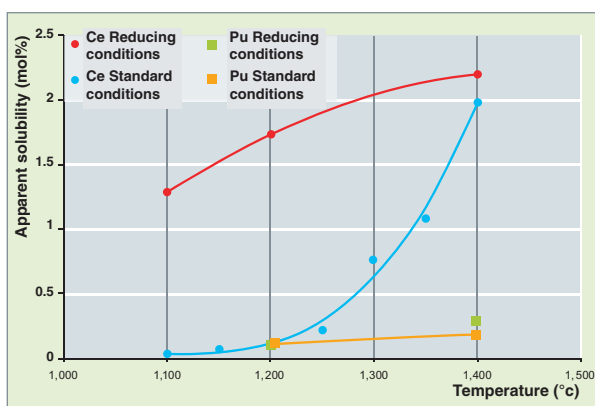
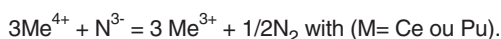


Fig. 39. Solubility limit of cerium and plutonium in borosilicate glasses as a function of the redox conditions and glass-making temperature.

The mechanism of cation reduction by the silicon nitride has not been clearly determined. Yet, bubble formation, which reveals a gas release, could be observed in glasses after cooling at room temperature. The reduction reaction proposed is thus as follows:



Though no action was taken to identify the nature of these gases, it appears that they could be nitrogen, as indicated in the previous reaction, or nitrous vapors NOx.

### The role of elements in glass structure as a function of their oxidation state

One of the possible approaches for investigating the role of the various elements in glass structure consists in measuring the characteristic quantities of the solubilized element local environment (length of the cation-oxygen bond, coordination number) by EXAFS\* analysis. These quantities were used to compute the field force parameter  $F = z / (d_{\text{Me-O}})^2$  defined by Dietzel [16] as the ratio of the cation charge  $z$  to the square of the cation-oxygen bond length. This parameter was used by Dietzel for classifying cations as a function of the field force value. To sum up it all, the network forming elements such as silicon or boron have a high field force ranging between 1 and 2 A<sup>-2</sup>. They make up the skeleton of the vitreous network by forming chains of polyhedra consisting of boron and silicon atoms surrounded with oxygen. Reversely, the network modifiers (alkalines, earth alkalines) have a low field force of 0.1-0.4 A<sup>-2</sup>. These elements cause the glass network to be depolymerized owing to the formation of non-bridging oxygen atoms. They also play the role of charge compensators between the network forming polyhedra. Intermediate elements can be found between these extreme values, which are either network formers or network modifiers depending upon the glass compositions under consideration. Now, the criteria defined by

Dietzel imply that the elements investigated (lanthanides, actinides, and hafnium) all have an intermediate role (Fig. 40). The same conclusions were drawn by Muller [13] as part of work relating to the electronic structure of the 5f orbitals in actinides and, more particularly, plutonium. The value of the field force parameter introduces an important difference between trivalent and tetravalent elements, which are respectively very close to network modifiers or to network formers. The results of the Si 29 analyses by NMR-MAS\* agree with this conclusion: for depolymerization of the glass network can be observed when incorporating a trivalent element such as lanthane, whereas no glass network evolution is revealed by this analysis when incorporating a tetravalent such as hafnium.

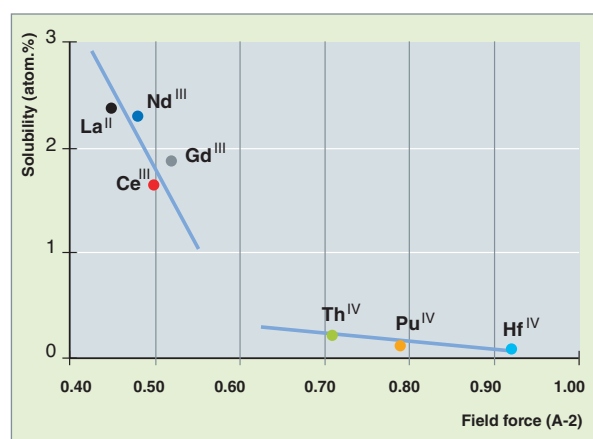


Fig. 40. Evolution of the apparent solubility versus the field force. The network formers (B, Si) have a field force higher than 1, whereas the network modifiers (Na, Ca, Li...) have a field force lower than 0.4.

As a conclusion, actinides and lanthanides have a similar structural role in the network of borosilicate glass used for nuclear waste conditioning. Technologically, this result raises the challenge of how going beyond the cumulated solubility limit of these elements with a view to advanced fuel treatment. Investigations are ongoing to verify the feasibility of vitrifying such FPs streams, especially with the option of reducing multivalent elements (Ce, Pu, Np) to the trivalent state in order to increase their solubility.

## Glass devitrification and thermal stability

Glass packages produced in vitrification workshops undergo a temperature rise due to a fraction of the energy arising from fission product and actinide decay. Typically, a R7T7 glass package of 150 L (400 kg of glass) has a specific thermal power of about 2 kW at the date of fabrication.

Concerns over the long-term thermal stability of the glass package make it necessary to define maximum admissible temperatures for glass and the environment. As stipulated in a basic safety rule (the so-called "RFS" III.2.b. article 2.6), *"the onsite storage of conditioned waste (glass canisters) shall be performed under conditions which guarantee that, in any circumstances, the core temperature is kept lower than the glass phase transformation temperature with a margin of at least 100 °C."*

Accordingly, a maximum temperature of 510 °C was determined for the R7T7 glass basing upon its crystallization characteristics. More generally, for each glass category, this temperature depends upon its chemical and radiochemical composition.

Thermal stability thus constitutes one of the prime criteria for confining matrix selection. It underlies the preservation of a homogeneous glass over time. Theoretically, glass may naturally evolve to a crystalline state thermodynamically more sta-

ble. But such transformation, thermally induced, gets dramatically slow (or even stops), when the glass is maintained at temperatures lower than the glass transition temperature ( $T_g$ ). Predicting thermal stability at low temperature and in the long term therefore requires experiments performed in supercooled liquids as well as modelling.

As regards nuclear glasses the main work in this field is that performed by X. ORLHAC [17], which helped confirm the R7T7 glass thermal stability in the very long term.

Devitrification experiments conducted on this glass made it possible to identify three major crystalline phases ( $\text{CaMoO}_4\text{CeO}_2\text{ZnCr}_2\text{O}_4$ ) and two minor phases (albite  $\text{NaAlSi}_3\text{O}_8$  and silicophosphate) between 630 °C and 1,200 °C. Yet, their crystallization remains limited (a maximum 4.24 wt%), for these phases consist of glass minor elements (Fig. 41). Even after a heat treatment resulting to a maximum crystallization (100 h at 780 °C), no change can be observed in the main properties of the nuclear glass (chemical durability and mechanical properties).

Plotting the nucleation and growth curves of these phases highlighted several essential points:

- nucleation sharply emerges during the first hours of the treatment, then stops beyond this period of time. Nucleation is heterogeneous, inducing crystallization on the already occurring active sites. Moreover, nucleation curves are strongly amplified and shift to lower temperatures in presence of platinoid insoluble particles;
- seed crystal growth is very low, and, after a few dozen hours, displays a saturation phenomenon;
- strong nucleation coupled with low growth globally leads to a material which can hardly be devitrified.

The stability of high-level R7T7-type nuclear glass at low temperature and in the long term was then investigated by modeling. The mathematical model selected is based on the KJMA theory (KJMA, for KOLGOMOROV, JOHNSON, MEHL, and AVRAMI), and describes the transformation kinetics as a function of time and temperature.

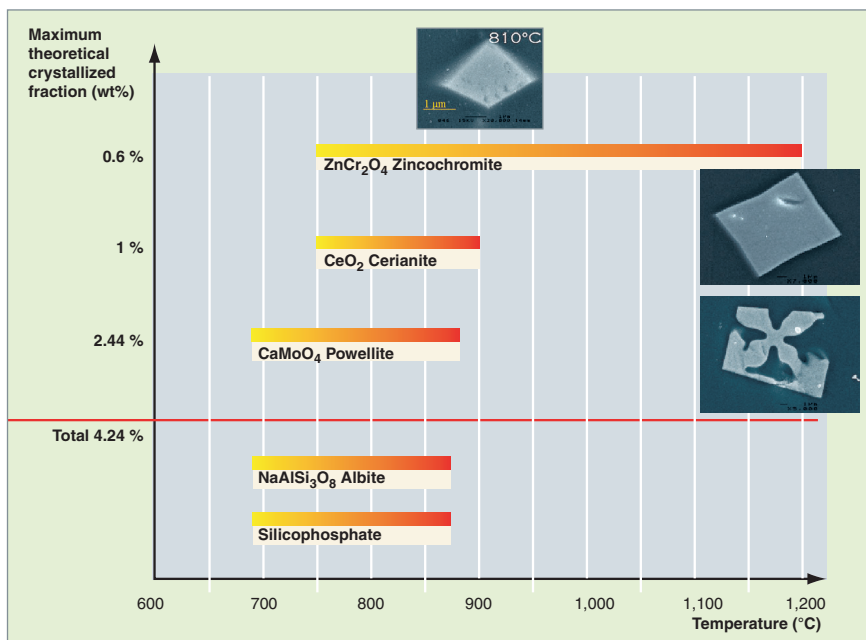


Fig. 41. Temperature range for the nucleation and growth of the main crystalline phases likely to be formed after a devitrifying thermal treatment of a borosilicate nuclear glass, which confines high-level effluents arising from UOX fuel treatment.



Atomic diffusion is the main factor which limits crystallization, as demonstrated by measuring the diffusion activation energy. Viscosity is therefore the key parameter which determines the nucleation-growth kinetics in glass: it is this very parameter which conditions diffusional atomic transport in the silicate-based liquid. Consistently, nucleation-growth kinetic processes can be determined by means of independent viscosity measurements in a broad range of temperatures.

The model validation was achieved under isothermal conditions on a simplified barium disilicate glass, known for its homogeneous, fast crystallization.

Applying this model to the R7T7 glass shows that periods of several millions of years are required for the three main phases to be completely crystallized. These results confirm the thermal stability of actual high-level waste confining glasses.

More generally, even if uncontrolled crystallization has of course to be avoided, it is noteworthy that crystallization is not absolutely an unfavorable phenomenon. It all depends upon whether its volume is significant and its distribution homogeneous, how radionuclides are localized among the various phases formed, and whether a chemically durable, residual vitreous phase has been preserved. Indeed, glass-ceramics materials may afford an innovating route to confine fluxes of radionuclides rich in elements of low solubility in glassy networks, provided that crystal nature, quantity, distribution, and physico-chemical stability are controlled and the residual vitreous phase is demonstrated.

## ► References

- [1] I. BARDEZ, "Étude des caractéristiques structurales et des propriétés des verres riches en terre rare destinés au confinement des PF et éléments à vie longue", Thesis, Paris VI University (2004).
- [2] A. QUINTAS, "Étude de la structure et du comportement en cristallisation d'un verre nucléaire d'aluminoborosilicate de terre rare", Thesis, Paris VI University (2007).
- [3] M.P. ALLEN, D.J. TILDESLEY, "Computer Simulation in Chemical Physics", Kluwer Academic Publishers, 1993.
- [4] F.H. STILLINGER, T.A. WEBER, *Phys. Rev. B* **31**, 5262 (1985).
- [5] L. CORMIER, D. GHALEB, J.-M. DELAYE, G. CALAS, *Phys. Rev. B*, **61** (2000), p. 14495.
- [6] A.C. WRIGHT, "Neutron and X-Ray Amorphography", Ch. 8, in *Experimental Techniques of Glass Science*, ed. C.J. Simmons, O.H. El-Bayoumi, *Ceramic Transactions* (American Ceramic Society, Westerville, OH, 1993), p. 205.
- [7] R.L. Mc GREEVY, *Nucl. Instrum. Methods Phys. Res. A* **354** (1995), p. 1.
- [8] C. SIMONNET, "Conductivité électrique des verres et fontes d'oxydes. Effet de l'incorporation de particules  $RuO_2$ ", Thesis, Montpellier II University (2004), CEA Report CEA-R-6048.
- [9] C. DINARDO, "Étude et contrôle des réactions d'oxydoréduction au cours de l'élaboration des matrices vitreuses de confinement des déchets nucléaires", Thesis, Montpellier II University (2003), CEA Report CEA-R-6029.
- [10] O. PINET, J. PHALIPPOU, C. DI NARDO, "Modeling the redox equilibrium of the  $Ce^{4+}/Ce^{3+}$  couple in silicate glass by voltammetry", *J. Cryst. Solids* **352** (2006), p. 5382.
- [11] V. MAGNIEN, D.R. NEUVILLE, L. CORMIER, J. ROUX, O. PINET and P. RICHER, "Kinetics of iron redox reactions: a high temperature XANES and Raman spectroscopy study", *J. of Nuclear Materials*, **352** (1-3), pp. 190-195, 2006.
- [12] V. MAGNIEN, "Étude cinétique des réactions d'oxydoréduction dans les silicates", Thesis, IPGP Paris (2006), CEA Report CEA-R-6118.
- [13] I. MULLER, W.J. WEBER (2001), *MRS Bulletin* **26-9**, p. 698.
- [14] C. LOPEZ (2002), "Solubilité des actinides et de leurs simulants dans les verres nucléaires. Limites d'incorporation et compréhension des mécanismes", Thesis, Paris XI University.
- [15] J.-N. CACHIA (2005), "Solubilité d'éléments aux degrés d'oxydation III et IV dans les verres de borosilicate. Application aux actinides dans les verres nucléaires", Thesis, Montpellier University.
- [16] A. DIETZEL (1942), "Z. Electrochimie", **48-9**.
- [17] X. ORHLAC, "Étude de la stabilité thermique du verre nucléaire. Modélisation de son évolution à long terme", Thesis, Montpellier II University (2000), CEA Report CEA-R-5895.

**Thierry ADVOCAT, Jean-Marc DELAYE,**  
**Sylvain PEUGET and Olivier PINET,**  
*Research Department of Waste Treatment  
and Conditioning*

**XAVIER DESCHANELS,**  
*Marcoule Institute for Separation Chemistry*



## Long-term behavior of glasses

In the case of a deep geological disposal for vitrified waste packages, underground water will come into contact with glass sooner or later, after corroding the containers and overcontainers. Now, glass matrix alteration by water is the chief factor likely to lead to the radionuclide release into the natural environment. It is still true, however, that the highly radioactive glass package undergoes self-irradiation, and irradiates the surrounding environment. As a matter of fact, the radioactive glass alteration by water depends upon this irradiation, at least in the two following ways. First, the radioactive glass irradiates the neighbouring underground water and generates potentially aggressive chemical compounds by radiolysis. Secondly, the glass network change induced by self-irradiation may a priori make the latter more vulnerable to alteration by water. Fortunately, as will be shown hereunder, these two effects are low, indeed.

### Nuclear glass alteration by water under disposal conditions

The mechanisms which control nuclear glass **leaching**\* kinetics are investigated taking account of environmental conditions. That allows to build computational models likely to be used for performance assessment of a geological repository, thereby verifying that its dose impact at the outlet remains below the authorized levels. These models have to be applicable to all the vitrified waste packages industrially produced, the chemical composition of which varies depending on both the manufacturing process and the fission products solutions to be vitrified (from the treatment of, e.g., the pressurized water reactor or natural uranium graphite gas reactor fuels).

Similarly to chemical element incorporation capacity or the industrial process feasibility, the composition effect on chemical durability is taken into account upstream at a very early stage, as soon as research work starts on glass compositions likely to confine a given type of waste (see "Nuclear glass formulation, structure and properties", pp. 33-49). This allows to give up early glass compositions likely to result in too fast alteration kinetics. This composition effect is then investigated more thoroughly in order to be integrated into models for long-term glass behavior. In the present contribution, the composition effects will be scrutinized referring to the several following approaches:

- the atomistic modelling of alteration;
- dependence of glass composition on the secondary-phase precipitation and renewed alterations;
- the dependence on the elements brought by the environment;
- using experimental matrices to determine by interpolation the alteration rate values over a whole industrial composition range.

#### Glass alteration mechanisms

Glass alteration is described in detail in the monograph "Corrosion". Whatever the glass composition may be, the different reactions involved are interdiffusion (proton - alkali ion exchange), hydrolysis (Si-O-Si bond rupture), dissolved species recondensation so as to form an amorphous alteration gel which constitutes a diffusive barrier between the glass and the solution, and the precipitation of secondary crystalline phases. By contrast, any of these reactions may be favored depending upon the glass composition (as well as the chemical species brought by the environment, and the solution renewal conditions, which will impact on the glass matrix alteration rate and, so, on the radionuclide release rate.

These reactions are structured as four simultaneous processes which are likely to be described in terms of kinetics:

- the oxide glass is turned into a porous, hydrated, hydroxide-type phase (the gel);
- this glass hydration reaction is limited by the water diffusion transport up to the reaction interface through the gel layer already formed: in other words; the gel has a passivating effect;
- the gel is dissolved on its external surface at a rate which is a function of the solution renewal conditions in the glass proximity;
- secondary phases precipitate, thereby consuming passivating-zone formers.

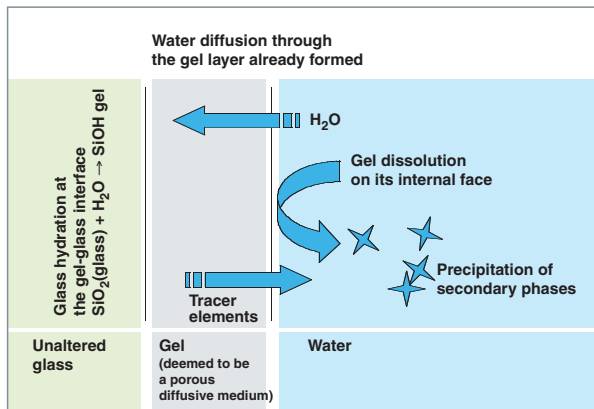


Fig. 42. The four processes involved in glass alteration.

These processes are sufficient to describe the various regimes of glass alteration rate:

- the “initial rate” is the easiest to measure: it can be observed when the prevailing reaction is hydrolysis and, first of all, only depends upon glass temperature, pH and composition;
- as regards the R7T7 glass, the “rate drop” is systematically evidenced in a closed system and in pure water: it is connected both with affinity effects (a decrease in the hydrolysis rate coupled with an increase in the concentrations in solution), and the forming of an alteration gel standing as a diffusive glass-solution barrier;
- the “residual rate” following the rate drop also includes the phenomena of gel dissolution and secondary phase precipitation; once established, this regime induces glass alteration at a steady rate. This rate may be very slow if the glass is placed in a soft environment (i.e. reduced flow of water in the vicinity of glass, and a quasi neutral pH).
- last but not least, the special cases when the alteration rate suddenly increases once a drop (or even residual) rate regime has been established, are called “renewed alteration” (or “alteration resumption”); this regime is coupled with high precipitation of specific secondary phases.

## Atomistic modelling of glass alteration mechanisms

The ingress of the aqueous species into the glass takes place both through exchange mechanisms between ions  $H^+$  and  $H_3O^+$  and the glass mobile elements as modifiers (mostly alkalis), and through molecular water diffusion. Simultaneously the glass network undergoes hydrolysis reactions through the water molecules which induce the opening of former – oxygen – former type bonds (with Si, B, or Al as the “former” atom). These atomic-scale reactions result macroscopically in the emergence of a gel - with an amorphous, porous and hydrated network -, and the more or less rapid change into solution of the various glass constitutive elements.

Two atomistic simulation approaches, the *ab initio* and “Monte Carlo” approaches, were implemented to give an insight into the atomic-scale mechanisms leading to gel hydrolysis, and to the macroscopic-scale mechanisms that govern the gel growth.

For example, performing *ab initio* calculations related to the interaction of a  $H_2O$  molecule with a glass network of type  $SiO_2 - Al_2O_3 - CaO$  made it possible to evidence the hydrolysis mechanisms of the Si-O-Si and Si-O-Al [1].

Contrary to the crystalline state, all the chemical bonds of type cation-O-cation in a glass are not equivalent. The local environment of the former cation strongly influences the hydrolysis energies of the cation-O bonds and, so, the final configurations following the reaction. Considering the simple glass under study, it appears that only some bonds Si-O-Si may favor a hydrolysis reaction from the energetic viewpoint. The final configuration then appears as two dissymmetrical silanol groupings (Si-OH) interconnected by a hydrogen bond between one of the oxygen atoms of a silanol grouping and the hydrogen atom of the second silanol grouping. This result explains why the number of silanol groupings in a hydrated glass starts increasing with the amount of dissolved water prior to stabilizing, with the water molecules in excess being left in a molecular state.

New results were acquired in relation to the hydrolysis of the Al-O-Si bonds. For example, the entity  $H_2O-AlO_3$  was evidenced and characterized structurally and energetically. In addition, all the steps of the protonation of a Si-O-Al bond were explored. As a first step, two silanol groupings Si-OH are formed, then a proton is fixed onto the Si-O-Al bond in order to form a protonated bond Si-O(H)-Al. For each of the previous mechanisms, i.e. the formation of  $H_2O-AlO_3$  or Si-O(H)-Al, a charge compensator of an Al atom is turned into a network modifier, and a nonbridging oxygen is formed (Fig.43).

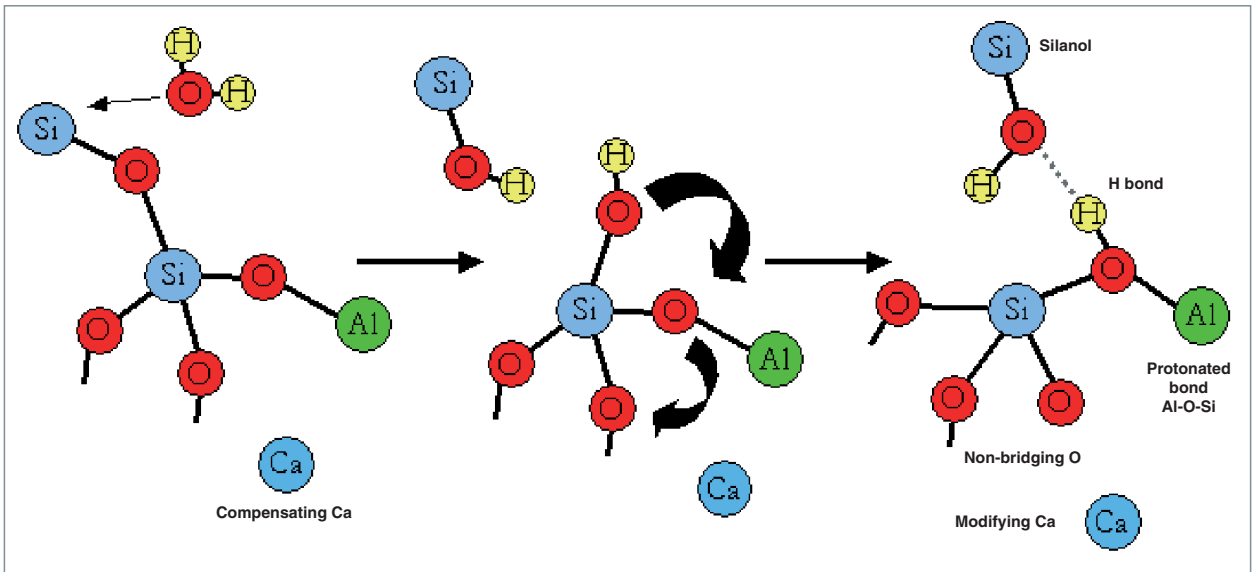


Fig. 43. Hydrolysis of a Si-O-Si bond, with the Si-O-Al bond protonation and the calcium change of state (conversion of compensating Ca to modifying Ca). In this very case, this is a concerted reaction.

A phenomenological model was put forth, referring to the basic mechanisms previously described. This model allowed to successfully reproduce the experimental profiles of H and Na concentrations for  $\text{SiO}_2 - \text{Al}_2\text{O}_3 - \text{CaO}$  on contact with a solution.

Lattice “Monte Carlo” calculations have been implemented at the CEA for several years in order to investigate the microscopic/macrosopic relationship and understand the gel role on glass alteration kinetics as a function of the glass chemical composition [2]. The glass is modelled in a simplified manner as a cubic lattice where some edges are deleted so as to reproduce the coordination number 4 of Si atoms and the coordination numbers 3 or 4 of B atoms (Fig.44). In this type of simulation, it is more important to comply with the coordination number of atoms and the hierarchy of the binding energies than with the network topology. Thus, selecting a crystal lattice means a significant gain in computational times without affecting the result. The modelled solid is contacted with an aqueous solution to simulate the hydrolysis/condensation mechanisms of the cations acting as network formers, a basic step in gel formation. This model has been recently improved so as to take into account the occurrence of 8-coordinated zirconium which behaves as a glass “hardener”, and that of calcium that may be either a charge compensator or a network modifier.

The reactivity of elements is defined by dissolution probabilities which depend upon the nature and coordination number of the atom under consideration, as well as a probability of recondensation which depends upon the concentration of species in solution. The model differentiates the soluble ele-

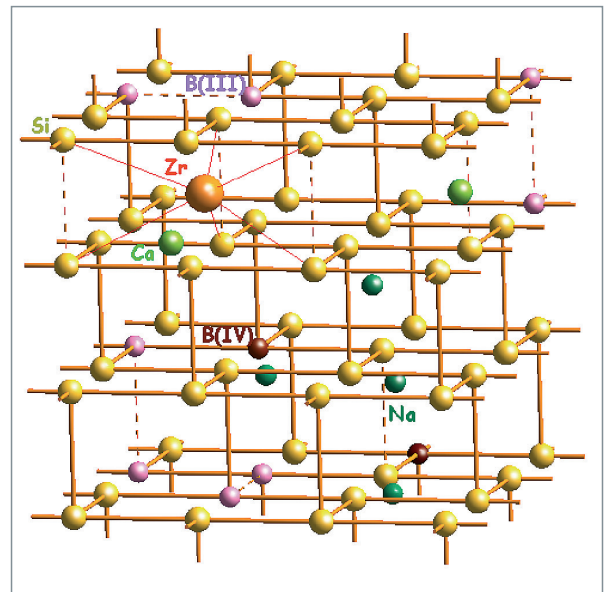


Fig. 44. Representation of the structure of the modelled glass used in the lattice “Monte Carlo” modelling.

ments (such as sodium or boron), which are systematically dissolved as soon as they meet a water molecule, and the hard-to-dissolve elements (such as silicon and aluminium), which have smaller dissolution probabilities and may condense at the glass/water interface. This method has the benefit of carrying out simulations over timescales similar to those of laboratory experiments and, so, to provide directly comparable results.

In the absence of Zr a silicate gel is very rapidly formed. This gel is, first, of small density and high porosity. The concentration of the dissolved Si, initially null, starts increasing, thereby speeding up the condensation phenomena. As a consequence, the condensation flux of silicon finally proves to com-

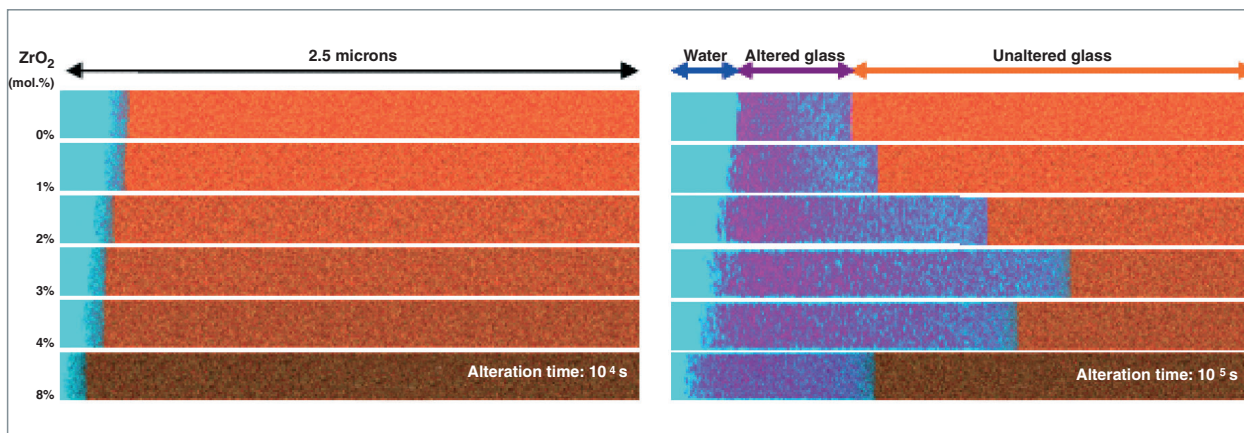


Fig. 45. "Monte Carlo" simulation of the alteration of 6 glasses of type  $\text{SiO}_2\text{-B}_2\text{O}_3\text{-Na}_2\text{O-CaO-ZrO}_2$ , the  $\text{ZrO}_2$  content of which varies from 0 to 8% (zirconium being a substitute for silicon) under initial alteration rate conditions (left figure) and after halting the alteration rate conditions (right figure). The longitudinal cutview of the glass shown in these figures highlights the gel alteration front and morphology. On these figures, water is shown in blue, silicon in red, zirconium in black, and boron in yellow. Such simulations make it possible to explain the nonlinear effect of zirconium upon glass alteration kinetics.

pensate that resulting from the silicate network dissolution, and the gel is densified and its pores are progressively shut. The gel alteration then comes to a halt, for no more exchange is possible with the solution. In real situations diffusion (not taken into account in this model) makes the drop in the glass alteration rate more progressive.

It is worthwhile mentioning, in addition, that the strongly nonlinear effect of Zr on the chemical durability of borosilicate glasses is very well predicted in the model (Fig.45). For high zirconium contents (8% in oxide moles), simulation highlights percolating paths which are the origin of alteration deep in the glass. Zirconium displays a hardening effect which limits the dissolution of neighboring atoms. This effect is favorable in so far as the initial dissolution rate of the glass is considered. Yet, it proves far less favorable in the long term, for Zr makes silicon condensation more difficult and, beyond a given threshold, prevents the gel porosity from being closed.

This mechanism, which had been observed experimentally, here finds an interpretation corroborated by simulation.

### Alteration gel and rate drop

Glass alteration rate drop originates in the alteration gel formed on the glass surface through recondensing of dissolved elements. This gel makes it possible to develop retention properties regarding some elements of the glass matrix, especially actinides. These properties may be influenced by the very structure of the gel, which itself depends on the chemical composition of the unaltered glass. Therefore it may be

useful to characterize the gel structure with respect to glass composition for better understanding of alteration mechanisms. Promising results have already been obtained on simplified glasses with NMR and SAXS, two structural investigation techniques.

Oxygen is the only element in oxide glasses whose nearest neighbours are both network formers and modifiers. Given this central position it is an ideal probe likely to be detected by oxygen-17 NMR after isotopic enrichment. Considering sodium calcium borosilicate glasses which contain zirconium and gels arising from the leaching of these glasses, investigations through O-17 NMR coupled with B-11 NMR have shown that calcium markedly remains in the alteration gel during alteration, either stabilized near non-binding oxygen atoms or behaving as a charge compensator of zirconium. The latter keeps the same coordination number as in glass. It rigidifies glass structure as it hinders silicon dissolution and reprecipitation, thereby slowing up the formation of a protective gel, which results in an increase of altered glass quantities.

Small Angle X-ray Scattering (SAXS) can be used to investigate the evolution over time of the porous texture of the gel formed during alteration. In some cases such studies make it possible to determine the pore size and the specific surface area developed by the gel. Investigating a series of simplified glasses containing Zr as a substitute for silicon has improved knowledge on the role of this element, of prime importance in long-term behavior. This study shows that smooth pores resulting from condensed silicon reorganization can be formed only if the content of hardening elements such as zirconium is not too high. As it highlights this fact and refers to alteration kinetics, it thus helps sustain the hypothesis that gel reorganization enhances the protective effect responsible for the rate drop. Such results are fully consistent with those from NMR and atomistic modelling studies.

### A phenomenon to be avoided: renewed alteration by zeolite precipitation

In some cases borosilicate glasses can be subject to renewed alteration (increase in glass dissolution rate as the glass is in a rate drop or residual rate mode). This phenomenon depends on glass composition and the geochemical conditions applied (pH, temperature, solution composition). In the case of the R7T7 glass, a pH sharply more basic than that imposed by glass - typically 11.5 at 90 °C- first slows down glass alteration rate due to the formation of a protective gel, as is traditionally observed at a lower pH. This step is followed with a renewed alteration after a few dozen days (Fig. 46). This renewed alteration results from the crystallization on the gel

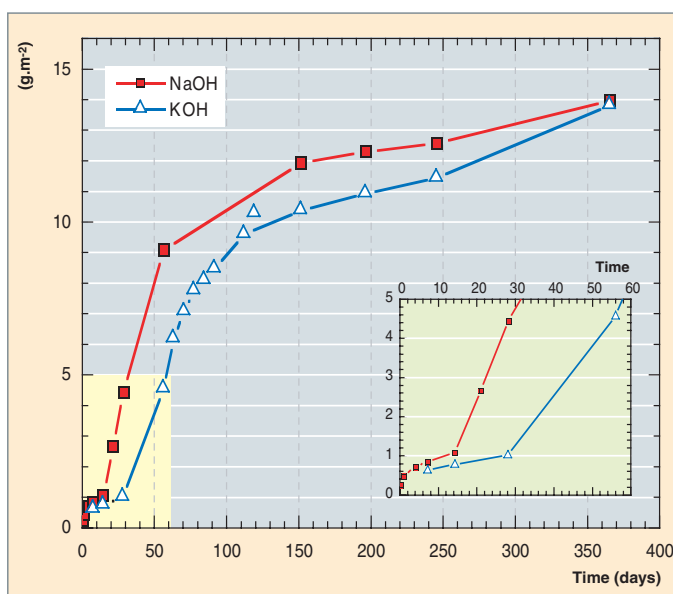


Fig. 46. Evolution of the altered glass quantities for a R7T7 inactive glass subjected to 90°C alterations in NaOH and KOH solutions with pH = 11.5. It can be observed in the 0-6 day zoom that renewed alterations do not occur at the same time. This is due to the formation of zeolites of various types.

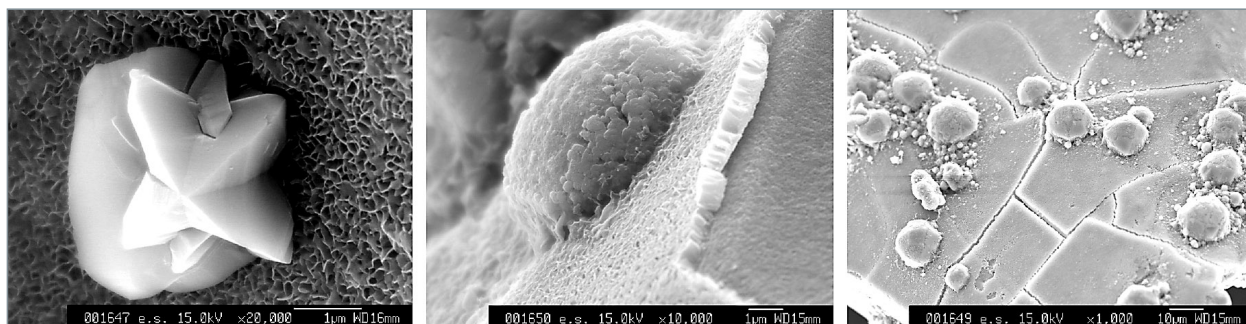


Fig. 47. SEM view of the inactive R7T7 glass altered at 90 °C, with pH 11.5 (NaOH), after (a) 14 days (x20,000) and (b,c) 91 days of alteration (x10,000). These pictures show the development of the analcime-type zeolites, responsible for alteration resumption phenomena.

surface of zeolite phases (analcime, merlinoite) (Fig. 47) which, as a first step, consume the aluminium in the solution, then the whole of aluminium and part of the silicon in the gel, thereby destabilizing the latter up to losing its protective character [3]. Delay of zeolite precipitation is attributed to a kinetic limitation at the nucleation step.

If the pH is not held at a very basic value, the system gets unstable, for significant boron release coupled with renewed alteration results in lower pH and zeolite dissolution. These investigations led to the conclusion that R7T7-type glasses in a geological disposal facility are not likely to undergo such brutal phenomena, for the pH conditions, aqueous species very slow transport, and the relatively low temperature cannot allow for a massive precipitation of crystallized phases liable to consume the gel elements.

A glass will be more or less liable to undergo renewed alterations depending upon, primarily, its chemical composition. For renewed alteration is more likely to occur with the two following factors: first, when the glass Al/Si stoichiometry is coming close to that of zeolites, and, secondly, when the glass composition tends to force a very basic equilibrium pH on the leachant. As evidenced in a past investigation on a hundred borosilicate glasses, there exists a pH threshold of 10.5 at 90 °C, so that glasses may be classified in two categories: those most likely or least likely to undergo a renewed alteration, depending on whether the pH is beyond or under the threshold. Therefore, as the glass equilibrium pH results from a balance between the so-called “basic” species (alkalis, alkaline-earths), the buffer effect species (boron), and the “acid” species (silicon), today it is possible to evaluate the risk *a priori* from the glass chemical composition alone. This approach was successfully applied in formulating ILW-LL-type glasses dedicated to the confinement of radionuclides occurring in decontamination effluents from nuclear facilities.

### Alteration dependence on the elements brought by the surrounding environment

It could be observed that some chemical elements had the same effect upon glass alteration rate, whether they are brought by the glass itself or by the environment. Such is the case, particularly, of calcium and magnesium.

As regards calcium, leaching experiments were performed on a series of 3-to-8-oxide simplified glasses with a stoichiometry similar to that of the R7T7-type glass. They highlighted the fact that the presence of calcium highly favors the alteration rate drop (Fig. 48) whereas its position as a network modifier

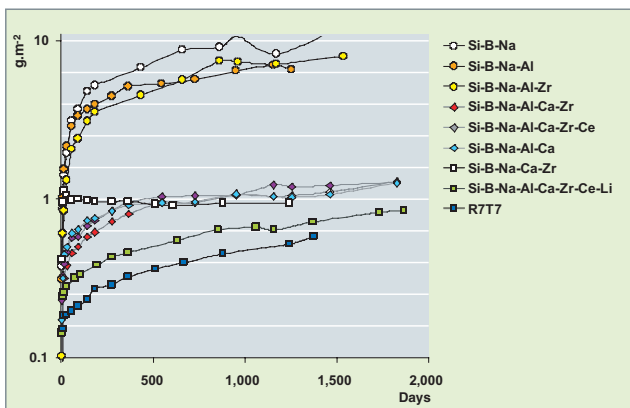


Fig. 48. Amount of altered glass versus time as measured on a set of 3-to-8 oxide simplified glasses with the same stoichiometry as the R7T7 glass. Alteration in the R7T7 glass is far lower than in simplified composition glasses. Occurrence of calcium in glass composition means decreasing the rate drop by one order of magnitude at least (considering experiments performed at 90 °C, with no water renewal, with initially pure water, and with a glass surface/solution volume of 80 cm<sup>-1</sup>).

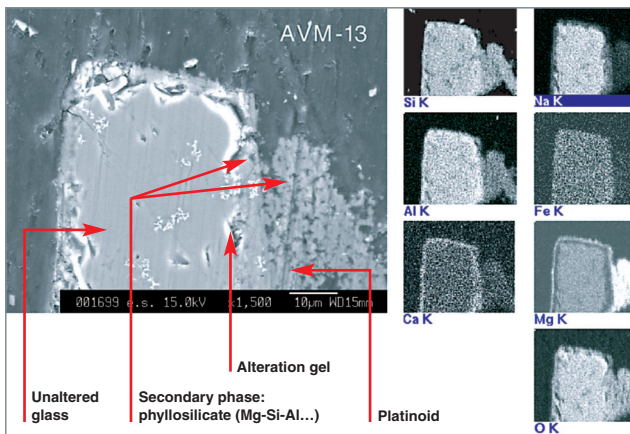


Fig. 49. SEM (x1,500) view of the alteration film on an AVM glass altered at 50 °C for one and a half year. As shown on the basic distribution maps, precipitated secondary phases appear significantly rich in magnesium.

generally makes it penalizing to the initial rate, highly sensitive to the polymerization degree of the silicate network.

Besides, as shown by leaching experiments on 5-oxide glass Si-B-Na-Zr with a calcium-bearing solution coupled with solid observations through TOF-SIMS, the solution calcium is integrated into the alteration gel and enhances its protective power. For, as a result of calcium addition, the diffusion coefficient of boron (an alteration tracer) in the gel is decreased by 3 orders of magnitude. The result is the same with calcium occurring at the very start of the gel alteration or if is added after a pure-water alteration step: in the latter case it is integrated into the gel already formed and improves its properties.

The magnesium case is symmetrical to that of calcium: the effect on alteration is still the same, whether magnesium is brought by glass or by the solution. However, although calcium and magnesium are relatively close from a chemical viewpoint, magnesium has a reverse effect compared with calcium: far from integrating into the gel and enhancing its protective power, it takes part in the precipitation of secondary-phases such as magnesian phyllosilicates: not only do these phases not act as a diffusive barrier between glass and the solution, but, moreover, do they tend to consume the gel-forming elements such as silicon, which degrades the gel properties all the more (Fig. 49). Taking the example of R7T7 glass, which does not contain magnesium, adding this element to the altering solution does increase the alteration rate (Fig. 50). Reversely, magnesium issued from the treatment of the natural uranium graphite gas (UNGG) reactor fuel is held responsible for the higher alteration rates in the (so-called “AVM”) resulting glasses as compared with the R7T7 glasses from the water reactor fuel treatment.

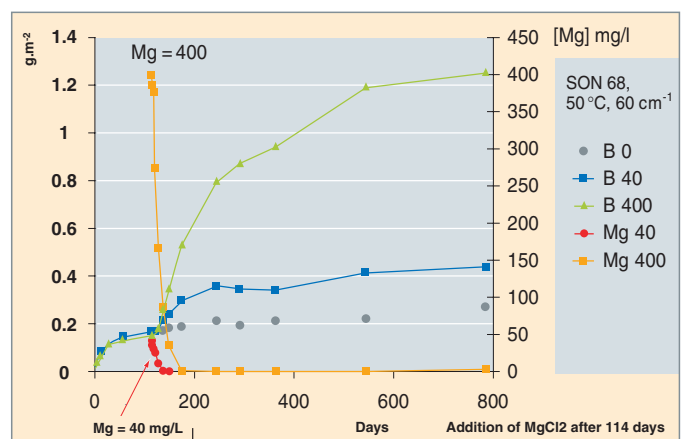


Fig. 50. Amount of altered glass (on the left axis, B0, B40, B400) and magnesium concentrations (on the right axis, Mg 40, Mg 400) versus time as obtained during the alteration of an inactive R7T7 glass, with 40 or 400mg/L of MgCl<sub>2</sub> added in the solution after 114 days of alteration. Adding magnesium to the solution entails a sharp resumption of the alteration (considering an experiment performed with no water renewal, at 50 °C, and with a glass surface/solution volume of 60 cm<sup>-1</sup>).



### Experimentation plans for studying glass alteration over a given composition range

The experimentation plan method is used when the study chiefly aims at characterizing a given composition range and applying to it the knowledge acquired on a well-characterized reference glass.

This method consists in defining the variables to be taken into account (chemical elements or groups of chemical elements), postulating a model which relates these variables to the data under investigation (e.g., the initial alteration rate or the solution pH), and building an experimental matrix which limits the number of experiments required to get all the model coefficients with the best possible accuracy. The behavior of a glass included in the composition range considered can therefore be obtained through interpolation of the results collected on the experimentation plan glasses.

This method is especially useful for investigating industrial glasses, in which some variation ranges in chemical composition are made necessary by the requirements of the glass-making process. However, due to the high complexity of these glasses (typically, an approximate thirty oxides), all the effects and interactions of the chemical elements cannot be exhaustively investigated (about 230 experiments would be required!). Therefore, a priori identification of the main elements and interactions to be considered is based upon more general knowledge acquired on the composition effect, which allows to "limit" the number of compositions to be investigated to about twenty or thirty.

Alteration rates observed during the leaching of nuclear glasses show several regimes: typically, e.g., for R7T7 type glasses in initially pure water, an initial rate regime is followed with a rate drop phase, then with a residual rate regime.

Exploring the composition ranges of industrial glasses (especially R7T7 and AVM) through experimentation plans made it possible to formulate simple statistical laws which couple the initial rate or the residual rate to main constituent contents in these glasses. For example, the empirical formula hereunder provides the value of the residual alteration rate at 50 °C for glasses in the R7T7 range with an accuracy of about  $0.2 \cdot 10^{-4} \text{ g}\cdot\text{m}^{-2}\cdot\text{d}^{-1}$  (considering an alteration in an initially pure and unrenewed water):

$$V_r (10^{-5} \text{ g}\cdot\text{m}^{-2}\cdot\text{d}^{-1}) = -261 \times \text{Si} - 1677 \times \text{B} - 431 \times \text{Na} - 359 \times \text{Al} + 61 \times \text{Fe} + 48 \times \text{FI} + 210 \times \text{FP} + 3207 \times (\text{Si} \times \text{B}) + 147 \times (\text{Si} \times \text{Na}) + 1513 \times (\text{Si} \times \text{Al}) + 602 \times (\text{Si} \times \text{Fe}) + 768 \times (\text{Si} \times \text{FI}) + 397 \times (\text{Si} \times \text{FP}) + 5389 \times (\text{B} \times \text{Na}) + 53 \times (\text{Na} \times \text{Al})$$

This formula expresses the weight content of the oxides corresponding with the 7 variables of the model - i.e. Si, B, Na, Al, Fe, fines (FI), and fission products (FP) - normalized to the sum of these constituents in the glass and expressed in per-

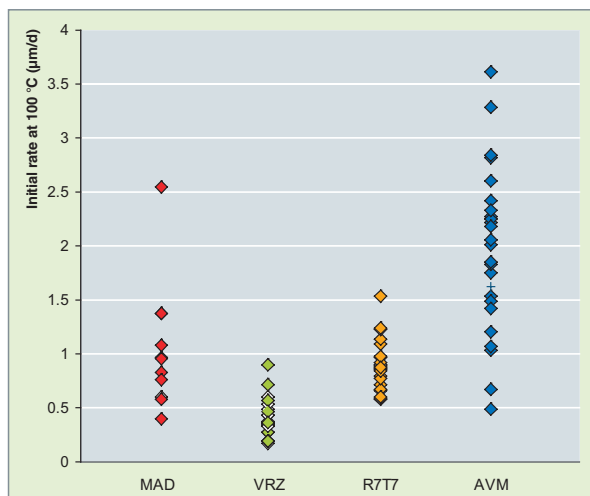


Fig. 51. Initial alteration rates at 100 °C in pure water for four composition ranges of borosilicate glasses (each dot stands for a given composition). MAD glasses are investigated with a view to ILLW conditioning; VRZ glasses are residual glasses from vitrocristallines which were candidate glasses for minor actinide specific conditioning; R7T7 and AVM glasses are industrial glasses respectively produced in La Hague and Marcoule plants. Comparing with the residual rate, the initial alteration rate is not very much dependent on glass composition.

cents. When applied to the reference glass R7T7, the model predicts a rate of  $0.45 \times 10^{-4} \text{ g}\cdot\text{m}^{-2}\cdot\text{d}^{-1}$  at 50 °C, in good agreement with the measurement.

Comparing the various composition ranges investigated highlights the following points:

- the values of the initial rates are of the same order of magnitude for all glasses, not only within a composition range, but also for all the glasses. They are approximately of a few  $\text{g}\cdot\text{m}^{-2}\cdot\text{d}^{-1}$  at 100 °C and with a pH of 7 (Fig. 51) and they increase with temperature and pH;
- reversely, the long-term rate values much depend upon the composition: some glasses display almost no rate drop whereas others, rich in Ca, Ti and Zr, show a null or quasi-null alteration rate in the long term.

These very values of alteration (initial and residual) rates, coupled with the fracturing rates of glass packages, are those which allow for lifetimes to be calculated for glass packages under disposal conditions. For example, for the whole of the R7T7 glasses in the specified composition range, operational models predict a lifetime of an approximate 300,000 years, which guarantees that doses released at the outlet of a disposal facility are far lower than the standards recommended by the safety authorities (the lifetime is defined as the time required for complete alteration of the glass matrix).

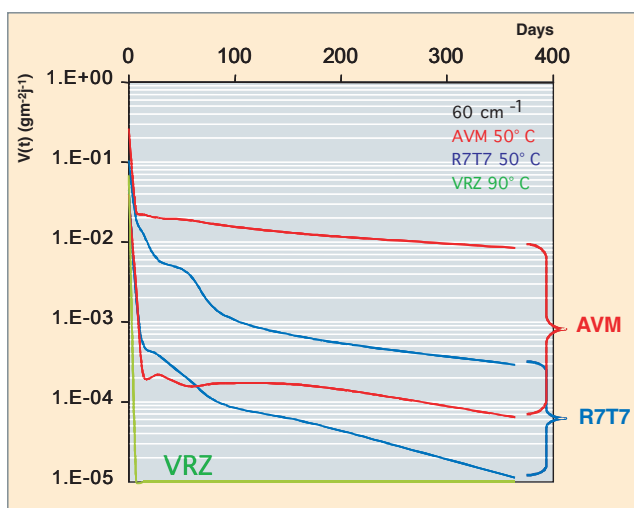


Fig. 52. Rates measured during the alteration of the glasses selected for the experimentation plans (R7T7, AVM at 50 °C, and VRZ at 90 °C for a S/V ratio of 60 cm cm<sup>-1</sup>). The curves shown hereabove are the envelope curves for the experimental curves obtained for the 25 glasses in each composition range. The residual rate is much dependent on glass composition.

### Glass alteration by water: conclusive remarks

The compilation of the data collected on hundreds of borosilicate nuclear glass compositions gives access to a good statistical representation of the composition effect on alteration rates in pure water for all composition ranges of industrial glasses. Besides, the role of major elements can now be interpreted: for example, a high silicon content is beneficial at all the steps of alteration; calcium increases the initial rate, but also favors the alteration rate drop as it integrates into the gel; oppositely, magnesium in the same conditions preserves high rates as it enhances the secondary phase precipitation; zirconium decreases the initial rate, but later on it slows down gel recondensation, and aluminium takes part in the fast precipitation of zeolites. For a high solubility due to a high pH (which may result from the alkaline content of the glass) and for a high Al/Si ratio, the zeolite formation contributes to gel destabilization, which induces high alteration rates.

The mechanisms involved in these composition effects are the same when the chemical elements are not issued from the glass itself, but from the alteration solution. These data can therefore be transposed to investigations on the environment dependence of alteration rates. In this case, however, one of the main factors is the element stream likely to be brought in or out by the environment. Therefore, these investigations will require a significant work of chemistry-transport coupling.

Last but not least, in parallel to studies on glasses of nuclear interest, laboratory works carried out on natural or man-made old silicate glasses have opened the way to concept generalization. Despite notable composition differences, water alteration mechanisms in all silicate glasses seem likely to be generalized (interdiffusion, hydrolysis, condensation, and secondary phase precipitation), and so it is of the related kinetic regimes (initial rate, rate drop, residual rate). Specimens of well characterized basaltic glasses or obsidians as well as Roman glasses weathered since the ancient times are used to validate the predictive models which help evaluate the performance of nuclear glass packages under disposal conditions.

### Glass resistance to self-irradiation

High-activity nuclear glasses aim at long-term confinement of most of the radioactivity of the waste arising from the nuclear industry. This is achieved through incorporating radioactive atoms into the glass network. These elements are by nature unstable and therefore spontaneously decay into other nuclei, which release energy in the glass as electromagnetic waves and charged particles in motion. Ensuring a good confinement of these elements in the long term requires evaluating the potential impact of this self-irradiation on the glass intrinsic properties.

#### Nature and origin of the various radiations likely to affect glasses

The main irradiation sources in nuclear glasses originate in:

- the  $\alpha$  disintegrations issued from minor actinides, especially Np, Am, and Cm, which result in the emission of two charged particles, a light helium nucleus (He), and a heavy recoil nucleus (the daughter in the disintegration chain);
- the  $\beta$  disintegrations issued from the fission products (FPs), which result in the emission of an electron or a positron and of a low-energy recoil nucleus (the nuclear daughter in the disintegration chain);
- the  $\gamma$  transitions coupled with  $\alpha$  and  $\beta$  disintegrations, which result in the emission of photons;
- and, to a lesser extent, ( $\alpha, n$ ) reactions, spontaneous or induced fissions, and ( $n, \alpha$ ) reactions the most frequent of which is reaction  $^{10}\text{B} (n, \alpha) ^7\text{Li}$ .

These different types of particles or radiations release their energy by interacting with glass atoms in two types of processes, i.e., inelastic interactions (electron excitations, ionizations), and elastic interactions (ballistic events likely to move the glass atoms).

Table 11.

<b>Characteristics of the various radiation sources in nuclear glasses</b> (the number of disintegrations per gram refers to the R7T7 glass used for vitrifying solutions arising from the treatment of PWR spent fuels with a 33GWd/t burnup).						
Radiation sources	Path in the glass	Energy deposited (Gy)		Number of atomic displacements per event	Number of disintegrations per gram of glass over 10 <sup>4</sup> years	Number of atomic displacements per gram of glass over 10 <sup>4</sup> years
		over 10 <sup>4</sup> years	over 10 <sup>6</sup> years			
<b>α disintegration</b>						
Helium ion (4 to 6 Mev)	~ 20 μm	~ 3.10 <sup>9</sup>	~ 10 <sup>10</sup>	~ 200	~ 3.10 <sup>18</sup>	~ 6.10 <sup>20</sup>
Recoil Nucleus (0,1Mev)	~ 30 μm	~ 6.10 <sup>7</sup>	~ 3.10 <sup>8</sup>	~ 2,000		~ 6.10 <sup>21</sup>
<b>β disintegration</b>	1 mm	~ 3.10 <sup>9</sup>	~ 4.10 <sup>9</sup>	~ 1	7.10 <sup>19</sup>	7.10 <sup>19</sup>
<b>γ transition</b>	qqs cm	~ 2.10 <sup>9</sup>	~ 2.10 <sup>9</sup>	~ 1	2.10 <sup>19</sup>	~ 2 10 <sup>19</sup>
Reactions (α, n)	1 m	~ 2.10 <sup>2</sup>	~ 9.10 <sup>3</sup>	200 to 2,000	3.10 <sup>12</sup>	6.10 <sup>14</sup> to 6.10 <sup>15</sup>
Spontaneous and induced fissions	FP : 10μm	~ 2.10 <sup>4</sup>	~ 4.10 <sup>4</sup>	10 <sup>5</sup>	10 <sup>11</sup> to 10 <sup>12</sup>	10 <sup>16</sup> to 10 <sup>17</sup>
	neutron: 1m			200 to 2,000		2.10 <sup>13</sup> to 10 <sup>15</sup>

Table 11, which details the various radiation sources, shows that most of the energy deposited in nuclear glasses results from *alpha* disintegrations, *beta* disintegrations, and *gamma* transitions. *Beta* disintegrations, *gamma* transitions, and helium nuclei resulting from *alpha* disintegrations mostly have electronic interactions with the glass network atoms. As for *alpha* disintegration recoil nuclei, they mainly lead to elastic interactions between nuclei and originate in most of the atomic displacements experienced by glass under disposal conditions.

In order to evaluate whether these various radiation sources may alter nuclear glass properties during their disposal, investigations were carried out in the CEA laboratories as early as the seventies, with special focus on differentiating the impact of the two interaction processes, i.e., electronic and nuclear effects.

### Methodologies for studying self-irradiation effects

The aim of these investigations is to determine whether the glass properties will be or not altered by the successive disintegrations occurring within glasses during their geological disposal.

Therefore, it is of prime interest to find how to speed up the timescale so as to simulate the potential consequences liable to occur on very long durations, typically from ten to several hundreds of thousands of years.

For this purpose, an approach based upon several complementary axes has been implemented at the CEA. It mainly consists of specific experiments allowing nuclear glass ageing under disposal conditions to be explored on the laboratory scale (over a period of about one year), as well as atomistic simulations which can help understand the origin of the observed phenomena at the atomic scale. This whole set constitutes the basis required to achieve robust long-term behavior models.

### Investigations of glasses doped with radioactive elements

The aim is to incorporate short half-lived radioactive elements into a glass in order to quickly accumulate the highest possible disintegration doses on the timescale of laboratory investigations. This study method displays the advantage of being the most representative, as the resulting irradiation of the whole of the glass volume is identical to the real case and all the disintegration com-

ponents are involved. For instance, as regards *alpha* disintegrations, this technique simulates the consequences of both the *alpha* particle (helium nucleus) and the recoil nucleus.

One of its drawbacks, however, is working on radioactive samples, thus limiting characterization to the techniques available in this environment. In addition, the effect of the dose rate has to be evaluated since disintegration doses in these laboratory materials are integrated more rapidly than under actual disposal conditions. This is achieved through making materials with various dopant contents likely to investigate irradiation effects at various dose rates.

Investigations of doped materials started at the CEA in the seventies and were first aimed at evaluating the impact of self-irradiation on glass macroscopic properties. They are still under way now as characterization techniques in radioactive environment have improved, and now extend to the behavior of glass atomic network.

### Investigations of real radioactive glasses

This technique lies in making laboratory-scale radioactive glasses with a composition similar to that of real glasses, or directly investigating radioactive glasses industrially produced. Though not allowing for accelerated ageing, it has the benefit of sticking to the actual case and giving access to significant observations on a human timescale ( $10^{-30}$  years). For almost half of the energy deposited by the *beta* and *gamma* disintegrations is deposited in the first 30 years. In the years 80-90 glasses simulating the actual glasses produced by AREVA were made at the CEA, and a sample of a radioactive glass produced by AREVA on the industrial scale is still used to validate the data from other investigation axes on a real object.

### External irradiation of glasses

This third investigation axis is based upon the use of nonradioactive simulant glasses in which irradiation stress is simulated by external irradiation techniques (neutrons, heavy ions, electrons,  $\gamma$ ). This axis aims at giving a relatively easy access through experimentation to macroscopic and microscopic evolutions in the material. This approach also give experimental access to the behavior of the glass atomic structure under irradiation characterizing glasses with improved spectroscopic techniques.

Moreover, the choice of the irradiation type makes it possible to simulate the various types of disintegrations as well as differentiate electronic effects from nuclear effects, which proves necessary to understand the origin of the observed phenomena.

The major disadvantages of this experimentation type consist of the upsetting effects of injected high dose rates and of irradiated low volumes. Accurate knowledge of these offsets allows relevant effects to be sorted from experimental artefacts comparing with the results of other axes. This type of study was undertaken as early as the eighties to evaluate the effects of *beta* disintegra-

tions and *gamma* transitions and was focused on the latter in the late 90's owing to experimental tool developing. In parallel heavy-ion irradiations were used to start investigating nuclear interaction effects in order to complete investigations of actinide-doped radioactive glasses.

### Atomistic modelling of glass self-irradiation

Outstanding progress achieved in calculation capacities in the past few years have paved the way for atomistic numerical simulation of the phenomena involved in glass self-irradiation.

Until now most of the studies carried out in this field have been molecular-dynamics studies in order to understand the ballistic (or nuclear) effects induced by the recoil nuclei emitted during *alpha* disintegrations. The advantage of this approach lies on the fact the path of the recoil nuclei is relatively short, the primary or secondary projectile energy decay duration is fast, and most of the energy decays is elastic. Simulating the path of a recoil nucleus and all the related dynamic phenomena thus becomes possible in models of glass systems including a few dozen to a few hundreds of thousands of atoms. This provides an atomic-scale view of the glass network under behavior irradiation.

The first studies of nuclear glasses through simulation started in the mid-nineties. Owing to the strong increase of calculation tools in the last few years, other studies were carried out, especially to simulate the doses corresponding with an actual glass disposal period of about 10,000 years.

Coupling these various investigation axes exhibits two benefits: first, evaluating the impact of glass self-irradiation on its macroscopic behavior, thereby assessing the extent to which radioactive-element confinement capacity can be maintained in the long term, and, secondly, understanding the atomic origin of the phenomena involved, a key element for the building of long-term behavior models.

---

### Effect of glass self-irradiation on its intrinsic properties

#### Effect of *beta* disintegrations and *gamma* transitions

The effect of electron interactions induced by *beta* disintegrations and *gamma* transitions is mainly investigated through external electron irradiations.

Glasses with chemical compositions representative of the industrially-produced nuclear glasses were thus irradiated to doses equivalent to those received in about 1,000 years of disposal, i.e., 70% of the total dose received in 1 million years.

These irradiations have not entailed detectable modifications of the macroscopic properties (density, mechanical properties). In addition, glass still displays a homogeneous microstructure after irradiation.

Now, various studies reported in literature mentioned deep modifications in the properties of some oxide glasses under electron bombardment. An analysis process was then set up to determine why nuclear glasses displayed no evolution.

As a first step, glasses with simplified chemical compositions (in contrast with nuclear glasses) were made which ensured easier study of the glass structure behavior [4], then chemical elements were progressively added to come close to the actual composition of nuclear glasses [5,6].

As shown in these investigations, even the simplest glasses exhibit outstanding evolutions liable to be induced by a migration of sodium atoms under electron irradiation. This migration mainly aims at increasing the connectivity (or polymerization) of the silicate glass network, partially moving from 4- to 3-coordinated boron atoms, and forming dissolved molecular oxygen.

Structural evolutions can be limited or even inhibited by adding some chemical elements, especially transition elements and rare earths, to these simplified glasses. As highlighted in the same studies, these chemical elements experience reduction processes under irradiation liable to prevent the emergence of the spot flaws which the structural evolutions observed on simplified glasses result from.

### Effect of *alpha* disintegrations

As mentioned above, *alpha* disintegrations constitute the main source of nuclear damage in glass under disposal conditions, through the atomic displacements induced by recoil nuclei, nuclear daughters of the *alpha* emitter.

The related effects were mainly investigated through studying glasses doped with a short half-lived actinide, i.e., the curium isotope with atomic weight 244. For owing to its short radioactive half-life (18.1 years), the glass under consideration can integrate within a few years doses equivalent to those to be delivered to the nuclear glass for thousands of years under disposal conditions. Besides, glasses with different burden rates were made and steadily observed in order to evaluate the possible artifacts induced by such time scale acceleration. For, comparing the properties measured on the various glasses for a same integrated dose provides information on the effect of the integration rate parameter.

In parallel, comprehension of irradiation effects of nuclear origin could be improved through external heavy-ion irradiations liable to simulate nuclear effects and molecular-dynamics atomistic simulations.

### Macroscopic behavior of a nuclear glass under *alpha* self-irradiation

*alpha* disintegrations induce a slight swelling in a nuclear glass. The relative variation of density is represented in Figure 53. Density experiences a fast decrease at the lowest doses, then stabilizes around a saturation threshold. This type of variation is confirmed by studies based upon external irradiations and molecular-dynamics modelling.

The experimental behavior is correctly reproduced by an exponential model of the same type as that developed by Marples [7], a model in which the sample volume variation is proportional to the fraction of the volume once damaged. Detailed analysis of this model makes it possible to determine an *alpha*-disintegration-damaged unit volume of about 280 nm<sup>3</sup>, i.e., a value fairly close to that of about 300 nm<sup>3</sup> obtained through molecular dynamics simulation. This result tends to confirm the results obtained through the various investigation methods.

The glass mechanical properties also depend on the cumulative *alpha*-decay events. For, whether curium-doped glasses or ion-irradiated glasses are considered, a decrease in hardness and the Young's modulus can be observed with the dose, followed with a progressive stabilization around saturation thresholds respectively at values about 35% and 15% lower than the initial values. It is also worthwhile mentioning that the glass tenacity, which characterizes its tensile breaking strength, increases with glass self-irradiation. These results thus reveal a global improvement of glass mechanical properties after irradiation.

The microstructure of the doped and externally irradiated glasses was also characterized as a function of the *alpha* disintegration dose. No microstructure alteration could be detected, whether on

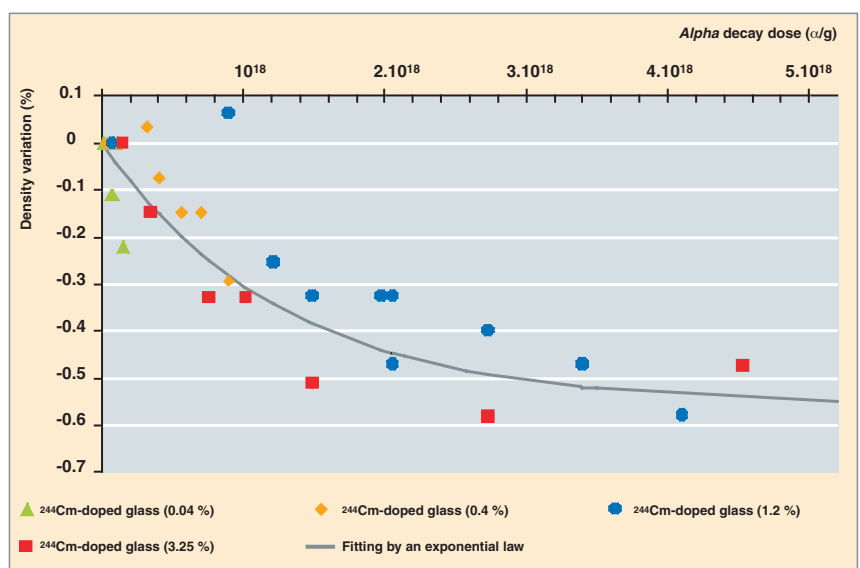


Fig. 53. Evolution of the density of curium-doped glasses with the *alpha*-decay dose. The unbroken curve stands for the fitting of the experimental points using an exponential model.

the SEM scale (resolution of about 100 nm) or the TEM scale (resolution of 1 nanometer). Despite the evolution of some glass macroscopic properties, glass microstructure thus proves to be still homogeneous as it shows no phase separation or crystallization under *alpha* self-irradiation.

The following conclusions can be drawn from the whole of the results available at the present time. On the one hand, following a minor evolution phase, macroscopic properties (swelling, hardness, elastic modulus) are stabilized with integrated doses around 1 to 2  $10^{18}$   $\alpha/g$ . On the other hand, there is no dose rate effect, as variations can be reproduced among the various glasses under study which exhibit quite different integration rates, spreading over four orders of magnitude.

This type of behavior on nuclear glasses studied could also be observed in other countries (United States, Germany, Japan) [8, 9].

### Structural behavior of a nuclear glass under *alpha* self-irradiation

The structural evolution of ion-irradiated glasses was analyzed by spectroscopic techniques (Raman, NMR, IR). As a first step, it was checked that the simplified glass behavior was similar to that of complex glasses under the same irradiation conditions. Then the structural evolutions of these simplified glasses were investigated.

The molecular dynamics method was used to simulate the effect of recoil nuclei upon the glass structure. Detailed at the beginning of the monograph (see supra "Nuclear glass formulation, structure and properties", pp. 33-49), this method was used to simulate the glass structure, then to subject these structures to series of displacement cascades of 600 or 4 eV (with energies lower than actual energies due to calculation times). Simulating a displacement cascade consists in "bombarding" the structure with a heavy projectile in order to investigate the consequences of the ensuing atom collision cascade. So this method is perfect to study ballistic effects in a model glass.

In a three-oxide ( $\text{SiO}_2$ ,  $\text{B}_2\text{O}_3$ ,  $\text{Na}_2\text{O}$ ) simplified nuclear glass, the Raman band is shifted at  $495 \text{ cm}^{-1}$  towards higher frequencies when the irradiation dose increases, an evolution which tends to a saturation threshold [10] (Fig. 54) as is the case for macroscopic properties. This shift may be interpreted as revealing the decrease of medium angles Si-O-Si, between the tetrahedra which constitute the silicate network. This phenomenon could also be observed through molecular dynamics, with an angular variation measured of about  $2^\circ$ .

Nuclear Magnetic Resonance (RMN) spectra obtained on unaltered and irradiated 5-oxide glasses show a slight depolymerization induced by irradiation as an increase in the concentration of 3-coordinated boron and non-bridging oxygens. Such observations are confirmed by the data obtained through molecular

dynamics which allow them to be quantified. The decrease in the polymerization induced by irradiation thus proves to be limited to about 1 to 2%.

In parallel the average distance Na-O decreases, which may be explained by an increase in the concentration of sodium atoms positioned as network modifiers. Moreover, Q3 species increase detrimentally to Q4 species, thus also explaining the slight glass depolymerization under irradiation (a Q4 species is a tetrahedron  $\text{SiO}_4$  containing four bridging oxygens whereas a Q3 species is a tetrahedron  $\text{SiO}_3$  containing three bridging oxygens and one nonbridging oxygen).

As shown in the data previously detailed, nuclear glass undergoes little change, both in its properties and structure, under *alpha* self-irradiation. Its evolutions are induced by the nuclear interactions due to the recoil nuclei emitted during *alpha* disintegrations. It is worthwhile noticing that such evolutions are similar to those observed on nonradioactive glasses, when increasing the material temperature.

This is the reason why studies were carried out in order to compare the properties and structure of irradiated glasses with those of glasses the structure of which was deliberately frozen in at high temperature by quenching. These studies are detailed in the previous chapter (see "Nuclear glass formulation, structure and properties", pp. 33-49). Their conclusions show that stresses due to ballistic processes and quenching do result in quite similar materials with a high fictive temperature.

A model of cumulative local quenching was built from these data in order to help explain the origin of the evolutions observed under irradiation, as well as the origin of their stabilization under high doses.

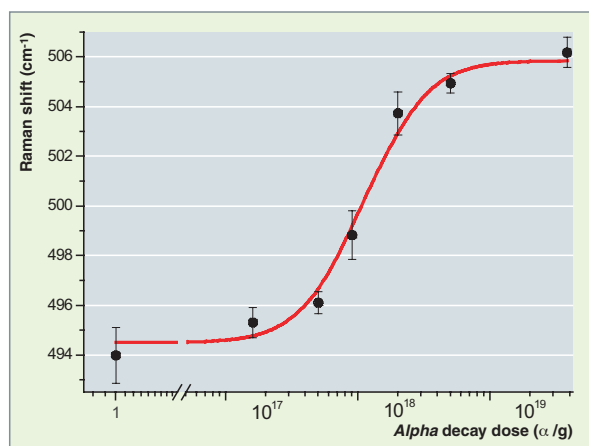


Fig. 54. Position of the vibrational band of the Si-O-Si bonds versus the radiation dose.

As displacement cascades accumulate, glass structure is fully destabilized by nuclear interactions (see the frame). Then the material can be quickly reconstructed without any external energy and its structure is close to that a glass frozen in at high temperature, which results in the observed evolutions.

When the whole of the glass volume has been damaged once by the displacement cascades, any new *alpha* disintegration produced will again temporarily destabilize the structure, but the latter will be rebuilt in the same way as after the first damage. So the glass no longer undergoes significant change, which could explain why its properties are stabilized beyond a given dose. It is worthwhile mentioning that the saturation dose experimentally observed in relation to macroscopic property evolutions (Fig. 53) coincides with that required for full glass damaging by displacement cascades, which corroborates the proposed model.

As a conclusion, the insignificant evolution of nuclear glasses under *alpha* self-irradiation with respect to some minerals [12] could be explained by its initially disordered nature.

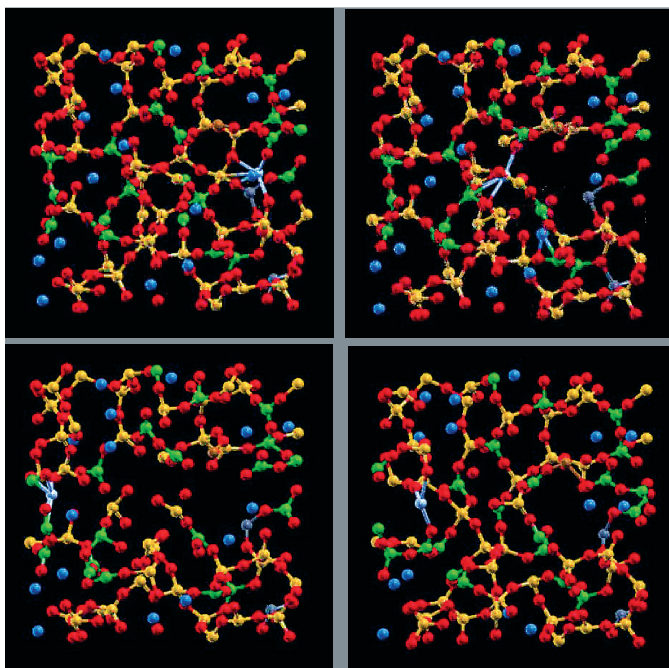


Fig. 55. Evolution of displacement cascade: four successive views. In the top left corner, the initial glass containing the uranium atom (sky blue atoms) to be accelerated with a 800 eV ( $t = 0$  ps). In the top right corner, starting ballistic phase induced by the uranium projectile ( $t = 0.013$  ps). In the bottom left corner, final step of the ballistic phase standing for the maximum broken bonds ( $t = 0.038$  ps). In the bottom right corner, reconstruction of the glass structure after the ballistic phase ( $t = 0.25$  ps).

### Molecular dynamics simulation as applied to investigations of glass behavior under irradiation

Molecular-dynamics calculations were initiated more than ten years ago and were first devoted to simulating individual displacement cascades over the whole energy range 0 keV - 100 keV. Actual energies of recoil nuclei could be reached [13], especially thanks to the development of a method called CoMoD (standing for *Combined Molecular Dynamics*), which couples two types of molecular dynamics. It could be highlighted that results proved coherent between low and high energies.

The following conclusions could be drawn from the whole of the calculations performed in relation to individual cascades in glasses:

- displacement cascades take place in two separate steps (Fig. 55):

- the step of the properly called collisions during which collisions between atoms take place as a whole. This phase coincides with the strong heating of the matrix and a depolymerization of the structure by interatomic bond breaking. In parallel, a decrease in atom density can be observed within the cascades;

- the relaxation step during which glass structure reconstruction takes place. The glass structure then experiences significant reconstruction to a state close to its initial state, but still with a slight structure depolymerization and a slight swelling on the whole;

- atomic displacements are of several types, as a function of collision energy:

- the most energetic collisions entail individual displacements, i.e., an atom is taken off from its site and its local environment is totally changed. These individual displacements occur in the early stage of the cascade when the atoms have high energies;

- the least energetic collisions entail collective displacements of a chain of interconnected atoms. These collective displacements mostly occur in the final stage of the cascade;

- the role of mobile elements (especially, Na) is important, for they endow the glass network with a reordering flexibility which reduces cumulative stresses and speeds up glass reconstruction to a state close to its initial state;

- displacement cascades are not homogeneous. It was proved that the reconstruction quality depended upon the local heating degree. A damage peak emerges for intermediate heatings between low energies, at which damage is low, and high energies, at which there is sufficient heating to ensure a better structure reconstruction.

## Is glass/water chemical reactivity modified by self-irradiation ?

Radioactive element confinement results in radiation fields within the glass matrix, which may lead to two types of effects:

- effects upon the solid structure likely to alter its physical properties and the glass/water chemical reactivity,
- effects at the solid/liquid interface which may affect the kinetics of glass alteration by water, especially owing to the formation of radiolytic species\*.

Two parameters will help characterize self-irradiation resulting from radioactive atoms under disposal conditions. The radiation activity, i.e., the number of disintegrations occurring in the interval of one second, progressively decreases with time, due to the steady disappearance of the most radioactive elements. The decay dose, which corresponds with the number of disintegrations accumulated between the material making and a  $t$  time of the disposal period, progressively increases with time, owing to the cumulative disintegrations during this period.

### $\alpha$ , $\beta$ , $\gamma$ radiation activity dependence of the chemical reactivity of glass with water

Experiments were performed on laboratory-scale radioactive glasses the content of which was deliberately fitted so as to simulate glass activities under disposal conditions. As a complementary step, under-water alteration tests were achieved on industrial radioactive glasses from La Hague plant in order to confirm the results on actual samples. The aim of these investigations is to evaluate whether water radiolysis induced by glass activity can modify the chemical reactivity of glass with water due to radiolytic species generation.

The initial alteration rates measured do not depend on  $\alpha$ ,  $\beta$ ,  $\gamma$  activities of the glasses [14]. Moreover, the temperature dependence of this rate is strictly the same as that of the inactive glass with the same composition, which means that the activation energy coupled with the hydrolysis reaction is identical (Fig. 56). It is worthwhile noticing as well that the nuclear glass behavior is very close to that of a natural basaltic glass.

These data show that the chemical reactivity of glass with water measured by the initial alteration rate does not depend upon the glass radioactive activity.

### Decay dose dependence of the chemical reactivity of glass with water

Investigating the effects potentially induced in glass by the cumulative  $\alpha$  decay events requires to find ways to speed up the timescale. For this purpose two types of glasses were prepared on the laboratory scale:

- glasses which only contained short half-lived radioactive iso-

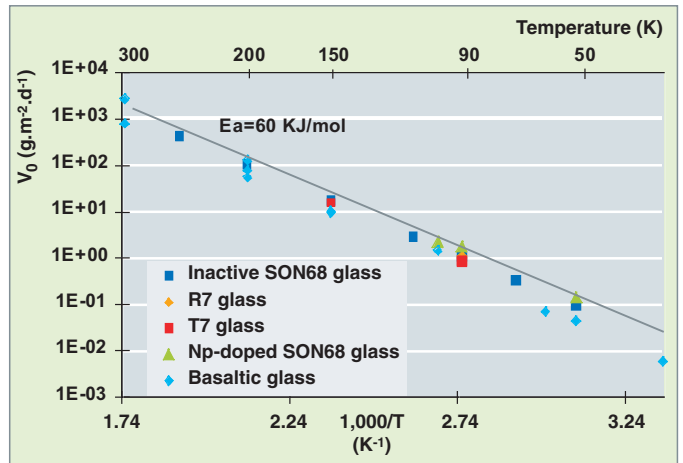


Fig. 56. Temperature dependence of glass alteration initial rate.

topes made it possible to integrate within a few years decay doses equivalent to those to be received by nuclear glasses during their thousands of years' disposal period;

- non-radioactive glasses were irradiated by charged particle beams in order to reproduce the damage due to the cumulative decay dose events.

$\beta$  disintegrations could thus be simulated in glass through electron irradiations. Glass alteration experiments were performed with the Soxhlet technique, i.e., with permanent pure water renewal, showed no difference between the irradiated glass alteration and that of the initial glass.

The effects related to the cumulative  $\alpha$  decay events were investigated on  $^{244}\text{Cm}$ -doped glasses and heavy-ion-irradiated glasses (Fig. 57). The initial alteration rate measured under the same conditions on a non-irradiated glass is highlighted by the black line. These data do not show any significant dependence

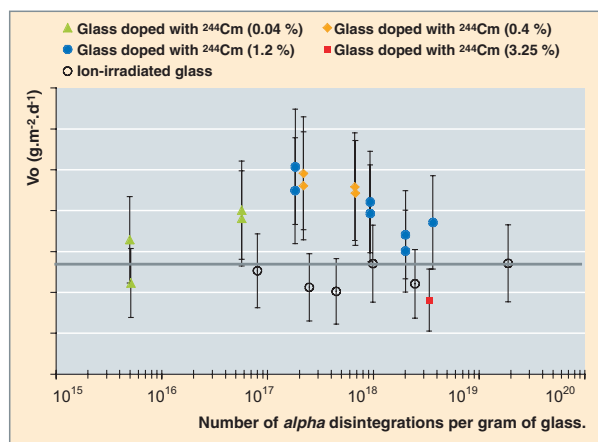


Fig. 57. Effect of the  $\alpha$  dose upon the initial alteration rate of a glass.



of this property on the *alpha* decay dose, whereas others (hardness, modulus of elasticity, density) prove to be affected.

This lack of impact can be explained by the nature of the glass structural modifications under *alpha* self-irradiation. For irradiation results in a glass with a nearly identical structure, but with a higher fictive temperature, i.e., with a slightly lower degree of polymerization (1 to 2%) and with slightly decreasing angles between silica tetrahedra. These low evolutions are not sufficiently significant to modify chemical reactivity between the glass and water, since this parameter is mainly controlled by glass chemistry, and structural parameters only play a secondary role. In contrast, some macroscopic properties, especially mechanical properties, are more sensitive to these parameters. In particular, a decrease in the boron average coordination number and an increase in the nonbridging oxygen number can have an impact on the network flexibility and, thus, its mechanical properties, whatever minor they may be.

## ► References

- [1] G. GENESTE, F. BOUYER, S. GIN, "Hydrogen-sodium interdiffusion in borosilicate glasses investigated from first principles", *J. Non-Cryst. Solids*, **352** (2006), p. 3147.
- [2] M. ARAB, C. CAILLETEAU, F. ANGELI, F. DEVREUX, L. GIRARD, O. SPALLA, *XI Int. Conference on the Physics of Non Crystalline Solids* (2006), Rhodes (Greece).
- [3] S. RIBET and S. GIN "Role of neoformed phases on the mechanisms controlling the resumption of SON68 glass alteration in alkaline media". *Journal of Nuclear Materials*, **324** (2004), p. 152.
- [4] B. BOIZOT, G. PETITE, D. GHALEB, B. REYNARD, G. CALAS, *Journal of Non-Crystalline Solids*, **243** (1999), p. 268.
- [5] N. OLLIER, "Verres de confinement de déchets nucléaires de type SON68 et leurs produits d'altération : spectroscopie optique des terres rares et de l'uranium", Thesis Claude Bernard - Lyon 1 University (2002).
- [6] F. OLIVIER, "Influence du dopage par certains éléments de transition sur les effets d'irradiation dans des verres d'intérêt nucléaire", Thesis, École Polytechnique (2006).
- [7] J.A.C. MARPLES, *Nuclear Instruments and Methods In Physics Research B*, **32** (1988), p. 480.
- [8] W.J. WEBER, R.C. EWING, C.A. ANGELL, G.W. ARNOLD, A.N. CORMACK, J.M. DELAYE, D.L. GRISCOM, L.W. HOBBS, A. NAVROTSKY, D.L. PRICE, A.H.M. STONEHAM, M.C.H. WEINBERG, *Journal of Materials Research*, **12** (1997), p. 1946.
- [9] Y. INAGAKI, H. FURUYA, K. IDEMITSU, T. BANBA, S. MATSUMOTO, S. MURAKO, *Materials Research Society Symposium Proceedings*, **257** (1992), p. 199.
- [10] J. DE BONFILS, "Effets d'irradiations sur la structure de verres borosilicates - comportement à long terme des matrices vitreuses de stockage des déchets nucléaires", Thesis, Claude Bernard - Lyon 1 University (2007).
- [11] S. PEUGET, J.-N. CACHIA, C. JÉGOU, X. DESCHANELS, D. ROUDIL, J.-C. BROUDIC, J.-M. DELAYE, J.-M. BART, *Journal of Nuclear Materials*, **354** (2006), p. 1.
- [12] R.C. EWING, W.J. WEBER, F.W. CLINARD, *Progress in Nuclear Energy*, **29-2** (1995), p. 63.
- [13] J.-M. DELAYE, D. GHALEB, *Physical Review B*, volume 71 (2005), p. 224203. *Physical Review B*, **71** (2005), p. 224204.
- [14] T. ADVOCAT, P. JOLLIVET, J.-L. CROVISIER, M. DEL NERO, *Journal of Nuclear Materials*, **298** (2001), p. 55.

**Stéphane GIN, Isabelle RIBET,**  
**Sylvain PEUGET and Jean-Marc DELAYE,**  
*Research Department of Waste Treatment  
and Conditioning*



## Cold crucible vitrification

### Cold crucible: a promising technology

Glass melters based on induction heating in a cold crucible were developed to take advantage of their two main features:

- the cooling of the crucible produces a thin layer of solidified (frozen) glass (the so-called “cold-skull”) that protects the crucible, thereby preventing corrosion, which allows to make materials highly corrosive in the molten state and significantly increases the crucible service life;
- direct induction heating in the molten glass bath paves the way to high temperatures and thereby increased capacity in glass fabrication, along with the development of new confining materials unachievable in the current process (see “Nuclear glass formulation, structure and properties”, pp. 33-49).

### Principles of the direct-induction cold-crucible vitrification technology

Direct induction melting consists in placing the glass to be heated in an alternating electromagnetic field generated by an inductor (the frequency of this alternating field is about a few dozen kilohertz). As the liquid glass is an electric conductor (with a resistivity ranging from 1 to 10 ohm.centimeter), the alternating electromagnetic field generates in it induced currents which dissipate energy due to the Joule effect.

The aim of direct induction is direct heating of the material to be melted, instead of the crucible. The latter is metallic (made of, e.g., stainless steel). It is cooled by water flow and subdivided into metal sectors (or segments) separated from one another by a thin layer of electric insulator in order to ensure a relative “transparency” to the electromagnetic field (Fig. 58).

Contact with the cold wall induces the formation of a thin layer of solidified (“frozen”) glass 5-10 mm thick, which separates molten glass from the wall cold metal. So the crucible metal does not come into contact with molten glass, which is fully contained in this “skin” or “crust” of frozen glass (the “cold-skull” or “skull”). Hence the term “self-crucible” assigned to the device. Now, this absence of contact between molten glass and the cold metal protects the crucible against any corrosion from the aggressive, high-temperature molten glass.

As glass is an insulating electric material at room temperature, it is necessary to pre-heat a glass feed to start induction. In nuclear applications, this pre-heating is achieved through placing a titanium or zirconium ring on the initial glass feed. This ring is heated under the effect of the electromagnetic field, then its oxidation brings energy to the glass, allowing it to be melt. At the end of this induction-initiating phase the fully oxidized metal is a constituent of the glass.

As in the current hot crucible process, the furnace operation is of the semi-batch type; it is continuously fed with the material to be melted whereas the pouring of the resulting glass into containers is sequential. At the end of each pouring a sufficient volume of molten glass is kept in the furnace so as to maintain induction and keep melting going on.

This direct-induction cold-crucible vitrification process is very compact compared with the electrode ceramic furnace process.

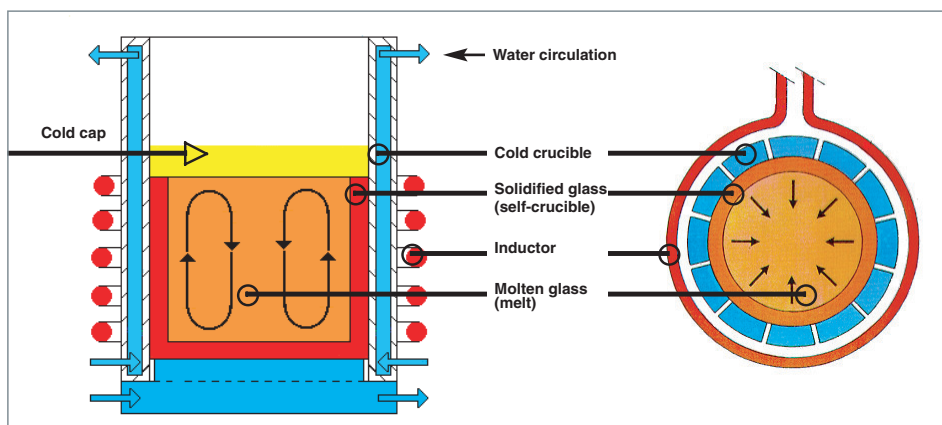


Fig. 58. Schematic overview of a glass melting furnace using direct induction in a cold crucible.

### State of the art and technological developments of direct-induction cold-crucible vitrification

The process for vitrifying fission products solutions by direct induction in a cold crucible is under development, mainly in France and Russia.

The CEA Marcoule started developing this technology more than 20 years ago, chiefly to process fission products solutions. A key step in this development was coupling a scale-1 furnace (i.e., including a crucible 650 mm inside diameter) with the calcinator and the gas scrubbing system of the inactive prototype at one of La Hague vitrification units (Fig. 59).

When this technology was deemed to be sufficiently mature, a three-partner working group gathering COGEMA, SGN, and the CEA determined the main technological design options relating to the development of the cold crucible vitrification process in such an environment as, typically, La Hague vitrification workshops.

The tests and developments performed resulted in the definition of an optimized crucible, strictly identical to that scheduled to be implemented at La Hague around 2010. The former furnace was replaced with a scale-1 cold-crucible pilot coupled

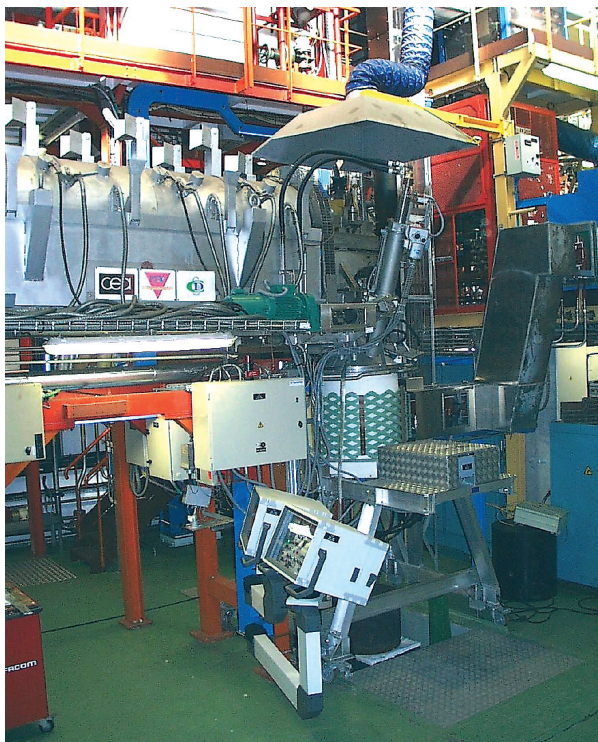


Fig.59. The Vitrification Evolutive Prototype (PEV) at the CEA Marcoule, equipped with a cold crucible furnace.

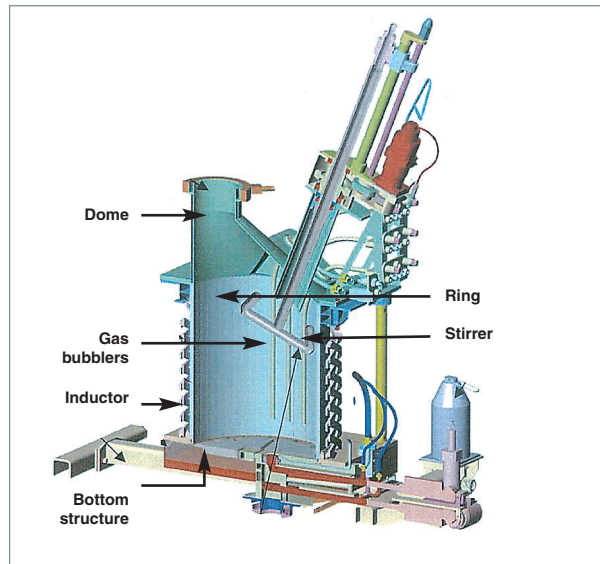


Fig.60. Sectional view of the cold crucible developed for the applications of the AREVA plant at La Hague.

with the calcinator of the existing Vitrification Evolutive Prototype PEV (*Prototype Evolutif de Vitrification*). The resulting inactive facility is quite representative of the process to be implemented at La Hague (Fig. 60).

The developments performed in the cold crucible of the PEV in the last ten years have taken into account industrial constraints.

The *ring* was optimized:

- the upper part of the *ring* now consists of a water box headed by a flange to which the dome is connected under satisfactory conditions of leaktightness;
- energy losses on the crucible structure were reduced by 30% through increasing its height and optimizing the size and form of the gaps between the *ring* metal sectors, thus improving the inductor-glass coupling.

The *dome* is equipped with:

- a cooled stirrer, which ensures thermal and chemical homogeneity in the glass bath. Hydraulic research work on an oil bath mockup has made it possible to optimize stirrer features (blade profile, turning velocity). The stirrer is retractable so that it can be recovered in the case of an outage.

- three instrumentation rods designed to perform:
  - a molten-glass bath level measurement using a cooled pneumatic bubbler,
  - two temperature measurements, one of which is a direct one performed by a partially cooled bubbler ended with a metal nozzle.

The *bottom structure* constitutes the lower part of the melter on which the ring is placed. It especially includes:

- the pouring unit. It consists of a set of two stainless steel slide valves (or “gate valves”) designed to slide into a body maintained in the bottom structure, thus obturating an outlet. The whole device is water-cooled. The opening of the first valve results in a progressive reheating of the solidified glass and, then, in its melting and pouring. Once the process has been triggered, the pouring rate is controlled by this valve. The second valve is a safety element to be used in the case of a first valve failure.

The *High-Frequency* electric supply consists of:

- A transistor power generator. It supplies 400 kW for a 300 kHz operating frequency. This choice makes it possible to supply the inductor with electric current under a voltage lower than 2,000 V, which limits the overheating risks on passing through the vitrification cell wall, and allows for the use of radiation-resistant insulating materials.
- The transmission line. Its self-inductance was minimized, which helps reduce voltage drops at its terminals. Taking account of active operation constraints led to a remotely dismountable design, so that the crucible could be removed under maintenance conditions.
- The cooled inductor consists of windings of rectangular cross-section and of same length, distributed in two layers. Such a design makes it possible to improve heating homogeneity as current flow is forced through the whole of the inductor. It is sized to ensure the restarting of a melter filled with solidified glass (400 kg) after an incidental shutdown.

---

### Modelling the cold crucible

Two-dimensional axisymmetrical models were developed in order to model cold crucible electromagnetic phenomena as well describe the thermal behavior of induction-heated glass. These models made it possible to improve crucible geometries: height, diameter, sector number, sector widths and geometry depending upon applications.

3D-models which couple electromagnetic and thermohydraulic phenomena, are under development. The aim is calculating motions and energy distribution in the molten glass bath, which can improve the process and reduce the number of pilot tests.

These models require good knowledge of the physical properties of the material to be heated, particularly its electrical and thermal conductivities. Specific investigations were carried out for better understanding of electrical and thermal conductivity phenomena in nuclear glasses and, thereby, better control of these parameters.

The studies relating to glass resistivity were developed at the CEA Marcoule, and triggered collaborations with the Montpellier II University and the Orléans Research Center on High Temperature Materials.

It was thus demonstrated that the electrical conductivity of an oxide melt can significantly vary through adding a low volume of platinoid-type particles (Pd, Rh, Ru). As revealed in a bibliographical study performed experimentally, only ruthenium occurring in glass as RuO<sub>2</sub> particles can result in a notable increase of the material electrical conductivity (see *supra* “Nuclear glass formulation, structure and properties”, pp. 33-49).

Operation of Joule-heated melters (direct-induction melters or electrode-heated ceramic melters) is significantly altered by such an increase of electrical conductivity.

---

### Developing the cold crucible direct induction in Russia

At Moscow the VNIIM is developing rectangular-shaped cold crucibles (0.6 m long, 0.2 m wide, 0.4 m high) which consist of a twofold set of stainless steel tubes. High-frequency generators supply a power of the order of 160 kW and operate with a 1.7 MHz frequency. This technology is scheduled to be transferred to the Ozersk treatment plant.

At Zagorsk, the SIA RADON is equipped with a cold crucible vitrification unit to treat low and medium level radwaste.

Last but not least, the St Petersburg’s KHLOPIN Institute is also developing cylindrical cold crucibles and cooperates with the INEEL (USA - Idaho) to assess the possibilities and performances of this technology.

---

### Non-nuclear applications for the cold crucible

Cold crucibles are of potential interest for a number of non-nuclear applications due to their reliability and their flexible use. For they offer significant benefits, indeed, due to their following features: no pollution by the refractory material, no temperature limitation for melting, easy and quick shutdown and restarting to change glass composition, and the ability to make low throughputs.

One example among the applications available is the production of colored glasses, in which the cold crucible makes it possible to change color without any risk of contamination.

As part of CEA's technological dissemination measures, two melters of 60 cm and 1.20 m respectively were licensed in 1995 and 1998 by the EFD company and commissioned by the FERRO company at Saint-Dizier. The 1.20-m diameter melter ensures a 40 t/month output of enamels for the manufacturing of enameled sheet.

It is presumable that cold crucible applications will develop.

**Roger Boën,**

*Research Department of Waste Treatment  
and Conditioning*

## Cements as confining materials

### Cementitious materials

Cement-based materials are widely used in the nuclear industry for radioactive waste conditioning and disposal. They result from the setting of a mixture of anhydrous cement, aggregates of various sizes, and water. Several categories may be distinguished depending on whether aggregates are present or not, their size, and the water/cementitious ratio:

- **pure pastes**, only consisting of cement and water;
- **grouts**, pure pastes or fine mortars with a low sand content and a high quantity of water (water volume > cement volume), which gives them the relevant rheology for the pouring that follows mixing;
- **mortars**, which contain aggregates (sand) under 6.3 mm in size (generally, the sand volume is higher than the cement volume, which is itself higher than the water volume);
- **concretes**, which, in addition to sand, include aggregates of a size between 6.3 and 80 mm. In order to increase their tensile strength, they may be armored with bars or reinforced with short metal fibers (fiber-reinforced concretes).

Grouts are mainly used as waste embedding matrices. Mortars are used for immobilization operations (immobilization of bulky waste in a container, immobilization of a primary

container in a secondary container). Last but not least, concretes are used for container manufacturing and for the making of structural components on disposal sites.

Except in such pathological cases as an alkali-aggregate reaction, aggregate properties vary little over time. The chemical evolution of cementitious materials is therefore chiefly governed by that of the cement paste. Cements are hydraulic binders: in presence of water they form hydrates by dissolution-precipitation and these hydrates organize themselves into a cohesive structure. After hardening they withstand the action of water, in contrast with other mineral materials such as plaster or non-hydraulic lime (calcium hydroxide).

The cement most commonly used is of the *Portland* type. It results from the grinding of clinker, an artificial rock made around 1,450 °C from limestone (80%) and clay (20%). Chemical elements recombine at high temperature to give four main crystalline phases: tricalcium silicate  $3\text{CaO}\cdot\text{SiO}_2$  (50-70% of clinker), dicalcium silicate  $2\text{CaO}\cdot\text{SiO}_2$  (5-25% of clinker), tricalcium aluminate  $3\text{CaO}\cdot\text{Al}_2\text{O}_3$  (2-12% of clinker), and tetracalcium aluminoferrite  $4\text{CaO}\cdot\text{Al}_2\text{O}_3\cdot\text{Fe}_2\text{O}_3$  (0-15% of clinker). In presence of water, these phases form hydrated calcium silicates (70%), calcium hydroxide or portlandite (20%), as well as hydrated calcium aluminates and sulfoaluminates (ettringite and monosulfoaluminate) (10%).

Table 12.

Composition of the cements most widely used in the area of nuclear waste conditioning and disposal. CEM I and CEM II Portland cements are those used conventionally in the building industry. CEM III and CEM V cements differ from the CEM I Portland cement by the addition of high quantities of blast-furnace slag and pozzolanic materials.

Composition of standardized cements								
Main types	Notation		Composition (wt.%)					
			Clinker	Blast-furnace slag	Pozzolans			Secondary constituents
					Natural	Natural calcinated	Silica-containing fly ash*	
CEM I	Portland cement	CEM I	95-100	-	-	-	-	0-5
CEM III	Blast-furnace cement	CEM III/A	35-64	35-65	-	-	-	0-5
		CEM III/B	20-34	66-80	-	-	-	0-5
		CEM III/C	5-19	81-95	-	-	-	0-5
CEM V	Composite cement	CEM V/A	40-64	18-30		18-30		0-5
		CEM V/B	20-38	31-50		31-50		0-5

At the clinker grinding step various minerals may be added to Portland cement in order to tailor its usual properties. Fillers obtained by fine grinding of rocks or aggregates, are chemically inert, but improve the physical properties of cementitious materials (controllability, impermeability, reduced crackability...).

Table 12 sums up the compositions of the standardized cements most widely used in the nuclear waste conditioning area.

Hydration reactions start as soon as cement and water come into contact. A few hours following mixing, the material sets: within a few seconds it turns from the suspension to the solid state. After the setting hydration goes on all along the hardening process. Mechanical features change very rapidly in the hours following the setting, then this evolution goes on more and more slowly for several months.

Hardened cement paste is a heterogeneous material which consists of a porous solid, a liquid phase and, generally, a gaseous phase present in the pores. The solid is formed with hydrated minerals and possibly of residual anhydrous cement. The interstitial solution is very basic (pH between 12.5 and 13.6) and its composition varies with the material age.

## Developing cementitious embedding material formulations tailored to various types of waste

### Diversity of the waste to be conditioned

Cementation is the oldest and most widespread process in France and abroad for low and intermediate-level waste conditioning. This waste shows high diversity.

**Origin-related diversity:** Waste arises from the different steps of the nuclear fuel cycle (uranium ore mining and fuel manufacturing, nuclear power plant operation, spent fuel treatment, facility dismantling). It is also worthwhile to mention, though to a lesser extent, waste issued from research centers, hospitals, and industries using or making radioelements.

**Nature-related diversity:** Waste is under such forms as aqueous solutions, suspensions (chemical co-precipitation sludges), or bulky or pulverulent solids. "Homogeneous" waste is intimately mixed with the cementitious binder (embedding) and are potentially reactive (evaporator concentrates, sludges, small-grain-sized pulverulent solids). "Heterogeneous" waste, more bulky and non-reactive in cementitious media, is subjected to a mere mechanical immobilization (plastic-material objects, rubble, some metallic waste...).

**Composition-related diversity:** The composition of the waste to be immobilized in cement depends on the activity it arises from, as well as the treatment and decontamination processes implemented upstream the conditioning stage. The contaminated aqueous waste volume can be thus reduced by evaporation or chemical co-precipitation (in order to insolubilize the radioelements), as well as filtration. In the first case, this results in a high-salinity solution (up to 600 g/L), and, in the second case, in a suspension in which the dry extract depends on the filtration process used. Besides, the composition of a given waste may vary significantly.

Such a diversity in waste implies diversity in embedding materials, based upon tailored formulations. The latter have to take into account both the constraints of the implementation industrial process and the specifications for further package disposal (see the frame hereafter).

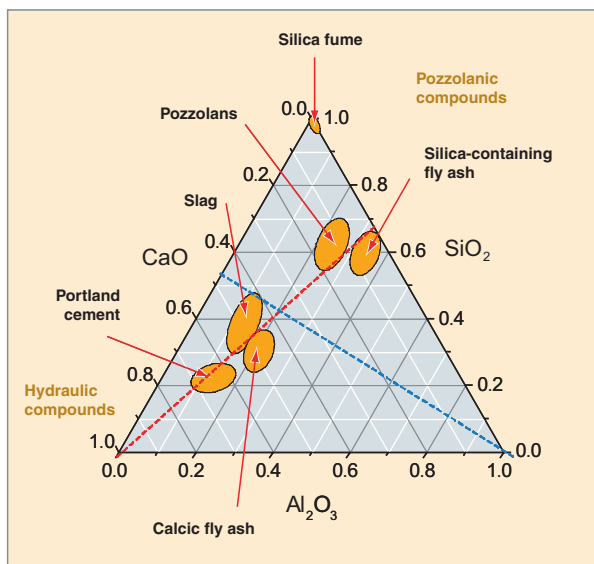


Fig. 61. Localization in the ternary diagram  $\text{CaO} - \text{SiO}_2 - \text{Al}_2\text{O}_3$  of the inorganic compounds usually added to the Portland cement.



## Properties required for a cementitious waste conditioning matrix

### Specifications inherent to the implementation industrial process

Cementation conditioning is generally performed near the waste-producing sites. The embedded waste preparation is carried out either in the container itself (in-container mixing), using (lost or retrieved) impeller blade stirring, or in a separate mixer, prior to pouring the mixture into the container (continuous processes). In contrast with civil engineering, a specific environment (shielded cells or glove boxes) is required due to the radioactivity of the mixed products.

The **rheology**\* of the embedded waste after mixing is an important criterion for assessing the quality of a formulation, especially when the latter is used in a mixer. The aim is a grout-type fluidity, with a durable workability retention. This facilitates mixer drainage, and reduces the volume of rinsing water (which stands as a secondary waste).

The **setting time** is also a key element to determine the process. It may be affected by the waste chemical composition. The final setting time should preferably be over 4 h so as to avoid any risk of setting in the mixer in the case of a dysfunctioning, but should not be too long (over 24 h) to avoid lower yields on the conditioning line.

### Specifications related to package disposal

Waste is acceptable for final disposal only if it consists of a solid, indispersible block which does not contain water liable to be leaked out. Packages should be easy to handle and shock-resisting. They should ensure durable confinement of the waste and exhibit satisfactory resistance to water leaching.

## Waste reactivity in a cementitious medium

The setting of a cementitious material involves a cascade of hydration reactions as well as a number of equilibria between hydrated phases and the interstitial solution. In such a context, it is understandable that waste incorporation into a cementitious matrix cannot be neutral: as it alters the hydration kinetics or upsets the equilibria, it can inhibit cement setting or alter the hydrated material properties. Cement-waste interactions fall into five categories.

### Adsorption

Adsorption phenomena take place on the various solid-liquid interfaces.

- adsorption of solutes brought by the waste to the surface of anhydrous cement grains. Such is the case, in particular, of low-concentration phosphates which slow down cement hydration by blocking calcium silicate dissolution sites.

- adsorption of solutes brought by the waste at the surface of hydrates. Calcium hydrosilicates (C-S-H), the major hydrates of Portland cement, can adsorb a high number of monovalent or divalent cations, thereby slowing down their migration through the cementitious material, which is an asset for confinement. For, owing to their nano-particular feature and their lamellar structure, these phases develop a very broad interface with the interstitial solution (about 250 m<sup>2</sup>/g) and have an exceptionally high surface charge density due to acid-base dissociation of silanols Si-OH.

- adsorption of the mixing water on the particles of a pulverulent waste. Adding waste with a large specific surface area may make the paste too viscous for the industrial process. In such a case, using a superplasticizer improves the embedded waste workability without excessively increasing water proportion.

### Precipitation / co-precipitation

During the mixing operation the solution is burdened with different ions, among which Ca<sup>2+</sup> and OH<sup>-</sup> ions with which many ions can precipitate (calcic precipitation: F<sup>-</sup>, SO<sub>4</sub><sup>2-</sup>, CO<sub>3</sub><sup>2-</sup>, B(OH)<sup>4-</sup>, PO<sub>4</sub><sup>3-</sup>...), precipitation under the form of an hydroxide: Pb<sup>2+</sup>, Cd<sup>2+</sup>, Sn<sup>2+</sup>, Ni<sup>2+</sup>, actinides, Mg<sup>2+</sup>, Co<sup>2+</sup>, Cu<sup>2+</sup>...). A high number of radionuclides is thus insolubilized, which constitutes one of the benefits of the cementitious matrix. Yet, some precipitations can exhibit negative effects: failure on the material setting, or on the contrary accelerated hydration.

Furthermore, salts initially dissolved in the aqueous waste (e.g., in sodium nitrate) can crystallize over time after water has been consumed by cement hydration reactions. The crystals grow in the pores, but are still extremely soluble. So they will be easily leached by an outer water source, displaying higher porosity and lower confinement power.

### Acid-base reactions

Cement paste neutralizes acid waste due to its buffer power. If the interstitial solution pH decreases to below 10.5, the cement hydrated phases become unstable and the material loses its cohesion. This critical situation may occur with some uranyl nitrate solutions issued from spent fuel treatment (concentration of 1,300 gU/L). Waste neutralization has then to be performed prior to embedding, despite the related drawback of volume increase.

### Redox reactions

Conditioning aluminium-containing metallic waste may result in the release of dihydrogen (H<sub>2</sub>) following the metal oxidation by the mixing water. Hydrogen bubbles are formed in the first stages of cement hydration, thereby creating a macroporosity. Further hydrogen generation in the material makes it subject to a risk of cracking if the gas cannot be released from the matrix.

## Phase separation

Some compounds do not show a good miscibility with the cement paste due to a polarity or density deviation. Such is the case of highly hydrophobic pulverulent graphite and magnesium (density of  $1.74 \text{ g}\cdot\text{cm}^{-3}$ ), two constituents of waste arising from the natural uranium graphite gas (UNGG) reactor system. This may result in an embedded waste heterogeneity unacceptable for disposal. Adding surface-active molecules improves graphite dispersion. Magnesium flotation is limited by selecting a high-viscosity formulation which helps fast setting.

## Defining an embedding material formulation

Figure 62 gives an overview of how an embedding formulation is developed, with the various steps.

Multiple parameters are involved in developing the embedding material formulation and investigating its robustness. Hence the use of experimentation plans to help define efficient experimental strategies.

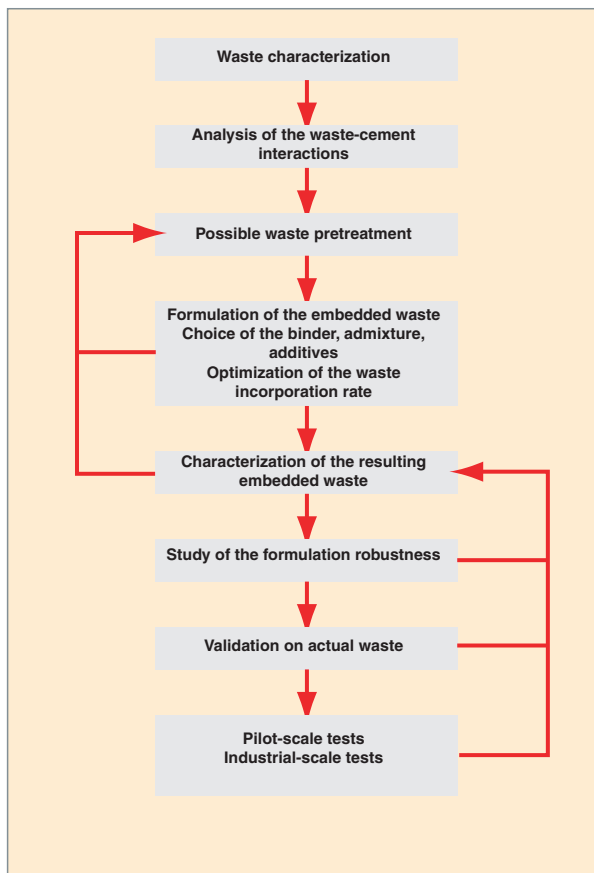


Fig. 62. General process for the formulation of a cementitious material designed for waste embedding.

Only the more informative experiments with respect to the aims fixed are achieved in the research area. The number and cost of the tests are therefore reduced.

Operational models are built in order to predict the embedded waste properties as a function of the formulation parameters or the waste composition. They may eventually be used to perform a multicriteria optimization of the formulation or to check through calculations that the embedded waste meets the specifications for all of the waste composition range (Fig. 63). Last but not least, these models might constitute an attractive tool for operating a conditioning workshop as they would enable the operator to gather waste streams under optimized conditions.

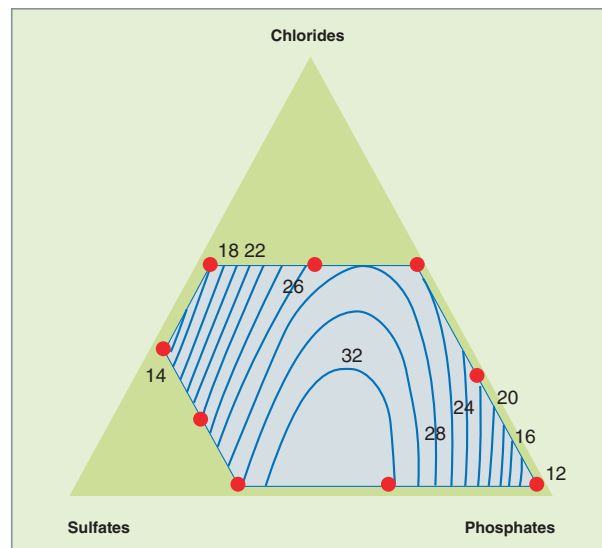


Fig. 63. Study of the sensitivity of an embedding formulation to the variation of the cemented waste composition. Iso-response curves, plotted in blue, are based upon a predictive model which couples the initial setting time (in hours) of the embedded waste to the waste concentrations in chlorides (1-20 g/L), sulfates (0.8-27 g/L), and phosphates (1-50 g/L).

## Finding new alternatives to improve conditioning

Using hydraulic binders as immobilization materials perfectly meets waste producers' needs; this operation is well controlled on the industrial scale and, as a consequence, has not spurred new developments. Yet, research work on embedding matrices is generally conducted in collaboration with waste producers, with a view to increasing waste incorporation rate and improving confinement performance of cementitious materials, bearing in mind two factors: the increase in waste volume after conditioning, and possible interactions between some waste constituents and cement phases, likely to upset cement hydration and influence the durability of the materials obtained.

### Better understanding of cementitious phase-waste interactions for better environment control

Phosphates are often present in variable concentration in the evaporator concentrates of effluent treatment stations. Immobilizing this type of waste in cement raises an issue, for phosphate ions are known to retard cement setting and deteriorate its mechanical properties. As part of a collaboration with the Institut Carnot de Bourgogne, the CEA has investigated the influence of orthophosphate ions on the hydration of a high-silica-content Portland cement commonly used for waste conditioning [2].

The hydration of cement pastes mixed with sodium phosphate solutions in increasing concentration was followed using isothermal microcalorimetry. This technique gives a general insight into thermal activity and provides information on binder hydration kinetics. For concentrations between 0 and 50 g/L, phosphates retard hydration, but not continuously and with a pessimum level towards 30 g/L (Fig. 64).

This 30 g/L concentration is found as a threshold value in dynamic rheometry experiments following cement paste structuration. As shown in Figure 65, e.g., referring to Time “100 min” after mixing, the elastic modulus first decreases as the concentration increases from 0 to 30 g/L, and increases beyond. The effect of phosphate ions on cement hydration kinetics could be explained with two opposite effects: under 30 g/L, the prevailing effect would be phosphate ion adsorption onto tricalcium silicate, which would block the silicate hydration. That would account for the delay observed in cement setting. Above 30 g/L, the precipitation of a calcium phosphate (hydroxyapatite) would also take place, inducing an increase in the elastic modulus of the cement paste. The concomitant depletion of the calcium solution would also explain the resumption of hydration acceleration.

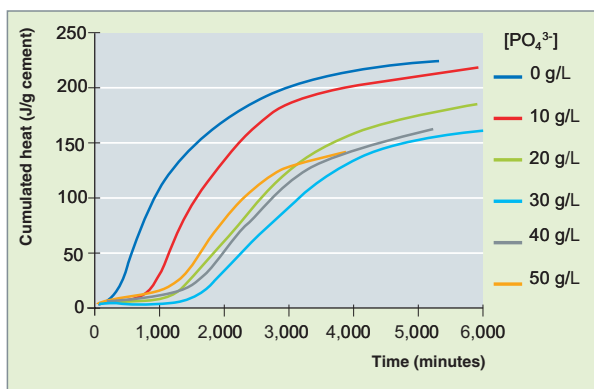


Fig. 64. Influence of the phosphate concentration of the mixing solution upon the hydration kinetics of a CEM I cement paste (water weight / cement weight = 0.3). [2]

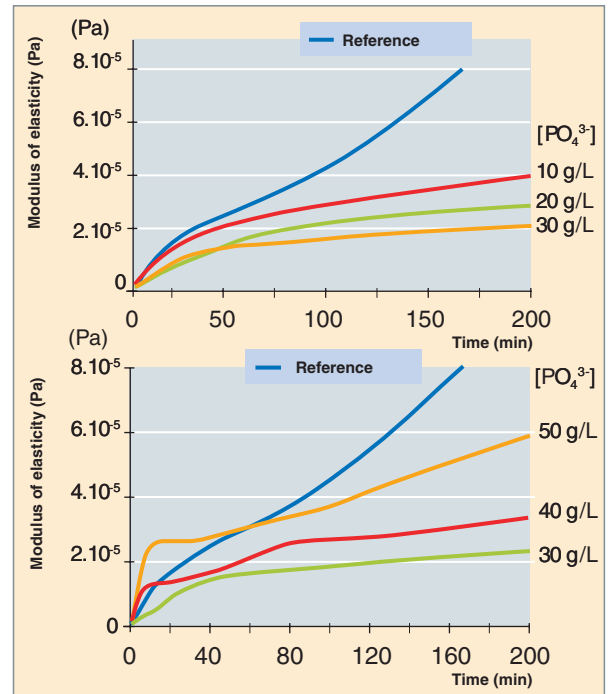


Fig. 65. Influence of the phosphate concentration of the mixing solution upon the structuration of Portland cement pastes (water weight / cement weight = 0.3). [2]

A possible solution derived from this study could be adding a small amount of hydroxyapatite to the binder, in order to improve the conditioning of phosphate solutions which significantly delay Portland cement hydration. This amount would act as a growth basis and would therefore foster phosphate ion precipitation, thereby reducing their adsorption onto calcium silicate dissolution sites. The investigation of cement pastes mixed with a sodium phosphate solution of 20 g/L confirms that the delay in hydration is strongly reduced by seeding the paste with hydroxyapatite crystals (Fig. 66).

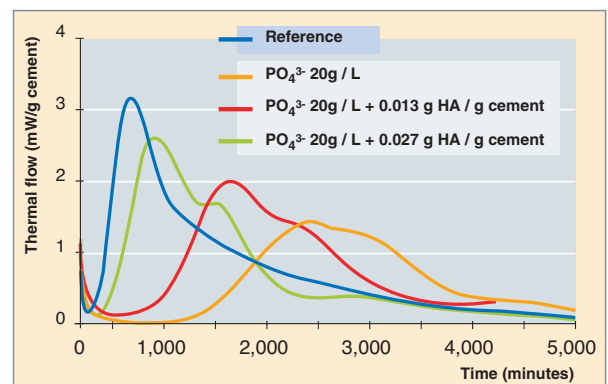


Fig. 66. Influence of the addition of hydroxyapatite seeds upon the hydration kinetics of cement pastes mixed with a solution of sodium phosphate (20 g/L). Phosphate ions slow down cement hardening, but adding hydroxyapatite seeds makes it possible to restore the process satisfactorily. [2]

### Calcium sulfoaluminate cements: cements with low hydration inhibition by heavy metals and borate ions

The usual strategy to limit the harmful effect of a waste upon a hydraulic binder hydration consists in turning the penalizing constituent(s) into a form which is thermodynamically stable in a cementitious medium. One alternative to avoid such pre-treatment would be using a binder with better chemical compatibility with the waste than calcium silicate cements. Sulfoaluminate cements might offer promising prospects for embedding waste with a high content of borate or zinc ions, the latter being two inhibitors of Portland cement hydration.

Sulfoaluminate cements are manufactured in two steps, (i) first calcination of limestone, bauxite, and gypsum mixture at 1,300-1,500 °C, then (ii) intergrinding the resulting clinker with gypsum, the content of which (up to 25%) may be far higher than in Portland cement (3-5%). They mostly consist of yeelimite ( $4\text{CaO}\cdot 3\text{Al}_2\text{O}_3\cdot \text{SO}_3$ ), gypsum, dicalcium silicate, and a ferritic phase. These cements mostly lead, through hydration, to the formation of ettringite ( $3\text{CaO}\cdot \text{Al}_2\text{O}_3\cdot 3\text{CaSO}_4\cdot 32\text{H}_2\text{O}$ ) and/or calcium monosulfoaluminate hydrate ( $3\text{CaO}\cdot \text{Al}_2\text{O}_3\cdot \text{CaSO}_4\cdot 12\text{H}_2\text{O}$ ), and, in smaller amounts, of calcium silicate and aluminate hydrates. A higher gypsum content of the binder enhances ettringite formation, whereas a low content induces the formation of calcium monosulfoaluminate hydrates.

Their properties vary with clinker composition and gypsum percentage, which allows for the formulation of a wide range of materials, including expansive cements as well as rapid-setting and hardening cements.

In the general context of the cement industry's durable development, sulfoaluminate cements stand as an interesting alternative to address the growing environmental concern for lower carbon dioxide emissions. Gains are expected due to the following set of factors:

- a clinkering temperature 100-150 °C lower than for Portland cement;
- a favorable stoichiometry, as yeelimite formation goes along with a lower  $\text{CO}_2$  release than dicalcium or tricalcium silicate formation;
- a clinker which can be ground more easily;
- the possibility to upgrade industrial residues such as slag or fly ash as raw materials.

As shown by recent results, sulfoaluminate binders could even prove to be attractive for the conditioning of zinc-containing waste such as ash arising from some technological waste incineration. Zinc is of little trouble for sulfoaluminate cement

hydration: no blockage of cement setting could be observed, even for an extreme zinc concentration of 1 mol/L in the mixing solution (Fig. 67). Conversely, the setting of Portland cement would be fully inhibited in such conditions. Besides, standardized mortars made from a sulfoaluminate binder with a gypsum content of 20% and a zinc chloride solution with a 0.5 mol/L concentration exhibit highly satisfactory properties over the 90 years of the investigation period:

- rapid hardening and high mechanical strength: compressive strength reaches 37 MPa after only 24 hours of hydration in a climate cell at 20 °C and a relative moistness of 95%, whereas for the same material prepared from a Portland cement setting could not have occurred by this deadline;
- very high confinement power of zinc: as shown in batch leaching tests performed on a material ground to less than a 100- $\mu\text{m}$  grain size, zinc concentration released in the solution is lower than 0.1 mg/L, which is the limit of detection for the analysis method used;
- low dimensional instability: when stabilized to 800  $\mu\text{m}/\text{m}$ , expansion under water does not exceed by more than 200  $\mu\text{m}/\text{m}$  that of the reference material prepared without zinc chloride.

Preliminary tests with nonradioactive ashes have shown that their rate of incorporation into the embedded waste could be presumably multiplied by two in contrast with present formulations, thereby reaching 10-20 wt%.

In the very case of a complex chemistry waste resulting from the mixing of a chemical co-precipitation sludge and an evaporation concentrate of 600 g/L salinity, it is worthwhile to men-

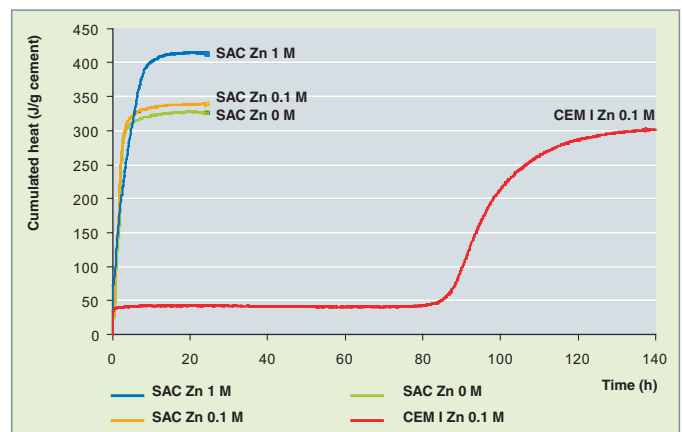


Fig.67. Influence of the zinc chloride concentration in the mixing solution upon the hydration kinetics of standardized mortars prepared from Portland cement (CEM I) or sulfoaluminate cement (SAC) with a gypsum content of 20%. Contrary to that of Portland cement, the setting of the sulfoaluminate cement is not inhibited by zinc chloride.

tion a significant breakthrough. Despite a high boron concentration in the waste liquid phase, direct waste cementation proved to be achievable with a binder containing 70% sulfoaluminate clinker and 30% CEM I Portland cement. In contrast, taking an ordinary Portland cement, the same concentration would have allowed the setting to be delayed by more than one week. Besides, two enhancements were brought to the reference process: the waste pretreatment step could be dropped and the waste incorporation rate into the embedded waste could be increased by a 1.8 factor.

### Bétons à bas pH pour le scellement des stockages de déchets

The study presented herein does not deal with waste embedding. As in previous examples, the aim is to develop a binder chemically compatible with the environment where it is located.

In the concept of long-lived intermediate-level waste deep disposal which is being investigated by the ANDRA, the sealing of a disposal cell is achieved using a swelling clay plug (bentonite) supported by two concrete blocks (Fig. 68) [3]. In this case two difficulties would have to be faced if using a Portland-cement conventional concrete:

- after percolation through this material, water would be highly alkaline and, so, very aggressive to clay, so that it would be likely to degrade its confinement properties;
- the high increase in temperature induced by cement hydration in the support block could give birth to microcracks harmful to the structure durability.

Investigations have been undertaken with the support of EDF and ANDRA in order to formulate a material complying with the following criteria:

1. a pH lower than 11 for the interstitial solution of the hydrated material in order to reduce clay alkaline attack (hence the name of “low-pH concrete”);
2. low heating during binder hydration (with a temperature increase lower than or equal to 20 °C on mortar in semi-adiabatic conditions);
3. high mechanical performance (i.e., a compressive strength higher than 70 MPa in the long term), as a durability factor for the structures built;
4. moderate shrinkage (<300 µm/m);
5. constituents easy to supply.

The most promising alternative seems to be pozzolan addition to a Portland cement which may have been mixed with slag [4]. For pozzolan compounds react with portlandite, a high-solubility phase requiring an approximate 12.5 equilibrium pH, thereby forming calcium silicate hydrates in which the Ca/Si ratio may be lower than that of Portland cement hydrates, hence a threefold benefit:

- the portlandite formed by Portland cement or slag hydration may be fully consumed if the type and proportion of pozzolan have been correctly chosen;
- alkaline element concentration in the interstitial solution may be reduced since the C-S-H ability to sorb Na<sup>+</sup> and K<sup>+</sup> ions increases as the Ca/Si ratio decreases;
- the equilibrium pH of the C-S-H decreases with the Ca/Si ratio.

After one year of hydration the interstitial solution of the “low-pH” cement pastes displays a pH between 11.7-12.2 according to the formulation, i.e., one unit lower than the reference Portland cement-based concrete specimens. This pH decrease goes along with a significant decrease in the alkaline element concentration of the pore solution. This result is interesting for the prospect of limiting, or diluting the alkaline plume generated by low-pH materials during the disposal site resaturation by water.

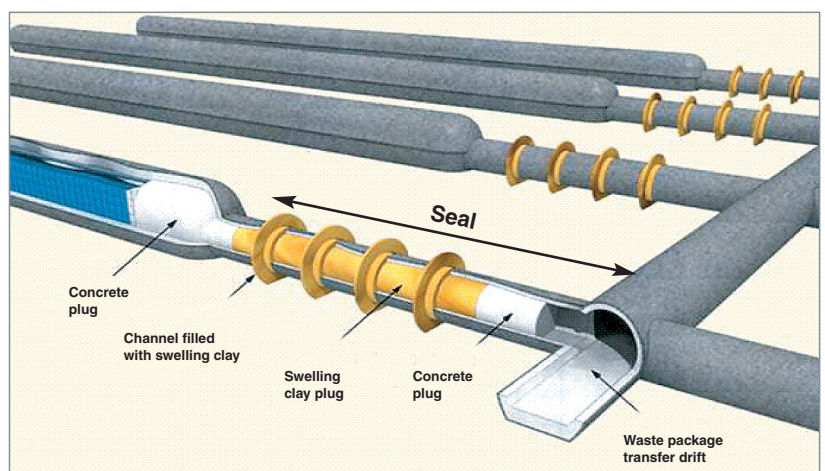


Fig. 68. Sealing principle for long-lived intermediate-level waste disposal cells, as proposed by ANDRA [3].

Dimensions:

- from the cell bottom to the first concrete plug: 200 m, for a drift diameter of about 11 m;
- seal: 50 m long for a 6-m diameter;
- access drift diameter: about 10 m;
- swelling clay core: about 35 m.

Last but not least, these binders would be successfully used to formulate concretes of sufficient workability likely to undergo low heating during hydration and show a compression resistance higher than 70 MPa after a 90-day curing (at 20 °C and with a relative moistness of 100%).

The material is made with a ternary binder consisting of Portland cement / silica fume / fly ash. It also displays dimensional variations under air (-400 µm/m) and under water (+50 µm/m) comparable to those of a Portland-cement standard concrete, and the pH of its interstitial solution reaches a value of  $11.0 \pm 0.3$  after 20 months in compliance with the prescribed specifications.

To sum up it all, the complexity of cementitious matrix formulation results from the following items:

- the huge diversity of the waste to be conditioned;
- the cement/waste interactions liable to degrade the quality of the resulting embedded waste;
- the specifications to be met for the final material, which depend upon its implementation process and its disposal conditions.

The improvements achieved originate in:

- a formulation process rationalized;
- a better understanding of the behavior of some waste constituents in a cementitious medium;
- newly developed binders likely to afford solutions tailored to specific waste conditioning or ensure better compatibility with the environment.

## Concrete containers

The container common to long-term **storage** and **geological disposal\***, jointly developed by the CEA and the ANDRA, stands for the external envelope in which several waste primary packages are placed. This container allows waste storage and disposal operations to be made rational and reliable through reducing the number of handled item flows, as well as standardizing the dimensions and handling modes of these items. As it is made of a low-alteration material, the common container allows for a possible waste retrieval over several hundreds of years for disposed waste, and over a 100-300 year timescale for stored waste (Fig. 69).

### Waste characteristics

Storage/disposal common containers are designed to house the whole inventory of Long-Lived Intermediate-Level (IL-LL) waste, i.e., all the types of primary packages identified in the Andra's inventory model (the so-called "MID", standing for "Modèle d'Inventaire et de Dimensionnement"). Six types of packages have been retained (Table 13).

The common container must be able to cope with the specific problems raised by any of these packages.

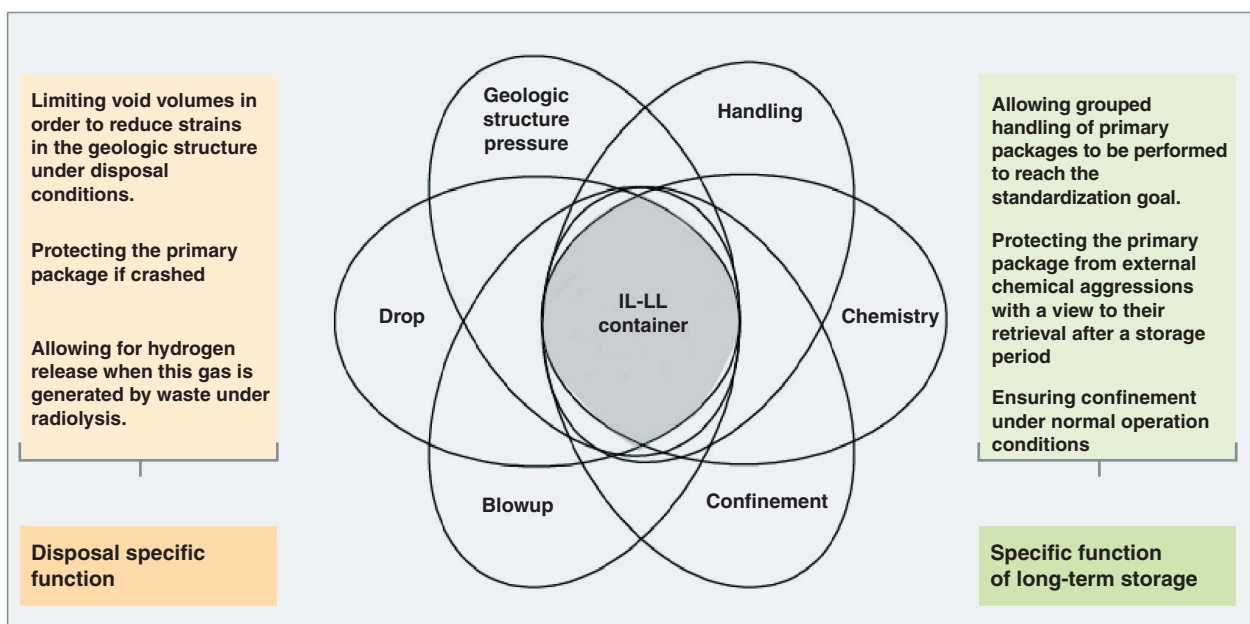


Fig. 69 : The functions of the concrete container.

Table 13.

The six waste package types likely to be conditioned in a concrete container.	
Families	Denomination
B1	Activated metal waste packages
B2	Bituminized sludge packages
B3	Cemented technological waste packages
B4	Cemented hulls and nozzles packages
B5	Compacted structural and technological waste packages
B6	Structural and technological waste packages in bulk containers

### Standard concrete container

The container body is a parallelepiped (Fig. 70). It also includes four housings designed to contain four primary packages. Its shape is adapted to the disposal cell size (Fig. 71).

Two concretes have been developed in order to comply with functional requirements, one for the container body, the other for its lid which is designed to allow for radiolytic gas release as a specific function. In the latter case, material porosity is enhanced by increasing water content and eliminating silica fume. The common feature of the two concretes is displaying metal reinforcements meant to improve their mechanical behavior: hook fibers and stainless steel bars. This characteristic enables container durability to be improved by limiting the impact of corrosion on concrete.

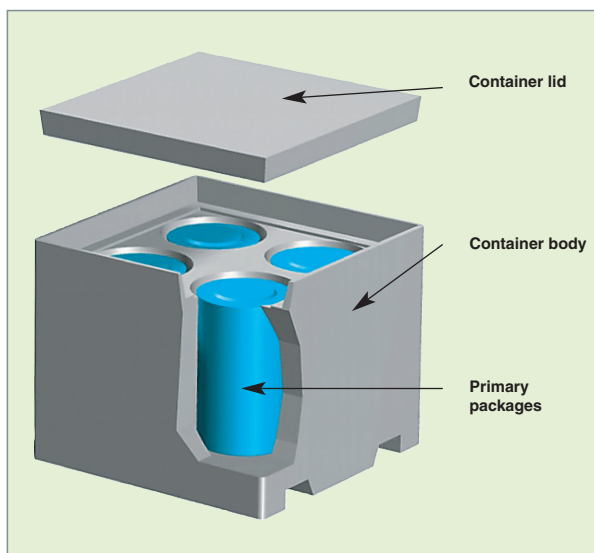


Fig. 70. The standard concrete container.

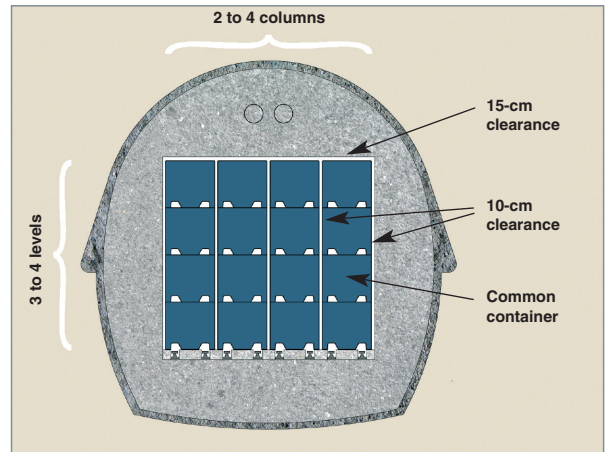


Fig. 71. Sectional view of a disposal cell (ref. ANDRA).

The lid is inserted in the top of the container body. The body walls thus go up to the lid level and support most of mechanical stresses under conditions of stacking. The body and lid are coupled by mortar and rods anchored within the body and screwed on the lid (Fig. 72).

Validation of material design and selection required to set up scale-1 demonstrators under industrial conditions, as well as develop various characterization tests in order to measure the container performance relevance to the attributed functions (durability, hydrogen release, mechanical behavior, handling). Two of these characterizations are developed hereafter.

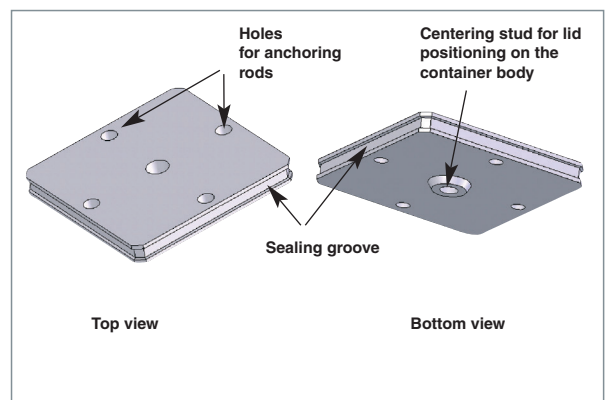


Fig. 72. Basic diagram of the container lid (ref. ANDRA).

## Container drop behavior

Containers in storage or disposal facilities are stacked on top of each other on four floors. Consequently there is a potential risk for containers to undergo a drop from more than the height of a pile, i.e., 6 meters. Primary packages can withstand a high-impact drop due to their mechanical behavior. It is however necessary to check whether degradations induced on the outer concrete container are likely to result in the dissemination of the elements contained in primary packages and, thus, the degradation of the latter's retrieval functions.

In order to limit the number of tests, two drop configurations deemed to be highly penalizing to the primary package behavior have been selected. The first one mimicks a drop on the upper corner of the container, the second a drop on a top edge. Drop height is fixed at 6 meters from the container lowest point along an axis passing through the container center of gravity so as to avoid its rotation during the drop. Especially penalizing conditions have been retained as the surface onto which the container is to drop is the top of a very rigid slab 4 m thick overheaded with a very rigid 100-mm thick plate. The drums used as container test load are actual stainless steel drums arising from industrial manufacture and filled with a mixture of thin sand (grain size  $< 350 \mu\text{m}$  as in embedded radioactive salts) and bitumen produced at the Marcoule effluent treatment station. As a result, density, filling rate and mechanical properties are identical to those of an actual waste drum. Every drum is filled to 80% of its height up to a 240-kg mass.

The containers are dropped using a pyrotechnic mechanism.

During the corner drop test, the mechanical behavior of the concrete envelope can be followed with the help of fast camera shots. The first fact to be observed is the rapid crushing of the corner along with concrete bursting and dissemination of the resulting fragments over several dozens of meters. This crushing is then suddenly stopped and strains are then displayed by two mechanisms: an overall shearing effect in the container and the cracking of its side walls induced by the shock wave spreading (Fig. 73). After filtering at 2 kHz, maximum decelerations recorded by the accelerometers for this test configuration are of the order of  $500 \text{ m}\cdot\text{s}^{-2}$ .

Few steel ruptures can be observed, which is a very favorable factor for the container integrity protection. The cell volume is well preserved on the average. Save for the impact area the lid undergoes little damage and the cracks that may be observed on it are very narrow (less than 0.1-0.2 mm).

Cracks on the container side faces are oriented  $45^\circ$  and open across a few millimeters. The jointing area is crossed by a crack in the area neighbouring the edges in contact with the impact area.

Following every test, the lid is cut off using diamond tools so as to access to the primary packages and check the inner part of the containers. The main overall shear cracks of the container are localized within the container. Yet damage to concrete is limited: few debris resulting from the drop can be found at the bottom of the cells.

Inspecting the bituminized waste packages after retrieval shows that they are not punctured and the general state of the envelope on the whole circumference is still reliable (Fig. 74). It can be observed in the impact area that the package top has collapsed by a few millimeters, and stainless steel undergoes local plastification. These degradations, however, do not affect the retrievability of packages.



Fig. 73. Container B2.1 as resulting from a drop test, after lid removal.



Fig. 74. Bituminized packages removed from the concrete container after corner drop test.



What makes the edge drop test different from the corner drop test is the higher deceleration which the container is subjected to. The evolution of the contact surface is far less progressive indeed in this configuration, which significantly enhances the shock: in this case decelerations are about 2,000 m.s<sup>-2</sup>. Besides, rupture mechanisms are slightly different: cracks oriented parallel to the drop axis can be observed, following the shock wave propagation, as well a shearing of the container body relative to the lid.

As the concrete areas affected on the periphery of the container are the thinnest, the role of reinforcing bars and stringers proves to be essential in drop behavior. The head of one of the stringers was torn out during a test, which gives a good example of the extreme stress level which they are subjected to. The container body residual motion relative to the lid is 6 cm. In contrast, the coupling between the two components is still robust, since the container can be handled in an upside down position with no additional damage.

### Gas diffusion in cementitious materials

The common container is designed to house very different types of primary packages. Therefore, it must be likely to meet the specific requirements which characterize them. Particularly, most of primary packages generate gases (hydrogen mainly) as a result of the radiolysis affecting embedding matrices and organic technological waste. These gases have to be removed to ensure container integrity and limit explosion risks associated with high hydrogen concentration in the container gas cover plenum.

In this context, selecting concrete as a constituent of the common container enables hydrogen to access to the open porosity network formed during the material set and hardening, and migrate through it.

### Pore structure in cementitious materials

The cement paste is a polyphase material, consisting of a mixture of residual, non porous grains of anhydrous cement, interstitial solution, and gas. Multiscale porosity resulting from the material texture generally falls into two families [5]:

- capillary porosity, which corresponds with residual space not filled by hydrates which initially separates anhydrous cement grains. Capillary porosity strongly depends upon the initial (mixing) water-to-cement ratio (w/c) (by weight), anhydrous cement fineness, and the amount of porous hydrates in the material, i.e., the age and chemical composition of initial reactants. Capillary porosity evolves with time along with hydrate precipitation, which results in a porosity with topological and morphological complexity;
- hydrate pores, mostly involved in the development of calcium silicate hydrates (C-S-H), which are the main cement paste

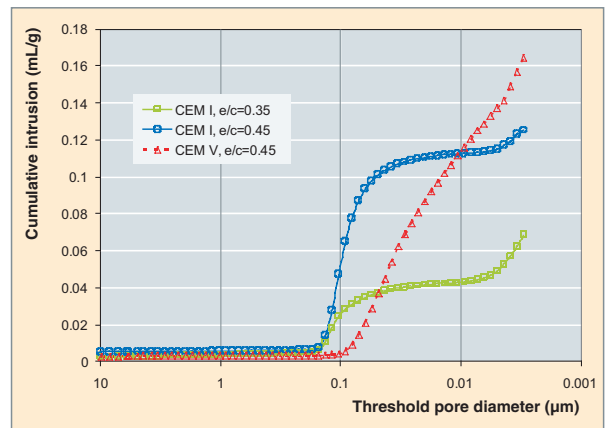


Fig. 75. Cumulated volumes of pores accessible to mercury, as obtained in cement pastes. Pastes of type CEM I display two pore classes respectively of about 0.1 µm and a few nanometers. In pastes of type CEM V, which include additives with a very thin grain size, the pore size distribution is more homogeneous and displays smaller sizes.

hydrates. The C-S-H are often described as amorphous aggregates of nanometric colloidal nodules displaying a sheet structure and are thus intrinsically porous. This porosity is practically independent from the w/c ratio, but varies with the chemical nature of anhydrous cement.

These main differences are illustrated by the curves of mercury intrusion porosimetry in Figure 75. For the same chemical composition of anhydrous cement, variation in the w/c ratio results almost exclusively in alterations in capillary porosity: for the same threshold pore diameter (also called “critical pore diameter”), capillary pore volume sharply increases from a CEM I cement paste of w/c ratio = 0.35 to a CEM I cement paste of ratio w/c = 0.45. Considering different chemical compositions of cementitious materials, herein CEM I and CEM V, the pore volume and distribution are strongly altered for a given w/c ratio, which means a fairly different organization of the material during its texturing. The threshold pore diameter of the CEM V cement paste is fairly lower than those measured on the CEM I cement paste.

Furthermore, concrete microstructure is significantly different from that of pure paste. For adding aggregates to the material formulation strongly alters anhydrous cement grain distribution in the vicinity of these aggregates. Hence the emergence of a transition ring, an area featuring higher porosity and a preferential orientation of hydrates.

This complex porosity area will be the medium through which gases generated during package radiolysis will be released to the environment.

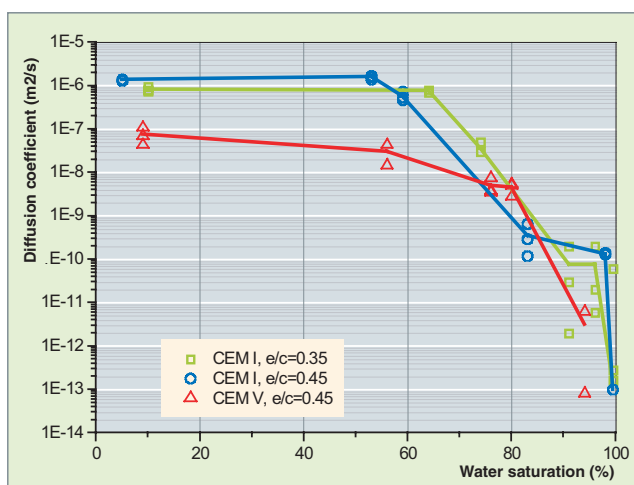


Fig. 76. Variation of the hydrogen diffusion coefficient in cement pastes versus the material saturation in liquid water. For a cement in storage conditions, the expected saturation ranges between 80 and 90%; for a container in deep geological disposal conditions, it is close to 100%.

### Gas transport and cementitious material saturation

As gas transfer is mostly induced by the hydrogen partial pressure difference between the inner envelope and the surrounding environment, the gas transfer mechanism encountered is mainly diffusive. Given the very low gas solubility in water, transport has to be ensured through an interconnected gas phase which percolates from the inner face to the outer face of the concrete container. The material saturation state is therefore of great importance, since preferential paths for gases depend upon this state, hence the evolution of the gas diffusion coefficient by several orders of magnitude (Fig. 76). Hydrus equilibrium, the total water amount, and its distribution among the pores mostly depend upon the outer environment of concrete, especially upon relative moistness [6] and temperature.

As regards gas diffusion through cementitious materials, the most important microstructural factors are the critical pore diameter and the capillary porosity volume.

When there is a pressure gradient within a cementitious material, permeation calculations show that under the hygrometric conditions expected to prevail under storage conditions, one square meter of a 15-cm thick concrete wall will let out about 1 millimole hydrogen per hour under a pressure gradient of 1 atmosphere. This “discharge capacity” will probably be sufficient to avoid radiolytic gas pile-up in the concrete container under dry-storage conditions. It will not be so for a container under geological disposal conditions. For a pressure increase will then be expected inside the container up to a level depending on the radiolytic gas generation rate. The extent and consequences of such pressure increase are still to be assessed.

## Irradiation effects in cementitious matrices

Whatever structural concretes of radioactive waste conditioning materials, cementitious matrices encountered in the back-end of the fuel cycle may undergo ionizing radiation effects.

On the average Portland-cement-based or aluminous concretes exhibit good behaviour for cumulated doses up to  $10^{10}$  or even  $10^{11}$  Gy, with no mineralogical transformation. In particular, the Ca/Si ratio of calcium silicate hydrate (C-S-H), the main hydrate in Portland cement pastes, remains unchanged.

Concerning some legacy packages of cemented hulls and nozzles, which release a hundred watts, thermal effects resulting from irradiation may entail a change in microstructure, creep, and the cementitious matrix desiccation. Conversely, as regards cemented waste generated at the present time, which release less than a few dozen watts per package, these thermal effects are negligible and, generally, their consequences are not to be feared.

As a matter of fact, irradiation consequences mostly emerge as the residual water radiolysis and gaseous dihydrogen emanation. The latter raises a safety issue in itself for cemented waste package management under storage or disposal conditions (hydrogen build-up in the package environment or overpressure in packages likely to make them burst). Of little impact in most cases, radiolytic  $H_2$  emanation proves to be significant only for some package families featuring a high  $\beta\gamma$  activity (fuel clads or activated control rod hulls up to  $10^{15}$  Bq per package), or a high  $\alpha$  activity (process sludges up to  $10^{11}$  Bq per package). Nevertheless, owing to their high number, lower-activity packages as a whole generate gas volumes to be taken into account in the design basis and ventilation of storage and disposal facilities.

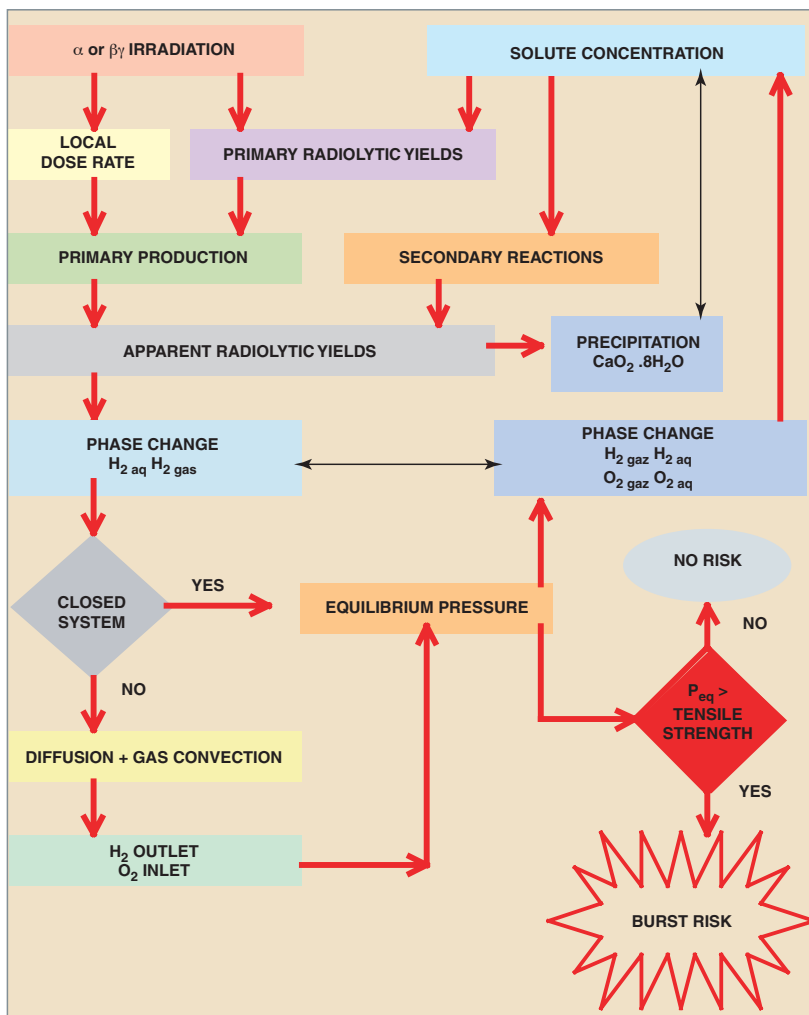


Fig. 77. Physico-chemical parameters and the related couplings involved in the radiolysis which occurs in cemented waste packages: the heterogeneous (solid-liquid and liquid-gas) equilibria are shown in thin lines.

### A prevailing phenomenon: water radiolysis in the cementitious matrix

Radiolysis is a chemical decomposition under irradiation. Only 2% of the total energy deposited by radiation within the material are turned into chemical energy, the latter 98% being degraded as heat.

Thus radiolysis is no more than a broad-amplitude effect of radiation-matter interaction. Only with sufficient radiation intensity (respectively towards  $10^{-3}$  and  $10^{-5}$  Gy/s for  $\beta\gamma$  and  $\alpha$ ) does its impact becomes significant, possibly combining then with heating effects. Contrary to the radiolysis of such organic matrices as bitumens or polymers, cementitious matrix radiolysis is strictly linked with the radiolysis of the water contained in the latter. During the radiolysis process, highly depending on medium porosity and mineralogical context, three components can be pointed out:

- **energy deposition**, induced by a radioactive source term which is most often internal and multi-emitting;
- **chemical reactions** in hyperalkaline solution ( $\text{pH} > 13$ ) in presence of calcium;
- **transport of the reactive gases** generated or consumed by radiolysis: mainly  $\text{H}_2$  and  $\text{O}_2$ .

The phenomenon starts with water primary decomposition. This step is nearly instantaneous ( $10^{-6}$  s). It must be emphasized that water decomposition does not depend upon the water amount involved (zero-order kinetics), and varies as the radioactive source term evolves. Then come secondary chemical reactions, phase changes (solution/gas and solid/solution) and gas transport. They may deeply alter the result of the primary step by their complex feedbacks in the short, medium, and long term.

The basis of the whole radiolytic physico-chemistry lies in the generation of the six primary species ( $e_{\text{aq}}^-$ ,  $\text{H}$ ,  $\text{OH}$ ,  $\text{HO}_2$ ,  $\text{H}_2\text{O}_2$ , and  $\text{H}_2$ ) is equal to the product of the dose rate by the specific primary yield of each species (which expresses radiation efficiency with respect to water decomposition). As dose rates and primary yields are specific to the radiation type, primary source term may become rather complex according to the radiological inventory occurring in the radioactive waste package matrix. For example, for  $\text{H}_2$ , primary production kinetics under multiple irradiation  $\alpha \beta \gamma$  takes the following form:

where  $c$ ,  $G$ , and  $D'(t)$  respectively represent a conversion coefficient, the primary yield, and the dose rate at time  $t$  for a given radiation.

$$\frac{d[\text{H}_2]}{dt} = c \cdot (G_{\text{H}_2}^\alpha \cdot D'_\alpha(t) + G_{\text{H}_2}^\beta \cdot D'_\beta(t) + G_{\text{H}_2}^\gamma \cdot D'_\gamma(t))$$

Considering the case of pure water radiolytic decomposition, the species produced at the primary step are involved in more than 60 reactions (including acid-base equilibria).

These reactions result in the secondary generation of molecules and radicals, either already known as primary products,

These reactions result in the secondary generation of molecules and radicals, either already known as primary products,

or new ( $O_2$  and  $O_3$ ). The presence of solutes arising from the cementitious medium (iron, sulfur) or from waste (nitrate, chloride, etc.) can make this basic design particularly more complex with several hundreds of additional reactions.

Within the cementitious matrix, dihydrogen initially generated as an aqueous phase turns to a gaseous state in the pore fraction unoccupied by the interstitial solution (Henry's law). Cumulated  $H_2$  in the matrix induces total or partial pressure gradients which respectively result in advective transports ("Darcy law") or diffusive transports ("Fick law") if the system is open to the atmosphere. In this case, atmospheric dioxygen inlet into the matrix leads to an aerobic evolution which favours the simultaneous generation of  $H_2$  and  $O_2$  as well as  $H_2$  outlet.

### Radiolysis effects

The high heterogeneity of the cementitious matrix, and the diversity and complexity of the phenomena involved (Fig. 77) result in a fairly nonlinear behavior of radiolysis, along with the further contribution of couplings and feedbacks between chemistry, decreasing radioactive source term, gas phase transport, solid precipitation, and temperature.

Because of these feedbacks, it proves very difficult to predict the radiolysis consequences upon cemented waste.

Concerning simulations relating to the overall description of package-scale radiolysis over a long time, their relevance depends on the number of elementary mechanisms taken into account in the modelling and quality of the data characterizing each of these mechanisms. These basic data fall into two main categories:

- package geometry and composition;
- physical or chemical elementary phenomena.

Generation of radiolytic  $H_2$  outside packages is much dependent on several variables. The first and most important is the **dose rate\***, which induces radiolysis: the higher the energy deposited in water, the higher the water amount decomposed and the  $H_2$  amount produced. The second is the system confinement, which determines whether a steady regime or an equilibrium pressure may be possibly reached. Other factors are involved as well, such as the radiation nature. For all radiations do not generate the same radicals in the same proportions. The pore saturation degree and the ratio  $H_{2\text{aq}}/O_{2\text{aq}}$  are also involved. These factors and their influence upon hydrogen generation are summed up in Table 14.

Given the diversity of conditionings and the specificity of operating conditions, measuring source term  $H_2$  for all package types cannot be contemplated. Using simulation is a must assuming that an integrated model is available, likely to manage a minima the radiological inventory evolution, in-solution reactions, homogeneous and heterogeneous equilibria, and gas transport. Developed at the Physico-Chemistry Department [7], the model DO-RE-MI (an acronym standing for *Description Opérationnelle de la Radiolyse de l'Eau dans les Matériaux Irradiés*: operational description of water radiolysis in irradiated materials) simulates radiolysis over several hundred years and evaluates the hydrogen amounts generated. Furthermore, simulation provides a tool for better understanding as it enables various configurations to be tested. The following prospective example shows how mixed radiation fields may influence radiolysis process.

When cemented waste packages display a complex radiological inventory with fission (or activation) products and actinides (fuel clads, for example), radiolysis follows a sequence where the  $\beta\gamma$  emissions of the first (short-lived isotopes) first prevail over the  $\alpha$  emissions of the second (long-lived isotopes) *prior to decrease significantly*. In the long term the initial trend of radiolysis is fully reversed, going from type  $\beta\gamma$  to type  $\alpha$ . This configuration can be simulated coupling, e.g., a short-lived  $\beta\gamma$ -emitter (Co 60,  $T_{1/2} = 5.27$  years) with a long-lived  $\alpha$ -emitter (Am 241,  $T_{1/2} = 432.6$  years) and attributing a dose rate a hundred times higher to the first one. Under these conditions, with a dose rate  $D\dot{\gamma} = 10^{-2}$  Gy/s, radiolysis simulation in a closed

Table 14.

The main variables controlling radiolysis in cemented packages and the related parameters				
Rank	"Variable"	Mode	Influence	Related parameters
1	Dose rate	Low High	Generation of small $H_2$ amounts Generation of high $H_2$ amounts, non-proportional to the dose rate	Primary yields
2	Closed/open system	Closed Open	Internal $H_2$ generation, with partial destruction External $H_2$ generation	
3	Saturation porosity	Low High	Increased gas exchange ( $O_2$ ), $H_2$ attack	Powers parameters
4	Precipitation $CaO_2 \cdot 8H_2O$	Without With	Evolution in a homogeneous solution Mineralogical control of the solution	$K_s$ , dissolution kinetics

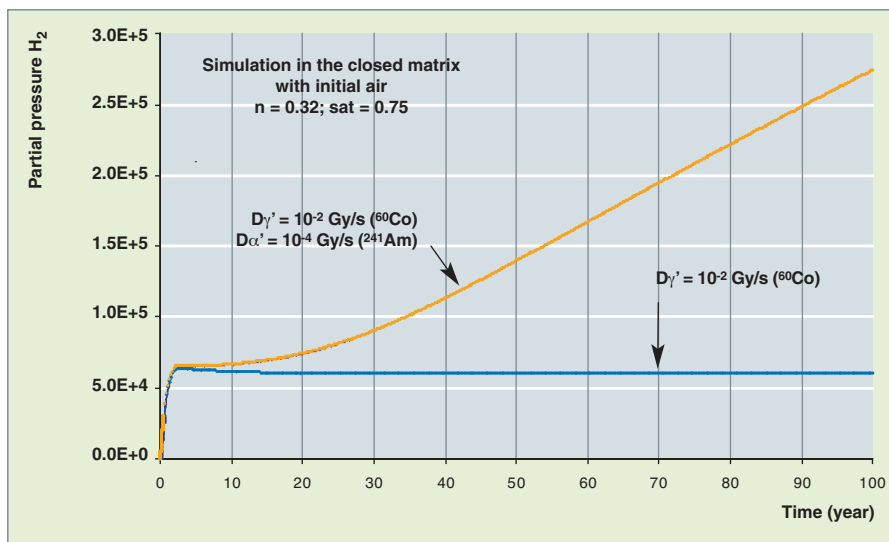


Fig.78. Compared evolution of the total effective amount of radiolytic hydrogen in the cementitious matrix of a closed package for a  $\gamma$  or mixed  $\gamma + \alpha$  source term.  $n$  and  $sat$  respectively stand for the porosity and liquid saturation degree taken into account in the model DO-RE-MI.



Fig. 79. "ERMITE" experiment: assembly of three 500-cm<sup>3</sup> mini-containers filled of cementitious material prior to being introduced into the irradiation device.

system leads to an identical evolution of partial pressures in early lifetime, with or without  $\alpha$  activity, for 10 years approximately. A drastic change in behavior occurs later on. When comparing the (aqueous + gaseous) H<sub>2</sub> amounts stored in the matrix (Fig. 78), it can be assumed that in presence of a mixed  $\alpha\gamma$  source, the loss of the long-term regulating effect is related to the unavailability of oxidizing radicals O<sup>-</sup> and OH<sup>\*</sup>, which alone are able to attack dihydrogen. For these radicals are produced massively by  $\gamma$  radiolysis and, in a very small proportion, by  $\alpha$  radiolysis.

Model checking requires to perform tests on simplified systems, such as

Test "ERMITE" (an acronym standing for *Expérience de Radiolyse en Mini-conteneurs irradiés sur un Temps Etendu*: Radiolytic Experiment in irradiated mini-containers over an extended time). This test, co-financed by CEA, EDF and ANDRA and brought to completion in 2006, consisted in following over more than one year, in a closed system, the total pressure and the H<sub>2</sub> generation of three 500-cm<sup>3</sup> containers including the same cementitious material, subjected to a  $\gamma$ -irradiation inducing a 0.1-Gy/s dose rate (Fig. 79). Results highlight the presence of both (predominant) H<sub>2</sub> and O<sub>2</sub> in the aqueous phase, as well as a good overall agreement between the evolution and level of the total (rather low) pressure and the simulation performed with the model DO-RE-MI (Fig. 80). Yet, comparing the simulation with the experiment shows that, if the values used for primary yields correctly describe how radiolysis starts, the discrepancy observed later on could be attributed to uncomplete description of the cementitious medium chemistry (the discrepancy, however, is kept at a factor 2 at the end of the test).

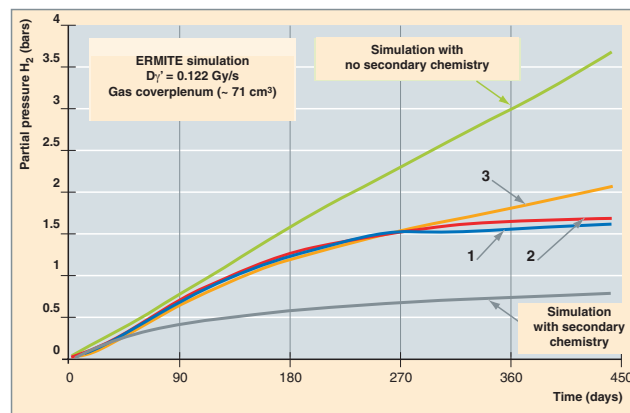


Fig. 80. Comparison between the "ERMITE" experiment (mini-containers 1 to 3) and the simulations performed with the model DO-RE-MI. Dispersion between curves 1, 2, and 3, which were measured independently on three identical mini-containers, gives an idea of experimental uncertainties.

Exploiting the experiment requires new investigations, such as performing validation tests at higher temperatures, and implies taking into account new parameters, such as iron species in the standard reactional system. It also induces to consider the concept of H<sub>2</sub> release “envelope” curve, quite useful to waste managers, as it applies the radiolysis model to an open system, taking into account hydrogen release as the gas is being generated.

## Long-term behavior of cementitious materials

Concretes have been widely used for decades to build structures and objects in relation to the long-term management of radioactive waste, such as, respectively, civil engineering works and engineered barriers for storage, as well as packages, conditioning matrices, and containers. Long-term behavior investigations are being conducted for twenty years or so, mainly focusing on cementitious materials physicochemical degradation in presence of water and its impact on their mechanical resistance. This research work made it possible to collect experimental data, improve knowledge about the phenomena involved, and set up behavior models to describe concrete evolution in different types of wet environment (whether saturated, i.e., under water, or unsaturated, as in free air) characterized by the occurrence of various aggressive agents in solution or in the atmosphere. Scientific process has always aimed at assessing the lifetime of objects and structures using a long-term predictive approach. As part of this framework, actions of understanding and modelling the alteration processes and mechanisms affecting materials initial properties have been extended to structure element behavior.

### Cement degradation mechanisms in unsaturated environment

The three main topics dealt with relate to mechanisms likely to impair the package structure and performances in an unsaturated environment: concrete atmospheric carbonation, reinforced concrete degradation by reinforcement network corrosion, and radiolytic phenomena (for this topic, see the part Irradiation effects in cementitious matrices, p. 82).

Atmospheric carbonation is a key component of the issue of reinforcement corrosion in cementitious medium. Under unsaturated conditions and excepting cases of industrial and/or marine environments exhibiting media highly enriched in chlorides, air CO<sub>2</sub> migration and the associated precipitation of calcium carbonate in the material porosity cause a pH decrease in the interstitial solution. This pH decrease stands as a major precursor phenomenon in the initiation of steel corrosion within cementitious media. Thus, the aim of research work on concrete atmospheric carbonation is twofold: knowing the material state following a storage period in air (whatever the type may be), and determining when the concrete reinforcement depas-

sivation is triggered, leading rapidly to the growth of an active corrosion. Studies on atmospheric carbonation of cementitious materials have been conducted at the CEA since the early 2000's. They are chiefly focused on improving and validating a numerical model using Cast3m [8]. The overall architecture of the model refers to the simplified chemical zoning approach as adopted in the operational model dedicated to concrete degradation. Recent work has been devoted to this model as part of the ALLIANCES platform development.

Considering that cemented waste packages (container + primary packages) are to ensure radionuclide confinement and are likely to undergo retrieval operations during storage and/or the disposal operational phase, long-term behavior of reinforced concretes has to be predicted. Similarly, some reinforced-concrete civil engineering structures have to keep their mechanical resistance over centuries. Therefore, ensuring the most passive management of these various reinforced-concrete objects requires to predict their durability with respect to reinforcement corrosion. This is the reason why a research program on (concrete) cementitious materials/(steel) metallic materials interactions has been set up since 2002, which takes into account the specific features of the nuclear field in relation to waste management (confinement, retrieval) as well as timescales (several hundred years). Since its has been initiated, the program CIMETAL has focused on knowledge acquisition and development of modelling tools dedicated to the predicting of reinforced concrete degradation in unsaturated environment. This program considers the microscopic approach (depassivation, corrosion rate, corrosion products nature and properties) as well as the macroscopic approach (concrete cracking, bearing capacity loss of structures), and integrates models coupling chemistry with transport and mechanics. The works completed today have allowed to build up a data base of solid phenomenological knowledge and initiate the development of a dedicated corrosion chemistry-transport, which, in the future, will be coupled to the macroscopic mechanical damage model CORDOBA (Fig. 81).

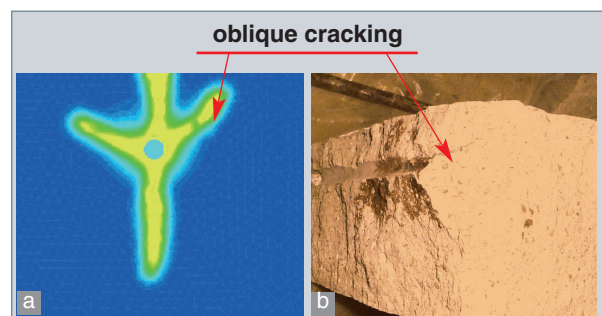


Fig. 81. Comparison of the cracking facies obtained by modelling with the CORDOBA tool and observed on a reinforced concrete beam during an accelerated corrosion laboratory experiment.

### Cementitious materials degradation mechanism in saturated environment and release model

In relation to the issue of waste geological management, R&D programs devoted to concrete behavior under saturated conditions and associated release phenomena stood as major research axes. Most of the efforts were focused on describing physico-chemical evolution with coupled chemistry-transport approaches taking into account dissolution-precipitation phenomena and the evolution of the material microstructure. These investigations were based on both an experimental approach (acquisition of phenomenological data related to materials) and a modelling approach (developing simplified models to be exported to numerical platforms such as the platform "ALLIANCES" developed through a cooperation of the CEA, EDF, and ANDRA). Their ultimate aim is to predict radionuclide release and waste package mechanical resistance over extended periods of time [9, 10].

From an experimental viewpoint, studies focused on describing cementitious materials behavior under very penalizing conditions (pure water leaching), taking into consideration various types of cements (CEM I, CEM V) and materials (pure pastes, mortars, concretes). As a second step, priority was given to the approach of realistic environmental conditions. Thus, aggressive-environment chemistry was complexified in successive steps in order to address such key issues as those related to carbonates (plugging effect) and sulfates (expansive phenomena [11], considered together with temperature dependence) [12].

The first phenomenological studies led to the development of a model describing the evolution of the cementitious system, especially the one based on CEM I cement [13]. The physical

phenomena involved are portlandite dissolution and the diffusive transport of species dissolved in the porous medium. This model takes into account the feedback of dissolution/precipitation phenomena on porosity and their influence on transport properties. It is worthwhile to mention, however, that this model was simplified by limiting to portlandite and C-S-H in order to allow evolutive boundary conditions to be managed. The simplifications achieved were validated by a number of experiments. The resulting simplified model (DIFFU-Ca) includes only one material balance equation for calcium:

$$\frac{\partial (\phi \cdot C_{Ca})}{\partial t} = \text{Div}(D_e \cdot \text{Grad}(C_{Ca})) - \frac{\partial S_{Ca}}{\partial t}$$

where  $t$  is time,  $C_{Ca}$  calcium concentration in the interstitial solution,  $S_{Ca}$  calcium concentration in the solid phase,  $\phi$  porosity, and  $D_e$  the effective diffusion coefficient of calcium in the material.

In this context, the equilibrium between calcium-rich phases ( $\text{Ca}(\text{OH})_2$ , C-S-H) and in-solution calcium concentration leads to a well-established relationship between calcium concentration in the solid phase ( $S_{Ca}$ ) and that in the solution ( $C_{Ca}$ ). Porosity evolution is directly linked with the mineralogical evolution of the system, which later on allows the diffusion coefficient of the material to be traced according to the material degradation state. The application of this model was fully validated on CEM I pastes and concretes and is under validation on CEM V materials. In the same context, important work focusing on the coupling between materials microstructure and diffusive properties have led to the building of the Microtrans model [14].

The developed tools were subjected to a number validation trials (Fig. 82). with special focus on mechanism prioritizing, cou-

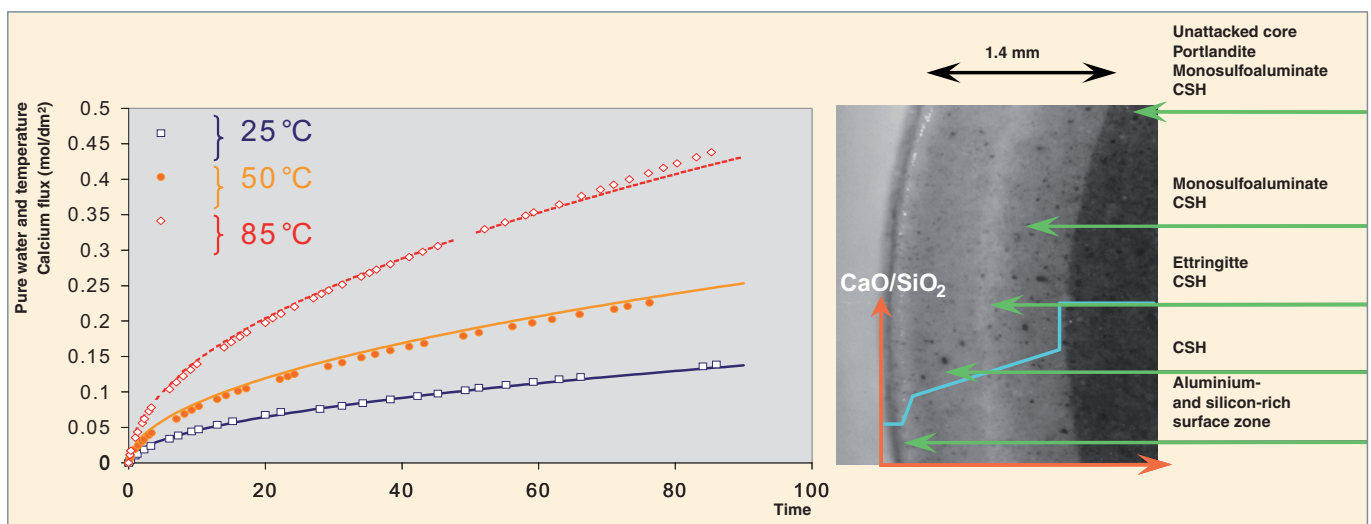


Fig. 82. Experimental quantification and modelling of leached species ( $\text{Ca}^{2+}$ ), along with the visualization of the associated solid phases during chemical degradation tests on CEM I-type cement pastes in pure water.

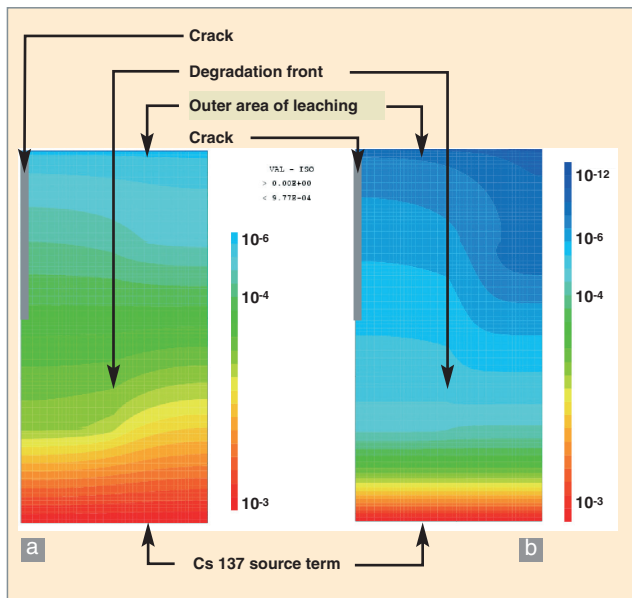


Fig. 83. Example of modelled 2-D concentration profiles in a container concrete wall subjected to superficial microcracking and chemical degradation by water over a 300-year period, referring to caesium 137: without (a) and with (b) allowance for the radionuclide sorption properties. Concentrations are expressed in arbitrary units.

plings, and input data validity. They should finally afford a robust description of waste package behavior and the associated radionuclide release.

A more thorough analysis of these mechanisms and their modelling can be found in the monograph “Corrosion” (to be published).

## Cementitious materials: a reliable confining matrix for low or intermediate-level waste

Cement-based materials are widely used in radioactive waste conditioning: grouts for waste embedding, mortars for immobilization operations (immobilization of bulk waste in a container, immobilization of a primary container in a secondary container, and concretes for container or structure elements manufacturing on disposal sites. Given the specific nature of the issues raised by cement/waste interactions and the timescales to be considered, a new approach of cementitious materials has emerged in which physico-chemistry has a predominant role and provides the data required for modelling the processes involved.

In relation to waste confinement, cementitious matrices display a number of assets which counterbalance the drawback associated with the significant volume of this conditioning type:

- versatility (ability to confine a number of physico-chemical wasteforms),
- low cost, easiness of implementation,
- good mechanical resistance,
- insolubilization of a high number of radionuclides owing to the interstitial solution basicity.

This Monograph highlights the outstanding advances achieved in cementitious material formulation as well as in the knowledge of their durability in a saturated or unsaturated medium and under irradiation. Cementitious matrices thus rank as reference materials for low and intermediate-level waste conditioning, whether for their storage or for their surface or geological disposal.

### ► References

- [1] CAU dit C. COUMES, S. COURTOIS, “Cementation of a Low-Level Radioactive Waste of Complex Chemistry: Investigation of the Combined Action of Borate, Chloride, Sulfate and Phosphate on Cement Hydration Using Response Surface Methodology”, *Cem. Concr. Res.* **33-3** (2003), pp. 305-316.
- [2] P. BENARD, S. GARRAULT, A. NONAT, CAU dit C. COUMES, “Hydration Process and Rheological Properties of Cement Pastes Modified by Ortho-Phosphate Addition”, *J. Eur. Ceramic Soc.* **25-11** (2005), pp. 1877-1883.
- [3] ANDRA, “Dossier 2005 Argile, Évaluation de la Faisabilité du Stockage Géologique en Formation Argileuse”, ISBN 2-951 0108-8-5 (2005).
- [4] M. CODINA, C. CAU dit COUMES, P. LE BESCOP, J. VERDIER, J.P. OLLIVIER, “Design and characterization of low-heat and low-alkalinity cements”, *Cem. Concr. Res.* **38-4** (2008), pp. 437-448.
- [5] ALIGIZAKI Kalliopi, “Pore Structure of Cement-Based Materials”, Taylor and Francis (2006).
- [6] M. MAINGUY, “Modèle de diffusion non linéaire en milieu poreux. Application à la dissolution et au séchage des matériaux cimentaires”, thèse de doctorat, École nationale des Ponts-et-Chaussées, France, (1999).
- [7] P. BOUNIOL, (2004), “État des connaissances sur la radiolyse de l'eau dans les colis de déchets cimentés et son approche par simulation”, CEA Report CEA-R-6069.
- [8] B. BARY, A. SELLIER, “Coupled moisture-carbon dioxide-calcium transfer model for carbonation of concrete”, *Cement and Concrete Research*, **34** (2004), pp. 1859-1872.
- [9] C. RICHET, P. LE BESCOP, C. GALLÉ, H. PEYCELON, S. BÉJAOU, I. TOVENA, I. POINTEAU, V. L'HOSTIS, P. LOVERA, “Synthèse des connaissances sur le comportement à long terme des bétons – applications aux colis cimentés”. CEA Report, CEA-R-6050, CEA Édition (DSI), Saclay, 2004.



- [10] C. GALLÉ, H. PEYCELON, P. LE BESCOP, S. BÉJAOU, V. L'HOSTIS, P. BOUNIOL, C. RICHEL, "Concrete long-term behaviour in the context of nuclear waste management: experimental and modelling research strategy", *Journal de Physique IV*, **136** (2006), pp. 25-38.
- [11] P. LE BESCOP, C. SOLET, "External sulphate attack by ground waters. Experimental study on CEM I cement pastes", *Revue européenne de génie civil*, **10-9** (2006), pp. 1127-1146.
- [12] H. PEYCELON, C. BLANC, C. MAZON, "Long-term behaviour of concrete: influence of temperature and cement binders on the degradation (decalcification/hydrolysis) in saturated conditions", *Revue européenne de génie civil*, **10-9** (2006), pp. 1107-1125.
- [13] F. ADENOT, "*Caractérisation et modélisation des processus physiques et chimiques de dégradation du ciment*", Thesis, Orleans University, France, 239 p., 1992.
- [14] S. BÉJAOU, B. BARY, S. NITSCHKE, D. CHAUDANSON, C. BLANC, "Experimental and modelling studies of the link between microstructure and effective diffusivity of cement pastes", *Revue européenne de génie civil*, **10-9** (2006), pp. 1073-1106.

**Céline CAU dit COUMES, Fabien FRIZON,**  
*Research Department of Waste Treatment  
and Conditioning*

**Nicolas MOULIN and Guillaume RANC,**  
*Fuel Cycle Technology Department*

**Pascal BOUNIOL, Christophe GALLÉ,**  
*Physico-Chemistry Department*



## Bitumens

**B**ituminization is used for embedding co-precipitation sludge arising from either effluent insolubilization treatments, or evaporator concentrates issued from spent fuel chemical treatment.

Co-precipitation consists in adding reagents to effluents so as to form various strongly insoluble salts. Radionuclides are carried over in the solid phases according to different mechanisms, which ensures effluent decontamination up to the levels prescribed by release standards (Fig. 84).

Co-precipitation treatments may vary according to the treatment station considered. Co-precipitation sludge generated in France at the present time mainly contains barium sulfate, nickel and potassium ferrocyanide, as well as different hydroxides, among which iron hydroxide. This sludge also contains variable contents in soluble salts, which mostly are sodium sulfate and sodium nitrate.

This wet sludge may then be cemented (see p. 71) or bituminized. Although bituminization is to be soon replaced by cementation, the amount of bitumen drums already produced in France and abroad justifies that a chapter of this monograph be devoted to this process.

### Bitumen package manufacturing

The embedding process consists in hot mixing of sludge waste to bitumen in an extruder (Fig. 85). The resulting mixture is dehydrated and poured into a steel drum (about 222 L) where it can cool. Hot extruding ensures both sludge dehydration, waste homogeneous dispersion, and radionuclide immobilization within the bitumen matrix. The waste incorporation rate into bitumen is an approximate 40 wt %. From a chemical viewpoint, the embedded waste mostly consist of salts insoluble in water (barium sulfate, ferrocyanides, cobalt sulfide), and soluble salts (sodium nitrate, sodium sulfate). Bitumen used in

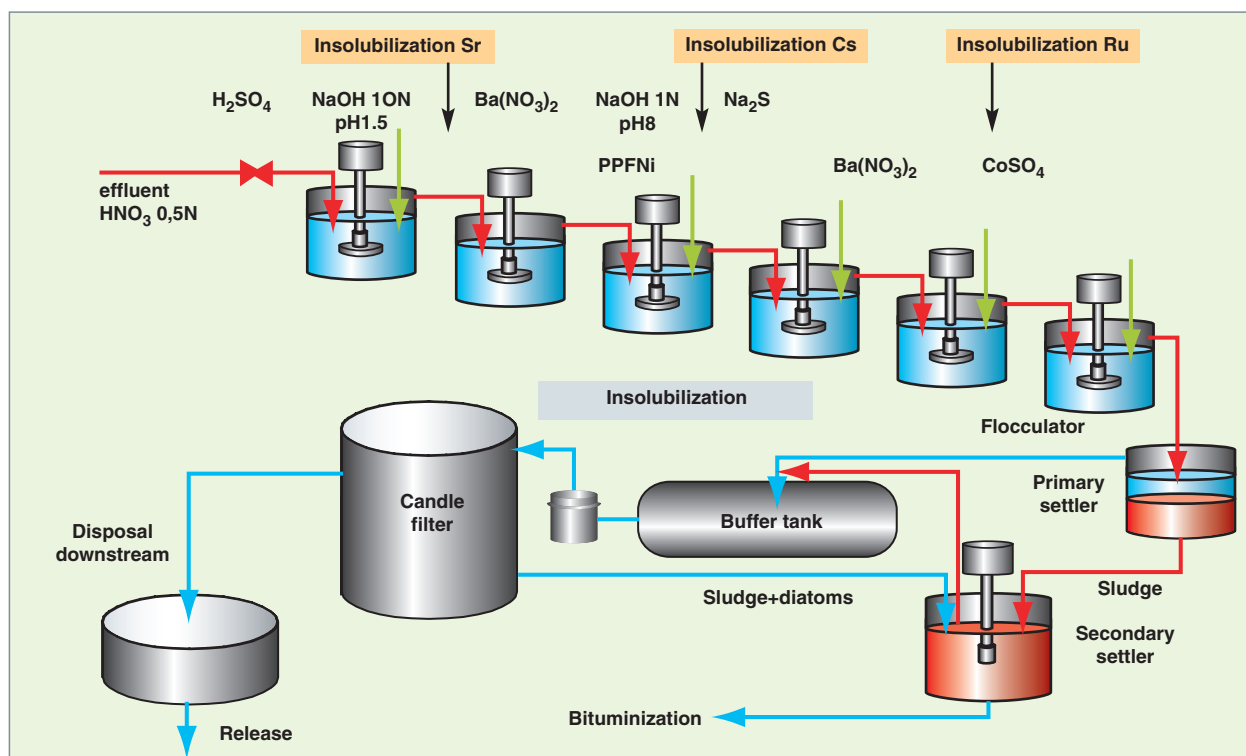


Fig. 84. Schematic of the liquid waste decontamination by co-precipitation under implementation in the STE3 Workshop at La Hague.

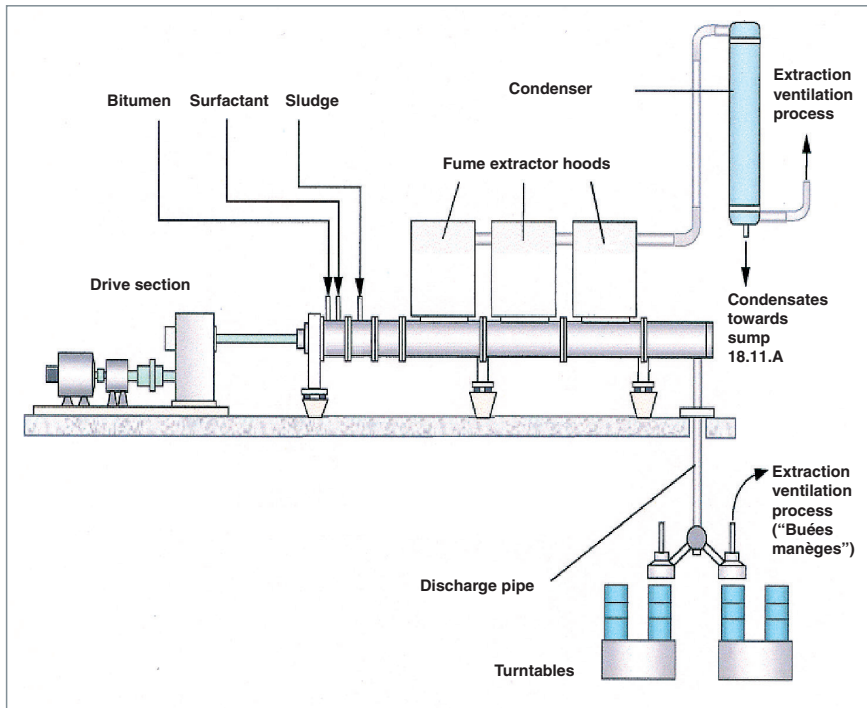


Fig. 85. Schematic of the industrial-scale process of bituminization in an extruder.

the French process arises from straight distillation of crude oils. It is a relatively soft bitumen (with 70/100 penetrability as defined by standards), which allows the embedding process to be implemented with moderate temperatures ranging between 130 and 180 °C in the extruder, thereby limiting fire risks.

The waste packages so produced are of low or intermediate-level and long-lived.

Once they have been cooled, packages are stored on the production sites and periodically followed pending their transfer to the disposal site. Most of the 70 000 bituminized packages produced in France since the sixties, were produced on the Marcoule site. A few thousand legacy packages had to be reconditioned there following drum corrosion or embedded waste overflow due to radiolytic swelling.

R&D studies in which the CEA is involved are first related to thermal behavior control in the short term, i.e., in the hours following the pouring so as to take into account fire risks (see the incidents at Saclay in 1991 and at Tokai Mura in 1997).

### Controlling fire risk during package manufacturing

In the French process embedded waste leave the extruder at a temperature close to 130 °C. As packages have a high thermal inertia, they remain at high temperatures (> 100 °C) for several hours. The risk associated with this temperature level is exothermal reaction development within the embedded waste, following heat-activated redox reactions, and resulting temperature rises likely to induce bitumen inflammation if the temperature goes beyond 250 °C.

These phenomena are primarily controlled upstream, where the potential reactivity of the embedded waste is checked by calorimetric measurements prior to bituminization. This reactivity may be caused by chemical reactions between the waste and bitumen or between the waste properly said.

Potentially reactive species were screened by calorimetry. These systematic investigations contribute to the industrial process safety by identifying these potentially reactive species.

For example, the NaNO<sub>3</sub>/cobalt sulfur mixture was identified as a reactant at embedding temperatures: a bituminized waste containing this mixture was synthesized at the laboratory and the microcalorimetry performed (Fig. 86) evidenced an exothermal peak between 100 and 170 °C.

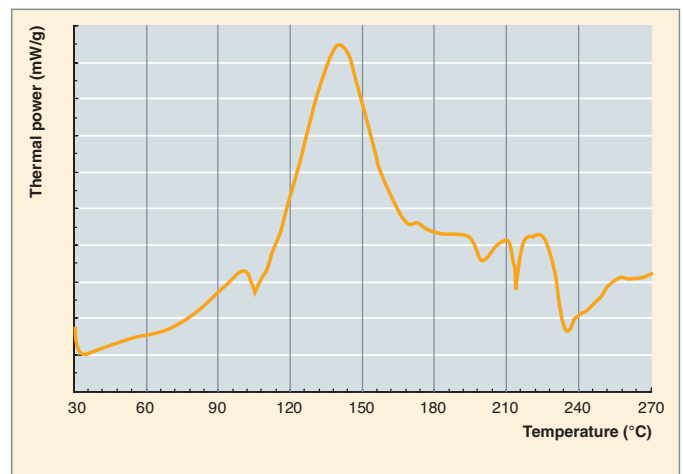


Fig. 86. Dynamic thermogram 30-270 °C at 0.1 °C/min of a modelled bituminized waste containing the mixture NaNO<sub>3</sub>/cobalt sulfur (50 wt %).

The limit below which bituminization is achievable can be evaluated basing upon feedback from former facilities which process waste streams of relatively steady composition. This limit can also be drawn from package cooling simulation. In the latter case experimental data resulting from the microcalorimetry are used as input data for the thermal conduction cooling model (Fig. 87), which also integrates in a conservative way parameters representative of extrusion industrial conditions (number of pourings, filling levels and delays...), as well as the physico-thermal parameters of the materials used.

In the case when there is a low heat release kinetics with respect to the characteristic time of activation of exothermal reactions, the limit predicted in terms of admissible thermal reactivity is of the order of a few dozen joules per gramme of embedded waste. This limit is fairly comparable to that drawn from feedback.

Once the bituminized package has been manufactured, its good behavior has to be ensured in the long term. The two phenomena to be considered are the **radiolysis\*** caused by the package self-irradiation and the leaching induced by a possible package contact with water.

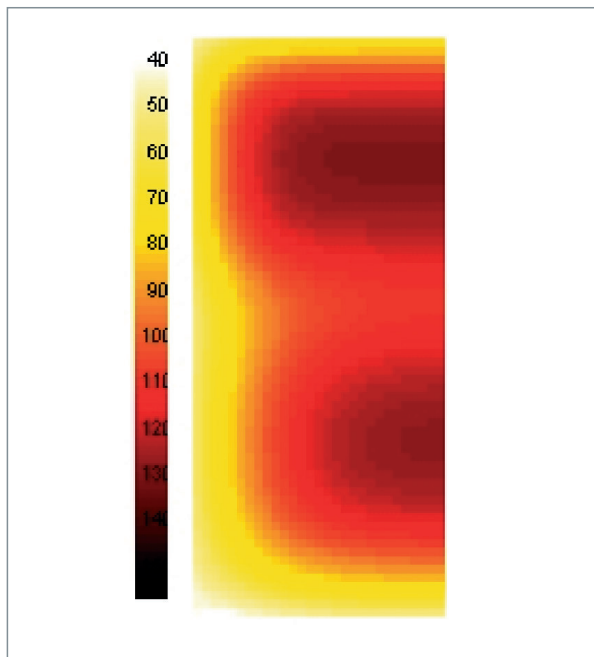


Fig. 87. "Temperature map" within a package 15 h after the first pouring step has started (a two-step pouring enables the temperature rise to be limited without significantly altering the industrial output rate).

## Bitumen package evolution under self-irradiation

Bitumen is a continuum of organic compounds of molar masses between 400-4,000 g/mol most of which are unsaturated and polycyclic. This organic composition endows bitumen with the property of emitting radiolytic gases, essentially hydrogen, under self-irradiation. These gases are issued from the cleavage of the existing C-H bonds.

According to the activity incorporated about 1-10 L of radiolytic gases per year are generated by a drum on the production line. The gas source term falls to less than one liter after one thousand years owing to decay. The volume of accumulated gas over one thousand years is about one cubic meter per drum.

The gases generated in the whole volume of the embedded waste first solubilize in the matrix up to saturation (about 1% in volume). Beyond this step hydrogen forms gas bubbles, the growth of which may lead to the swelling of the embedded waste (Fig. 88). A swelling rate of about one centimeter per year could be observed in some packages.

In some cases (e.g., packages manufactured with no apical vacuum), swelling evolution can cause the embedded waste overflowing out of its container, or even induce their pressurization if the overflow is halted (e.g., by a lid). This swelling does not impair bitumen confinement properties with respect to radioactivity, but requires a suitable package management during the storage period and the reversibility period of the geological disposal phase.



Fig. 88. X-radiographic cut of a synthetic bituminized waste which is subjected to an external *gamma* irradiation of about 1 MGy at 25 °C. Initially, the waste occupied half the experimental specimen.

### Swelling management by limiting incorporated activity and drum filling rate

As a matter of fact, the swelling impact is limited by two mechanisms of release of the generated gases. The first one originates in the gas bubble upward migration following the density discrepancy relative to the embedded waste. At a 25 °C temperature migrating bubbles are typically centimeter-sized. This mechanism is all the more efficient as bubbles are voluminous (hence with significant swelling) and as the embedded waste viscosity is low (hence with a high storage or disposal temperature). The second mechanism, dissolved gas diffusion/permeation, contributes to the release of at least 1 L/year gas.

These mechanisms of gas generation, buildup and release are integrated into a predictive modelling implemented in the JACOB2 code. It is thus possible to determine the swelling evolution (Fig. 89), which typically follows a bell-shaped curve, reaching a peak within a few dozen years following the bitumen drum production. The maximum swelling level is mainly dependent on the incorporated activity and the package storage temperature. Therefore, the JACOB2 code is used to optimize bitumen package manufacture parameters so as to prevent any risk of drum overflow.

### Swelling management by radiolytic hydrogen trapping

A further way to control embedded waste swelling consists in adding a trapping hydrogen salt to the waste to be bituminized in order to eliminate this radiolytic gas. This strategy is under testing for the bituminization of legacy waste. The trapping salt retained is obtained through precipitating cobalt sulfur in aqueous medium. This product presents the benefit to be already well-known, as it is one of the reagents used for decontaminating effluents by ruthenium co-precipitation prior to bituminization.

The effect of cobalt sulfur trapping by hydrogen was evidenced after following up the high-level experimental drums produced in the early nineties that displayed a very light swelling since then. External *gamma* irradiation experiments performed on cobalt-sulfur-containing bituminized inactive waste also confirmed a strong decrease in the radiolytic hydrogen generation (Fig. 90).

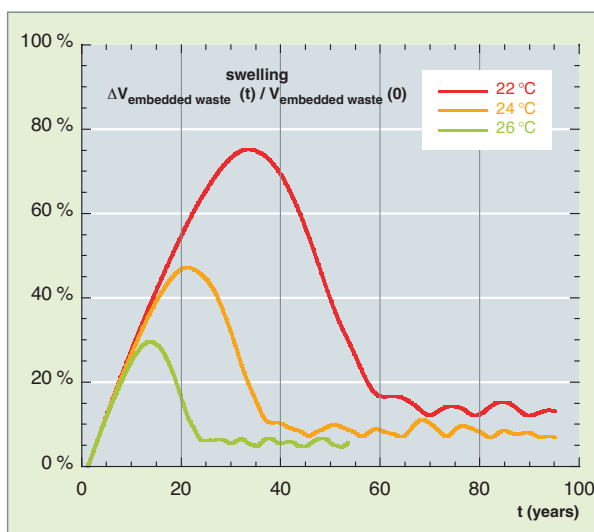


Fig 89. Variation with temperature of the swelling kinetics of a reference bituminized waste. The embedded waste viscosity depends on temperature, which thus has a determining effect upon the capacity to release radiolytic gases through upward migration of the bubbles generated.

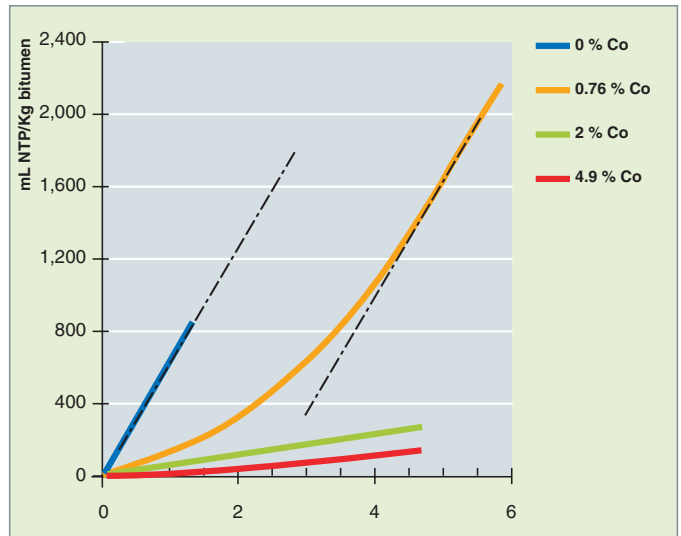
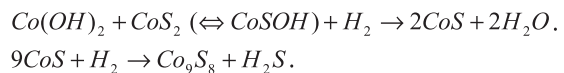


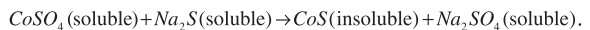
Fig. 90. Hydrogen release from the radiolysis of inactive bituminized waste irradiated by a *gamma* source (Co 60). The bituminized waste contain 10 wt% salts with variable amounts of cobalt sulfur and barium sulfate. The average dose rate is 400 Gy/h.[1]

Various studies were conducted by the CEA [1,2] and, then, independently corroborated by University laboratories [3,4] to improve understanding and quantifying of cobalt sulfur with respect to hydrogen. Cobalt sulfur chemically reacts with hydrogen and turns it into water irreversibly according to a stoichiometry close to 1/2 mole of hydrogen per cobalt mole. The trapping balance equations are as follows:

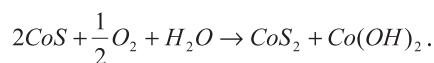


The generation of a partially  $\text{Co}_9\text{S}_8$ -crystallized phase and of an amorphous phase with a stoichiometry close to  $\text{CoS}$  was demonstrated by characterizing the solid after trapping.

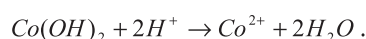
The trapping salt synthesis was achieved in two steps. First, a step of  $\text{CoS}$  insoluble product precipitation from cobalt sulfur and sodium sulfur:



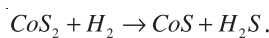
Secondly, a step of partial oxidation by oxygen through mere stirring of the suspension in air:



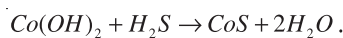
In the trapping mechanism of this cobalt bisulfide and hydroxide mixture  $\text{H}_2\text{S}$  gas is involved as a reaction intermediate. For it was experimentally demonstrated that  $\text{CoS}_2$  can be isolated by selective dissolution of cobalt hydroxide in an acid medium according to the following relationship:



The insoluble  $\text{CoS}_2$  can thus be isolated by washing. Once contacted by hydrogen in a closed reactor, this product does not trap much of hydrogen but can form significant amounts of sulfurized hydrogen according to the following reaction:



In the trapping mixture the  $\text{H}_2\text{S}$  gas is then trapped by cobalt hydroxide according to the following reaction:



This mechanism was confirmed experimentally putting the two phases  $\text{CoS}_2$  and  $\text{Co(OH)}_2$  separately in a same closed reactor (Fig. 91). It was observed that the total amount of trapped hydrogen (as measured by the pressure drop in the reactor) is close to the amount of sulfur transferred to the cobalt hydroxide phase. Trapped hydrogen excess with respect to the sulfur fixed by  $\text{Co(OH)}_2$  can be explained by the formation of the compound  $\text{Co}_9\text{S}_8$  from the  $\text{CoS}$  issued from the previous mechanism.

In order to simulate radiolytic hydrogen production of an embedded waste and measure its trapping capacity an experimental device was developed. This device confronts the embedded waste, in a closed reactor (Fig. 92), with hydrogen amounts standing for several-century radiolytic generation, which speeds up the trapping phenomenon and allows the embedded waste trapping capacity to be measured within a few months. Hydrogen consuming can be deduced from the total pressure drop of the gas in the reactor.

This trapping capacity so measured can be coupled with a trapping duration provided that radiolytic hydrogen generation over time is known, excepting the trapping effect. Though

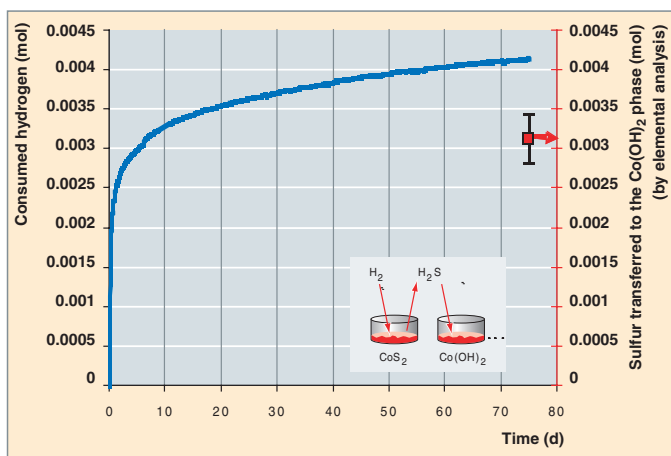


Fig. 91. Hydrogen trapping experiment performed on two separate phases in a same closed reactor: a  $\text{CoS}_2$  phase (4 mmol) extracted from the trapping salt and a  $\text{Co(OH)}_2$  phase (16 mmol) of commercial cobalt hydroxide.

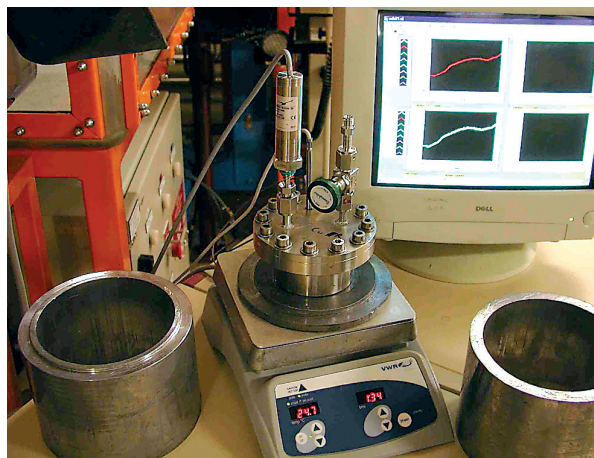


Fig. 92. Photograph of the measuring device of the hydrogen trapping capacity in bituminized waste: stainless steel made closed reactor fitted with a filling valve and a gas pressure sensor.

depending upon the radionuclide spectrum of the package, this capacity is mostly proportional to cumulated doses and *alpha*, *beta*, *gamma* radiolytic yields.

Embedded waste trapping effect can also be evidenced qualitatively through measuring its hydrogen release in a closed reactor where the gas builds up before being analyzed. In the case when the embedded waste contains hydrogen trapping salts, the gas quantities released are very low with respect to the theoretical release as calculated from its radiological activity.

In contrast with swelling management through limiting incorporated activity or package filling rate, using a hydrogen trapping salt could allow the activity incorporated per package to be significantly increased, while preventing any overflow for a given period thanks to the trapping salt quantity used.

## Bitumen alteration by water [5,6]

Although pure bitumen is not much permeable to water and dissolved species, the initial presence of salts favors water uptake through diffusion and osmosis. On contact with water within the embedded waste, the most soluble salts are dissolved locally. Formation of saline solution bags results in porosity developing, which facilitates the dissolved species diffusion back to the outer leachant.

The kinetics that characterize water uptake and the release of the most soluble salts, comply with square-root laws for time, specific of a diffusion mechanism. These kinetics are chiefly controlled, first, by the contents and solubilities of the various embedded saline species, and, secondly, by the leaching solution (Fig. 93).

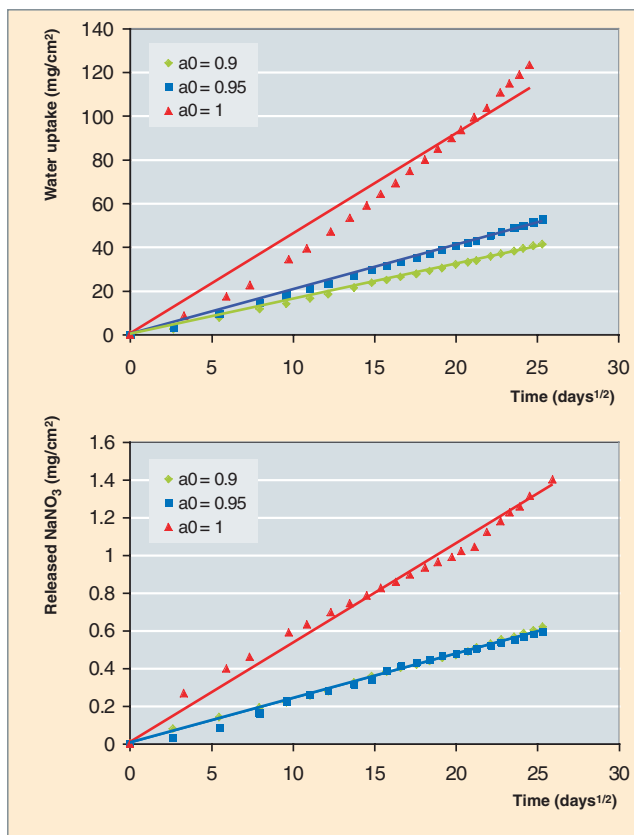


Fig. 93. Experimental leaching kinetics of a synthetic bituminized waste (water uptake and tracer salt release) as a function of time and for three activity conditions ( $a_0$ ) of the leachant periodically renewed.

It is noteworthy that for a given alteration time water uptake is about 100 times faster than the release of the most soluble salts, a fact to be referred to the values of effective diffusion coefficients which have been determined separately by experiments, of the order of  $10^{-15}$  m<sup>2</sup>/s for solubilized salts. This difference results in the swelling of the embedded waste, due to the porous area maturation and the leaching front progress (Fig. 94). Regarding the latter, it proceeds at a rate of the order of mm/yr<sup>1/2</sup>.

All the experimental data obtained for a variety of boundary conditions - leaching under renewed or stagnant liquid water, pure water or water representative of an argilous or cementitious medium, and alteration by air moistness - were integrated into the operational code COLONBO, in which a chemistry-transport coupling is used, together with a penalizing approach, to determine material transfers between an embedded waste under leaching, its disposal package, and the engineered barrier.

Last but not least, it is worthwhile mentioning that these studies are performed taking as a reference the release of high-solubility tracer salts such as sodium nitrate. Trials on active

embedded waste have corroborated the penalizing character of this approach: it was demonstrated that radionuclide release rates are two to four orders of magnitude lower than those of tracer salts.

All things considered, bitumen is a reliable confining matrix: radionuclide release rates, which are governed by diffusion within the matrix, are slow and show high compatibility with the safety requirements of a disposal facility. Industrial feedback tends to indicate that fire risk does exist initially, but can be controlled if sludge chemical reactivity is correctly analyzed and taken into account. Similarly, swelling can be tackled by limiting package activity, forcing a sufficient vacuum at the top of the package, or adding cobalt salts. However, prospects for output look rather dull since bitumen is still a matrix of the organic type – hence flammable and sensitive to radiolysis –. So, this conditioning material is progressively replaced by hydraulic binders that allow for homogeneous cementation or immobilization in mortar. In other cases, changing the effluent management system allows to concentrate these streams so that they may be grouped with fission products solutions to be vitrified.

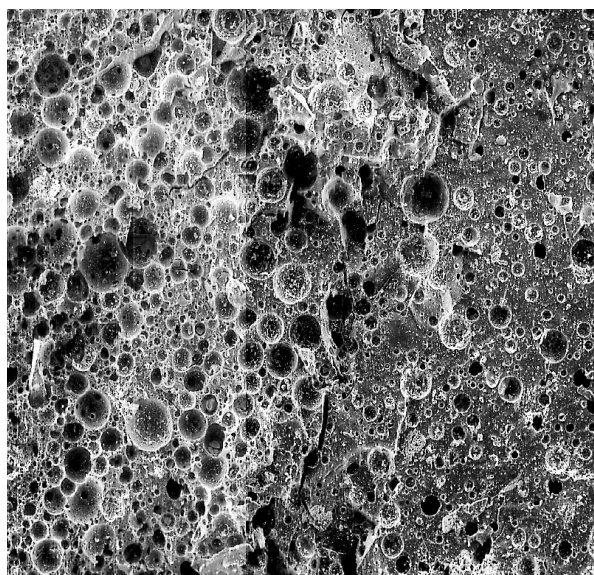


Fig. 94. Crosscut of a synthetic bituminized waste (BW) altered in one year in periodically renewed pure water, as observed using an “Environmental” Scanning Electron Microscope (SEM). Dark craters, which are more numerous in the BW top area, highlight saline solution bags formed on water uptake. The white dots occurring mainly in the lower area are dry salts, unreached by water by this time.



## ► References

[1] C. RIGLET-MARTIAL, F. ADENOT, S. CAMARO and V. BLANC “A New Chemical Process to Prevent the Swelling of the Radioactive Waste Packages in Organic Media”, *Global* (2005), Stukuba, Japan.

[2] S. CAMARO, Q. RAGETLY, C. RIGLET-MARTIAL “Composé piègeur de l'hydrogène, procédé de fabrication et utilisation”, Patent 2, 859, 202 (2003)

[3] C. LOUSSOT, “Étude du phénomène d'inhibition par le sulfure de cobalt de la production de gaz de radiolyse lors de l'irradiation de molécules organiques modèles”. Thèse de doctorat, Lyon 1 University, France (2006).

[4] C. PICHON, “Étude de l'inhibition de la production d'  $H_2$  par radiolyse (problème des boues radioactives bitumées)”. Thèse de doctorat de l'École Nationale Supérieure des Mines de Saint-Étienne, France (24 novembre 2006).

[5] J. SERCOMBE, B. GWINNER, C. TIFFREAU, B. SIMONDI-TEISSEIRE, F. ADENOT, “Modelling of bituminized radioactive waste leaching. Part I : Constitutive equations”. *Journal of Nuclear Materials*, 349 (2006), pp. 96-106.

[6] B. GWINNER, J. SERCOMBE, C. TIFFREAU, B. SIMONDI-TEISSEIRE, I. FELINES, F. ADENOT “Modelling of bituminized radioactive waste leaching. Part II: Experimental validation”. *Journal of Nuclear Materials*, 349 (2006), pp. 107-118.

**David CHARTIER, David LAMBERTIN, Aurélien LEDIEU,  
and Christophe JOUSSOT-DUBIEN**  
*Research Department of Waste Treatment  
and Conditioning*



## Metallic structure waste conditioning

Once the spent fuel has been dissolved in the treatment plant, there remains, first, the dissolution solution which contains valuable materials (U, Pu) together with fission products and minor actinides and, secondly, metallic residues which arise from the shearing of the clads constitutive of the fuel assembly. This structural waste consists of zircaloy hulls (Fig. 95) and structural materials (nozzles, grids and guide tubes) made of stainless steel and nickel alloy.

Despite enhanced flushing at the outlet of the dissolver, these hulls and nozzles contain radioactive activation products, and part of the contamination results as trapped in the clad peripheral area. Consequently, this waste contains too high an  $\alpha$  and  $\beta$  activity to be admitted to a surface storage site.

So this waste falls into the class of intermediate-level, long-lived (IL-LL) waste, the so-called "B-type" waste.

Between 1990 and 1995 this waste is conditioned in concrete (Fig. 36).

The cemented package is 1.69 m high and has a 1.06 m diameter, a volume of about 1.5 m<sup>3</sup>, and a mass of the order of four tons (Fig. 97).

Its average activity is 50 TBq  $\beta\gamma$  and 0.1 TBq  $\alpha$ , which results in a contact dose rate of the order of 10 grays/hour. Today 1517 packages containing cemented hulls and nozzles are stored in La Hague plant.



Fig. 95. Zircaloy-made cladding hulls.

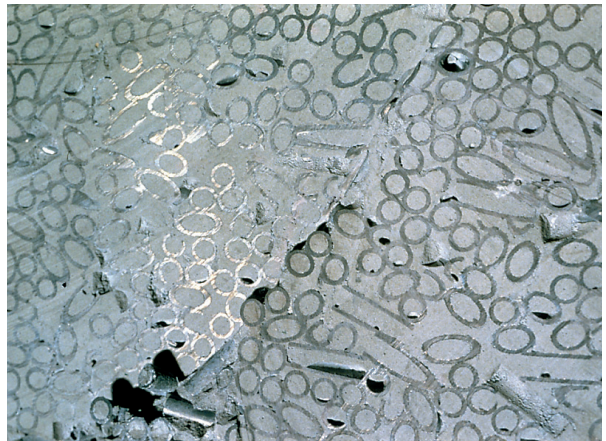


Fig. 96. Example of cladding hulls immobilization by injection of a hydraulic binder. (Sectional view of a package).



Fig. 97. Drum of cemented hulls and nozzles.

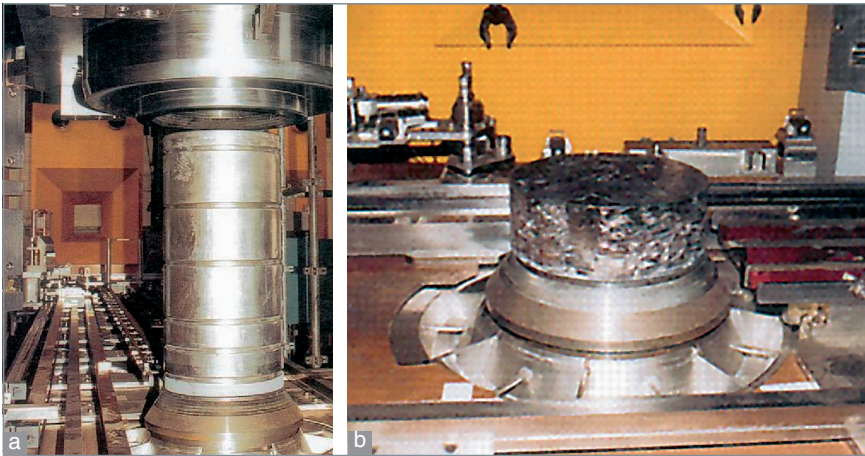


Fig. 98. a: Press and case prior to compaction. b: the compacted pancake.

### Fuel clad compaction process

From the year 2000 the cementation process was replaced by a cladding hulls compacting process which allows for a volume reduction by about a factor 5 with respect to the cementation process for this IL-LL (“B-type”) waste likely to be sent to a geological disposal site.

Cladding hulls are introduced into metallic cases (Fig. 98a), then compacted with a press which allows the waste density to be increased up to 65% of the metal density; the resulting pancakes (Fig. 98b) are piled up in a stainless steel container.

The compacting workshop in La Hague plant is fitted with a press of 2,500 T (Fig. 98). It is designed to produce 2,400 packages per year.

### The standard package for compacted waste

The resulting package is the so-called “CSD-C”<sup>3</sup> which does not include any immobilizing material. Each container encloses five to ten pancakes (seven on the average) depending on whether there are nozzles or not in the package. As part of a standardization approach these containers have the same outer geometry – D = 0.43 m, h = 1.3 m, Volume = 180 L – than the standard container (or package) for vitrified waste (CSD-V\*, for *Conteneur ou Colis Standard de Déchets Vitrifiés*). The only visible difference is that the weld closure is achieved at the top of the cylindrical drum, and not of the upper ring (Fig. 99).

3. CSD-C: for “Colis Standard de Déchets Compactés”, standard package for compacted waste. Standardizing the packages intended for deep geological disposal can but make their further handling easier.

The initial activity of this package is about a few hundred TBq  $\beta\gamma$ . It also contains  $\alpha$  emitters.

Similarly to the cemented package, it is a long-lived intermediate-level (IL-LL) waste, the so-called “B-type waste”.

It contains three types of radionuclides:

- **activation\*** products coupled with the impurities in all of the structural materials;
- fission products: about 0.2% of the fission products contained in spent fuel can be found in clads;
- actinides: about 0.03% of the actinides contained in spent fuel can be found in clads.

The total amount of structure activation products is spread through the metal thickness.

Fission products and actinides are included either in the clad metal (zircaloy), or in the surface oxide (zirconia) about 100  $\mu\text{m}$  thick.

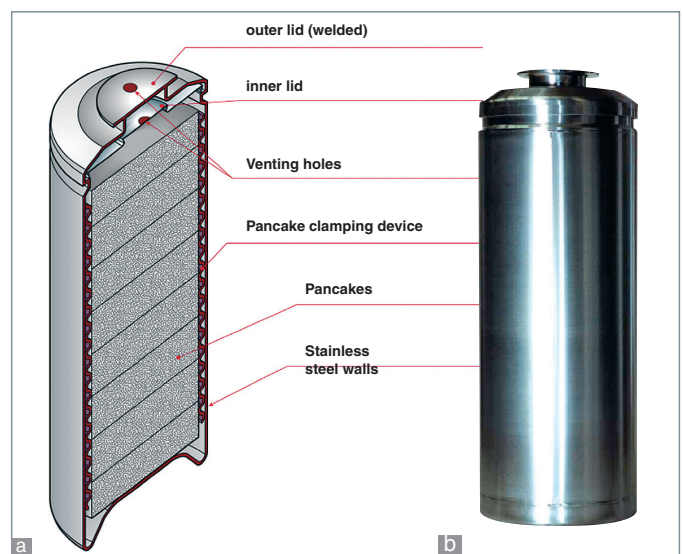


Fig. 99. a. Piled-up pancakes in their container; b. The CSD-C (for “Colis Standard de Déchets Compactés”, standard package for compacted waste).

## Long-term behavior of packages for compacted metallic waste

The standard packages for compacted waste (CSD-C) are heterogeneous packages. Their potential radionuclide-confining properties are linked with the durability of the radionuclide-loaded materials within the package (metal, oxide, hydrides...).

During the first decades (up to about 300 years), the package integrity is preserved.

Later on release of radionuclides depends upon their localization within the package.

As part of a safety approach, when radionuclides are not included in a massive material or when the alteration of their host material is not sufficiently understood or not sufficiently slow, they are considered as “**labile\***”, i.e., likely to be readily turned into solution when ingress water comes into contact with the package. Thus their release only depends upon their physicochemical state and environmental conditions (water nature and renewal). So will it be of the radionuclides occurring in fines and depositions on the clad surface, or of those contained in technological waste which might possibly be conditioned with compacted clads.

Reversely, the release of the radionuclides incorporated into the durable materials mass is dependent upon the degradation of those materials, which stand for the confining matrix. This degradation is itself much dependent on the surrounding environment.

Prevailing alteration mechanisms are zirconia dissolution and the corrosion of zircaloy (today 90 wt% of the assembly consist of Zircaloy-4 clads) as well as nickel-based alloy.

The radionuclide release model put forth by the CEA is thus based upon the localization of the radiological inventory with, on the one hand, a portion deemed to be labile, and, on the other hand, a confined portion the release of which is controlled by the alteration of the material standing as the matrix.

Until today only zircaloy, stainless steel, and nickel-based alloy have been seen as likely to play a confining role, which couples very penalizing conditions with this model.

This very model is the one that has been selected by the ANDRA for safety analyses relating to deep geological disposal.

Release can then be calculated pace by pace, radionuclide by radionuclide, as a function of the localization of the radionuclide considered and the corrosion rate of the material possibly confining this radionuclide. Typical confining times are about 10,000 years for zircaloy, 100,000 years for stainless steel, and 1,000 years for the nickel-based alloy, with, for the latter, a corrosion rate presumably higher than the actual value. The first performance assessments and sensitivity studies will allow to evaluate whether this model has to be completed taking into account the confinement by other materials occurring in the package, especially zirconia, so as to make it more realistic and less penalizing.

## Prospective research on cladding hulls melting

In the eighties cladding hulls melting was investigated in order to apply this process to the metallic waste arising from fast neutron reactor spent fuel treatment [1, 2].

Clad treatment by melting addresses the following aims:

- performing maximum volume reductions by making a massive ingot through melting and continuous drawing: Table 15 hereafter details the maximum volume reductions deemed to be reachable;
- decontaminating the ingot by transferring  $\alpha$  emitters, Cs and Sr to a slag (a mixture of oxides and/or fluorides) easy to separate from the ingot and likely to be vitrified;
- fabricating an alloy featuring the best corrosion resistance;
- homogenizing the residual activity in the whole volume of the ingot;
- performing a maximum reduction of the waste surface likely to be possibly exposed to leaching.

In order to reach these objectives the CEA has developed a cold crucible induction melting process with continuous drawing of the ingot from the bottom of the crucible (Fig. 100-101). The process is comparable to the conventional process implemented in the metallurgical industry for metal purification by zone melting.

Clad metal melting by cold crucible induction allows melting to be performed under controlled atmosphere, with no temperature limitation, no crucible corrosion, and, last but not least,

Table 15.

Maximum volume reduction achievable through hulls melting			
	Hulls bulk density	Ingot density	Volume reduction factor
Fast neutron reactor clads (Phénix)	1,500 kg/m <sup>3</sup>	8,000 kg/m <sup>3</sup>	5.3

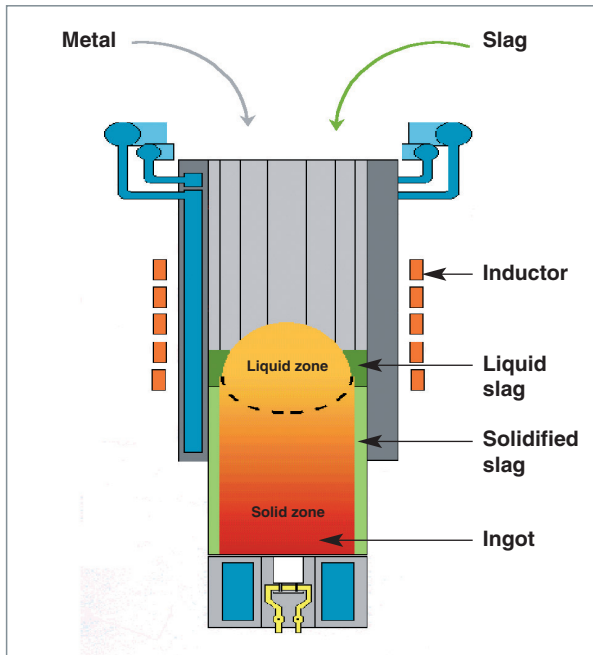


Fig. 100. Principle of clad metal melting through cold crucible induction.

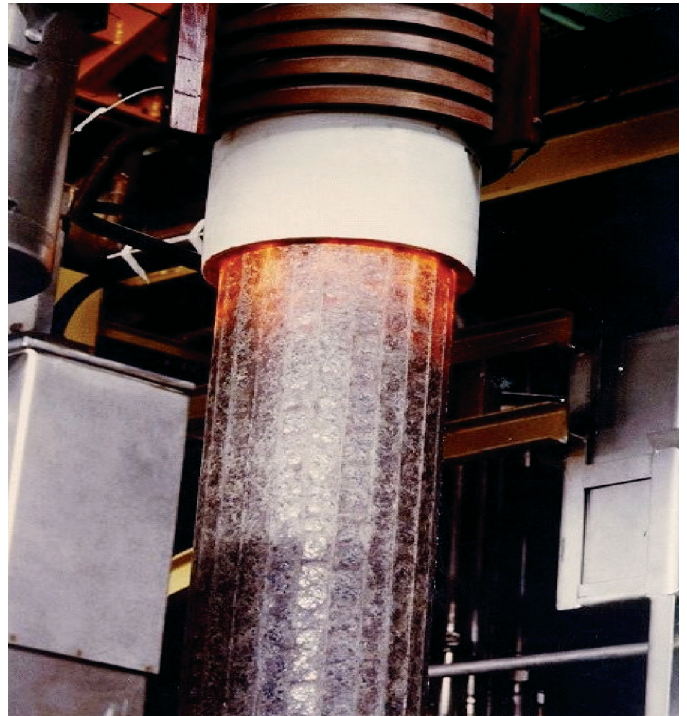


Fig. 101. Principle of clad metal melting through cold crucible induction.

a strong electromagnetic mixing of the metal which favors oxide transfer to the slag.

Continuous drawing of ingots avoids the problems generated by continuous casting in ingot molds: metal-slag remixing, occurrence of a shrinkage cavity, difficulties for maintaining controlled atmosphere. The slag embeds the ingot. So it can be separated mechanically or chemically. Continuous drawing also allows molten metal mass in the crucible to be minimized (for example, there are only 20 kg of liquid metal for an ingot of 250 kg).

### **R&D work on cladding hulls melting has been conducted alongside four axes**

- Electromagnetic, hydraulic and thermal modelling of the furnace. This model was used to define furnaces on the laboratory and the technological scale, as well as associated high-frequency generators.
- Developing the process and technology on inactive Scale 1.

An inactive prototype was achieved and implemented. It allowed to pull ingots 200 mm diameter and 1 m long, fitted with gas scrubber.

It made it possible to check the technological feasibility as 100 ingots were manufactured from the stainless steel clads simulating the cladding hulls of fast neutron reactors. The melting

capacity is of the order of 60 kg/h. The slag is a mixture of fluorides -  $\text{CaF}_2$  (75%),  $\text{MgF}_2$  (25%) - or oxides -  $\text{BaO}$  (75%),  $\text{B}_2\text{O}_3$  (25%) - . Its content varies from 0.3 to 3% of the metal mass.

Promising preliminary tests for the specific vitrification of these slags were performed, but complete characterization has not been achieved due to the program being halted.

- Checking the process safety.

In order to evaluate the risk of water-molten metal interaction, tests putting water and molten metal into contact were performed and demonstrated that no explosion or sharp boiling can be evidenced on a 4-kg molten metal scale.

- Investigating the radionuclide distribution in spent fuel clads from fast neutron reactors.

In order to evaluate the radionuclide distribution in the process, a melting rig was built around a cold crucible 60 mm diameter, placed in a shielded cell. This rig allowed to melt 20 kg of real clads and pull eight ingots of about 3.4 kg of clads from fast neutron reactors.

These tests have shown that:

- the initial clad activity is distributed among the dusts retrieved in gas scrubbing, the melting flow, and the ingot;
- the ingot decontamination factor reaches 2,000 for  $\alpha$  emitters, and at least 100 for Sr and Cs;
- activation products prove to be immobilized in the ingot;
- and so is it of most of tritium;
- the metallic matrix arising from melting is compact and homogeneous.

Applying this process to cladding hulls from fast neutron reactors is promising due to its benefits: volume reduction through melting is maximum, and it can be assumed from the resulting  $\alpha$ -emitter decontamination factors that this waste could possibly be decategorized.

#### ► References

- [1] P. BERTHIER, J.P. RUTY, C. LADIRAT, R. PICCINATO, "Compactage par fusion haute température de déchets de gaines actives en creuset froid. Rapport final. Contrat CCE FI 2W-CT 90052" (1993).
- [2] R. PICCINATO, J.P. RUTY, R. CARABALLO, N. JACQUET-FRANCILLON, "Compactage par fusion haute température des déchets de gaines actives des creusets froids – Rapport final CCE – Contrat n° FI 1W 00 14 F" (1991).

**Roger BOËN and Étienne VERNAZ,**  
*Research Department of Waste Treatment  
and Conditioning*

**Guy BRUNEL,**  
*Communication and Teaching Action*





## Plasma benefits for incineration/vitrification waste treatment. The Shiva process

Plasma heating makes it possible to reach extreme temperatures locally and very rapidly. Plasma is of high interest for waste treatment, for it allows most of them to be decomposed, whether they are solids, liquids, organic materials or minerals. Indeed, waste treatment and conditioning processes using plasma have been investigated all around the world, and even industrialized in some cases such as, for instance, the Zwiilag facility in Würenligen Center, in Switzerland.

To the physicist plasma is the extension of the gaseous state; for it exists beyond this state when the energy contained in matter is sufficient to ionize a high number of the constitutive atoms. So plasma is a mixture of molecules, atoms, ions and electrons with specific physical properties. Produced at the atmospheric pressure, plasma can easily be made to reach temperatures in excess of 6,000 °K. Simultaneously very hot and very chemically reactive, owing to the occurrence of highly excited atoms and ions or molecules unusual in conventional chemistry, this very plasma can be used by the engineer to process some especially “delicate” waste categories. For instance, the waste concerned may be ion exchange resins or, more generally, technological waste including an organic fraction that would not allow them to be directly vitrified or would make uncertain their embedding into a cementitious matrix.

There exist various techniques for producing a thermal plasma; it all depends on how energy is brought to turn gas into plasma. Energy can be brought by an electromagnetic field, microwave, or still electrical discharge in a gaseous flow – the technique mostly used –, the nature of which may range from argon to oxygen or water vapor... Indeed, it is the chemical process considered which determines the choice of a given gas. Current density in an arc column can reach such values as  $10^6$  A/m<sup>2</sup> or more; it is even higher on the electrodes where current density can even go beyond  $10^{10}$  A/m<sup>2</sup>. Associated densities of heat flow rate are about  $10^{10}$ - $10^{11}$  W/m<sup>2</sup>, which requires a specific design of electrodes in order to ensure a lifetime compatible with and industrial-scale use. As almost any chemical composition can be reached at very high temperatures, this can be useful, e.g., to produce by synthesis in a reducing medium, or to rapidly destroy molecules in a highly oxidizing medium... which is the main application of plasma in waste treatment.

The assumption of a local thermodynamic equilibrium in the arc column is generally verified. Plasma can therefore be deemed to be a mixture of ideal gases in thermodynamic equilibrium, which allows to determine its chemical composition as a function of temperature or pressure. The method used lies in minimizing the free enthalpy of the system, taking mass balance and electroneutrality as the two conditions. Figure 102 gives the example of the chemical composition expressed as the mole number which characterizes a plasma of argon and water vapor at a 1 bar pressure, a case which can be faced in organic waste incineration. Atoms, free radicals, e.g., O, as well as ionized species and electrons can be pinpointed on Figure 102. The chemical reactions involved and their kinetics highly depend on these occurring species and the respective efficiencies of processes are significantly increased. Gas flow rates can be low due to the highly reactive mixtures. Consequently plasma reactors can be small-sized and the downstream gas processing units can be small-dimensioned. This is a major benefit for some applications, especially in radwaste treatment where facilities must be small-sized. Another advantage of the reactor small size is decreasing their thermal inertia. This results in high flow rates of processed waste relative to the size of plasma reactors.

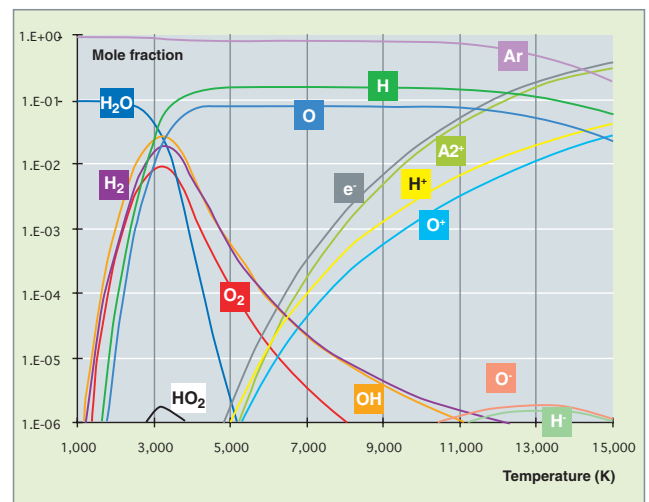


Fig. 102. Evolution of the composition of a Ar/H<sub>2</sub>O plasma versus temperature at a pressure of 1 bar.

These physical particularities endow the plasma processes with high flexibility of use, so that a broad range of waste can be concerned by plasma treatment. Moreover, carrying out several stages of waste processing in a single reactor may be contemplated, in contrast with conventional processes. Such is the case, for example, of organic technological waste incineration/vitrification on a glass bath in a plasma reactor where the ash complete combustion and incorporation can be performed in the same apparatus.

In order to perform solid waste treatment, the CEA has initiated research aimed at proposing a process likely to destroy waste organic fractions while stabilizing and confining their mineral fractions. This type of treatment called “incineration-vitrification” is to generate a vitrified-slag-type ultimate waste with sufficient qualities to be directed to a disposal site. Basing upon its solid background in incineration, high temperature chemistry and associated technologies, as well as vitrification with such advanced techniques as direct-induction cold-crucible melting, the CEA has started to make the whole of its knowledge available for the plasma system in order to propose new processes such as SHIVA (a French acronym for *Système Hybride d’Incineration Vitrification Avancé*: Advanced Hybrid System for Incineration and Vitrification). As shown in the overview of the SHIVA process in Figure 103, SHIVA is at the convergence of knowledge from the areas of incineration, vitrification and research on materials likely to be used in confinement matrices. The IRIS process (IRIS: Installation de

Recherche en Incinération des Solides, facility for research in solid incineration) was developed to incinerate organic waste highly burdened with chlorine so as to generate carbonless ash (see *supra* “Decontamination and treatment processes for effluent and technological waste”, pp. 13-26). Its development made it necessary to combine it with a very high-performance gas scrubbing using filters without filtration medium. The FID (“*Fusion par Induction Directe*”: Direct Induction Fusion) is a cold crucible vitrification process that was developed to protect fusion pots and thereby reduce secondary waste generation. The need for higher treatment capacities oriented the process to the CFA (“*Creuset Froid Avancé*”: Advanced Cold Crucible) (see *supra* “Cold crucible vitrification” pp. 67-70), substituting plane inductors for the induction windings. Knowledge already available on all these technologies made it possible to contemplate incineration-vitrification coupling through organic material feeding on a melting glass bath. As using inductive heating alone did not prove sufficient for efficient oxidization of organic matter, plasma torch implementation was investigated and resulted in the proposal of a hybrid process.

The convergence of the various research routes hereabove mentioned allowed for the proposal of a very compact process, likely to combine in a single reactor waste combustion, gas afterburning (an often voluminous process component ) and the vitrification of the mineral load which contains the major part of activity [1].

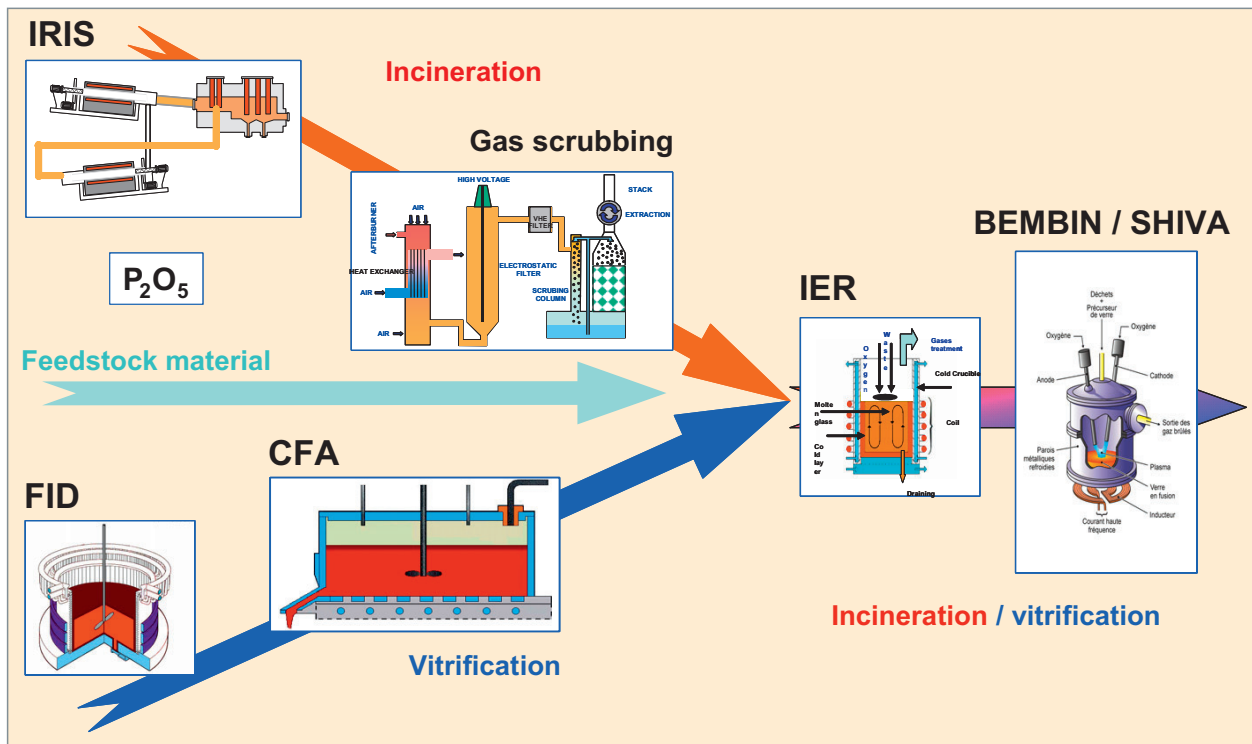


Fig. 103. SHIVA, a waste treatment process issued from several converging research axes at the CEA.

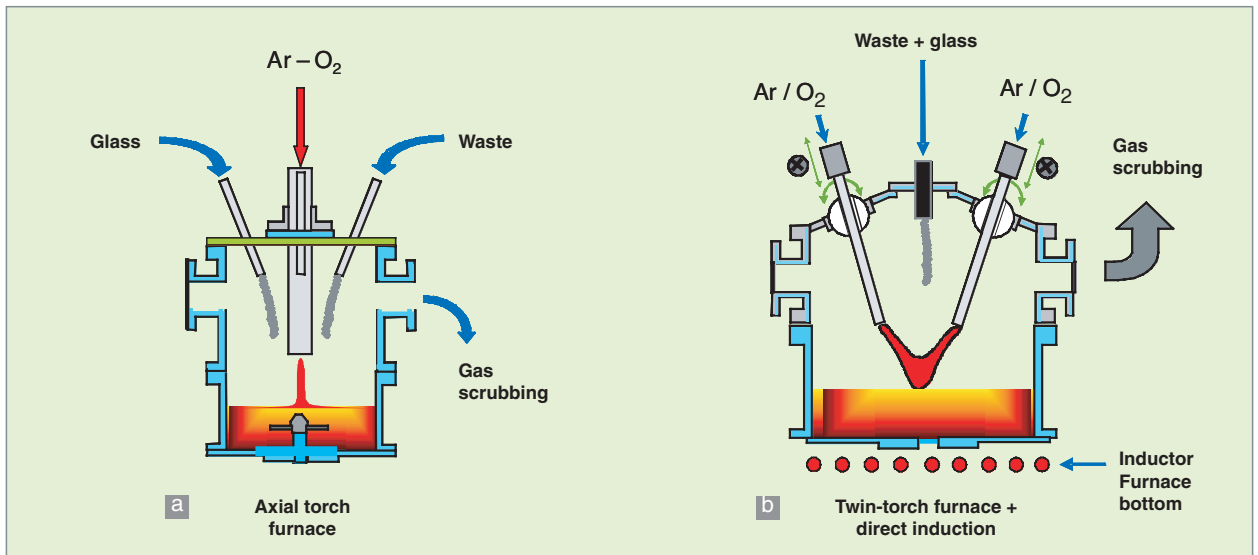


Fig. 104. Incineration/vitrification process: a. in its initial form, b. in its present form SHIVA.

The reactor already set up is issued from several evolutive steps the aim of which was to progressively combine plasma torches and induction techniques, two heating processes. Initially fitted with a transferred arc plasma torch, using an anode immersed in the melt, the reactor turned to the cold crucible concept equipped with an inductive floor overheaded with twin plasma torches of opposite polarity. Figure 104 gives a very schematic view of that evolution.

As shown in Figure 104b, the SHIVA process is currently equipped with a crucible totally cooled by water circulation, which avoids important corrosion on internal walls, and a cooled dome bearing two plasma torches. A planar inductor is placed in the crucible sole plate made of silicon carbide. The process principle lies in waste feeding directly onto the molten glass bath and under the plasma plume which ensures combustion of the waste organic fraction, as well as gas afterburning in the area overheading the molten bath. As for the mineral load, it is progressively incorporated into glass after being stabilized at high temperature. If plasma helps bring the energy required for the various chemical- reactions involved, it is also used to initiate glass melting, thereby avoiding the addition of the metal components necessary to trigger glass melting. The process principle lies in continuous feeding in fragmented waste onto a molten glass bath. After reaching the surface, waste constitutive materials are subjected to a high temperature which has a twofold effect: first, causing a direct combustion phenomenon between the occurring oxygen and the organ matter surface, and, secondly, a pyrolysis for materials unexposed to oxidants. This pyrolysis is responsible for the generation of fuel gases (CO, miscellaneous hydrocarbides) with high calorific value. The volatile compounds released in or near the plasma plume are oxidized quite rapidly as they

are subjected to extreme temperatures and to highly reactive species such as those described in Figure 102. As regards the waste mineral load, one part is vaporized under the effect of high temperatures while the other is incorporated into the glass matrix through a digestion process at the interface. The three main functions of incineration-vitrification are thus gathered within one and the same reactor. This reactor is coupled to a gas scrubbing system which is aimed at cooling and filtering reactive species, and then neutralizing them at low temperature. As shown in Figure 105, the ultimate waste arising from the process are of various types. The gases released are thoroughly decontaminated inert gases, mainly consisting of  $H_2O$ ,  $N_2$  and  $CO$ . The final solid waste is a vitrified slag including nearly all the radioelements occurring in the initial waste, to be directed to a final disposal site. Last but not least, gas scrubbing also generates a scrubbing effluent which, whether liquid or solid depending on the technique used, is fully decontaminated as it is released downstream a high efficiency particulate air filter (HEPA).

One part of the investigations carried out on this topic have demonstrated the importance of treatment conditions in the incorporation of mineral compounds within the glass matrix. For instance, if oxidatino conditions are optimal, the compounds can be introduced as soluble oxides into the molten glass bath. Reversely, some insolubles can be formed at the interface and generate inclusions in the molten glass bath. Such is the case, e.g., of sulfur, depending on whether it is vaporized as  $SO_x$  or retained as sulfides under the form of balls which move into glass. Using plasma torches is of prime importance in this case since it conditions temperature levels at the interface. As shown in Figure 106, when treating with ion exchange resins, some of which are endowed with

sulfonated groups, plasma torch heating limits sulfur ball formation quite significantly, as opposed to a treatment without plasma, which allows for a high number of sulfur balls.

The SHIVA technology was developed to process very different types of wastes. Among them can be mentioned ion-exchange resins, bituminized chlorinated technological waste, and spent fuel treatment sludge. The latter two cases may be quoted as examples [2].

### Chlorinated waste incineration

Technological waste consist of cellulose, plastic materials and a variety of polymers. Their average density is low: 0.16. The chlorine contained results from the wide use of various types of PVC. As any other waste, this waste has a relatively significant mineral loading.

Chlorinated organic waste treatment started to be investigated as part of the incineration described in a previous paragraph (see *supra* "Decontamination and treatment processes for effluent and technological waste", pp. 13-26). This investigation demonstrated that such occurring elements as chlorine in the mineral load induces the formation of volatile compounds which may have devastating effects upon facilities if some pre-

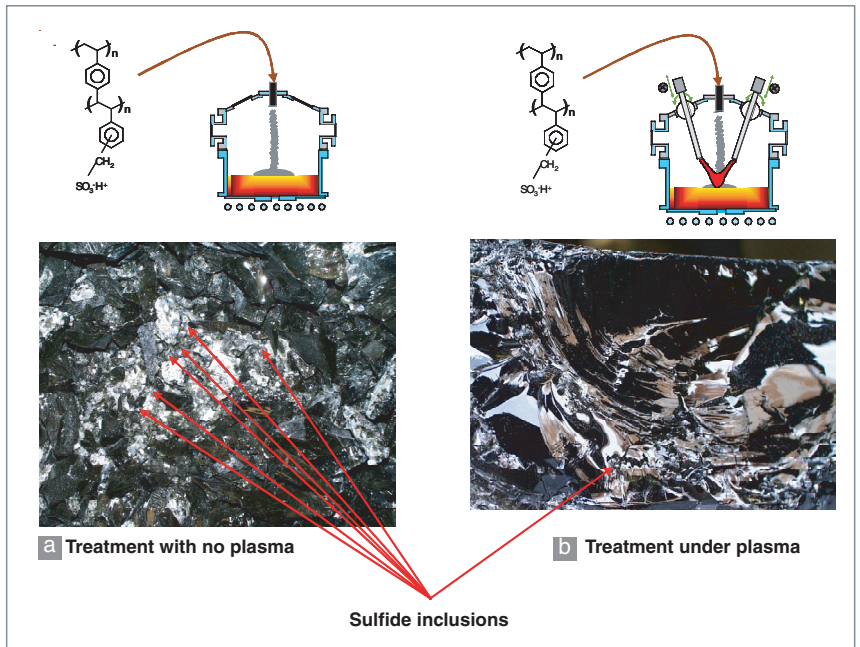


Fig. 106. Photographs of the different outcomes of minerals depending on treatment conditions. On the left-hand side, their treatment of sulfured cation ion exchange resins, with no plasma, results in the formation of sulfur balls. On the right-hand side, their treatment under plasma results in a sharp decrease of the number of balls produced.

cautions are not taken. As demonstrated by the results obtained, substantial benefit may be drawn from substituting phosphorus for chlorine in some volatile chlorides in order to generate stable dusts compatible and liable to be contained in a glass matrix. As the most penalizing compound is zinc chloride  $ZnCl_2$ , the amount of phosphorus introduced shall be adapted to the zinc amount occurring in waste. Currently, a ratio  $Zn/P = 1 \pm 0.1$  seems to ensure sufficient stability of dusts in the case of a rehydration likely to result in the formation of corrosive compounds (hydrated chlorides or polyphosphatic compounds). Phosphorus addition may be performed in various ways, either in solid form through pink PVC (a polymer made fireproof by a tri-aryl phosphate type molecule), which induces an increase in the waste thermal load, or TBP (tributylphosphate), a molecule currently used for spent fuel treatment. The latter alternative is attractive as it provides a new outlet for solvent treatment.

As part of feasibility and development studies, treatment tests are performed in the SHIVA reactor as described in Figure 107. It is coupled with its gas scrubbing system which includes an air quenching device, an electrostatic precipitator and a scrubbing tower.

Plasma (50 kW) - induction (283 kHz-100 kW) coupling gives quite satisfactory results in treatment with an average waste feed flow rate of about 3 kg/h as a first step. As shown in

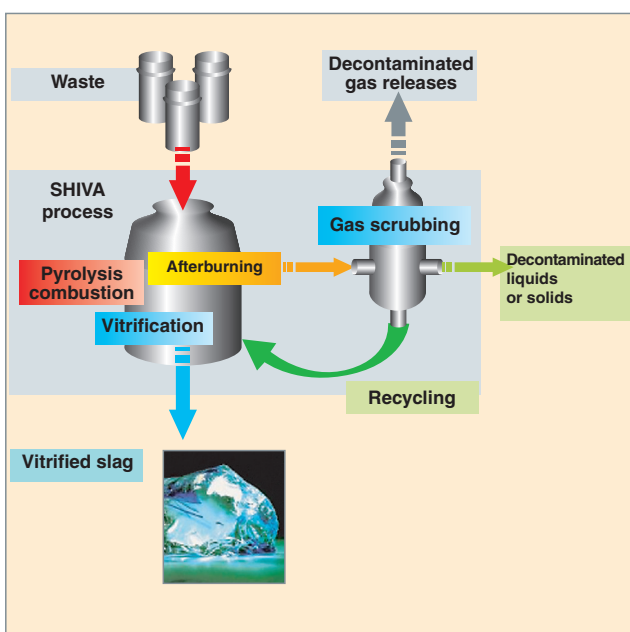


Fig. 105. SHIVA: an integrated process for waste treatment.

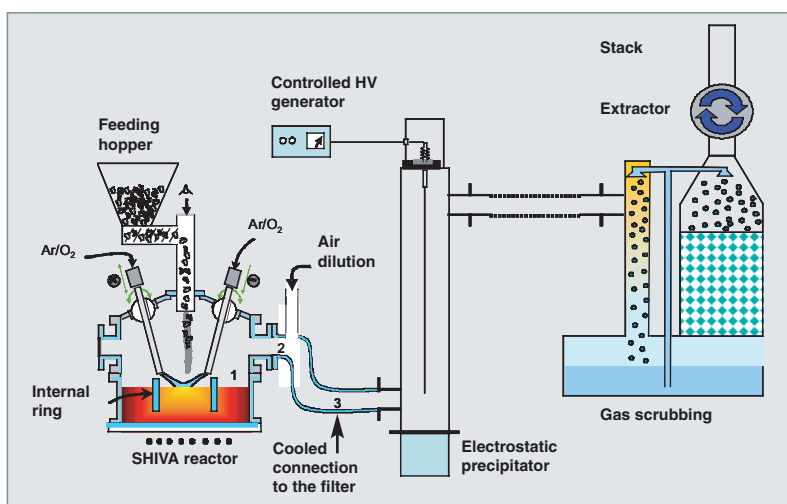


Fig. 107. The whole SHIVA process line. Its consists a waste feeding hopper, the SHIVA reactor, an air quenching device, an electrostatic precipitator, and a scrubber.

Table 16, it emerges from the results collected in a first analysis that the elements occurring in the waste are distributed among reactor glass and filters.

Whereas chlorine is distributed among the reactor and glass, it is obvious that phosphorus, initially gaseous under the form of anhydride  $P_2O_5$ , chiefly occurs in dusts, which highlights the efficiency of chloride phosphatization in a SHIVA-type structure.

Table 16.

Distribution of the mineral loading between the SHIVA reactor glass and the filter				
Element	Reactor	Filter	Compound	Glass (wt %)
C	1.55	1	$SiO_2$	51.69
Cl	18.4	26	$Na_2O$	9.60
S	1.4	0.62	$B_2O_3$	15.45
P	4.6	11.5	$Al_2O_3$	6.60
Na	6	9.5	$P_2O_5$	2.40
K	2	3.25	$K_2O$	0.39
Mg	1.25	0.25	$CaO$	4.80
Ca	6.2	1.25	$Fe_2O_3$	0.34
Zn	18.5	20	$ZrO_2$	2.11
Al	16.5	1.9	$BaO$	0.16
Si	4.3	1.9	$Sb_2O_3$	0.67
Sb	0.9	1.5	$ZnO$	2.80
Ni	1.3	0.1	$TiO_2$	0.15
Fe	6.4	1.1	$MgO$	0.66
Cr	1.6	0.15	$Li_2O$	2.18
Ba	1.6	0.25	$Cr_2O_3$	0.02
B	1.45	3.1	–	–
O	4.8	15.7	–	–

## Sulfur-containing waste incineration

Sludges arising from spent fuel treatment contain many sulfates, which makes difficult their conditioning with conventional methods (cementation, bituminization). Hence the interest of vitrification as part of a SHIVA-type process which, due to its two heating pathways, provides sufficient energy to dry waste and incorporate it into a glass melt. Apart from occurring water, these sludges arising from effluent treatment stations mainly consist of barium sulfate, as shown in Table 17.

The main technical challenge to be faced in processing these sludges is ensuring sulfate decomposition while allowing bar-

ium to be incorporated into molten glass. Tests performed up today have confirmed that the process is feasible on condition that sludges are wholly subjected to the high temperatures coupled with plasma. Oppositely, in the case when part of the sludges happens to be deviated from the plasma zone, sulfate proves to be only partially decomposed. This observation is directly related to species stability, as indicated in Figure 108 which shows how the composition of a  $H_2O/BaSO_4$  equimolar system can proceed between 1,200 and 2,000 °C. As the plasma torches are positioned at the center, the point with the higher temperature corresponds with the crucible center. Then temperature progressively decreases from the center to the outer edge of the ring. So the technological evolution of the process naturally brings it to an internal ring system which retains materials to be processed under the plasma torches, within the plasma plume. This type of ring is represented in Figure 108.

As regards the behaviour of mineral species, the analytical values measured on glass collected from the crucible central part are in excellent agreement with the compositions calculated referring to a R7T7-type glass of known composition that con-

Table 17.

Average composition of STE2-type sludge	
Compound	wt %
$BaSO_4$	62.00
$Ni_2Fe(CN)_6$	6.74
$K_4Fe(CN)_6$	5.26
$CoS$	8.00
$NaNO_3$	9.00
$Na_2SO_4$	9.00

tains the elements listed in Table 18. These values are confronted in Table 18, which shows that today barium incorporation rate is higher than 70%. This result will be improved by determining an appropriate glass formulation.

As a conclusion, plasma-induction coupling in a cold crucible technology allows a wide range of waste to be processed on a semi-industrial scale. Nevertheless source separation is still a pending issue in cases when a high fraction of metals is contained in the materials to be processed. In order to avoid this preliminary step, sometimes hard to cope with depending on waste ages and activity levels, a study is currently under way to propose new routes likely to favor the emergence of a safe, efficient treatment process for this so-called “mixed” waste.

Table 18.

Glass composition analytical values after STE2 sludge treatment under SHIVA plasma		
Compound	Calculated composition	Measured composition
SiO <sub>2</sub>	48.5	49.3
Na <sub>2</sub> O	12.0	13.8
B <sub>2</sub> O <sub>3</sub>	16.8	15.5
Al <sub>2</sub> O <sub>3</sub>	7.3	6.7
ZnO	1.6	1.3
ZrO <sub>2</sub>	0.3	0.4
CaO	2.5	2.3
Li <sub>2</sub> O	1.2	1.1
CoO	0.9	1.0
Fe <sub>2</sub> O <sub>3</sub>	2.7	2.3
NiO	0.4	0.4
K <sub>2</sub> O	0.4	0.6
BaO	5.6	3.9

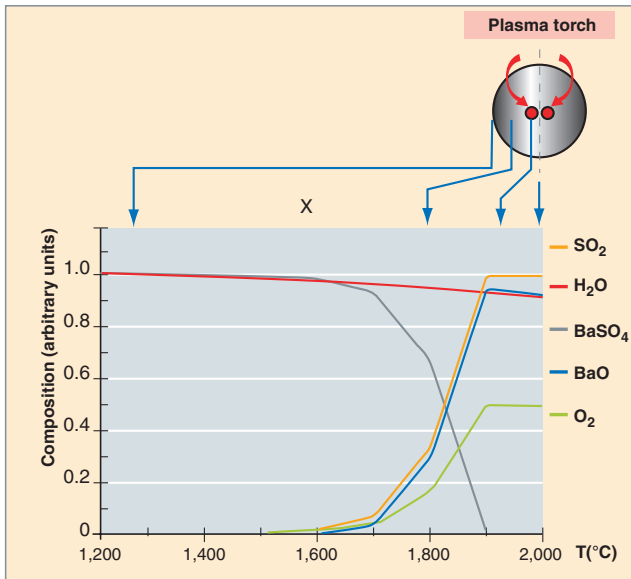


Fig. 108. Evolution of the composition of a BaSO<sub>4</sub> + H<sub>2</sub>O mixture versus temperature. The latter depends on how the material to be processed is positioned relative to the crucible center.

#### ► References

- [1] F. LEMORT, C. GIROLD, O. PINET, “The SHIVA Process: A Tool for the Incineration Vitrification of Hazardous Organic Wastes” IT3’03 Conference, May 9-14, 2005, Galveston, Texas.
- [2] C. GIROLD, O. PINET, F. LEMORT, “Mixed Organic and Mineral Waste Processing by Incineration-Vitrification: Case of Bituminous Media” MRS 2005, September 12-16th 2005, Gand, Belgique.

**Florent LEMORT and Christophe GIROLD,**  
*Research Department of Waste Treatment  
 and Conditioning*

## Alternative confining matrices

### Tailored ceramics for the confinement of specific radionuclides

Today vitrification constitutes “the” reference solution for conditioning high-level waste.

Yet, conditioning some radionuclides within a glass matrix may prove to be difficult owing to low solubility in the glassy network or to high volatility during high-temperature manufacturing.

Though they do not display the chemical flexibility of a glassy matrix (i.e. the capacity to integrate into the structure a number of elements), ceramics can be optimized for the radionuclide considered, thereby presenting the best confining properties.

A first trial in formulating ceramic matrices and qualifying their intrinsic properties was performed in the framework of the French Act of 30 December 1991 on nuclear waste management. The aim was to investigate a route alternative to enhanced separation-transmutation of minor actinides (Np, Am, Cm) and caesium, and a solution for conditioning non-transmutable radionuclides such as iodine.

These studies were conducted in co-operation with academic institutions within a research group (GDR Nomade) and based upon a method coupling an experimental approach and atomistic modelling. They were aimed at determining formulations both able to show a good behavior in the long term, in terms of self-irradiation and leaching resistance, and tailored to each radionuclide to be confined.

Bibliographical analysis and natural analog study served as a guidance to choose the matrix, tending to a high incorporation rate of the radionuclide compatible with the matrix stability:

For minor actinides: zirconolite ( $\text{CaZrTi}_2\text{O}_7$ ), britholite ( $\text{Ca}_9\text{Nd}(\text{PO}_4)_5(\text{SiO}_4)\text{F}_2$ ), monazite / brabantite ( $\text{LaPO}_4/\text{La}_{0.825}\text{Ca}_{0.088}\text{Th}_{0.088}\text{PO}_4$ ), thorium diphosphate phosphate ( $\text{Th}_4(\text{PO}_4)_4\text{P}_2\text{O}_7$ ). Incorporation rate to be reached: 10 wt%.

For caesium: hollandite ( $\text{BaCS}_{0.28}(\text{Fe}_{0.82}\text{Al}_{1.46})\text{Ti}_{5.72}\text{O}_{16}$ ). Incorporation rate to be reached: 5 wt%.

For iodine: vanado-phospho-lead-apatite ( $\text{Pb}_{10}(\text{VO}_4)_{4.8}(\text{PO}_4)_{1.2}\text{I}_2$ ). Incorporation rate to be reached: 7 wt%.

For all these mineral phases (excepting iodine), synthesis is performed through a four-step process:

1. precursor synthesis through the dry or wet route or the sol-gel process;
2. calcination;
3. powder grinding followed by pelletizing;
4. natural **sintering\*** in air.

#### Iodine confinement in apatitic minerals

The volatile character of iodine makes it necessary to develop processes which implement a reactive sintering, thereby allowing to minimize the number of high-temperature operations (one-step synthesis and sintering).

Sintering under uniaxial hot pressing UHP (630 °C-90 min-25PMa) [1] results in composite ceramics consisting of an iodoapatite core surrounded by a lead phosphovanadate jacket (PbVP). It is based upon a reaction between lead iodide and PbVP in excess (Fig. 109). The leaktightness of the system (which prevents from iodine loss) is ensured by PbVP densification at a sufficiently low temperature and with a higher kinetics than iodine release.

Yet, this process at best means a 88.5% densification of the iodoapatite core and a 3% iodine incorporation rate in the composite.



Fig. 109. Photograph of chopped pellets ( $\text{Pb}_{10}(\text{VO}_4)_{4.8}(\text{PO}_4)_{1.2}\text{I}_2$ ), in yellow, and ( $\text{Pb}_3(\text{VO}_4)_{1.6}(\text{PO}_4)_{0.4}$  in grey), for iodine confinement.

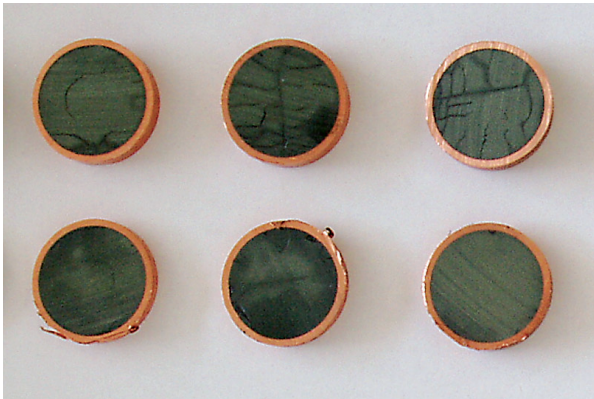


Fig. 110. Iodoapatite pellets obtained by hot isostatic pressing, with their copper envelopes.

Two other processes allowing to make without the PbVP jacket are under evaluation:

- Hot Isostatic Pressing (HIC) enables more than 90% lead iodine to be directly converted into dense iodoapatite (Fig. 110). Once the reactants have been shaped by cold isostatic pressing, prior to being subjected to the HIC cycle, pellets are inserted into a twofold container consisting of a copper-made internal envelope and a steel-304L-made internal envelope designed to ensure leaktightness after welding.
- Flash sintering through Spark Plasma Sintering enables centimetric items to be densified by letting a pulsed direct current flow through the material [2]. This current is approximately 400A and has a step profile, i.e., a 12-ms pulse followed with a 2-ms stop. It is applied between two electrodes which press upon the sample within a graphite cylindrical matrix. Iodoapatite densification is obtained for temperatures of 400-500 °C, with a temperature plateau of 5-20 min (heating rate 50 °C/min) and a densification rate higher than 97%.

Evaluating the underwater behavior of ceramics requires a fine description of alteration mechanisms and kinetics. The data acquired for all these matrices in pure water make it possible to describe the inner behavior of the ceramic (as regards this topic, see the paragraph written by J.-E. Lartigue in the "Corrosion" Monograph to be published).

However, once placed under disposal conditions, these matrices will undergo internal irradiations due to particle emission during the disintegration of the incorporated radionuclides, which can lead to the **amorphization**\* of the crystalline structure (due to  $\alpha$  particles), and entail a potential alteration of its chemical durability in water.

Similarly, the interstitial water could be irradiated by the  $\alpha$  particles emitted during the disintegration of the radionuclides disposed of: it would be then **radiolyzed**\*, which would entail the formation of unstable, reactive radical species ( $\text{HO}^\bullet$ ,  $\text{H}^\bullet$ ,  $\text{e}^-_{\text{aq}}$  ...), along with the formation of stable molecular species ( $\text{H}_2\text{O}_2$ ,  $\text{H}_2$ ).

### Self-irradiation dependence of zirconolite leaching [3]

Synthetic zirconolites amorphized by ( $\text{Pb}^{3+}$ , 360 keV) heavy-ion beam bombardment as well as metamict natural zirconolites (Phalabowra Carbonatite Complex, South Africa), rich in U and Th and aged  $2.10^9$ , were leached to evaluate their chemical durability.

Despite the structure amorphization, the chemical durability is not significantly altered: the initial alteration rate varies by less than a factor 1.5 compared with the results obtained on the unirradiated ceramic. Following a few years, the rate decreases by more than four orders of magnitude just as did the sound ceramic (Fig. 111).

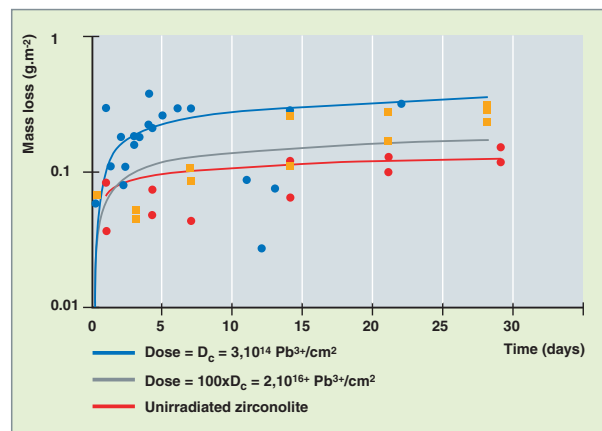


Fig. 111. Alteration by water of Nd-doped zirconolites, leached in the Soxhlet mode, at 100 °C, in initially pure water, before and after their irradiation by heavy ions. Calcium standardized mass losses – noted as PMN(Ca) – are in red for unirradiated zirconolite, in blue after irradiation by Pb ions (dose =  $3 \times 10^{14}$  ions/cm<sup>2</sup>), and in grey after irradiation by Pb ions (dose =  $2 \times 10^{16}$  ions/cm<sup>2</sup>).

### Water radiolysis dependence of zirconolite leaching [4]

Water radiolysis was generated by *alpha* particle or proton beams from the outside, with a flow higher than the values expected under disposal conditions by about 5 orders of magnitude so as to enhance the effects of water radiolysis.



Titanium, neodymium and zirconium releases increase by one to two orders of magnitude under radiolytic conditions comparing with releases measured without any radiolysis, whatever the temperature (20 or 50 °C), the zirconolite state of surface (sound or amorphous), and the experimental conditions (with or without irradiation of the solid) (Fig. 112). This effect cannot be only attributed to the redox reactions between oxidizing radiolytic species and zirconolite constitutive elements, for the latter are in their higher oxidation degree. Yet, it is assumed that  $H_2O_2$  plays a role through **complexation\*** reactions. It is also worthwhile to mention that aluminium and calcium releases are not significantly altered under radiolytic conditions, since they are higher by 1 to 3 orders of magnitude than those of titanium, zirconium and neodymium, which keeps the dissolution incongruent.

Concerning release evolution, it can be first observed a kinetically controlled phase. During this phase the dissolution rate, based upon neodymium releases, is higher by five orders of magnitude to the rate determined without performing a radiolysis; Yet this step is very short under radiolytic conditions, i.e., a few hours. When the leachant gets saturated with the zirconium and titanium hydroxides, releases become constant: from then the dissolution is controlled thermodynamically. During this thermodynamic step Ti, Zr and Nd concentrations are controlled by the solubility of titanium and zirconium hydroxides, which is very low in water (about  $10^{-8}$  mol.L<sup>-1</sup>). Assuming the dissolution to be homogeneous, these concentrations represent an altered thickness of about a few nanometers. However, this very fine alteration layer could not be observed on the solid.

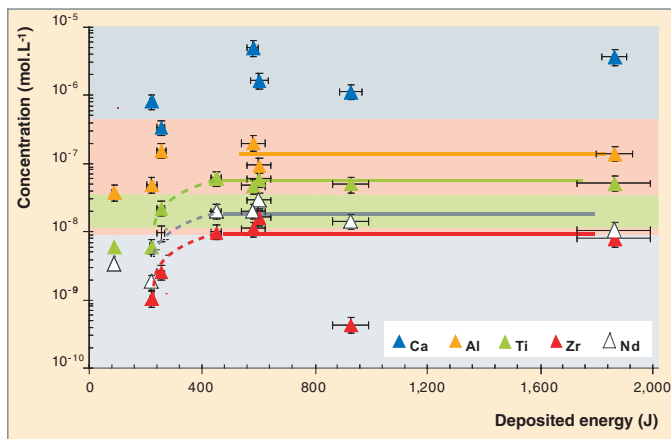


Fig. 112. Total basic contents released for zirconolite in equilibrium in water under radiolytic conditions as a function of the energy deposited. The energy deposited quantity is a function of the irradiation time: 1 hour stands for 115 J. The green and red-colored areas represent the solubility limits of titanium and zirconium hydroxides issued from literature [5,6].

In addition, under radiolytic conditions, the occurrence of a complexing agent for titanium and zirconium ions (fluoride ions) induces an increase of their releases in solution.

The dissolution then gets congruent for all the elements save neodymium, the releases of which are not affected by the occurring complexing species.

As shown by the analyses performed on the solid, alteration occurred preferentially at the grain boundaries. All these results are in agreement with the experiments achieved without any radiolysis.

As a conclusion, even under very aggressive conditions (water radiolysis, occurring complexing agents), zirconolite exhibits excellent chemical durability properties.

### Apatite leaching

Natural apatitic minerals are known for their stability and low solubility over very long periods.

A comparative study of alteration rate evolutions as a function of pH (90 °C) was conducted for a britholite  $Ca_9Nd(PO_4)_5(SiO_4)F_2$ , a fluoroapatite  $Ca_{10}PO_4)_6F_2$ , and an iodoapatite of composition  $Pb_{10}(VO_4)_{4,8}(PO_4)_{1,2}I_2$ . It shows that the three apatitic matrices display very similar behaviors in the pH range investigated. Alteration rates are low, between  $10^{-3}$  g.m<sup>-2</sup>.j<sup>-1</sup> for a pH of 5.5 - 6.5, and 1 g.m<sup>-2</sup>.j<sup>-1</sup> for the most acid pH. The three rates increase linearly with the decreasing pH, with very similar slopes. Thus the anion (I or F) seems to have a very limited influence upon the matrix alteration mechanism. A similar behavior can therefore be assumed for chloroapatite.

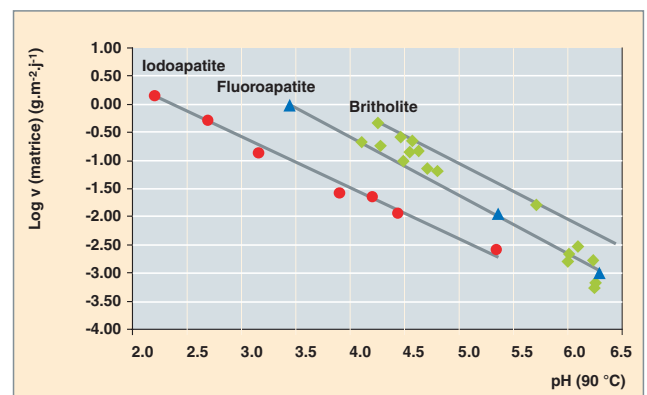


Fig. 113. Evolution of the alteration rate (log) as a function of pH at 90 °C for fluoroapatite  $Ca_{10}(PO_4)_6F_2$  (FAp), iodoapatite  $Pb_{10}(VO_4)_{4,8}(PO_4)_{1,2}I_2$  (IAp), and britholite  $Ca_9Nd_1PO_4)_5(SiO_4)F_2$ . The alteration tracer is Ca in the case of FAp, and britholite in the case of iodoapatite.

## Irradiation effects on confining ceramics

The main decay mode of minor actinides Np, Am, and Cm is the  $\alpha$  disintegration mode. *Alpha* disintegration causes to emerge a recoil nucleus with an energy between 70-100 keV, and an *alpha* particle with an energy between 4-5.5 MeV, which generates a helium atom in the structure by capturing two electrons. These two particles lose their kinetic energy through elastic (nuclear) interactions, and inelastic (electron) interactions with the atoms of the host matrix. More precisely, the recoil nucleus transfers about the two thirds of its energy through elastic interactions, which induces the generation of atomic displacements - i.e., about 1,500 per event - over a very short distance –  $10^{-40}$  nanometers –. Oppositely, more than 99% of the *alpha* particle energy is transferred as inelastic interactions over a few dozen micrometers. The remaining part of the energy of this particle generates about 100 atomic displacements in the host matrix in the end of its path [7].

Two techniques were used in order to study the effects of these events upon the structure of the ceramics contemplated for minor actinide conditioning (zirconolite, monazite-brabantite, britholite, thorium phosphate diphosphate). The first technique lies in achieving materials doped with short-lived radionuclides - Pu 238, with an 87-year half-life) which allow for the rapid buildup of a significant integrated dose, as represented in Figure 114. The second technique consists in irradiating the ceramics with ions. Helium ions were used to simulate, first, the electron energy deposition, and, secondly, helium generation in the structures under investigation, whereas the multi-energy mode irradiations with heavy ions (Au, Si) allowed to simulate the damage caused by the recoil nucleus. It must

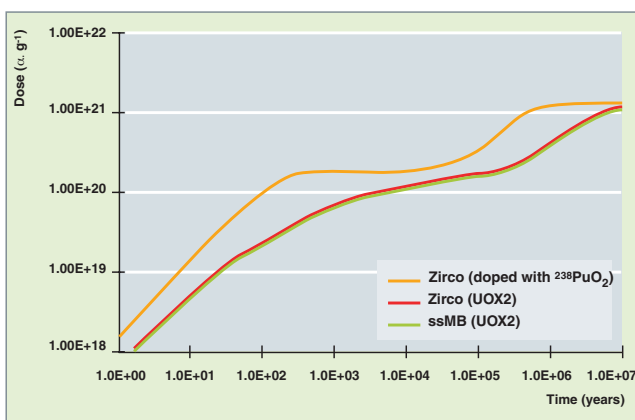


Fig. 114. Evolution of the integrated *alpha* dose obtained as a function of the disposal time for zirconolite pellets doped with 10 wt%  $^{238}\text{PuO}_2$  and for pellets of zirconolite and monazite brabantite solid solution (ss MB) containing 10 wt% minor actinide oxides incorporated in proportions corresponding with the radionuclide annual amounts arising from UOX<sub>2</sub> fuel treatment.

be emphasized that investigations on doped materials have not proceeded at the same pace, which made it difficult to compare the materials considered. Oppositely, studies based upon external irradiations allowed the first results to be obtained in this field.

## Evolution of materials properties under irradiation

The **amorphization\*** critical dose measured on the zirconolite doped with Pu 238 is close to  $4 \cdot 10^{18} \alpha.g^{-1}$ , which is consistent with the results published [7]. Recrystallization of the 2M-monoclinic structure of zirconolite is achieved in several steps: atom rearrangement from 500 °C, transition to a rhomboedric structure, and finally recrystallization of the 2M-monoclinic phase from 850 °C. Though the amorphization process has never been observed for natural monazites [7], it could be observed indeed for externally-irradiated monazites, as well as on americium-doped samples. The amorphization critical dose measured for this material is  $2.2 \cdot 10^{18} \alpha.g^{-1}$  [8].

The macroscopic swelling measured on Pu 238-doped zirconolites reaches about 6% on saturation (Fig. 115). This saturation phenomenon emerges for an integrated dose corresponding with the amorphization critical dose of the structure, which, as highlighted by CLINARD [9], shows that the two phenomena are linked. CLINARD deduces from it that these evolutions originate in the radiation damage caused to the structure by the recoil nucleus. In addition, the results obtained through ion or multi-energy mode external irradiation also exhibit swelling saturation for an approximate value of 6% (Fig. 110).

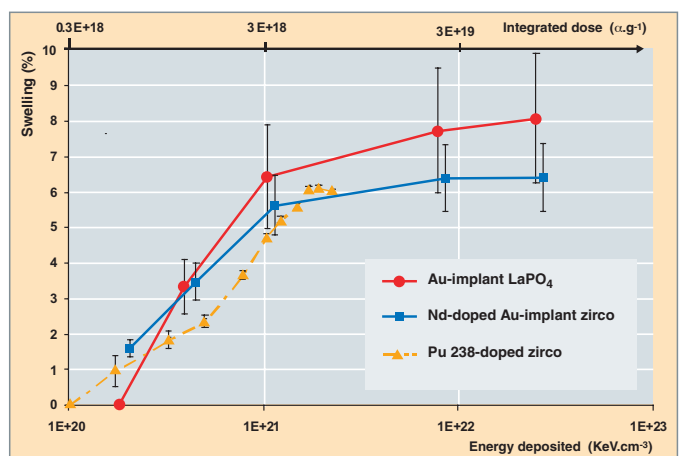


Fig. 115. Macroscopic swelling expressed as a function of the incident particle nuclear energy deposited: a recoil nucleus for Pu238-doped zirconolite, and Au ion in other cases. The nuclear energy deposited per unit volume was calculated by the computer code SRIM; correspondence with the integrated *alpha* dose is indicated. Swelling is measured by hydrostatic weighing on the Pu 238-doped samples, and by optical interferometry on the samples irradiated by ion beams.

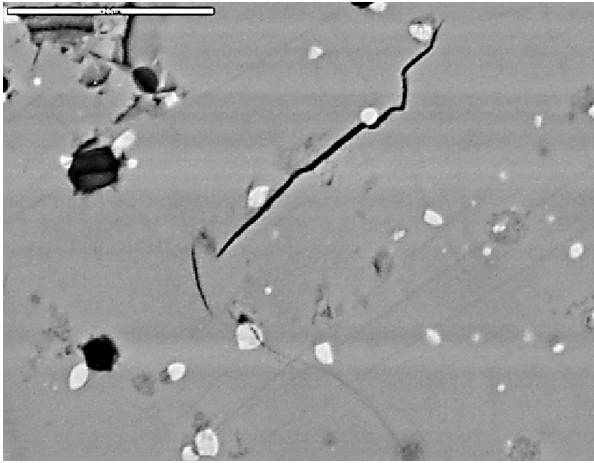


Fig. 116. Microstructure showing the presence of a microcrack in a Pu238-doped zirconolite pellet which has received a dose of  $2.1 \times 10^{18} \alpha.g^{-1}$ .

This corroborates the hypothesis that the nuclear energy deposited (i.e., radiation damage) is at the origin of the swelling observed. It can be seen on the same figure that the swelling measured in the monazite solid solution is slightly higher than in zirconolite, since it reaches about 8% on saturation. It is also noteworthy that macroscopic swelling is more predominant than microscopic swelling (i.e., 2% as regards zirconolite) measured by X diffraction prior to structure amorphization. According to Weber [7], this difference can be explained by three contributions: expansion of the crystal cell, amorphous area swelling, and swelling resulting from the emergence of extended defects (bubbles, microcracks, dislocations...). Microcracking could be observed in the case of Pu 238-doped zirconolite (Fig. 116), whereas no bubble could be evidenced on TEM examination of helium-implanted zirconolite samples.

Helium-3 profiles implanted in different pellets were measured using the nuclear reaction  $3He(d,p)4He$ , which made it possible to determine diffusion coefficients of this element in the ceramics investigated (britholite, zirconolite, and monazite). Basing upon these results, helium migration over a 10-micrometer distance (i.e., approximately the size of one grain) would last 100,000 years for britholite and 10 million years for zirconolite at the temperature of the geological disposal facility (50 °C), which implies a high amount of helium being retained in these structures. Yet, data relating to thermal diffusion have to be completed for a real material, for the diffusion process may be strongly speeded up, especially at low temperatures. Research work is under way to evaluate irradiation impact on this parameter in zirconolite. Preliminary measurements of helium release have been performed at the Karlsruhe ITU on plutonium-doped zirconolites (Fig. 117). The results obtained confirm high helium holdup in this structure and show the important role of the material structural state upon release:

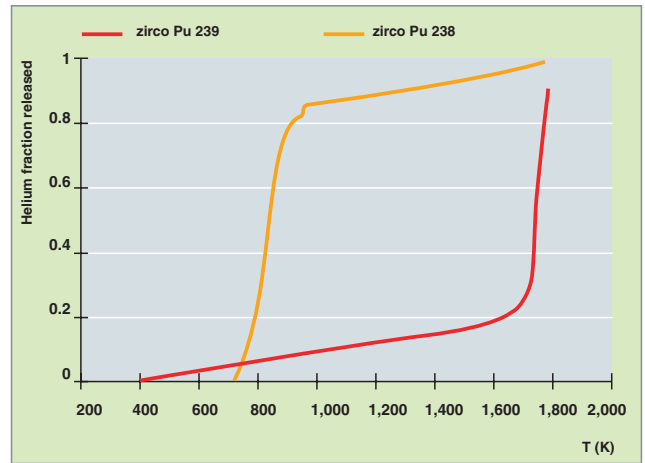


Fig. 117. Helium fraction released by zirconolite under annealing until reaching its melting temperature. The curve in red was obtained on a zirconolite displaying a crystallized structure (integrated dose:  $4.10^{16} \alpha.g^{-1}$ ), the curve in orange on a zirconolite exhibiting a metamict structure (integrated dose:  $4.10^{18} \alpha.g^{-1}$ ).

- for Pu239-doped crystallized materials, a release can be observed at a temperature close to the zirconolite melting temperature ( $T > 1,600$  K);
- for Pu238-doped metamict materials, a significant portion of helium ( $\approx 85\%$ ) is released as the structure is being recrystallized ( $500 > T > 700$  °C).

As a conclusion, in an initial phase (integrated dose lower than  $5 \times 10^{18} \alpha.g^{-1}$ ), swelling and amorphization of the ceramics investigated (zirconolite, monazite-brabantite) are chiefly due to radiation damage and, particularly, ballistic effects of the recoil nucleus. In this very phase, the helium generated by the *alpha* disintegration is in too low a concentration ( $>500$  ppm) to play an important role in swelling. Yet, for higher integrated doses likely to be reached in a disposal scenario ( $10^{20}$  to  $10^{21} \alpha.g^{-1}$ ), this element behavior will have to be defined more precisely.

## Atomistic modelling benefits

The term “atomistic modelling” usually designates two types of methods: the so-called *ab initio* quantum chemistry modelling, and a molecular dynamics simulation method. Studies based upon atomistic modelling bring out two types of information. On the one hand, modelling can help calculate quantities accessible to experimentation such as thermodynamic quantities, without having to synthesize the solid of potential interest for a given application. On the other hand, it affords better understanding of the basic mechanisms which govern the structure/reactivity relations. (“Reactivity” here means both chemical stability and the more or less high ability to swelling, as well as radiation and leaching behavior.

*Ab initio* atomistic modelling gives direct access to the geometries of crystalline structures and so informs about whether a given composition may be stable or not. For example, caesium conditioning in an apatitic matrix proved to be impossible, because the caesium ion size did not allow for the building of a stable crystallographic pile-up [12]. Nevertheless, similar calculations made it possible to consider all of the compounds of the lead vanadate apatite and demonstrate the occurrence of a solid solution continuous from the phosphate to the vanadate pole. Figure 119 gives an insight of the cell of the lead vanadate apatite, of composition  $Pb_{10}(VO_4)_6I_2$ .

Once the crystalline structure of a potential matrix is known, atomistic modelling can be used to calculate some thermodynamic quantities such as formation enthalpy, cohesion energy, or calorific capacities [13]. Consistency with experimentation is so high that modelling can now be used for predictive purposes. Figure 120 gives an insight of the calorific capacity values versus temperature for fluoroapatite, as well as predictions for the hereabove mentioned lead vanadate apatite.

Incorporating actinides (RN) into apatites has also been investigated, both from the macroscopic (geometry and formation energy) and the mechanistic viewpoint, to highlight the parameters likely to further the stability of a radionuclide in the host matrix [14,15]. Substituting divalent ions for tri- or tetravalent ions gives, by charge compensation,  $Ca^{2+} + PO_4^{3-} \rightarrow RN^{3+} + SiO_4^{4-}$  or  $Ca^{2+} + 2PO_4^{3-} \rightarrow RN^{4+} + 2SiO_4^{4-}$  which respectively lead to apatites of formula  $Ca_9RN(PO_4)_5(SiO_4)F_2$  and  $Ca_9RN(PO_4)_4(SiO_2)_2F_2$ . At the energetic level, it can be observed a stabilization of the structure relative to fluoroapatite

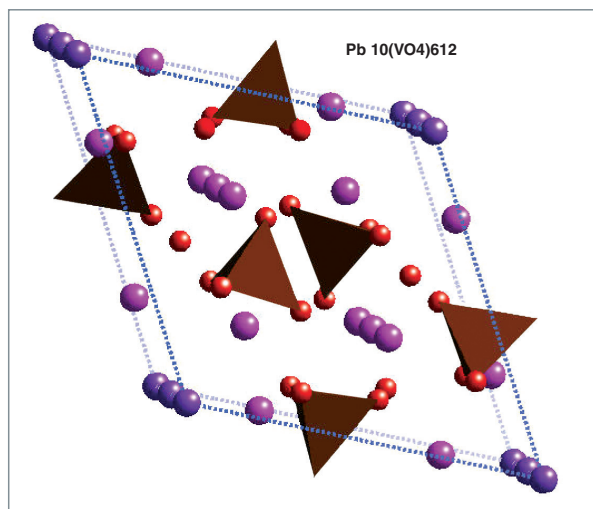


Fig. 119. Crystalline cell of the apatite  $Pb_{10}(VO_4)_6I_2$  (the brown triangles represent phosphate ions while the pink spheres stand for the lead ions, and the violet spheres for the iodide ions).

whatever the ion incorporated. Yet, this stabilization is higher for tetravalent ions than for trivalent ions. Consequently, the radionuclides are incorporated preferentially into the apatite as tetravalent. Analyzing the electron density shows that the bonds formed are not merely ionic (Fig. 121). The decrease in the charges of the RN and their neighbours, especially F, shows that the bonds formed by the RN are partially covalent, and that charge transfer is, first, higher for actinides (e.g., U) than for lanthanides (e.g., Ce), and, secondly, higher for ions 4+ than for ions 3+, which is directly correlated with the relative stabilities observed. The relation between bond covalence and the structure stability seems to be established.

Diverse molecular dynamics studies (see “*Glasses: a waste conditioning matrix for the long term*”, pp. 27-70) help simulate the effects of heavy-ion irradiations on crystalline matrices. As shown by a computational study on a pyrochlore structure ( $Ab_2B_2O_7$ ) after stress-relieving at constant pressure, the pyrochlore crystalline structure is consistent with experimental observations [16] (Fig. 122).

Modelling and simulation coupled with the experimental investigation methods thus allow to have a fine knowledge of the mechanisms and properties useful for a given purpose.

#### Ab initio methods for ceramics structure calculation

The so-called *ab initio* methods are calculation methods which do not call for any experimental datum, as they only require knowing the nature of the atoms which constitute the structure. Describing interactions between these atoms lies upon the writing of an operator composed of all physical basic interactions between particles of matter (electrostatic forces) [11].

Concerning the most simple apatite, fluoroapatite of formula  $Ca_{10}(PO_4)_6F_2$ , initial knowledge is given in Figure 118.

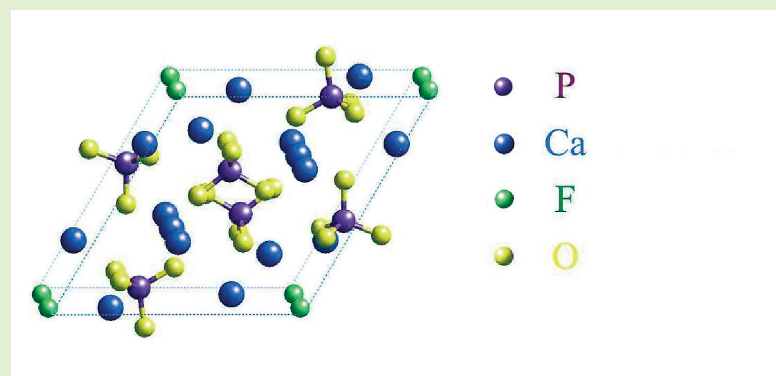


Fig. 118. Structure of fluoroapatite.

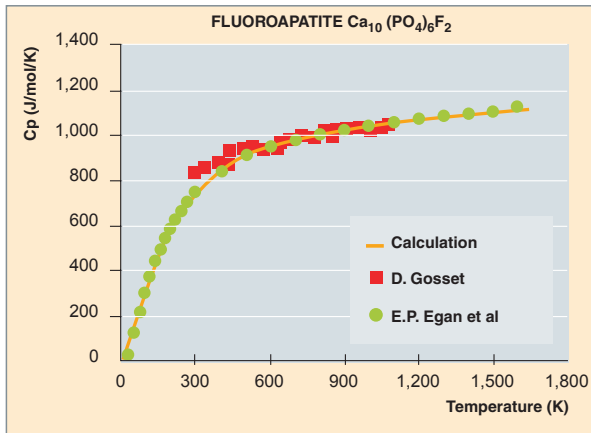


Fig. 120. Specific heat of fluoroapatite as a function of temperature [3].

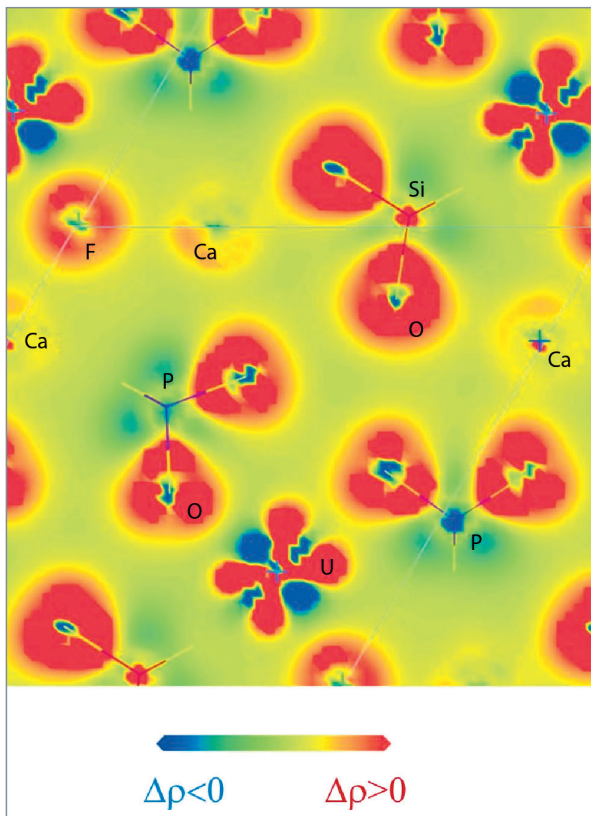


Fig. 121. Chart showing the deformation of charge densities in a (001) plane of the most stable configuration of the  $U^{4+}$ -containing apatite.

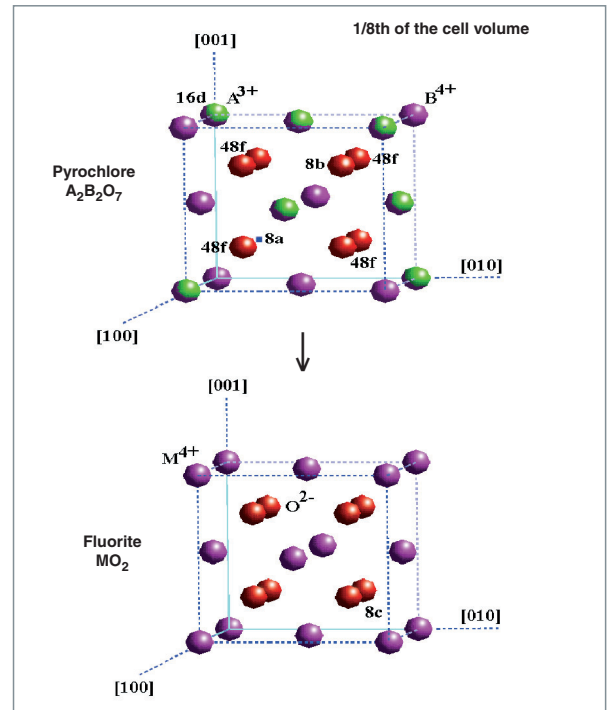


Fig. 122. Irradiation damage in a fluorite-type structure.

## Open prospective research for future conditioning materials

Alternative conditioning matrices are still very far from being implemented industrially. It is not obvious that their benefits in terms of safety do compensate the manufacture-related overcost and all of the resulting secondary waste. Yet, they could prove to be of interest for managing the waste associated to some advanced fuels.

### References

- [1] F. AUDUBERT, "Mise au point d'une matrice apatitique pour le confinement de l'iode 129", Thesis, Institut national polytechnique de Toulouse (1995).
- [2] Z.A. MUNIR, U. ANSELMINI-TAMBURINI, M. OHYANAGI, "The effect of electric field and pressure on the synthesis and consolidation of materials: a review of the spark plasma sintering method", 2006, *J. Mat. Sci.*, 41, pp. 763-777.
- [3] C. FILLET, T. ADVOCAT, F. BART *et al.*, "Titanate-based ceramics for separated long-lived radionuclides", *C. R. Chimie* 7 (2004), pp. 1165-1172.
- [4] M. TRIBET, "Étude de l'effet de la radiolyse de l'eau sur la lixiviation de la zirconolite", Thesis, Claude-Bernard Lyon1 University (2007).
- [5] K. G. KNAUSS, M. J. DIBLEY, W. L. BOURCIER *et al.*, "Ti(IV) hydrolysis constants derived from rutile solubility measurements made from 100 to 300 °C", *Applied Geochemistry*, 16 (2001), p. 1115.

- [6] P. L. BROWN, E. CURTI, B. GRAMBOW, "Chemical thermodynamics of zirconium", Elsevier, *Chemical thermodynamics*, **8** (2005).
- [7] WEBER W.J., EWING *and al.* *J. Mat. Res.*, **13** (6), 1998, pp. 1434-1484.
- [8] BREGIROUX, BELIN *et al.*, *J.N.M.* **366**, 2007, pp. 52-57.
- [9] F.W. CLINARD, *Am. Cer. Soc. Bull.*, **65** (8), 1986, pp. 1181-1187.
- [10] X. DESCHANELS *et coll.*, CEA rapport CEA/DTCD/2005/02, 2005.
- [11] M.C. PAYNE, M.P. TETER, P. ALLAN, J.D. JOANNOPOULOS, "Iterative Minimization Techniques for *Ab Initio* Total Energy Calculations: Molecular Dynamics and Conjugate Gradients", *Rev. Mod. Phys.*, **64**, pp. 1045-1097 (1992).
- [12] A. CHARTIER, C. MEIS, J. D. GALE, "A computational study of Cs immobilization in the apatites: in  $\text{Ca}_{10}(\text{PO}_4)_6\text{F}_2$ ,  $\text{Ca}_4\text{La}_6(\text{SiO}_4)_6\text{F}_2$  and  $\text{Ca}_2\text{La}_8(\text{SiO}_4)_6\text{O}_2$ ", *Phys. Rev. B* **64** (2001), p. 85110.
- [13] J.L. FLECHE, "Thermodynamical functions for crystals with large unit cells such as zircon, coffinite, fluorapatite and iodoapatite from *ab initio* calculations", *Phys. Rev. B* **65** (2002), p. 245116.
- [14] M. BERTOLUS, M. DEFRANCESCHI, "Towards the comparison of Rare Earth Elements and actinide behavior in materials: a computational study of Ce and U-bearing britholites", *J. Phys. Chem. B* **110**, p. 19226 (2006).
- [15] M. BERTOLUS, M. DEFRANCESCHI, "Optimizing the formula of Rare Earth-bearing materials: a computational chemistry investigation of Nd-bearing apatite", *Int. J. Quant. Chem.* **107**, 712 (2007).
- [16] J.-P. CROCOMBETTE, A. CHARTIER, "Molecular dynamics studies of radiation induced phase transitions in LZ pyrochlore", *Nucl. Instrum. Meth. Phys. Res. B* **255** (2007), p. 158.

**Catherine FILLET, Magaly TRIBET and Sylvain PEUGET,**

*Research Department of Waste Treatment and Conditioning*

**Xavier DESCHANELS,**

*Marcoule Institute for Separation Chemistry*

**Mireille DEFRANCESCHI,**

*Simulation and Experimental Tools Division*

## Confinement of waste from pyrochemical processes: status of research

**P**yrochemical route treatment consists in treating spent fuel after dissolving it in an appropriate molten salt, generally made of a eutectic mixture of chlorides or fluorides.

Most of **pyrochemical**\* techniques have been developed only on the laboratory scale. Two processes alone have emerged on the pilot scale, for metallic fuel treatment at ANL (*Argonne National Laboratory USA*) and for oxide fuel treatment (UOX, then MOX) at the RIAR (*Research Institute of Atomic Reactors, Russia*). In both cases, treatment includes an electrolytic stage in a molten chloride medium at a temperature between 500-700 °C.

The process aims at separating spent fuel into two components:

1. the valuable material: i.e., uranium, plutonium, and minor actinides recovered under metallic form. These elements are intended to be recycled as part of a new fuel;
2. the waste: i.e., first, contaminated, highly reactive salt, which contains fission products of the alkaline, alkaline-earth, and lanthanide types, and, secondly, metallic waste containing the so-called “reducible” fission products.

Renewed interest in these processes has emerged as part of the developing of the nuclear systems of the future, especially in the Russia and the United States. However, due to their chemical composition and low chlorine solubility in glasses, high-level salt-bearing waste will not be likely to be vitrified according to the present process of metallic crucible vitrification. Besides, their direct conditioning through vitrification or any other comparable process would mean a very significant increase in the high-level waste volume owing to the occurring solvent.

In France, the CEA is developing a process for reducing extraction in molten fluoride medium. Vitrification through an advanced “cold-crucible” vitrification process of the high-level salt-bearing waste could induce a glass-ceramic material compatible with incorporation rates of about 15% of the initial waste. (See *infra* the frame “Fluoride vitrification”).

As previously shown, the USA have developed a process to treat a metallic fuel in a molten chloride medium (a LiCl/KCl

mixture). This process is now being developed on the industrial pilot scale in the USA, for it was selected by ANL to treat spent fuels from the Experimental Breeder Reactor EBR-II (a sodium-cooled fast neutron reactor). As for fluorinated salt confinement, a new vitrification process could be contemplated. However, it seems that chlorine solubility in glasses is highly limited, hence the need for developing other, ceramic-type matrices.

The process investigated by ANL to condition this salt-bearing waste consists in performing the reactive sintering of zeolites after adding to them the fission products-containing salt, as well a glassy binder. The material so obtained is a glass/sodalite composite (see the frame “Glass-sodalite composite”), which contains a few wt% fission products. These radioactive elements are distributed depending upon their chemical nature: alkaline and alkaline-earth elements insert themselves within the borosilicate glass phase whereas the lanthanides can be seen as crystals distributed around the sodalite grain area. As regards chlorine, it is integrated into sodalite.

Other routes in a lesser state of advancement are also considered for chloride conditioning. On the one hand, the aim is to develop chlorinated apatitic ceramics, analogically to the studies conducted on apatitic phases for conditioning another halogen, iodine. The major asset of these matrices is their high resistance to leaching (pp.111-118).

In parallel to these studies, more innovating works are also under way with a view to salt recycling, together with the fission products selective conditioning. Fission products selective precipitation reactions are thus investigated so as to decontaminate salt and thereby allowing it to be used again. The chemical families to be taken into account, ranked in increasing order of difficulty, are lanthanides, alkaline-earths and alkaline elements. The aim is to form intrinsically durable mineral phases with reaction yields close to 100%, by adding carefully selected reactants (see *infra* the frame “Fission products selective precipitation in molten salts”).

Reducible fission products constitute a group the composition of which depends upon the fuel nature, burnup, and clad, as well as the pyrometallurgical process itself. The main elements to be considered are Ru, Rh, Pd, Mo, Tc, Ag, Sb, and Nb. The vitrification of such a mixture can be contemplated, but it requires the oxidation of most of the elements and the incorporation rate of such a stream is strongly limited by the fact that most of the constitutive elements occur as crystals within the molten glass. These occurring crystals (especially  $\text{RuO}_2$  pins and Pd beads) cause potential problems such as electrical resistivity drops or massive settling of metallic phases at

### Fluoride vitrification

Borosilicate glasses have the capacity of incorporating fluorine and fission products into their network by forming Si-F bonds which entail a progressive glass depolymerization (Fig. 123). This depolymerization potentially induces a degradation of chemical durability. In order to limit this effect, glass compositions have been chosen so as to induce fluorine crystallization as calcium fluoride, which “traps” fluorine in a crystalline phase of good intrinsic durability (Fig. 124), and allows the glass network to keep its confinement properties.

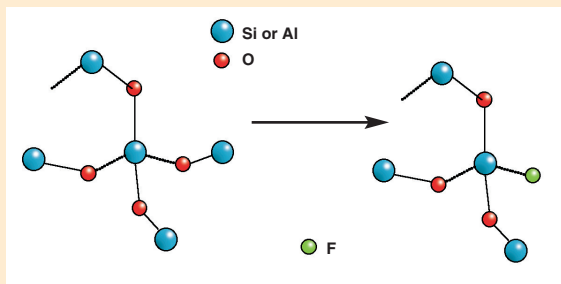


Fig. 123. Schematic representation of the structure of a silicate glass network.

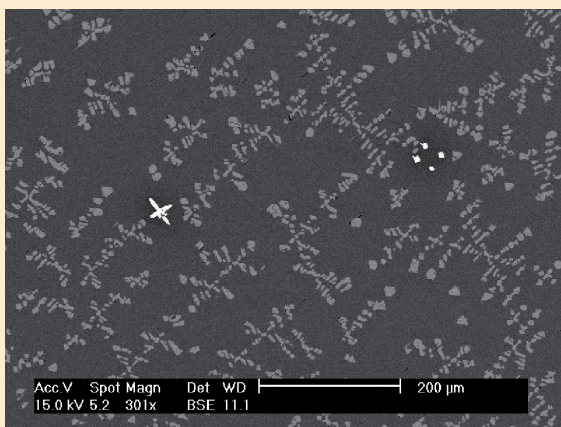


Fig. 124. SEM view of a glass-ceramic containing 15 wt% fluorinated salt. Crystals shown in light grey are of fluorite  $\text{CaF}_2$ .

### Glass-sodalite composite

A.N.L.'s developing the sodalite/glass composite for a contaminated chlorinated salt lies on the ion exchange properties of the zeolite family compounds, natural minerals of the silicate family.

Their structure results from the chaining of coordination polyhedra  $[\text{SiO}_4]^{4-}$  and  $[\text{AlO}_4]^{5-}$  only bound by their tops, thereby forming a negatively-charged open network displaying tunnels and cavities (cf. Fig. 125). The negative charge of this network is compensated by the presence of cations, generally Ca, Na, and K as regards natural minerals.

So some cations or small-sized molecules may be mobile in the crystalline network without leading to it being destroyed, which attributes ion-exchanger and molecular absorber properties to these minerals.

Initially it was scheduled to use zeolites as molecular sieves in order to separate fission products chlorides (to be conditioned) from the chlorides of the chlorinated salt (to be recycled). This process was then dropped and direct conditioning of the whole salt was selected.

These salt-loaded zeolites are mixed with a glass binder, then sintered by hot isostatic pressing at an approximate  $850^\circ\text{C}$ , thereby producing a dense ceramic of “glass-bonded sodalite” type through zeolite transformation.

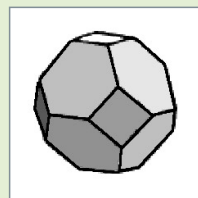


Fig. 125. a. Truncated octahedron, the basic figure of zeolites, analogue to the sodalite  $\beta$  cage (each dot stands for a Si-O-Si or Si-O-Al bond).

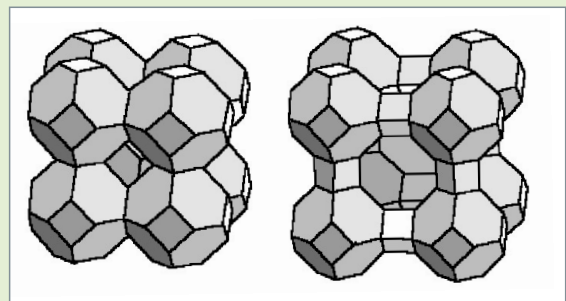


Fig. 125. b. Left: sodalite structure consisting of the combination of the octahedra truncated by their square faces. Right: zeolite A structure; it is noteworthy that the central cage is enlarged owing to the presence of prisms between the truncated octahedra.



### Fission products selective precipitation in molten salts

The selective precipitation of the lanthanides contained in a eutectic mixture LiCl/KCl as minerals of the monazite type  $\text{LnPO}_4$  was investigated in laboratory experiments on one-dozen gram scale. The principle lies in adding a phosphate precursor to the molten salt at 500 °C, in this case  $\text{NH}_4\text{H}_2\text{PO}_4$ , which induces monazite precipitation (Fig. 126 and 127).

Studies related to alkaline-earths and alkaline elements are proceeding with the final aim of solvent recycling.

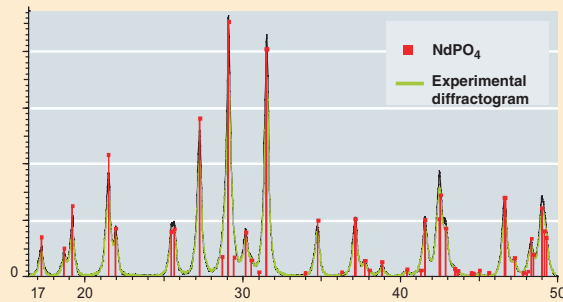


Fig. 126 a. A salt block as it appears after cooling (a): the occurrence of monazite-structured  $\text{NdPO}_4$  can be observed at the bottom of the crucible, as confirmed by the X-ray diffractogram (b).

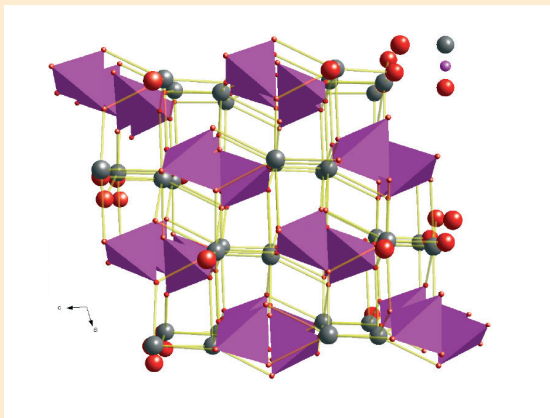


Fig. 127. Crystallographic structure of the monazite phase, projection onto plane (010).

the bottom of the crucible. These are the reasons why developing a metallic matrix is to be considered, and several cupronickel-type alloys adapted to this stream are under investigation at the CEA. Another evaluation to be undertaken will deal with the electrochemical corrosion of these phases in an aqueous medium under irradiation as a function of the metal (nature, surface state, microstructure...).

**Florence BART, Isabelle BARDEZ, Agnès GRANDJEAN and Damien HUDRY,**

*Research Department of Waste Treatment and Conditioning*



## Spent fuel: a possible confining matrix?

**O**n unloading from the reactor, spent fuel may be considered in two completely different ways depending on the policy guidelines implemented in relation with fuel cycle.

If the closed cycle has been selected, spent fuel is above all deemed to be a resource: in addition to 1.5% **fissile\*** material, i.e., twice more than natural uranium, it also contains 94% **fertile\*** material which holds an energetic potential of 2 oil equivalent tons per gram. Spent fuel treatment is then pending: the fuel is **stored\*** (temporarily, by definition) in the interval.

If the open cycle has been selected, the spent fuel is deemed to be a waste. It will then have to undergo not only storage, but again geological **disposal\*** (which by definition is final, though with a reversibility option). Although the open cycle option has not been retained by France<sup>4</sup>, it is interesting to see where it leads as regards waste management, were it not for comparison with the French option for treatment-recycling.

So, whatever the option chosen, spent fuel will have to undergo a storage period over a period of time between five years (a minimum time to let fuel “cool” prior to treatment operations), and a hundred years. Even in the “closed cycle” option, the storage time may be as long as that: for example, MOX spent fuels, not easily to recycle in present water reactors, will have to be stored until the park is endowed with fast neutron reactors able to use their plutonium efficiently.

Whatever the type of storage retained – dry or wet storage –, in any case the spent fuel clad must play its role and prevent the dissemination of the radionuclides generated by the fuel in the reactor. In dry storage spent fuel is enclosed in a container which protects it, allows it to be handled, and acts as a confining barrier. Then is raised the issue of dry corrosion and of the mechanical behavior of spent fuel rods which will be heated and undergo the pressure of the gases generated by the fuel actinide radioactive disintegrations (see *infra* “Spent fuel initial characteristics”, p. 125).

In wet storage, the temperature reached by the fuel is less high. The thermomechanic problems likely to affect the spent fuel are less acute, but attention must still be paid to aqueous corrosion problems that may be favored by radiolysis (see *infra* “Spent fuel evolution in a dry storage facility”, pp. 129-132).

In the “open cycle” option, the spent fuel will then be placed under disposal conditions. Surrounded by its container, it will have to ensure radionuclide retention for an even longer period of time. Several hundreds of thousands of years will prove to be necessary for spent fuel radiotoxicity to be brought back to the initial uranium ore level by radioactive decay. It will probably be impossible to avoid the direct contact of the fuel ceramic with the underground water. For the metallic envelopes surrounding the ceramic cannot withstand corrosion over so long periods of time. In this very case the issue to be investigated is that of ceramic **leaching\***.

Contrary to glasses, which display a homogeneous, amorphous microstructure, fuel ceramic is heterogeneous and polycrystalline. In addition, it is highly fragmented owing to the temperature gradients which it is subjected to in the reactor, and to gas buildup in it. When the fuel ceramic is in contact with the underground water, part of the radionuclides localized at the interfaces and grain boundaries will be rapidly released. This **labile\*** portion, too, will be investigated, for it is the prevailing component of the “**source term\***” in a deep repository for spent fuel. All of the phenomena hereabove described were modelled at the CEA with a view to achieving the safety analysis of a spent fuel storage facility and a spent fuel disposal facility (see *infra* “Modelling the long-term spent fuel behavior”, pp. 133-135).

Last but not least, concepts of spent fuel cases and containers have been developed at the CEA. They are briefly described hereafter (see *infra* “Spent fuel containers in long-term storage and direct disposal concepts”, pp. 137-139).

4. In the French Act of 13 July 1992 an ultimate waste is defined as a waste “which is no longer likely to be processed in the present technical and economic conditions, especially by extraction of the valuable part or reduction of its polluting or dangerous character”. More generally, spent fuel is not an ultimate waste according to this Act.



## Spent fuel initial characteristics

The nuclear fuel of the **PWR**\* (Pressurized Water Reactors) consists in an assembly of 264 **fuel rods**\* of 9.5 mm outside diameter and about 4 m long, interconnected with 8 grids of 24 tube guides (Fig. 128). Each rod consists of a clad of zirconium alloy 570  $\mu\text{m}$  thick in which the pellets are piled up: uranium oxide **pellets**\*  $\text{UO}_2$  for **UOX**\* fuel or mixed oxide  $(\text{U,Pu})\text{O}_2$  for MOX fuels. Each pellet is obtained by sintering uranium oxide powders (or mixed oxide powders in the case of MOX). It consists of grains of about  $8\mu\text{m}$  average diameter stuck on each other (grain boundaries). Further, **MOX**\* fuel is characterized by the occurrence of plutonium-enriched zones, called plutonium agglomerates, of a diameter between a few  $\mu\text{m}$  and a few dozen  $\mu\text{m}$ , which are distributed homogeneously in the pellet.

The fuel rod undergoes a number of transformations as it stays in the reactor. Its state after irradiation constitutes the initial state of spent fuel prior to transportation, and then, possibly, storage or disposal. Its long-term evolution depends upon this state. The purpose of this chapter is to describe the physico-chemical state of spent fuel pellets after in-reactor irradiation.

### Post-irradiation chemical composition of spent fuel pellet

The chemical composition of the nuclear fuel is altered during irradiation by the formation of fission products in the place of the fissile elements, and by the generation through neutron **capture**\* of other U and Pu isotopes and of additional actinides.

The elements occurring in spent fuel spread over a broad part of the Mendeleev table (Fig. 129). They may be classified according to their chemical form in the rod:

- the soluble elements in the fluorine network of the matrix such as actinides (Pu, Np, Am, Cm) - the element class with the highest weight percentage in irradiated fuel -, lanthanides (La, Ce, Pr, Nd, etc.), and soluble elements as oxides (Zr, Nb, Sr);
- the elements occurring as oxide precipitates: Rb, Cs, Ba, Zr, No, Mo, Te;
- the fission products (FPs) occurring as metallic precipitates: Mo, Tc, Ru, Rh, Pd, Ag, Cd, In, Sn, Sb, Te;

- fission gases - Kr, Xe, He -, helium from *alpha* decay, and in-reactor volatile FPs - I, Br, Rb, Cs, Se, Te.

Despite these different transformations, the fuel oxygen potential experiences little evolution under irradiation.

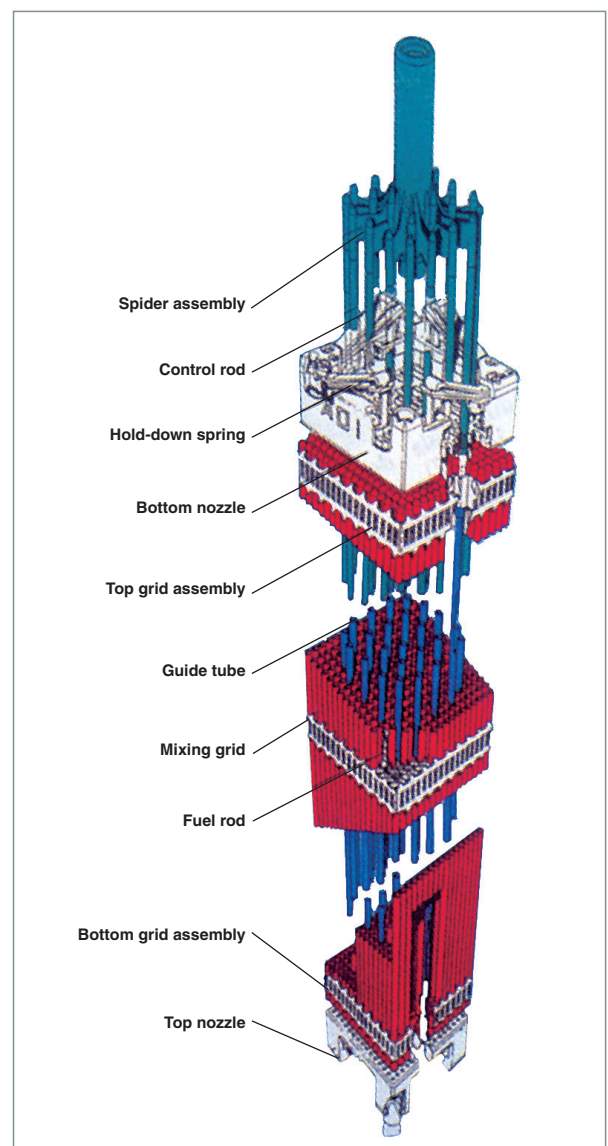


Fig. 128. A PWR fuel assembly.

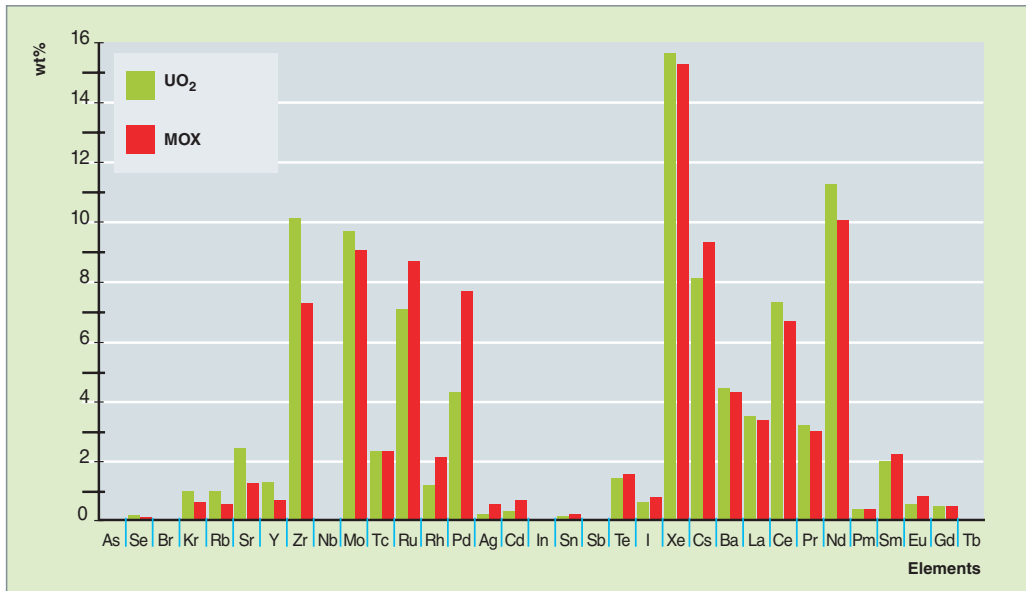


Fig. 129. Relative abundance of fission products for UO<sub>2</sub> fuels recycled in MOX with a 60-GWd/t specific burnup.

### Post-irradiation physical state of spent fuel pellet

The developing of a high radial temperature gradient in the pellet during its in-reactor irradiation induces considerable mechanical constraints which lead to the pellet cracking. Whatever the specific burnup (or burnup) reached, the spent fuel pellet after in-reactor irradiation may be seen as cut into fifteen fragments or so on the average (Fig. 130).

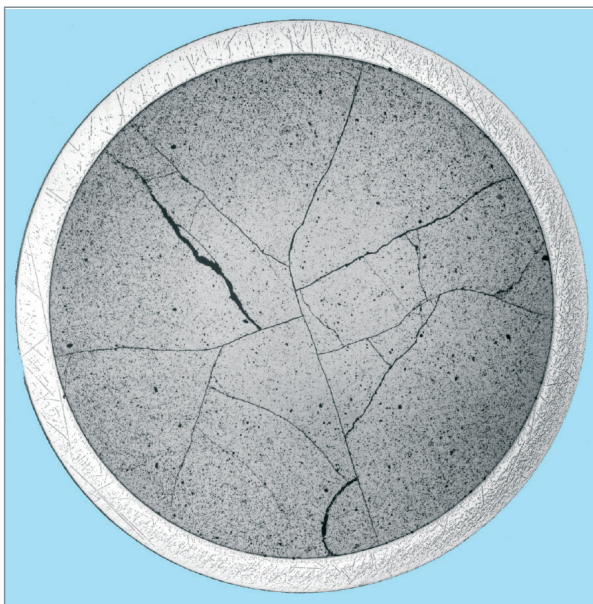


Fig. 130. Radial macrography of a spent fuel plate.

The macroscopic swelling observed during the irradiation results from fission products formation, irradiation defects, and emerging fission gas bubbles in UO<sub>2</sub> grains.

In-reactor irradiation strongly alters the microstructure of the fuel pellet, especially in the two following zones:

The grain boundaries in which metallic precipitates as well as fission gas bubbles pile up (Fig. 131). Even if the grain boundaries withstand high constraint levels, they are made more fragile by in-reactor irradiation. For the burnups and irradiation temperatures considered herein, post-irradiation fractographies of spent fuel pellets evidence chiefly intergranular ruptures, save in the central zone of the pellet, whereas they are of the transgranular type in the unirradiated fuel.

The restructured zones in the peripheral part of the pellet (rim), in UOX fuels where burnup is higher than 40 GWd.t<sup>-1</sup> and in big Pu-rich aggregates (of size >10 μm) located in the outer zone of the MOX fuel pellet. These restructured zones are characterized by a porosity of micrometric size of about 10% (closed after in-pile irradiation) and small-sized grains (0.1 to 0.2 μm) (Fig. 132).

### Irradiated clad state

During in-reactor irradiation, the microstructure of clad and structure materials is altered on account of both irradiation (alteration of the dislocation structure) and corrosion (oxidation and hydride formation). In-reactor irradiation thus results in a strong hardening of materials.

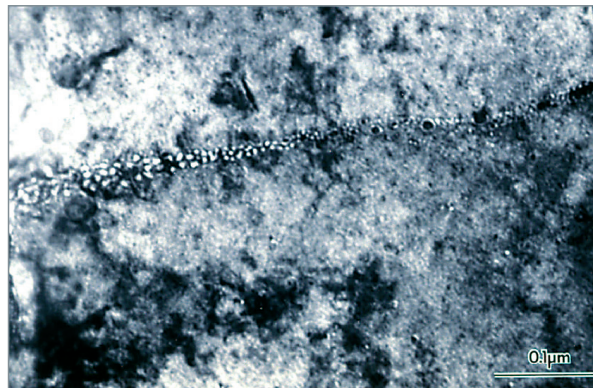
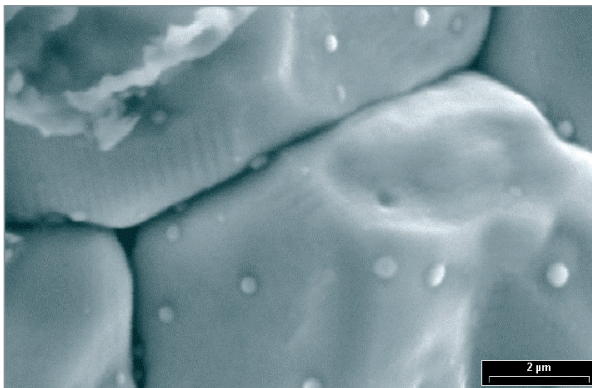


Fig. 131. SEM (left) and TEM (right) microphotographs of the ceramic after irradiation. They show a buildup of metallic precipitates (left) and of gas bubbles on grain boundaries (right).

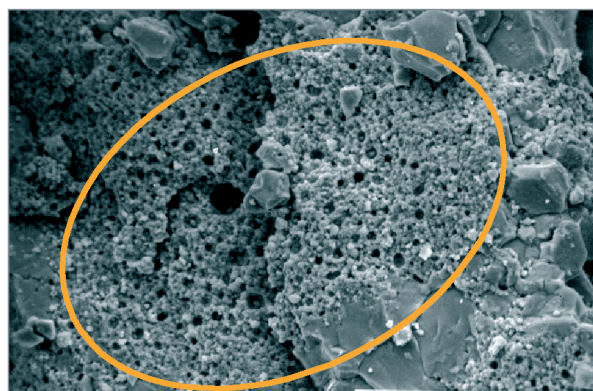
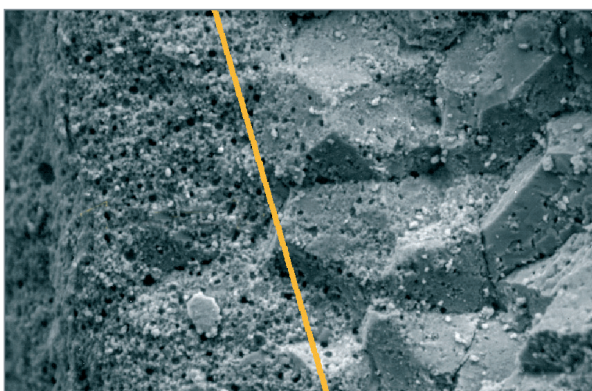


Fig. 132. Microphotographs of restructured zones on the pellet circumference in an UOX fuel (left) and in a MOX fuel plutonium agglomerate (right).

The thickness of the oxidized layer depends upon the axial temperature profile during irradiation and the type of alloy used. Internal oxidation remains low, about 10 μm. Outer irradiation of clads is higher: it reaches a maximum level in the hotter area, and generally remains lower than 100 μm in the clad alloy Zircaloy-4 (it is reduced to 25 μm after 6 irradiation cycles in the new alloy M5™ developed by AREVA NP, which means an outstanding progress).

On the other hand, clad oxidation by water releases hydrogen, part of which is absorbed into the metal. This hydrogen forms hydride plates which make the clad more fragile.

Besides, following the fission gas release in the free volumes of the rod, the pellet swelling, and the clad creep under the coolant external pressure during in-reactor irradiation, the rod internal pressure after irradiation is higher than the filling pressure. For UOX fuel rods clad with Zircaloy-4, it is 40 bars on the average (after cooling) for an initial helium pressure of 26 bars and a burnup of 60 GWd.t<sup>-1</sup>. In the same conditions, it is slightly higher for a MOX fuel (50 bars).

It is this very clad, with enhanced fragility and high stresses following in-reactor irradiation, which will have to contain radioactivity in spent fuel under storage conditions. This implies that the weaknesses mentioned above will have to be taken into account in the design of containers and storage facilities.

#### ► Bibliography

CEA, "Les déchets radioactifs à haute activité et à vie longue/ Recherche et Résultats". Axe 3. Rapport final. Décembre 2005.

**Cécile FERRY,**  
Physico-Chemistry Department





## Spent fuel evolution in a dry storage facility

Let us consider the case of storage, as practiced in the United States, or the containment phase of a deep geological disposal facility, prior to water income into the package. In this context, spent fuel assemblies only exchange energy with the outside, whether as heat (thermal impact of irradiated fuels), or as radioactivity (residual radioactivity  $\alpha$ ,  $\beta$  and  $\gamma$  of irradiated fuels). We call these boundary limits a “closed system”, for there is no material exchange between the system and the outer environment. These conditions correspond with the nominal operating conditions under storage conditions.

As opposed to the closed system, a system is said to be “open” in the case when confinement is lost due to container degradation and spent fuel rod clad rupture. Material exchange with the outside is then possible in addition to energy exchange. The alteration of the uranium dioxide ceramic takes place in a gaseous phase not saturated with vapor, in presence of oxidizing species (oxygen, nitrogen oxides generated by radiolysis...). These are the degraded conditions to be seen in a dry storage facility.

### Fuel evolution in a closed system

Radionuclide radioactive decay is the origin of the physico-chemical phenomena which characterize the long-term intrinsic evolution of spent fuel. On the one hand, it leads to the formation of elements with different oxidation states likely to affect the fuel oxygen potential. On the other hand, the *alpha* disintegrations generate helium atoms within the crystal and are also responsible for self-irradiation damage, the latter being induced by heavy atom recoil over a very short distance, about a few nanometers. A significant consequence of this evolution might be grain boundary damaging in the irradiated oxide, as well as a potential increase of the labile radionuclide inventory, which, on water ingress, could be disseminated in the spent fuel assembly package under disposal conditions.

The chemical composition of the irradiated oxide is altered by the *beta* decay of fission products, such as Cs 137 conversion into Ba 137, and of actinides, such as Pu 241 decay to Am 241. Thermochemical equilibrium calculations for timescales up to 300 years have shown that this evolution of chemical composition is not sufficient to affect irradiated fuel oxidation state after in-reactor irradiation. Molybdenum, an abundant fission product, and clad zirconium constitute a buffer which allows the varying oxidation state in fission products to be accommodated.

Helium generation through *alpha* decay of actinides raises a major issue for the long-term behavior of spent fuel. Figure 133 shows a typical calculation of the residual activity on a timescale of ten thousand years for an irradiated uranium dioxide fuel with a burnup of 47.5 GWd/Tu. Helium concentration will reach 0.7 at % per heavy metal atom over 10,000 years. For a MOX fuel with the same discharge burnup, it would reach 4%. Would helium be released to the free volumes of the fuel rod, this would entail a significant increase of internal pressure in the rod, and, consequently, of the clad tangential constraint.

Reversely, should helium be retained in the fuel pellet, helium could precipitate as nanometric-sized bubbles, or pile up at the grain boundaries (trapping in pre-existing fission gas bubbles) in the event of reduced mobility in the crystalline network. Research work has focused on helium mobility in  $UO_2$  and the consequences of buildup at grain boundaries in the polycrystalline solid.

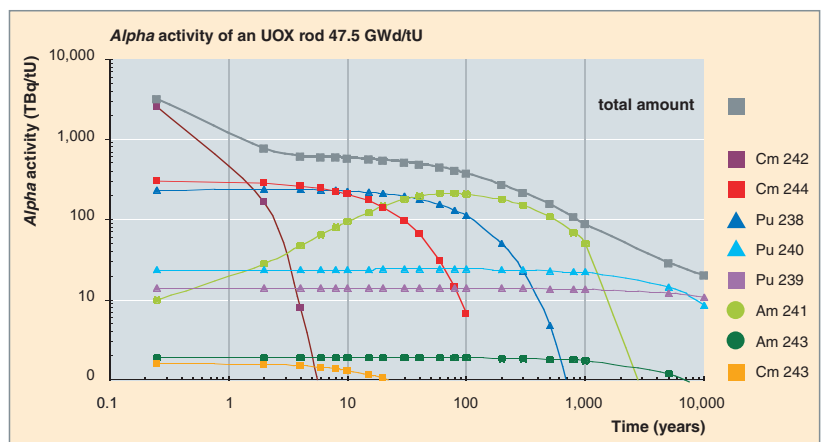


Fig. 133. Evolution of the *alpha* activity of an irradiated UOX fuel versus time.

An apparent diffusion coefficient was evaluated by experiments of helium implantation into  $\text{UO}_2$  samples followed by thermal treatments in controlled atmosphere, so as to avoid any oxidation during the test. In parallel, helium desorption measurements were conducted at the Institute for Transuranium Elements at Karlsruhe (ITE) on fuels doped with plutonium 238, which have a decay half-life of 87.7 years. By extrapolating the results at lower temperatures to the experimental temperatures, it can be observed in Figure 134 that helium mobility is higher than xenon diffusion and strongly varies with the fuel damage level. Focusing on the role of grain boundaries and of the damage generated by ion implantation, it could be demonstrated that helium mobility is speeded in the

vicinity of grain boundaries in a temperature range of 750-1,300 °C, whereas it was fairly lower at the core of grains, as helium was presumably trapped in the crystal defects or precipitated as nanobubbles (Fig. 135) [1]. This research has been achieved in cooperation with the CNRS/CERI at Orleans and the LPS at Saclay. At the present stage of development, our conclusion is that extrapolation to the temperatures of a dry storage facility evidences a limited mobility of helium in the fuel, at least in the event of a damage in a storage facility of one hundred years. The  $\alpha$  decay of actinides is also at the source of the irradiation damage induced by atomic displacement cascades in the crystal network. An atomistic study in molecular dynamics is under way to simulate the radiation damage effects upon the  $\text{UO}_2$  crystal and its grain boundaries. Experimental work also deals with the physical characterization of fuel natural analogues: uraninites and older fuels doped with actinides. An example is put forth in Figure 136: this Scanning Electron Microscope (SEM) photograph displays the microstructure of a  $^{238}\text{PuO}_2$  pile after thirty years, as 21% of plutonium has decayed by this age. Small bubbles and cracks have emerged around a few grain boundaries at a damage level which was higher by several orders of magnitude than the dose to be reached by an irradiated fuel within ten thousand years. This study is going on on doped fuels which reach intermediate irradiation doses.

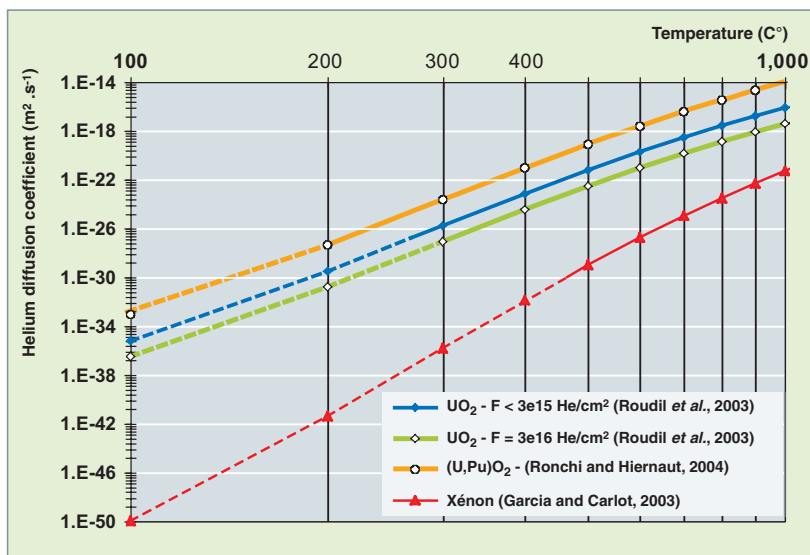


Fig. 134. Apparent diffusion coefficients of helium in nuclear fuels. Comparison with the diffusion coefficient of xenon in  $\text{UO}_2$ .

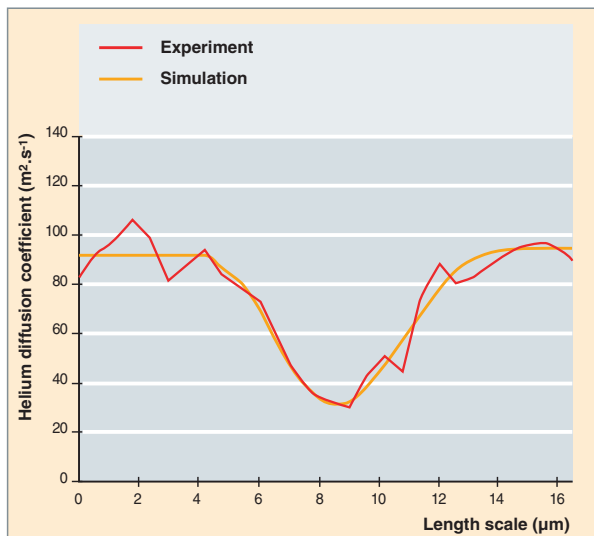


Fig. 135. Helium concentration profile around a  $\text{UO}_2$  grain boundary. Helium-implanted and 1,300 °C-annealed polycrystalline sample.

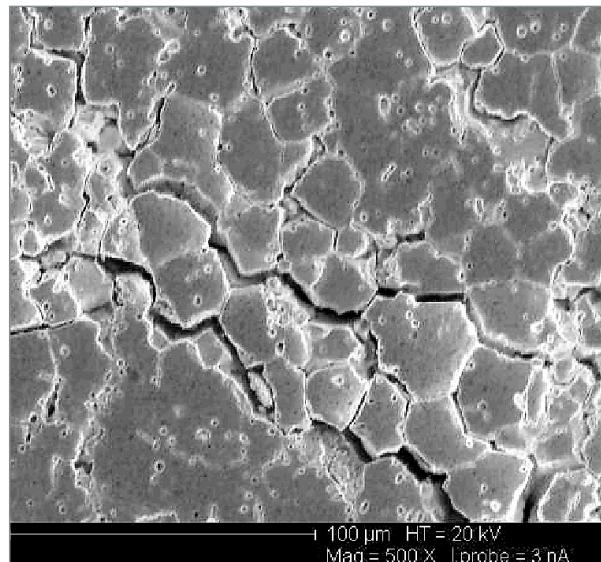


Fig. 136. SEM image of a 30-year-old  $^{238}\text{PuO}_2$  pile [2].

## Fuel evolution in an unsaturated open system

Under incidental conditions in a dry storage facility, the irradiated fuel runs the risk of being in contact with air or an oxidizing gaseous atmosphere.  $\text{UO}_2$  conversion into  $\text{U}_3\text{O}_8$ , a pulverulent oxide with a density much lower than that of  $\text{UO}_2$ , constitutes a major risk of fuel rod degradation under storage conditions.

A basic investigation of oxidation mechanisms has been undertaken with the aim of understanding all the steps of oxygen atom insertion into the  $\text{UO}_2$  crystalline network, in order to confirm the oxidation kinetic equations and their extrapolation on timescales unreachable with laboratory experiments. In particular, a neutron diffraction study was performed in order to pinpoint the localization of the oxygen atoms inserted in the network for compositions ranging between  $\text{UO}_2$  and  $\text{U}_3\text{O}_8$  (Fig. 137) [3].

In parallel, oxidation kinetics is being investigated in the long term in relation to high-burnup irradiated fuels. The typical schematic of this kinetics is represented in Figure 138. The intermediate plateau stands for the formation of species of type  $\text{U}_4\text{O}_9$  and  $\text{U}_3\text{O}_7$ , slightly denser than the initial oxide. This is illustrated in Figure 139, which reproduces a cross-sectional examination by optical microscopy of a fuel fragment after irradiation and oxidation for 5,000 hours at 200 °C. At this temperature oxygen intake has reached a plateau: emerging cracks can be observed as a result of the formation of intermediate compounds. This plateau is all the more extended as the temperature is low.

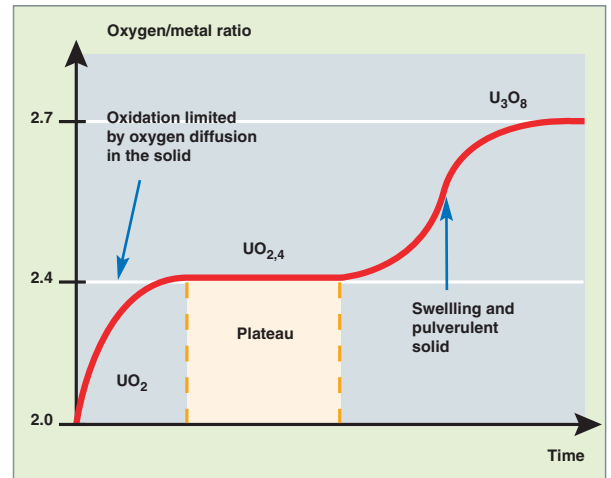


Fig. 138. Schematic view of the oxygen intake of an irradiated fuel versus time, during oxidation under air.

The data collected during these experiments as well as their interpretation will be used for making an operational behavior model for spent fuel if ever it is faced with an oxidizing atmosphere.

### ► References:

- [1] G. MARTIN *et al.*, "A quantitative  $\mu\text{NRA}$  study of helium intergranular and volume diffusion in sintered  $\text{UO}_2$ ", *NIMB*, **249** (2006), pp. 509-512.
- [2] D. ROUIL *et al.*, "Effects of a self-irradiation on actinide doped spent fuel surrogate matrix", *M.R.S. Symp.*, **932** (2006), pp. 529-536.

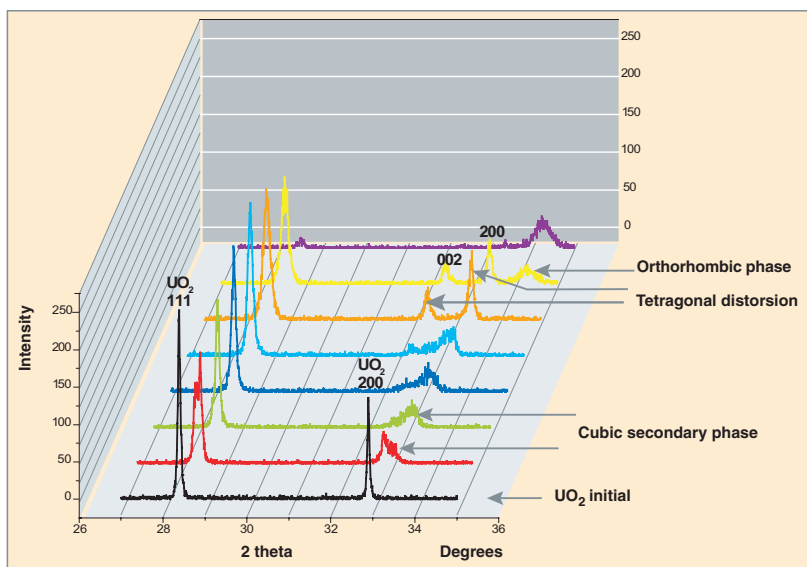


Fig. 137. X-diffraction spectrum of a uranium oxide sample displaying the structural evolution during oxidation of (cubic)  $\text{UO}_2$  to (orthorhombic)  $\text{U}_3\text{O}_8$  at 250 °C under a partial oxygen pressure of 0.2 atm. [3].

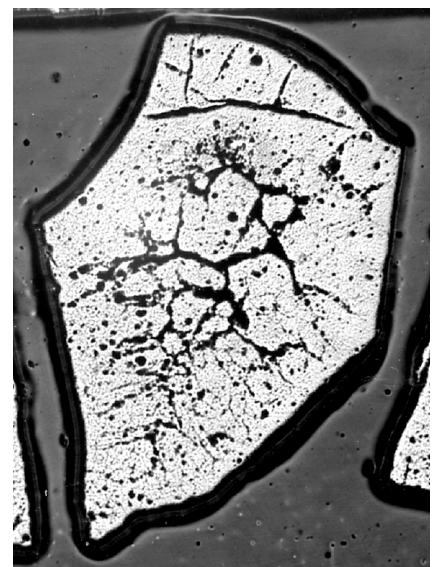


Fig. 139. Fuel fragment cross-sectional examination through optical microscopy after irradiation and oxidation for 5,000 hours at 200 °C.

[3] G. ROUSSEAU *et al.*, "A detailed study of  $\text{UO}_2$  to  $\text{U}_3\text{O}_8$  oxidation phases and the associated rate-limiting steps", *J. Nucl. Mat.*, **355** (2006), pp. 10-20.

**Jean-Paul PIRON,**  
*Fuel Research Department*

## Modelling the long-term spent fuel behavior

Studies intended to understand fuel behavior under dry and wet conditions make it possible to build long-term behavior models for spent fuels in these different contexts. The aim of these models is to predict radionuclide release in the event of a storage facility incident or of water ingress into the containers of a direct disposal facility. Behavior models developed by the CEA [1] aim at ensuring the robustness of evaluations, and so represent a simplified view of spent fuel evolution. Pessimistic hypotheses are integrated into the models in order to take into account the uncertainties relating to long-term behavior of spent fuels.

### Modelling the spent fuel pellet behavior

The irradiated fuel pellet evolution is mainly due to the decay of the nuclei occurring in it, which results in a buildup of radiation damages, the alteration of chemical inventories, and a significant helium generation by  $\alpha$  decay. The evolution of chemical inventories has no significant impact upon the oxidation state of the fuel pellet. In contrast, decay entails the buildup of a high helium amount in the pellet, especially for fuels rich in  $\alpha$  emitters as MOX fuels (Fig. 140) (see also *supra* "Spent fuel evolution in a dry storage facility", p.129-132). The challenge to be faced is the future of this gas mainly generated in the fuel pellet grains, and its consequences on the mechanical behavior of the grain boundaries, made more fragile by irradiation.

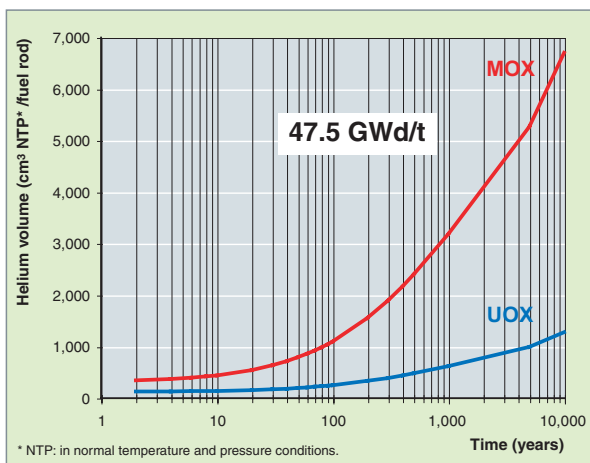


Fig. 140. Amount of helium accumulated over time in UOX and MOX fuel rods.

A macroscopic modelling was achieved basing upon the knowledge gained in relation to helium behavior in fuel and the mechanical properties of the spent fuel pellet. Its conclusion is that the helium amount formed within 10,000 years in UOX fuels is not sufficient to alter the initial microstructure of the spent fuel pellet [2]. For helium is expected to remain trapped in the grains and pores of the rim\*.

However, this recent result has still to be validated by models and experiments on the microscopic scale and the case of MOX fuels is still to be assessed.

### Modelling radionuclide release from spent fuel under disposal conditions

Deep geological disposal inevitably leads to the progressive rupture of the various package envelopes (chiefly by corrosion), and to underground water ingress and contact with the fuel. Schematically, the fuel evolution takes place during the corrosion period of the metallic envelopes, without being subjected to any alteration by ground waters. As is the case under storage conditions, its evolution goes on in an intrinsic way, under the influence of its internal disequilibria and decay reactions. Fuel evolution during this first stage determines its future state when water ingresses later on. In the following stage, the fuel is altered in presence of water, and progressively releases part of the radionuclides which it contains, around the package.

#### Instantaneous release of radionuclides on water income

As it comes into contact with the spent fuel, water solubilizes all of the radionuclides occurring in the voids and on the surfaces which can be accessed by the fuel. This results in an instantaneous release of this **labile\*** portion. The amount of radionuclides so released depends on the place where they are located in the rod when water comes into contact with the fuel. As it took into account the intrinsic evolution expected in the long term, a conservative release model was developed: it sets out that 8% of the most mobile fission products (I, Cs) are directly available on water income after 10,000 years. This assessment relates to an UOX fuel with an average burnup of 60 GWd/t.

### Radionuclide release on fuel matrix alteration

$\text{UO}_2$  is relatively stable in a deep geological medium owing to the reducing character of the host medium ( $\text{UO}_2$  solubility is extremely low:  $\sim 10^{-9}$  mol/L). Yet, the residual radioactivity of a spent fuel (especially the *alpha* radioactivity prevailing in the long term) leads to the radiolysis of water molecules at the fuel/water interface. The oxidants so generated oxidize the fuel surface (from U(IV) to U(VI), which entails its dissolution and the release of the occluded radionuclides. Figure 141 affords a schematic view of all of the alteration mechanisms in presence of a radiolysis.

Modelling these phenomena is extremely complex in so far as radiolytic reactions are numerous (more than 150 reactions in the models widely used), display not only high but also varied kinetics, and largely depend upon the environment.

Predicting the very long-term evolution requires to simplify phenomenology only retaining the prevailing reactions. In consistency with this approach the CEA has developed a model to describe radionuclide release by radiolytic dissolution. This model allows the fuel alteration rate to be assessed over time as shown in Figure 142. The assessment method is a highly pessimistic one indeed, which integrates all of the present uncertainties on both models and the parameters involved in fuel alteration. For the studies performed by European teams [4] have shown that radiolysis effects should be very limited over time (i.e., between 5,000 and 15,000 years for an UOX fuel with a 60 GWd/t burnup). Beyond this step, the matrix dissolution will be controlled by the fuel solubility, and so, particularly, by the concentration in dissolved uranium.

Consequently, alteration will be all the more sensitive to the environmental conditions imposed by the package near field (hydrogen, engineered barrier, rock).

In addition, it is presumable that part of the elements released by dissolution of the fuel (uranium, minor actinides, and fission products) precipitate in the vicinity of the fuel as new so-called “secondary” minerals. The latter may influence fuel alteration if they are able to maintain a uranium concentration lower than in fuel. They may also contribute to confinement under disposal conditions if they are likely to retain part of the radionuclides present in the fuel.

As a conclusion, long-term evolution mechanisms of nuclear spent fuel packages have been fully highlighted, even if some features of their evolution are still unknown.

Using a macroscopic approach of the intrinsic evolution characterizing the pellet microstructure made it possible to reduce part of the conservative parameters introduced in the first assessments of the labile fraction. The latter is deemed to be 8% of the inventory on water income for a UOX fuel with an average burnup of 60 GWd/t. A considerable research effort is focused on understanding grain boundary evolution at the microscopic scale in order to validate the proposed model.

As regards the underwater evolution of the spent fuel pellet, investigations are going on to take into account environment coupling. They will allow to reduce margins with respect to those introduced in the present model of strictly radiolytic dissolution.

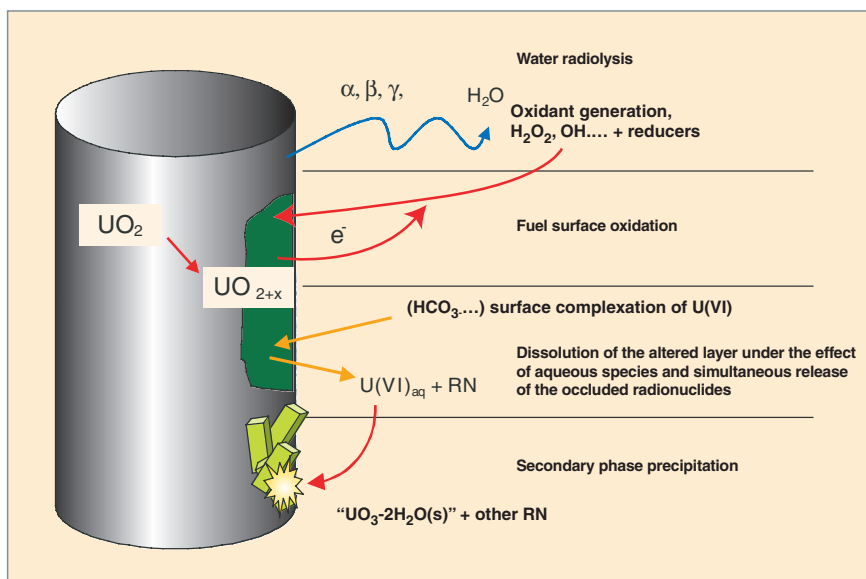


Fig. 141. Generic alteration mechanisms of spent fuel in presence of water.

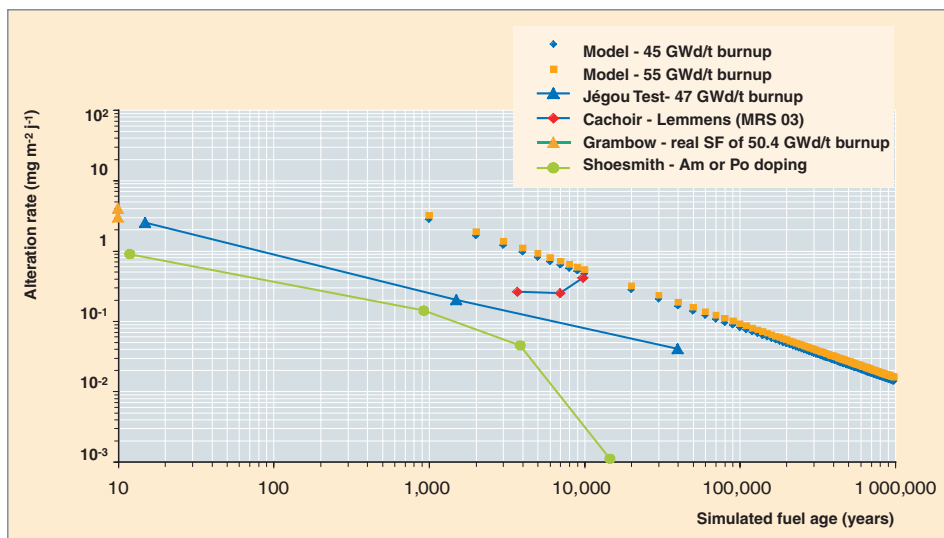


Fig. 142. Comparison between spent fuel alteration rate calculated as a function of time and experimental data. [3].

### ► References

[1] CEA, "Les déchets radioactifs à hautes activités et à vie longue/ Recherche et Résultats". Axe 3. Rapport final. Décembre 2005.

[2] C. FERRY, J.-P. PIRON, A. POULESQUEN and C. POINSSOT, "Radionuclides Release from the Spent Fuel under Disposal Conditions: Re-evaluation of the Instant Release Fraction, Basis: Nuclear Waste Management XXX", *Mat. Res. Soc.*, **985**, p. 65.

[3] C. POINSSOT, C. FERRY, P. LOVERA, C. JÉGOU, J.M. GRAS (2005), "Spent fuel source-term model for assessing spent fuel performance in geological disposal. Part II: Matrix alteration model and global performance", *J. Nucl. Mat.*, **346**, pp. 66-77.

[4] "Final Report of the European project spent fuel stability under repository conditions", CEA report CEA-R-6093 (2005), collective work.

**Cécile FERRY,**  
Physico-Chemistry Department





## Spent fuel containers in long-term storage and direct disposal concepts

As part of the review of the various alternatives for nuclear spent fuel management, the CEA has started investigating the following option: fuel assembly disposal following a preliminary step of long-term storage. After the storage step, fuels would be transferred without being opened from the storage container to the disposal container. These two types of packages will be described hereafter.

### Long-term storage and the dedicated container

The aim of long-term storage is to afford a transient solution in the waste management stream ensuring storage conditions likely to meet the following requirements:

- preserving primary package integrity for a period of time between a hundred and three hundred years, in order to allow it to be retrieved for further prospects;
- ensuring safety for workers, the public, and the environment during all these operations.

The general design principles for storage containers are the same whatever the content: UOX or MOX spent fuels, or again vitrified waste packages.

The container described herein is designed to house UOX-type spent fuels with a view to dry storage over hundreds of years.

Two main functions alone are attributed to the container:

- the “confinement function”;
- the “retrievability” function.

Secondary functions are derived from these main functions:

- the function “ability to release fuel residual heat”;
- the “guaranteed subcriticality” function;
- the “ability to be handled” function.

The further functions are transferred to the store (i.e., biological shielding, physical protection, external cooling).

Fulfilling these functions has made it necessary to design a double-confinement-barrier container (Fig. 143):

- the first barrier consists with a case which houses only one assembly: in addition to its confinement function, this case stands for the basic component compatible with further treatment or with specific containerization for a possible geological disposal;

- the second barrier consists of a container with a seven-case capacity.

The case is a cylinder 330 mm outside diameter, 4,893 mm high, and 4 mm thick, with a 1-assembly capacity. It is made of steel-304L, closed by TIG\* welding.

It has been designed so as to exhibit a suitable behavior on a 9 m drop, particularly, and be retrievable after a three-hundred-year period of time (Fig. 144).

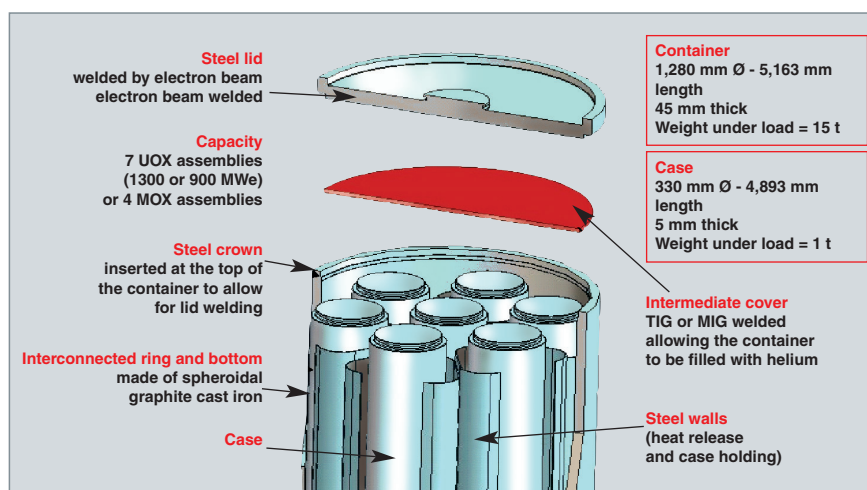


Fig.143. Long-term fuel storage package.



Fig. 144. Scale-1 demonstrator of the individual case for a spent fuel assembly.

The container which constitutes the second confinement barrier, is a cylinder 1,280 mm outside diameter, 5,168 mm high, and 45 mm thick for a capacity of 7 UOX spent fuel cases.

It consists of a spheroidal graphite cast iron body 400-15, fitted with a steel crown for better weldability, and a steel-S235 lid electron beam welded over 45 mm (Fig. 145).



Fig. 145. Scale-1 demonstrator of the storage container for 7 spent fuel assemblies.

### A cast iron container

Corrosion may be a cause of failure of the storage container. Metallic materials have been considered taking into account their behavior in corrosion.

#### “Passivable” materials

“Passivable” materials (stainless steels, Hastelloy, Inconel) seem to be attractive for storage. Yet, localized corrosion phe-

nomena (stress corrosion, pitting) may emerge depending on the medium and the local mechanical constraints applied to the material. The other passivable or thermodynamically stable metals under storage conditions (titanium, copper, tantalum, gold...) have been screened out for cost and/or availability reasons.

In contrast to localized corrosion, the evolution of homogeneous corrosion is more easily predictable. Two families of current industrial metals have finally be contemplated: low-alloyed or unalloyed steels and some cast irons. Compared with steel, cast iron displays several benefits: the ability to make the container body in a single, unwelded part, a best corrosion resistance, and a cost twice lower. The option “spheroidal graphite cast iron” allows for a tensile strength comparable with that of a mechanical engineering steel. Ultimate elongation remains slightly lower than in steel, but is compatible with the mechanical design criteria selected.

The relative drawback of “full-depth” welding of cast iron could be compensated inserting a steel crown into the upper part of the container during the casting step. This crown makes it possible to perform a steel/steel welding between the lid and the container during the final closure following the loading. The feasibility of this cast iron-steel crown coupling was validated on different scales.

### A challenge: how to close the container

Several systems of container closure have been investigated which, all of them, required to optimize their implementation in the prospect of long-term storage.

Three “full-depth” welding techniques of cast iron were assessed: TIG welding, electron-beam welding, YAG laser welding. Concerning TIG welding, the technique feasibility was demonstrated, but the shrinkages measured (comparing before and after welding) arer significant and presumably generate residual constraints not to be neglected. As regards YAG laser welding, the examinations performed after welding highlighted welding defects. This process does not prove difficult to implement in hostile media. However, further optimization is still needed indeed.

The electron-beam welding technique is characterized by the fact that welding is performed in only one step. Welding rates are very high since the welding of a container should be fully achieved in less than two hours. Qualification tests have also allowed to check whether the weld seam quality had been preserved in early and final welding steps.

The demonstration program has integrated the scale-1 manufacturing of a storage container, as well as small-scale drop tests onto objects.

## Disposal container

As mentioned in the introduction, once the storage phase has elapsed, leaktight cases shall be able to be transferred into the disposal container without being opened, thereby ensuring continuity between storage and disposal.

Specific constraints in terms of heat and criticality have led to select one conditioning unit for four UOX assemblies.

This package consists of three parts (Fig. 146):

- a ring: it is a forged part made of unalloyed steel, 110 mm thick;
- an insert: this part is cast directly into the container, and includes four cells in the case of the UOX fuel. The casting process alone can allow for sufficiently small container-insert clearances, so that, under disposal conditions, the container does not undergo any deformation exceeding the elastic limit of the constituent steel in spite of the environmental external pressure;
- a lid: it is welded in full depth by an electron beam in a shielded cell after the assemblies have been introduced into the container. This process has been selected for the reasons already mentioned above.

As a conclusion, the technical components required for spent fuel long-term storage and disposal do exist now thanks to the developments carried out at the CEA. Thus, these options for spent fuel management are available from now on, should industrialists and the Public Authorities wish to implement them instead of the treatment-recycling strategy retained at the present time.

## ► Bibliography

CEA, "Les déchets radioactifs à hautes activités et à vie longue/ Recherche et Résultats". Axe 3. Rapport final. Décembre 2005.

**Nicolas MOULIN,**  
*Fuel Cycle Technology Department*



Fig. 146. The disposal container for spent fuel assemblies.



## Spent fuel storage and direct disposal: results and outlooks

**T**he previous chapters show that spent fuel is not a confining matrix. After irradiation in the reactor, the fuel rod still displays leaktighness, indeed, but its state cannot ensure radionuclide confinement in the long term. The ceramic matrix has been damaged by irradiation. The fuel rod is overpressurized owing to the buildup within it of fission products and helium. Last but not least, the clad has been made more fragile by irradiation; besides it has been corroded internally by fission products, and, externally, by the reactor pressurized water. Despite that all, and as shown by studies on corrosion kinetics, spent fuel will be able to confine radionuclides under storage conditions, i.e., protected from outer aggressions for a limited period of time. As oxidation under dry conditions and corrosion under water are slow-proceeding phenomena, dry storage and wet storage are both feasible. A preliminary step shall be to make certain that the storage facility has been well designed and that the fuel is maintained in suitable temperature conditions. As regards disposal conditions, the corrosion

of the metallic envelopes and of the clad will proceed in the long term, thereby contacting the ceramic with underground water. The “labile” fraction, i.e., a few percents of the radioactive inventory, will then be released. The countries which have chosen spent fuel direct storage – Sweden, Finland, the United States – are faced with this difficulty. In order to solve this problem, they propose to base the safety of the disposal facility upon very sophisticated engineered barriers able to ensure radionuclide confinement in the long term. In the Sweden concept, by far the most advanced one, steel-copper containers are used, which are able to withstand corrosion for very long periods of time. How difficult the undertaking is clearly shown by the special attention paid by Sweden engineers to the manufacture of these containers, particularly for metallic impurity control and weld inspection. Definitely, the alternative based upon the closed fuel cycle and waste vitrification ensures a more rational waste management...

**Bernard BONIN,**  
*Scientific Division*



## Conditioning: a major asset for nuclear waste management

**N**uclear waste is often highlighted by the media as an unsolved problem liable to strongly penalize the future of this source of energy, and so is it considered by the public.

Nevertheless, this industry was the first to have concern for the future of its waste, and implement proven technical solutions.

From Spring 1957, when the first confinement glasses were manufactured at Saclay, to the most advanced research work now conducted at the Marcoule Center on plasma-assisted incineration-vitrification, the CEA has been rich of a long-lasting tradition of research in the field of nuclear waste conditioning. This research policy has made it possible to permanently improve the industrial practice of treatment-recycling chosen by France from as early as its first nuclear program.

Today, France holds a mature industry to condition its nuclear waste, based upon a strong network of basic and technological research work. Basic research has favored a good understanding of the physico-chemical mechanisms involved during the matrix manufacture or ageing. This acquired knowledge has paved the way for a true science dedicated to the long-term behavior of materials, which can support safety demonstration for each package type. Concerning technological research, it ensures facility operation in good conditions, continuous improvement of processes, and their tailoring to new problems.

Adapted forms of conditioning are available for all existing waste:

- fission products and minor actinide solutions, by far the most radiotoxic, are vitrified. Since 1978, vitrification industrial workshops have been operating almost continuously, thereby demonstrating the reliability of the technology. The quality of the glasses produced is also fully demonstrated. For example, it is noteworthy that the so-called "R7T7" glass developed to contain fission products arising from "light-water" reactor fuel treatment has become a world reference in this field. The alteration of this glass has probably induced more scientific papers in international periodicals than any other industrial glass (sheet glass, Pyrex...);
- structural waste from spent fuel assemblies is compacted and introduced into steel containers identical to those used for glass pouring. The impact of this compacted waste on the activity possibly released by a geological disposal facility is negligible;

- most of the technological waste arising from nuclear facility operation is cemented. Most of these concrete packages consist of short-lived, low and intermediate-level waste which is disposed of at the Aube Disposal Center (Soulaïnes). A broad range of hydraulic binders was developed to adapt to the diversity of this solid or liquid waste. These concrete packages are well characterized, and sufficient knowledge of their alteration mechanisms allows required confinement performances to be ensured.

An important work is under way in order to retrieve legacy waste.

Most of this waste is located at the Marcoule site, which was the cradle of the French nuclear industry. It is true that some confinement systems achieved more than forty years ago may legitimately seem to be obsolete today (bulky waste in pits, corroded black-steel-made drums, etc.). Yet, it must be kept in mind that by the standards of those years they were performing, then (many countries disposed of their technological waste directly to sea...), and they have satisfactorily fulfilled their confinement function till today. Two dedicated funds, one civil and the other military, are devoted to financing the reconditioning operations of this waste until all of it has joined the available waste streams.

Moreover, the (background) basic research work undertaken by the CEA in the field of spent fuel treatment-recycling and waste conditioning paves the way to wide prospects of progress which, if need be, will help further decrease the fraction of ultimate waste, and improve its confinement safety.

In this basic research work, sufficient time was devoted to studying such alternative solutions as spent fuel direct disposal or specific conditioning of partitioned actinides. Only after performing this thorough study of the background did France choose optimal spent fuel recycling and ultimate residue vitrification following valuable materials separation.

This significant stock of knowledge, going from the atom to the scale-1 industrial prototype, also allows to approach such an issue as nuclear waste of the future with an overall view. Contrary to the Generation-I and -II reactor parks, where waste management had to adapt to the fuels produced, ultimate waste minimization and conditioning optimization will be taken into account in Generation-IV reactors as soon as they are designed.

Waste conditioning is no more than one step in the waste management process from the place of waste generation to the final host site: processes for cementing intermediate-level waste, compacting hulls, and vitrifying minor actinide solutions and fission products are flexible, simple, and easy to implement. So the first two steps of the chain, spent fuel treatment and waste conditioning, jointly implemented at La Hague plant, “combine” rather consistently. Once waste has been conditioned as packages has been performed, it is still has to be determined what to do with the so-called packages. Thanks to their excellent chemical stability and to their compact and robust form, existing conditioning forms (cements, compacted metallic waste, glasses) can easily take place either in a surface storage facility, in the case of short-lived waste packages, or successively in a storage facility and, then, a deep geological disposal facility, the reference solution selected by the French Act of 28 June 2006 for long-lived waste packages. It is noteworthy that the steps of the waste management process thus display an overall consistency.

It must be kept in mind that these “high-tech” conditioning forms developed and optimized for each waste category are available today at a cost acceptable for society. This cost is taken into account in the kWh price, and the corresponding provisions are prepared by EDF.

Last but not least, all national and international studies demonstrate that nuclear waste environmental impact will remain negligible, including in the long term, provided that tailored treatments are implemented.

To put it in a nutshell, today the following conclusion can be drawn, even if not shared by most of public opinion: “Nuclear waste, we *do* know what to do with it, indeed”.

In a period when a worldwide nuclear revival seems to be inescapable given the world’s energy needs and the necessity to limit the share of fossil energies, France’s leading role in nuclear waste conditioning is an outstanding asset likely to be used, not only on the international, industrial scale, but also in terms of social acceptance, showing the public that France may be exemplary in nuclear waste management. May this book help spread this idea.

**Étienne VERNAZ,**  
*Research Department of Waste Treatment  
and Conditioning*



# Glossary – Index

**Note to readers.** This set of terms and definitions is strictly intended to be a translation of the French DEN Monograph Glossary and is provided only for convenience purposes. Accordingly, the definitions herein may differ from standard or legally-binding definitions prevailing in English-language countries.

**Actinides:** the rare earth element group with atomic numbers 89 to 103, corresponding to electron subshells 5f and 6d. Actinides have very close chemical properties. **7, 10, 45-47, 100, 111-117, 123.**

**Activation** (radioactivation): action tending to make certain **nuclides\*** radioactive when bombarded by **neutrons\*** or other particles, particularly within reactor structural materials. **99, 100, 103.**

**Activity:** 1) for a radioactive substance: the number of spontaneous nuclear transitions per unit time within a radionuclide or mixture of radionuclides. It is expressed in **becquerels\*** (Bq). A becquerel is equivalent to one disintegration per second. **7, 8, 129.**

2) in a chemical reaction: the chemical activity of a species corresponds to the active concentration of this species. Electrostatic interactions between the various species within a solution reduce their reactivity potential. Therefore, the concentration term must be corrected with a coefficient lower than one unit, the so-called “activity coefficient”. Substituting activity for chemical species concentration allows the mass-action law to be applied. **41, 42, 96.**

**Alpha:** see **Radioactivity.**

**Alpha particle** (or *alpha* radiation, *alpha* ray): a positively charged particle made up of two neutrons and two protons. It is the least penetrating of the three forms of radiation most commonly encountered. It can be stopped by a mere sheet of paper. **7.**

**Amorphous:** of a solid with a disordered crystalline structure. **11, 36, 51, 52, 81, 113, 115, 123.**

**ANDRA:** *Agence Nationale pour la gestion des Déchets RAdioactifs.* The French National Radioactive Waste Management Agency. **7, 8, 77, 78, 87, 101.**

**Assembly:** see **Fuel assembly.**

**ATALANTE:** a nuclear facility of the CEA Marcoule dedicated to R&D in spent fuel treatment from fuel dissolution to waste vitrification, involving the implementation of real radioactive products. It includes high-performance analytical and process scientific equipment coupled with containment enclosures (gloveboxes and shielded cells), which allow to investigate (hydrometallurgical and pyrometallurgical) treatment processes, and manufacture compounds for actinide recycle tests. **24.**

**Barrier** (confinement): see **Confinement barrier.**

**Becquerel** (Bq): a unit of radioactive decay equal to one disintegration per second. 37 billion becquerels are equal to 1 curie (Ci). 30,000 disintegrations per second occur in a household smoke detector. As the becquerel is a very small unit, large multiples are often used: mega-, giga-, and terabecquerel (MBq, GBq, and TBq, respectively). **27.**

**Beta particle** (or *beta* radiation, *beta* ray): an electron (or a positively charged particle with a mass equal to that of an electron) emitted from a radionuclide. It means less damage than the same dose of *alpha* radiation, but has a higher penetrating power. A *beta* radiation can be stopped by a thin sheet of metal or plastic. **7.**

**Burnup** (or burn-up, burn-up fraction, burnup rate): strictly speaking, it corresponds to the percentage of heavy atoms (uranium and plutonium) that have undergone **fission\*** over a given time interval

(referred to as the “**burnup fraction**”). It is commonly used to determine the thermal energy produced in a reactor per unit mass of  **fissile\*** material, between fuel loading and unloading operations, expressed in megawatt.days per ton (MW-d/t). (See also **Specific burnup\***). The **discharge burnup\*** is the value for which a fuel assembly must be effectively unloaded (i.e., after several irradiation cycles). **27, 33, 44, 59.**

**Burnup rate** (or burn-up rate): see **Burnup\***. **27, 33, 44, 59.**

**Capture:** the capture of a neutron by a nucleus. The capture is said to be “radiative” if it is immediately followed by emission of *gamma* radiation. It is said to be “fertile” if it induces the generation of a fissile nucleus. **125.**

**Cell:** see **Hot cell.**

**Chain reaction:** a series of nuclear **fissions\*** during which released **neutrons\*** generate new fissions, which, in turn, release new neutrons generating new fissions, and so on.

**Clad** (or cladding): the envelope surrounding the fuel material, intended to ensure its insulation and mechanical resistance within the reactor core. **84, 99-103, 123-126.**

**Cleanup** (radioactive): all the operations intended to reduce radioactivity in a facility or at a site, especially by decontamination or equipment removal. **7.**

**Complexation:** the capacity of a chemical species to form stable groups with one or more ligands through electrostatic interaction. **113, 134.**

**Conditioning** (of radioactive waste): all the successive operations to be performed to bring radioactive waste to a stable, safe form suitable for its future management, whatever the option chosen: **storage\***, **transmutation\***, or **disposal\***. In particular, these operations may include compaction, **embedding\***, **vitrification\***, and placing in containers (packaging). **8.**

**Confinement barrier** (or containment barrier): a device able to prevent or limit dissemination of radioactive materials. **7, 10, 11, 51, 86, 123, 137, 138.**

**Containment barrier:** see **Confinement barrier.**

**Contamination** (radioactive): see **Radioactive contamination.**

**Criticality:** a configuration characteristic of a mass of material containing fissile elements, and possibly other elements, with a composition, proportions, and a geometry such that a fission **chain reaction\*** can be maintained within it. **18.**

**CSDV** (or **CSD-V**): *Conteneur ou Colis Standard de Déchets Vitrifiés*: standard container for vitrified waste. A glass package of 200 liters and 400 kg poured into a stainless steel enclosure, selected by the ANDRA as a standardized waste form. **30.**

**Decay** (radioactive): the transformation of a radionuclide into a different nuclide by spontaneous emission of *alpha*, *beta*, or *gamma* radiation, or by electron capture. The final product is a nucleus of lower energy and higher stability. Each decay process has a well-defined radioactive half-life. **8, 129.**

**Decontamination** (radioactive): see **Radioactive decontamination**.

**Deep geological disposal** (of radioactive waste): see **Disposal** (of radioactive waste)\*.

**Direct disposal**: the act of sending spent fuel to a disposal facility without going through the steps of treatment and recycling. **11, 133, 137, 141**.

**Discharge burnup**: see **Burnup\***. **27, 33, 44, 59**.

**Disposal** (of radioactive waste): the action of radioactive waste emplacement in a facility specifically laid out to confine it in a potentially permanent way. The disposal facility in which waste is placed without intent to retrieve it is called **repository**. Retrieval would still be possible, however, in the case of a reversible disposal (see also **Storage\***). **Deep geological disposal** of radioactive waste is the disposal of such waste in an underground facility specifically laid out for this purpose (referred to as a “deep geological repository”). **8-11, 57-61, 137-141**.

**Dose**: a general term for the amount of energy from radiation that is absorbed in a specific mass. **59-65, 82-84, 94, 95, 99, 114, 115, 131**.

**Dose rate**: the intensity of irradiation (energy absorbed in matter per unit mass and per unit time). The SI standard unit is the gray per second (Gy/s). **60, 83-85, 94, 99**.

**Effluents**: the residues of a chemical treatment under liquid or gaseous form. In some cases these unwanted residues are released to the environment. Another option widely practised in the nuclear industry is to separate the toxic fraction, and condition it into a tailored matrix so that the remainder may be released with no significant harm to the environment. Radioactive waste discharges to the environment are subject to authorization and control. **7, 9, 13, 15-19, 21-26**.

**Embedding** (or **immobilization** US, **immobilisation** UK, **encapsulation**) (of radioactive waste): the immobilization of radioactive waste through fixation within a material in order to obtain a solid, compact, and stable product which is physically indispersible. **71, 72, 88, 99, 100**.

**Encapsulation** (of radioactive waste): see **Embedding** (of radioactive waste).

**EXAFS**: *Extended X-ray Absorption Fine Structure* (see **XAS**). **35, 38, 39, 47**.

**Fast neutron reactor** (or **fast reactor**): referred to in French as “RNR” (standing for *Réacteur à Neutrons Rapides*). **29, 101, 103**.

**Fertile**: refers to a material the nuclei of which yield **fissile\*** nuclei when they absorb neutrons. This is the case with uranium-238, which yields plutonium-239. Otherwise, the material is said to be sterile. **123**.

**Fissile**: refers to a nucleus capable of undergoing **fission\*** through **neutron\*** absorption. Strictly speaking, it is not the so called “fissile” nucleus that undergoes fission, but rather the compound nucleus formed after neutron capture. **123, 125**.

**Fission**: the splitting of a heavy nucleus into two fragments of approximately equivalent masses. This transformation, a special case of radioactive decay in some heavy nuclei, releases a large amount of energy, and is accompanied with neutron and *gamma* radiation emission. The fission of the so-called “fissile” heavy nuclei can be induced by a collision with a neutron. **7**.

**Fission products** (FPs): **nuclides\*** generated either directly through nuclear fission, or indirectly through the disintegration of fission fragments. **7**.

**Fly ash**: the pulverulent residues resulting from combustion. They fall into two categories - calcium fly ash arising from the incineration

of some lignites recovered in thermal power plant scrubbers, and coal fly ash arising from pulverized coal combustion, which mostly contain silica and alumina in a glassy form. Fly ash may be used as additives in concretes. **71, 72, 78**.

**FPs**: see **Fission products**.

**FR**: Fast Reactor. See **Fast Neutron Reactor**.

**Fuel**: the constituent material of a nuclear reactor core which contains the **fissile\*** nuclides maintaining the **chain reaction\*** in the core. **7**.

**Fuel assembly**: in the core of a water reactor, fuel rods are gathered together in clusters of suitable rigidity which are set in place with a definite position in the reactor core. The so-called “assembly” is the whole of this structure, grouping one hundred to a few hundred rods, which is loaded into the reactor as a single unit. **13, 99, 101, 125, 129, 137, 139, 143**.

**Fuel cycle**: the industrial operations which **fissile\*** materials are subjected to. The cycle includes ore mining, fissile material concentration, enrichment, fabrication of fuel elements, fuel use in reactors, spent fuel treatment, waste conditioning, and the disposal of the resulting **radioactive waste\***. **7, 123**.

**Fuel pellet**: see **Pellet (fuel)**.

**Fugacity** (for a gaseous substance): an expression of chemical **activity\*** (see acceptance 2). The fugacity of a gas equals its partial pressure weighed by its activity coefficient. This is also the pressure that the real gas would have if behaving as an ideal gas. **42, 43**.

**Gamma radiation** (or **gamma rays**): high-energy, short-wavelength, electromagnetic radiation emitted from atomic nuclei. It can be stopped by a sufficient layer of lead, concrete, or other materials. **7**.

**Geological repository (Deep)**: see **Disposal** (of radioactive waste)\*.

**Glove box**: an enclosure in which materials can be handled while being sealed off from the surroundings, thereby protecting the operator. Handling operations are performed through hermetically sealed glove openings in the chamber wall. The relative pressure inside the enclosure is generally kept negative to contain radioactive substances. **24**.

**GTA welding**: see **TIG welding**.

**Half-life**: the time it takes for half the initial number of **radioactive\*** atoms in a radioactive nuclide sample to disappear by spontaneous decay. **59, 61, 114, 130**.

**Hot cell**: highly shielded cell of a hot laboratory in which high level substances are handled using remote manipulator arms. **17, 30, 103, 139**.

**Immobilization** (or **immobilisation** UK) (of radioactive waste): see **Embedding** (of radioactive waste).

**Inventory** (of radionuclides): see **Radionuclide inventory**.

**Ionizing radiation** (or **ionising radiation** UK): radiation capable of producing ions when it passes through matter. **7**.

**Isotopes**: the different forms of atoms of the same chemical element, the nuclei of which have an identical number of protons, but a different number of neutrons (i.e., the same atomic number, but different atomic masses). Uranium-238 and uranium-235 are uranium isotopes. Isotopes may be stable (i.e., not decay spontaneously) or unstable (i.e., decay spontaneously emitting ionizing radiation). **84, 125**.

**Labile**: refers to the radionuclide fraction likely to be released very rapidly from a waste on contact with water. **18, 101, 123, 133, 134, 141**.

**Labile release:** the radionuclide inventory fraction likely to be released instantaneously when the irradiated fuel is contacted by water. It mainly consists of fission products soluble in solution, and does not depend upon the confinement properties of the irradiated fuel various layers. It is mostly dependent on water accessibility and on the amounts of fission products segregated or sorbed outside the fuel. [18](#), [101](#), [123](#), [133](#), [134](#), [141](#).

**Lanthanides:** the rare earth element group with atomic numbers 57 to 71, corresponding to electron subshell 4f. Lanthanides have very close chemical properties. They also have very close chemical properties to those of actinides. Separation of actinides and lanthanides in spent nuclear fuel constitutes a major challenge. [36](#), [45](#), [47](#), [119](#), [121](#), [125](#).

**Leaching:** the contacting of a solid body with a liquid with the purpose of extracting some elements. By extension, refers to any experiment focusing on the alteration of a solid in a liquid. [54](#), [56](#), [73](#), [77](#), [87](#), [88](#), [93](#), [96](#), [111-113](#), [116](#), [119](#), [123](#).

**Major actinides:** heavy nuclei of uranium and plutonium occurring or formed in nuclear fuel. [7](#).

**MAS-NMR:** Magic-Angle Spinning Nuclear Magnetic Resonance. An analytical technique which brings out information on the chemical environment of an element in a solid. [35](#), [38](#), [39](#), [45,47](#), [54](#), [62](#).

**Metamict:** refers to a rock amorphized by the self-irradiation due to its radioactive element contents. [112](#).

**Micella:** a colloidal particle formed by aggregation of small molecules or ions. [18](#).

**Minor actinides:** heavy nuclei formed in a reactor through successive neutron captures from the fuel nuclei. These **isotopes\*** mainly are neptunium (237), americium (241, 243), and curium (243, 244, 245). [7](#), [33](#).

**Mixed OXide fuel:** see **MOX**.

**MOX (Mixed Oxides) (or Mixed OXide fuel):** a nuclear fuel containing Mixed OXides of (natural or depleted) uranium and plutonium. [7](#), [119](#), [123-127](#), [129](#), [133](#), [137](#).

**Nuclear waste:** an unusable residue arising from nuclear energy utilization. [7](#).

**Package:** the packaging with its specified radioactive contents, as presented for transport, storage and/or disposal. [8-11](#), [27-31](#), [48](#), [49](#), [73](#), [78-85](#), [91](#), [100-102](#).

**Partitioning:** see **Separation**.

**Pellet (fuel):** a small cylinder made of a ceramic consisting of uranium, plutonium or other actinides, which is used as **nuclear fuel** and stacked within a **clad\*** to make up a **fuel rod**. [125-127](#), [133-135](#).

**Potential radiotoxicity** (of a certain quantity of radionuclides, e.g., in waste): radionuclide inventory multiplied by ingestion dose factor, indicating the potential harmfulness of a given quantity of radionuclides under accident conditions. [7](#), [8](#), [123](#), [143](#).

**PWR:** *Pressurized Water Reactor*. [7](#).

**Pyrochemistry:** high-temperature chemistry (several hundred Celsius degrees). Pyrochemistry does not involve water or organic molecules, only liquid metals and molten salts. [119](#).

**Radioactive cleanup:** see **Cleanup (radioactive)**.

**Radioactive contamination:** the undesirable presence of a radioactive substance on the surface of or within a medium. [13](#).

**Radioactive decontamination:** partial or total removal of radioactive contamination through methods that allow contaminating materials to be recovered in a controlled way. [13-18](#), [91](#), [99](#), [119](#).

**Radioactive half-life:** see **Half-life (radioactive)**. [59](#).

**Radioactive waste:** any radioactive substance for which no subsequent use is planned or contemplated. Ultimate radioactive waste is radioactive waste which can no longer be treated under current technical and economic conditions, especially through extracting its valuable content or reducing its polluting or hazardous character. [7](#).

**Radioactive waste disposal:** see **Disposal** (of radioactive waste).

**Radioactivity:** the property of some isotopes with an unstable nucleus to spontaneously emit *alpha* and *beta* particles or *gamma* radiation. This term more generally designates the emission of radiation accompanying the **decay\*** of an unstable element. [7](#).

**Radiolysis:** the breakdown of molecules by ionizing radiation. [11](#), [51](#), [64](#), [79-85](#), [92-97](#), [112](#), [113](#), [123](#), [134-135](#).

**Radiolytic species:** products arising from water **radiolysis\*** by ionizing radiation. They fall into two categories, radical species ( $e_{aq}^-$ ,  $\cdot OH$  ...) and molecular species ( $H_2$ ,  $O_2$ ,  $H_2O_2$ ...). Radiolytic yields associated with the generation of the various species depend upon the radiation type through linear energy transfer. [64](#), [113](#).

**Radionuclide:** an unstable **nuclide\*** of an element which spontaneously decays emitting radiation. [27](#), [49](#), [51](#), [73](#), [87](#), [88](#), [101](#), [111](#), [114](#), [123](#), [133](#), [134](#).

**Radionuclide inventory:** quantities of fission products and actinides contained in irradiated fuel, generally expressed in Bq/gIHM (Becquerels per gram of initial heavy metal) or g/tIHM (grams per ton of initial heavy metal). These quantities and the associated isotopic spectra depend on various parameters, such as fuel type and irradiation conditions (burnup, etc.). Average inventories are calculated at a given date using computer codes. Conversely, distribution of radionuclide inventories, which depends on irradiation conditions and fuel thermal behavior, requires the implementation of characterization tools (electron microscope). [83](#), [101](#), [129](#), [133](#), [141](#).

**Radiotoxicity (potential):** see **Potential radiotoxicity**. [7](#), [8](#), [123](#), [143](#).

**Recycling (or recycle):** reuse in a reactor of nuclear materials derived from spent fuel **treatment\***. [123](#), [139](#), [143](#).

**Repository:** see **Disposal** (of radioactive waste).

**Reprocessing:** see **Treatment** (of spent fuel).

**Rheology:** the study of the deformation and flow of materials. It includes the study of viscosity, elasticity, and plasticity. [33](#).

**Rim effect** (or rim): see **Rim zone**.

**Rim zone:** the restructuring of a zone on the very edge of the pellet as a result of irradiation and thermal gradient. [133](#).

**Rod:** a small-diameter tube closed at both ends, making up the core of a nuclear reactor and containing fissile, fertile or absorbing material. When containing fissile material, the rod is a fuel element. [11](#), [123](#), [125](#), [127](#), [131](#), [133](#), [141](#).

**Separation:** a chemical process among **treatment\*** operations through which the various constituent elements of spent fuel are separated. The PUREX process isolates uranium and plutonium. Other more advanced chemical processes (DIAMEX, SANEX, GANEX) are currently being studied to separate actinides from lanthanides, or actinides from one another (which is referred to as **partitioning**). [8](#), [111](#), [143](#).

**SF:** see **Spent fuel**.

**Silica fume:** it consists of particles approximately a hundred times smaller than cement grains (about 0.1  $\mu m$  average diameter), and display pozzolan properties due to its high amorphous silica content. Besides, it completes cement grain sizes in the ultrafine range. [72](#), [79](#).

**Simulant:** work in a radioactive environment involves complex logistics conditions, hence the frequent use of stable isotopes of the same element, or of elements displaying chemical characteristics comparable to those of the radionuclides being investigated (oxidation degree, ionic radius, electronic configuration). These elements are referred to as *simulants*. **28, 30, 45, 46, 60.**

**Sintering:** an operation which strengthens grain bonding in a metal or ceramic compacted powder by heating this powder below its melting point. **111, 112, 119, 125.**

**Sorbed:** see **Sorption**. **15, 127.**

**Sorption:** the light, reversible fixation of an atom or a molecule onto a solid surface. **73-75, 88.**

**Source term:** the nature and quantity of radioactive products released or likely to be released from a nuclear facility or a package of radioactive materials. In particular, the "source term" used in computational models can help evaluate the consequences of an accidental radioactive release into the environment. **83-85, 93, 123.**

**Specific burnup (or specific burn-up, burn-up rate, burn-up):** the total amount of energy released per unit mass in a nuclear fuel. Generally expressed in megawatt x day per ton (MW·d/t). **27, 33, 44, 59.**

**Spent fuel (or spent nuclear fuel, SF):** the fuel assemblies definitively removed from a nuclear reactor after a period of useful energy output. They are also referred to as "irradiated fuel". **7, 125-141.**

**Spent fuel treatment:** see **Treatment** (of spent fuel).

**Spent nuclear fuel:** see **Spent fuel**.

**STEL:** *Station de Traitement d'Effluents Liquides*, effluent treatment station. **13, 15, 26.**

**Storage** (of radioactive materials or waste): the action of placing radioactive materials or waste temporarily in a surface or subsurface specially designed facility, pending their retrieval. The facility in which waste is placed with the intention of further retrieval is referred to as a "storage facility" (see also **Disposal**). **7, 8, 10, 11, 29-31, 78, 123, 127-141.**

**Structure factor:** a function characterizing the interference of waves scattered from the atoms of a material in a (neutron or X-ray) diffraction experiment. This function contains information about how matter is structured on the atomic scale. **38, 39.**

**TIG (or GTA) welding:** (abbreviations, respectively standing for *Tungsten Inert Gas* and *Gas Tungsten Arc*) an arc welding process with a refractory tungsten electrode in an inert-gas atmosphere, used to obtain a very high welding quality (pressure vessels). **137.**

**Transmutation:** the transformation of one nuclide into another through a nuclear reaction. Transmutation considered in relation to radioactive waste management aims at converting a long-lived nuclide into a shorter-lived or stable nuclide. **8, 111.**

**Treatment** (of spent fuel) (or **reprocessing, spent fuel treatment**): an operation that consists in separating valuable materials in spent fuel from the remainder, which can be then considered as waste and conditioned accordingly. **7-10.**

**UOX:** the standard fuel used in light-water reactors, composed of uranium oxide enriched with uranium-235. **41, 48, 114, 119, 125-127, 129, 133, 134, 137-139.**

**Uranium:** the heaviest natural element with an atomic number of 92. **7.**

**Vitrification:** an operation which consists in incorporating radioactive waste into a glass melt to ensure its conditioning under a stable form as packages likely to be stored or disposed of. **9, 27-70, 105-107, 119, 141, 143, 144.**

**Waste** (nuclear): see **Nuclear waste**.

**Waste** (radioactive): see **Radioactive waste**.

**Waste immobilization** (or **waste immobilisation** UK): see **Embedding** (of waste).

**XANES:** *X-ray Absorption Near Edge Structure* (see **XAS**). **38, 43, 46.**

**XAS:** X-ray absorption spectroscopy used for measuring the modulations in the X-ray absorption coefficient in an energy range of a few hundred electronvolts beyond the ionization threshold of a chemical element. This analysis provides information on the electronic characteristics (oxidation degree) of the element being probed (XANES), as well as its atomic environment: nature, distance, and number of atoms in the vicinity of the analyzed element (EXAFS). **38.**

**Zircaloy:** an alloy of zirconium and one or several other metals (tin, iron, chromium, nickel), which displays outstanding mechanical strength and chemical resistance. It is used for water reactor fuel clads\*. **99-101, 127.**

**Zirconium:** a metallic element with atomic number 40. Zirconium alloys are widely used for water reactor fuel clads. **27, 125, 129.**

# Table of contents

Foreword	5
Introduction	7
Waste volumes and streams	7
Waste management in terms of strategy and steps	7
Waste conditioning in steady progress	8
Waste and effluents	8
Conditioning processes	9
Conditioning systems designed for durability	10

## Decontamination and treatment processes for effluent and technological waste

Aiming at “cleaner” waste and effluents	13
Decontamination processes	15
Liquid waste decontamination	15
Solid waste decontamination	16
Organic waste treatment	19
Incineration processes for organic technological waste	19
Chemical and thermal oxidation of organic waste in supercritical water phase (SCWO)	23

## Glass: a waste conditioning matrix for the long term

Glass packages and manufacturing processes	27
Glass as a confining material	27
The confinement process	28
How to manage glass packages	30
Waste vitrification in other countries	31
Prospects for vitrification	31
Nuclear glass formulation, structure and properties	33
Tailored glasses for various types of waste	33
Determining glass composition	33
Chemical reactivity during glass making	34
Glass structure	35
Atomistic modelling of glasses: structure, physical properties, and quench effects	36
How to optimize physico-chemical properties in nuclear glasses	40
Redox phenomena in glasses	41
Specific oxide solubility	43
Actinide solubility in glass	45
Glass devitrification and thermal stability	48
Long-term behavior of glasses	51
Nuclear glass alteration by water under disposal conditions	51
Glass resistance to self-irradiation	58
Cold crucible vitrification	67
Cold crucible: a promising technology	67

## Current conditioning systems for low and intermediate level waste

Cements as confining materials	71
Cementitious materials	71
Developing cementitious embedding material formulations tailored to various types of waste	72

Concrete containers	78
Irradiation effects in cementitious matrices	82
Long-term behavior of cementitious materials	86
Cementitious materials: a reliable confining matrix for low- or intermediate-level waste	88
<b>Bitumens</b>	<b>91</b>
Bitumen package manufacturing	91
Bitumen package evolution under self-irradiation	93
Bitumen alteration by water	95
<b>Metallic structure waste conditioning</b>	<b>99</b>
Fuel clad compaction process	100
The standard package for compacted waste	100
Long-term behavior of packages for compacted metallic waste	101
Prospective research on cladding hulls melting	101

### Researching alternative matrices and processes for waste treatment and conditioning

Plasma benefits for incineration / vitrification waste treatment.	
The Shiva process	105
Chlorinated waste incineration	108
Sulfur-containing waste incineration	109
Alternative confining matrices	111
Tailored ceramics for the confinement of specific radionuclides	111
Irradiation effects on confining ceramics	114
Atomistic modelling benefits	115
Open prospective research for future conditioning materials	117
Confinement of waste from pyrochemical processes: status of research	119

### Spent fuel: a possible confining matrix ?

Spent fuel: a possible confining matrix?	123
Spent fuel initial characteristics	125
Post-irradiation chemical composition of spent fuel pellet	125
Post-irradiation physical state of spent fuel pellet	126
Irradiated clad state	126
Spent fuel evolution in a dry storage facility	129
Fuel evolution in a closed system	129
Fuel evolution in an unsaturated open system	131
Modelling the long-term spent fuel behavior	133
Modelling the spent fuel pellet behavior	133
Modelling radionuclide release from spent fuel under disposal conditions	133
Spent fuel containers in long-term storage and direct disposal concepts	137
Long-term storage and the dedicated container	137
Disposal container	139
Spent fuel storage and direct disposal: results and outlooks	141

### Conclusion

Conditioning: a major asset for nuclear waste management	143
Glossary - Index	145

---

Contributors to this Monograph:

Thierry Advocat  
Catherine Andrieux  
Isabelle Bardez  
Florence Bart  
Roger Boën  
Pascal Bouniol  
Guy Brunel  
David Chartier  
Céline Cau dit Coumes  
Jean-Marc Delaye  
Xavier Deschanel  
Sylvain Faure  
Cécile Ferry  
Catherine Fillet  
Bruno Fournel  
Fabien Frizon  
Christophe Gallé  
Stéphane Gin  
Christophe Girold  
Agnès Grandjean  
Damien Hudry  
Christophe Jousset-Dubien  
David Lambertin  
Aurélien Ledieu  
Florent Lemont  
Nicolas Moulin  
Sylvain Peugot  
Olivier Pinet  
Jean-Paul Piron  
Guillaume Ranc  
Isabelle Ribet  
Stéphane Sarrade  
Magaly Tribet  
Étienne Vernaz (Topic Editor).

... along with, of course, all the members of the DEN Monographs  
Editorial Board:

Bernard Bonin (Editor in chief), Alain Forestier (CEA Saclay Center),  
Martine Dozol (CEA Cadarache Center),  
Michaël Lecomte (CEA Marcoule Center),  
Bernard Bouquin (Communication Division), Michel Beauvy,  
Georges Berthoud, Mireille Defranceschi, Gérard Ducros,  
Yannick Guérin, Christian Latgé, Yves Limoge, Charles Madic †,  
Philippe Moisy, Gérard Santarini, Jean-Marie Seiler,  
Pierre Sollogoub, Étienne Vernaz.